

# **Effects Of COPD And Its Treatment On Cardiovascular Structure And Function Assessed Through Advanced Imaging Techniques**



**Doctor Ian Stone MRCP, MBBS**

A dissertation submitted in partial fulfilment of the requirements of the degree

of

**Doctor of Philosophy**

of the

**University of London**

Respiratory Research Centre

and

Advanced Cardiovascular Imaging NIHR Biomedical Research Unit

William Harvey Research Institute

Queen Mary University of London

## Statement of Originality

I, Ian Steven Stone, confirm that the research included within this thesis is my own work or that where it has been carried out in collaboration with, or supported by others, that this is duly acknowledged below and my contribution indicated. Previously published material is also acknowledged below.

I attest that I have exercised reasonable care to ensure that the work is original, and does not to the best of my knowledge break any UK law, infringe any third party's copyright or other Intellectual Property Right, or contain any confidential material.

I accept that the College has the right to use plagiarism detection software to check the electronic version of the thesis.

I confirm that this thesis has not been previously submitted for the award of a degree by this or any other university.

The copyright of this thesis rests with the author and no quotation from it or information derived from it may be published without the prior written consent of the author.

Signature:

A handwritten signature in black ink, appearing to read 'Ian Stone', enclosed within a thin black rectangular border.

Date: 1<sup>st</sup> February 2016

## Details of collaboration and Published Manuscripts:

Doctor Redha Boubertakh provided physics and programming support related to the results in chapters 6, 7 and 8. Dawn Midwinter (GSK) provided statistics support. Doctor Mohammed Khanji is conducting the HAPPY London Study which provided the control group in Chapter 7.

**Chronic obstructive pulmonary disease: a modifiable risk factor for cardiovascular disease?** Ian S Stone, Neil C Barnes, Steffen E Petersen

*Heart* 2012;**98**:14 1055-1062

**Raised troponin in COPD: clinical implications and possible mechanisms** Ian S Stone, Steffen E Petersen, Neil C Barnes *Heart* 2013;**99**:2 71-72

**Reproducibility of arterial stiffness and wave reflections in chronic obstructive pulmonary disease: The contribution of lung hyperinflation and a comparison of techniques.** Ian S Stone, L John, SE Petersen , NC Barnes. *Respir Med.*2013; **107**(11): 1700-8

**Lung Deflation and Cardiovascular Structure and Function in COPD: A Randomized Controlled Trial** Ian S Stone, Neil C Barnes, Wai-Yee James, Dawn Midwinter, Redha Boubertakh, Richard Follows, Leonette John, Steffen E Petersen *Am J Respir Crit Care Med.* Epub 10/11/2015 (In press)<sup>1</sup>

## Overview of Thesis

Significant cardiovascular morbidity and mortality exists in chronic obstructive pulmonary disease independent of traditional risk factors. A number of different hypotheses exist to explain this association including the contribution arterial stiffness and lung hyperinflation.

Non-invasive cardiovascular imaging and assessment are ideal methods through which this relationship can be further studied although a number of the techniques have yet to be validated in COPD. In this thesis we aimed to achieve a number of goals. First, we aimed to assess the reproducibility and level of agreement between different measures of arterial stiffness in stable hyperinflated COPD. Second, we hoped to establish the utility of 3 different measurement techniques for measuring intrinsic cardiac function in stable hyperinflated COPD. Third, in a case-control study we compared surrogates of cardiovascular risk in hyperinflated COPD patients and a group matched for cardiovascular risk with normal lung function. Finally, we sought to understand the impact of pharmacologically reducing lung hyperinflation on cardiovascular structure, function and arterial stiffness.

We have firstly demonstrated that non-invasive measures of arterial stiffness are reproducible in stable hyperinflated COPD. Secondly, we have established the level of agreement and reproducibility of three different CMR techniques for measuring intrinsic myocardial function which will provide important information for the powering of future CMR studies in COPD. Thirdly, we have shown that surrogates for cardiovascular outcomes are adversely affected in COPD compared to a group matched for global cardiovascular risk, suggesting that current scoring systems may be suboptimal in risk prediction in COPD. Finally, we have demonstrated that pharmacological lung deflation has consistent and physiologically plausible beneficial effects on cardiac structure, function and the pulmonary vasculature. Whether intrinsic myocardial function can be modulated through prolonged periods of lung deflation is as yet unverified and should be the focus of future clinical trials.

# Contents

<b>STATEMENT OF ORIGINALITY</b>	<b>2</b>
<b>OVERVIEW OF THESIS</b>	<b>4</b>
<b>CONTENTS</b>	<b>5</b>
<b>ACKNOWLEDGEMENTS</b>	<b>9</b>
<b>ABBREVIATIONS</b>	<b>11</b>
<b>FIGURES</b>	<b>15</b>
<b>TABLES</b>	<b>17</b>
<b>INTRODUCTION</b>	<b>19</b>
<b>CHAPTER ONE: CHRONIC OBSTRUCTIVE PULMONARY DISEASE</b>	<b>20</b>
Pathogenesis and pathophysiology	20
Inhaled Pharmacological Treatment of COPD	25
The complexity of COPD	27
Clinical Phenotype	28
Pharmacological Treatment of lung hyperinflation: Bronchodilator Therapy	34
<b>CHAPTER TWO: CO-MORBIDITY AND THE COPD CARDIOVASCULAR PHENOTYPE</b>	<b>37</b>
Increased cardiovascular morbidity and mortality in COPD	38
The impact of shared exposures	43
Models Explaining The Interaction Between COPD And Cardiovascular Disease	45

<b>Evidence That COPD Treatment Reduces Cardiovascular Morbidity And Mortality</b>	<b>52</b>
<b>Could The COPD Models Explain The Beneficial Effects Of COPD Treatment?</b>	<b>54</b>
<b>CHAPTER THREE: IMAGING AND ASSESSMENT OF CARDIAC STRUCTURE AND FUNCTION</b>	<b>57</b>
<b>THE AORTA AND AORTIC FUNCTION</b>	<b>58</b>
<b>Regional assessment of Aortic Function</b>	<b>59</b>
<b>Global assessment of Aortic function</b>	<b>60</b>
<b>Pulse wave velocity (PWV)</b>	<b>60</b>
<b>Augmentation Index: The assessment of wave reflections</b>	<b>65</b>
<b>CARDIAC MRI</b>	<b>68</b>
<b>Cardiac Volumes and Function</b>	<b>69</b>
<b>Tagging and other non-invasive measures of myocardial deformation</b>	<b>70</b>
<b>Imaging of Pulmonary Arteries</b>	<b>72</b>
<b>Pulmonary Artery Pulsatility</b>	<b>72</b>
<b>CHAPTER 4: METHODS</b>	<b>74</b>
<b>Ethics</b>	<b>75</b>
<b>Patient Selection</b>	<b>75</b>
<b>Patient eligibility</b>	<b>75</b>
<b>Lung function measurements</b>	<b>76</b>
<b>Bedside measurements of PWV and Augmentation index</b>	<b>77</b>
<b>CMR data acquisition</b>	<b>79</b>
<b>Feature and Tissue tracking</b>	<b>82</b>
<b>CSPAMM Tagging</b>	<b>83</b>

<b>Statistical methods</b>	<b>84</b>
<b>CHAPTER FIVE: REPRODUCIBILITY OF ARTERIAL STIFFNESS AND WAVE REFLECTIONS IN CHRONIC OBSTRUCTIVE PULMONARY DISEASE; THE CONTRIBUTION OF LUNG HYPERINFLATION AND A COMPARISON OF TECHNIQUES</b>	<b>85</b>
<b>Abstract</b>	<b>86</b>
<b>Introduction</b>	<b>87</b>
<b>Materials And Methods</b>	<b>88</b>
<b>Results</b>	<b>89</b>
<b>Discussion</b>	<b>94</b>
<b>CHAPTER SIX: FEATURE TRACKING, TISSUE TRACKING AND TAGGING ASSESSMENT OF MYOCARDIAL FUNCTION IN STABLE HYPERINFLATED COPD: A VALIDATION STUDY</b>	<b>98</b>
<b>Abstract</b>	<b>99</b>
<b>Introduction</b>	<b>100</b>
<b>Methods</b>	<b>101</b>
<b>Results</b>	<b>102</b>
<b>Discussion</b>	<b>109</b>
<b>CHAPTER SEVEN: THE APPLICABILITY OF CURRENT CARDIOVASCULAR RISK SCORES AND CARDIOVASCULAR SURROGATES IN COPD: A CASE-CONTROL STUDY</b>	<b>113</b>
<b>Abstract</b>	<b>114</b>
<b>Introduction</b>	<b>115</b>
<b>Methods</b>	<b>116</b>
<b>Results</b>	<b>118</b>

<b>Discussion</b>	<b>124</b>
<b>CHAPTER EIGHT: THE EFFECT OF PHARMACOLOGICAL LUNG DEFLATION ON CARDIOVASCULAR STRUCTURE AND FUNCTION IN STABLE HYPERINFLATED COPD: A SINGLE-CENTRE RANDOMISED CONTROLLED CROSSOVER TRIAL</b>	<b>132</b>
<b>Abstract</b>	<b>133</b>
<b>Introduction</b>	<b>134</b>
<b>Methods</b>	<b>134</b>
<b>Results</b>	<b>138</b>
<b>Discussion</b>	<b>143</b>
<b>CHAPTER NINE: SUMMARY OF THESIS AND FUTURE PROSPECTS</b>	<b>151</b>
<b>UNRELATED PUBLISHED MANUSCRIPTS ARISING DURING MY PHD PERIOD</b>	<b>155</b>
<b>APPENDIX</b>	<b>156</b>
<b>Section one</b>	<b>156</b>
<b>Section Two</b>	<b>165</b>
<b>REFERENCES</b>	<b>168</b>



## Acknowledgements

I am indebted to my two supervisors, Professor Steffen Petersen and Professor Neil Barnes who showed great faith in me and provided invaluable professional support as well as personal guidance when times were tough. I am truly grateful to have had the opportunity to work alongside them both over the past 4 years. I will never forget the opportunity given to me and will look back on these years at the London Chest Hospital with great fondness.

I would like to thank my colleagues in the Advanced Cardiovascular Imaging Unit who all contributed to make my research fun and enjoyable. To Jane who knew how and where to do everything; to the company of Filip and Felix and the Italians, Alexia, Federica, Ermanno and William. I owe special thanks to my closest collaborators Dr Redha Boubertakh and Dr Mohammed Khanji.

The nature of my project has involved almost every corner of the London Chest and I owe a debt of gratitude to many people. Kathy, Leonette and Chris all have important roles to play in the day-to-day running of the clinical trial and I am very grateful to their efforts that often go unnoticed.

Thanks should also go to the hard work and dedication of the many staff at the Clinical Research Centre at the William Harvey Research Institute including Dr David Collier, Justin Watts and Carolyn Dawson. Particular mention should go to Wai-Yee James, whose drive to succeed is unrelenting and whose commitment to hard work over and above the call of duty is something I will be ever grateful for.

This project would not have been possible without the faith shown in our research proposal by GlaxoSmithKline and by further financial support provided by Bart's Charity Special Purpose Fund. Dawn Midwinters' statistical support and advice was outstanding and has formed an integral part of my PHD project.

Finally, special thanks must go to my parents for their emotional as well as financial support during my early years as a medical trainee and instilling in me the drive and focus necessary to undertake a body of work such as this. And last but by no means least I must thank my wife Kay. Over last four years our lives have changed unrecognisably with the arrival of our beautiful and inspiring first child Dora. Though

life has thrown some complex challenges our way Kay has provided me with the unconditional support and understanding necessary to reach this point.

“Fill your paper with the breathings of your heart.”

— William Wordsworth

## Abbreviations

AAMI	Association for the advancement of medical instrumentation
ABA	Abdominal aorta
ACS	Acute coronary syndrome
AE	Adverse event
AI	Augmentation index
ANOVA	One-way analysis of variance
ATS	American Thoracic Society
BMI	Body mass index
BNP	Beta natriuretic peptide
BP	Blood pressure
BSA	Body surface area
CAD	Coronary artery disease
CAT	COPD assessment test
CCF	Congestive cardiac failure
cfPWV	Carotid-femoral pulse wave velocity
CHF	Congestive heart failure
CI	Confidence interval
CMR	Cardiac magnetic resonance
COPD	Chronic obstructive pulmonary disease
COR	Co-efficient of reproducibility
CRP	C-reactive protein
CRQ	Chronic respiratory questionnaire
CSPAMM	Complimentary spatial modulation of magnetisation
CT	Computerised tomography
CV	Co-efficient of variation
CVD	Cardiovascular disease
DBP	Diastolic blood pressure
DLCO	Diffusion capacity for carbon monoxide
DP	Diastolic peak
DRP	Diastolic reverse peak
ECG	Electrocardiogram
ECLIPSE	Evaluation of COPD Longitudinally to Identify Predictive Surrogate Endpoints
EDV	End-Diastolic volume
EDVI	End diastolic volume index
EELV	End expiratory lung volume
EF	Ejection fraction
EFL	Expiratory flow limitation
eGFR	Estimated glomerular filtration rate
ERS	European Respiratory Society
ESV	End-systolic volume
ESVI	End systolic volume index
FEV <sub>1</sub>	Forced expiratory volume in 1 second
FF	Fluticasone Furoate

FP	Fluticasone propionate
FRC	Functional residual capacity
FT	Feature tracking
FVC	Forced Vital Capacity
GOLD	Global initiative for chronic lung diseases
HAPPY	Heart Attack Prevention Programme for You
HARP	Harmonic phase
HR	Hazard ratio
HRV	Heart rate variability
HT	Hypertension
IC	Inspiratory capacity
ICC	Intraclass correlation co-efficient
ICS	Inhaled corticosteroid
IL	Interleukin
INSPIRE	Investigating New Standards for Prophylaxis in Reducing Exacerbations
ISOLDE	ICS in Obstructive Lung Disease in Europe
ISS	Ian Steven Stone
LA	Left atrium
LABA	Long acting beta-2 agonist
LAESVI	Left atrium end systolic volume index
LAMA	Long acting muscarinic antagonist
LHS	Lung Health Study
LOA	Limits of agreement
LPA	Left pulmonary artery
LRTI	Lower respiratory tract infection
LV	Left ventricle
LVEDVI	Left ventricle end diastolic volume index
LVESVI	Left ventricle end systolic volume index
LVH	Left ventricular hypertrophy
LVM	Left ventricular mass
LVMI	Left ventricle mass index
LVRS	Lung volume reduction surgery
LVSVI	Left ventricle stroke volume index
MACE	Major cardiovascular events
MAP	Mean arterial pressure
MESA	Multi-Ethnic Study of atherosclerosis
MI	Myocardial Infarction
MMP	Matrix metalloproteases
MPA	Main pulmonary artery
MPA	Main pulmonary artery
MRC	Medical research council
MRI	Magnetic resonance imaging
MYK	Mohammed Younis Khanji
NETT	National Emphysema Treatment Trial
NHANES	National Health And Nutritional Examination Survey
NHS	National Health Service

NICE	National Institute for Clinical Excellence
NYHA	New York Heart Association
OR	Odds ratio
P	Peak
PA	Pulmonary artery
PAP	Pulmonary artery pressure
PDE	Phosphodiesterase
PH	Pulmonary hypertension
POET	Prevention Of Exacerbations with Tiotropium study
PP	Pulse pressure
PR	Pulmonary rehabilitation
PVR	Pulmonary vascular resistance
PWA	Pulse wave analysis
PWV	Pulse wave velocity
RAC	Relative area change
RCT	Randomised controlled trial
ROI	Region of interest
RP	Reverse peak
RPA	Right pulmonary artery
RR	Relative risk reduction
RV	Right ventricle
RVEDV	Right ventricle end diastolic volume
RVEDVI	Right ventricle end diastolic volume index
RVEF	Right ventricle ejection fraction
RVESVI	Right ventricle end systolic volume index
RVol	Residual volume
RVSVI	Right ventricle stroke volume index
SABA	Short acting beta-2 agonist
SAL	Salmeterol
SAMA	Short acting muscarinic antagonist
SAX	Short axis
SBP	Systolic blood pressure
SD	Standard deviation
SE	Standard error
SFC	Salmeterol/fluticasone propionate combination
SFL	Smoke free legislation
SGRQ	St. Georges respiratory questionnaire
SNS	Sympathetic nervous system
SP	Systolic peak
SPAMM	Spatial modulation of magnetisation
SRP	Systolic reverse peak
SSFP	Steady-state free procession
SV	Stroke volume
SVC	Slow vital capacity
SVI	Stroke volume index
TAA	Thoracic ascending aorta

TAC	Total arterial compliance
TDA	Thoracic descending aorta
TGV	Thoracic gas volume
TLC	Total lung capacity
TLCO	Carbon monoxide transfer factor
TNF $\alpha$	Tumour necrosis factor $\alpha$
TORCH	TOWards a Revolution in COPD Health
TRISTAN	Trial of inhaled Steroids and Long-acting $\beta$ 2-agonists study
TT	Transit time
UK	United Kingdom
UPLIFT	Understanding Potential Long-Term Impacts on Function with Tiotropium
US	Ultrasonography
VCS	Vicorder comparison study
VI	Vilanterol
VRS	Vicorder reproducibility study
WCC	White cell count

# Figures

## CHAPTER ONE

<b>Figure 1</b> Schematic representation of the different types of emphysema in relation to the acinar architecture of the lung.	21
<b>Figure 2</b> Associations between symptoms, spirometric classification and risk of future exacerbations.	23
<b>Figure 3</b> Diagram of Lung volumes.	29
<b>Figure 4</b> The natural history of chronic obstructive pulmonary disease	33
<b>Figure 5</b> Proposal of pharmacological treatment COPD according to clinical phenotypes.	34

## CHAPTER THREE

<b>Figure 6</b> Measurement of carotid-femoral PWV with the foot to foot method.	62
<b>Figure 7</b> Different measurement techniques for path length.	64
<b>Figure 8</b> Carotid pressure waveform as recorded by applanation tonometry	66
<b>Figure 9</b> Feature tracking analysis for radial and longitudinal velocities of the left ventricle.	72

## CHAPTER FIVE

<b>Figure 10</b> a) Scatterplot of repeat Vicorder pulse wave velocity measurements. b) Bland-Altman plot of the differences between repeat Vicorder pulse wave velocity measurements.	90
<b>Figure 11</b> a) Scatterplot of repeat Vicorder augmentation index measurements. b) Bland-Altman plot of the differences between repeat Vicorder augmentation index measurements.	91
<b>Figure 12</b> a) Scatterplot of Vicorder and SphygmoCor pulse wave velocity. b) Bland-Altman plot of the differences between Vicorder and SphygmoCor pulse wave velocity.	93
<b>Figure 13</b> a) Scatterplot of Vicorder and SphygmoCor augmentation index. b) Bland-Altman plot of the differences between Vicorder and SphygmoCor augmentation index.	93

## CHAPTER SIX

<b>Figure 14</b> A schematic diagram explaining the derivation of parameters for strain and strain rate analysis.	103
---	-----

**Figure 15** Bland-Altman plots showing inter-study reproducibility for global, systolic and diastolic strain and strain rate parameters derived from tagging, feature tracking and tissue tracking analysis. 108

**Figure 16** Bland-Altman plots showing extent of agreement between feature tracking and tissue tracking versus tagging for mid-ventricular global strain (%) and diastolic and systolic strain rate (%/s) measurements. 109

## CHAPTER SEVEN

**Figure 17** Bland-Altman plots showing agreement between measurements of a) Left ventricular End Diastolic Volume Index (LVEDVI), b) Central Pulse Pressure, c) Left Ventricular Stroke Volume Index (LVSVI), d) Thoracic Ascending Aorta Pulsatility, e) Left Ventricular Mass Index, f) Pulse Wave Velocity, g) Abdominal Aorta Pulsatility and h) Thoracic Descending Aorta Pulsatility. 120

**Figure 18** Differences in pulse wave velocity, total arterial compliance and their relationship to QRISK®2 in COPD compared to controls matched for cardiovascular risk. 124

## CHAPTER EIGHT

**Figure 19** Study design enrolment and outcome 135

**Figure 20** Box-plot of change from baseline in right ventricular end diastolic volume index for fluticasone furoate/vilanterol 100/25 µg once daily versus placebo following 7–14 days of treatment. Baseline is the assessment taken at pre-dose on Day 1 139

**Figure 21** Forest plot of other cardiovascular efficacy outcomes. 144



# Tables

## CHAPTER ONE

<b>Table 1:</b> Gradation of severity of airflow obstruction	22
--	----

## CHAPTER TWO

<b>Table 2:</b> Proportion of deaths attributed to cardiac disease in patients with COPD	41
--	----

## CHAPTER FIVE

<b>Table 3:</b> Demographic characteristics for Vicorder reproducibility study and Vicorder comparison study	90
--	----

<b>Table 4:</b> Haemodynamic Parameters for the Vicorder reproducibility study and comparison study	91
---	----

<b>Table 5:</b> Mean transit time and path length data	92
--	----

<b>Table 6:</b> Correlation between measures of lung hyperinflation and the variability of repeat AI and PWV measurements in the Vicorder reproducibility study and the Vicorder comparison study	94
---	----

## CHAPTER SIX

<b>Table 7:</b> Baseline demographics	104
---------------------------------------	-----

<b>Table 8:</b> Interstudy reproducibility of global, systolic and diastolic end-points for tagging, feature tracking and tissue tracking	105
---	-----

<b>Table 9:</b> Agreement between different strain measurement techniques.	110
--	-----

## CHAPTER SEVEN

<b>Table 10:</b> Demographic and pulmonary function characteristics of COPD and control groups matched for global cardiovascular risk	119
---	-----

<b>Table 11</b> Demographic and pulmonary function characteristics of all eligible patients from the COPD cohort and HAPPY London cohort used in univariate and multivariate analyses	123
---	-----

<b>Table 12:</b> Comparison Of Cardiovascular Endpoints Between COPD And Control Group Matched For Global Cardiovascular Risk	126
---	-----

<b>Table 13:</b> Univariate And Multivariate Predictors Of Pulse Wave Velocity	127
--	-----

<b>Table 14:</b> Univariate and Multivariate predictors of cardiac chamber size and stroke volume	128
---	-----

## CHAPTER EIGHT

<b>Table 15:</b> Demographic baseline clinical characteristics of patients in the efficacy population.	139
<b>Table 16:</b> Baseline data of cardiovascular efficacy endpoint	142
<b>Table 17:</b> Results of cardiovascular efficacy outcomes of FF/VI 100/25 versus placebo	145
<b>Table 18:</b> Results of pulmonary efficacy outcomes of FF/VI 100/25 versus placebo	147
<b>Table 19:</b> Summary of on-treatment adverse events	148

## APPENDIX

<b>Table 20:</b> Tagging Interstudy reproducibility	156
<b>Table 21:</b> Feature tracking interstudy reproducibility	158
<b>Table 22:</b> Tissue tracking interstudy reproducibility	160
<b>Table 23:</b> Agreement between different strain measurement techniques.	162

# Introduction

## Chapter One:

# Chronic obstructive pulmonary disease

An estimated 3 million people have chronic obstructive pulmonary disease (COPD) in the UK. The prevalence of an abnormal forced expiratory volume in 1 second (FEV<sub>1</sub>), the hallmark of COPD, is approximately 9% in primary care. About 900,000 have a confirmed diagnosis of COPD, whereas an estimated 2 million people have COPD which remains undiagnosed.<sup>2</sup> The true mortality of COPD is difficult to ascertain for a number of reasons: some die with the disease rather than because of it whereas others are misclassified at the time of death, dying of causes related to COPD but certified as being as a result of these associated complications. Despite this COPD is the third largest cause of respiratory death in the UK, accounting for 30,000 (23%) of respiratory deaths.<sup>3,4</sup> Furthermore COPD patients have an increase in all cause mortality, highlighting the co-morbid nature of the condition.<sup>5,6</sup> In men, age standardised mortality rates from COPD have fallen progressively since the 1970s, but in women there has been a small but progressive increase.<sup>7</sup>

### Pathogenesis and pathophysiology

Cigarette smoking is implicated in the pathogenesis of COPD in 90% of cases, although a significant genetic component also exists since only 15-20% of heavy smokers develop COPD.<sup>8</sup> The term COPD historically has principally encompassed two conditions, chronic bronchitis and emphysema.

Chronic bronchitis can be defined clinically based on sputum production: The presence of chronic cough and sputum production on most days for a minimum of 3 months a year for two successive years. Mucus hypersecretion takes place in the central airways and contributes, along with remodelling of the central airways as a result of inflammation and oedema, to the airways obstruction.<sup>9</sup>

However emphysema is based on radiological or histopathological findings and is characterised by irreversible damage to lung parenchyma and vasculature. Emphysema can be conveniently classified into 2 types, depending on how the acinus is destroyed: a) The most common form in smokers, centriacinar

(centrilobular) emphysema which is characterised by focal destruction of the bronchioles and central portions of the acinus and surrounded by grossly normal lung parenchyma and b) panacinar (panlobular) emphysema in which the whole acinus is uniformly involved (Figure 1).<sup>10</sup>

Pathologically, biopsy and broncho-alveolar lavage studies have found the predominant finding is parenchymal infiltration by CD8-lymphocytes and polymorphonuclear cells with destruction of the normal architecture of alveolar spaces and thickening of submucosal glands with intact epithelium.<sup>11, 12</sup> Induced sputum studies confirm a predominance of neutrophils within the airways, although eosinophils are present in a significant proportion of patients, particularly at exacerbation.<sup>9, 13-16</sup> Both chronic bronchitis and emphysema contribute to expiratory flow limitation.

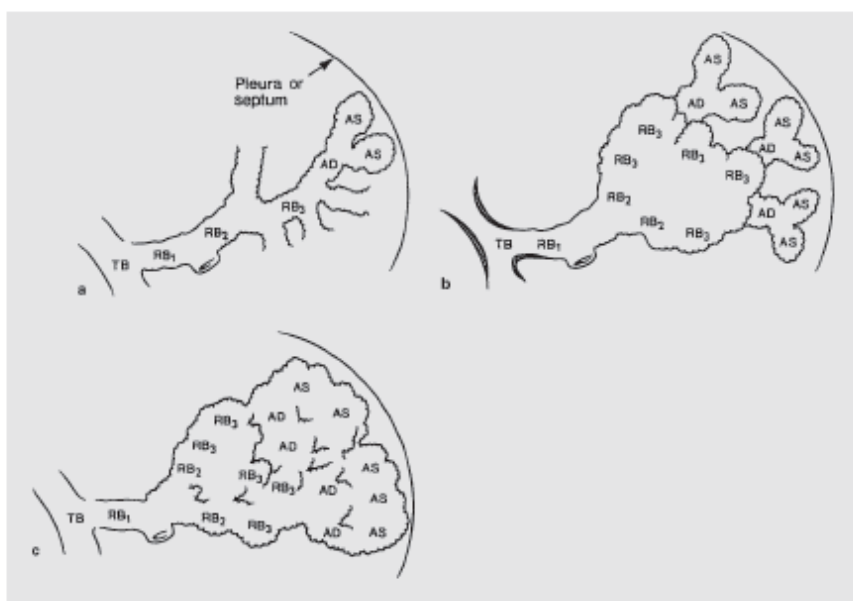


**Figure 1 Schematic representation of the different types of emphysema in relation to the acinar architecture of the lung.** TB: Terminal bronchiole; RB1–3: respiratory bronchioles; AD: alveolar duct; AS: alveolar sacs. a Normal acinus; b Centriacinar emphysema, in which the respiratory bronchioles are predominantly involved, whereas alveolar ducts and sacs are still normal; c Panacinar emphysema in which there is destructive enlargement of all air spaces distal to the terminal bronchiole and the acinus is more or less uniformly involved. (reproduced with permission from Turato et al<sup>10</sup>, published in *Respiration* by S. Karger AG)

Expiratory flow limitation in the presence of airflow obstruction is a hallmark of COPD. Most accepted definitions of COPD define airflow obstruction as a ratio of less than 70% of the FEV<sub>1</sub> to Forced vital capacity (FVC). Patients are said to be flow limited when the expiratory flow they generate during tidal respiration represents

the maximal possible flows that they can generate at that lung volume. Expiratory flow limitation can be characterised by FEV<sub>1</sub> and is one method by which the severity of COPD is defined (Table 1).

**Table 1 Gradation of severity of airflow obstruction (adapted from Nice guidelines 2010<sup>2</sup>)**

		NICE 2004	ATS/ERS 2004	GOLD 2008	NICE 2010
Post bronchodilator FEV/FVC	FEV % predicted	Severity of airflow obstruction			
			Post Bronchodilator		
<0.7	≥ 80 %		Mild	Stage 1: Mild	Stage 1: Mild
<0.7	50-79 %	Mild	Moderate	Stage 2: Moderate	Stage 2: Moderate
<0.7	30-49 %	moderate	Severe	Stage 3: Severe	Stage 3: Severe
<0.7	< 30 %	severe	Very Severe	Stage 4: Very Severe	Stage 4: Very Severe

Up until the most recent Global initiative for chronic lung diseases (GOLD) guidelines, COPD was staged exclusively based on the extent of airflow limitation and exacerbation frequency with pharmacological and non-pharmacological management largely being based on this. The dependency on FEV<sub>1</sub> to stage the disease is problematic in that not all aspects of the disease are properly captured and large heterogeneity exists within the COPD population with respect to clinical course and the efficacy of interventions. More recent guidelines have developed a more multi-dimensional approach, taking into account symptoms as well as exercise limitation, categorising patients into 4 groups A,B,C,D (see Figure 2). Specifically, they recommend the employment of the Medical Research Council dyspnoea (MRC) score and the COPD assessment test (CAT) score, discussed in more detail below. The groups no longer represent a linear increase in severity since, when the MRC score is used as the measure of symptoms, the risk of hospitalisation and mortality are similar in groups B and D. Furthermore, they do not differentiate active from inactive disease since the rate of lung function decline was similar between groups.

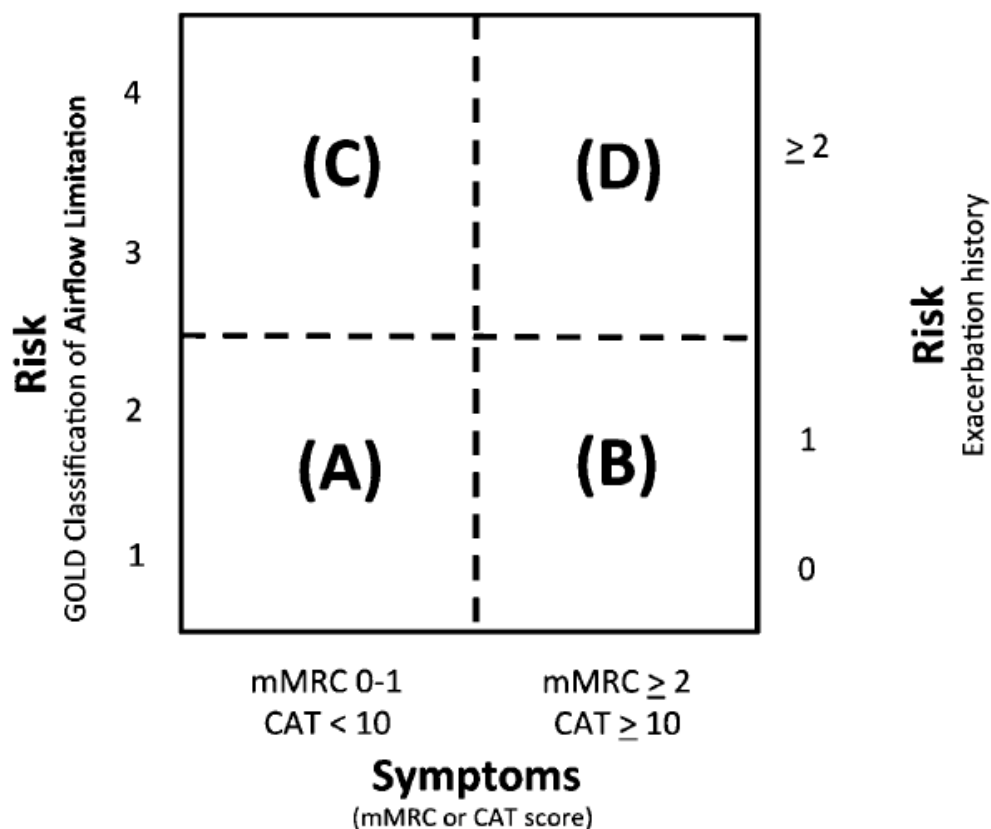


**Figure 2 Associations between symptoms, spirometric classification and risk of future exacerbations.** CAT: COPD assessment test; mMRC: modified Medical Research Council score. Reprinted with permission of the American Thoracic Society. © 2015 American Thoracic Society. The *American Journal of Respiratory and Critical Care Medicine* is an official journal of the American Thoracic Society<sup>17</sup>

### COPD exacerbations

An exacerbation of COPD is an acute event characterised by worsening of the patient's respiratory symptoms that is beyond the normal day-to-day variations and leads to a change in medication.<sup>17</sup> The manifestations of these exacerbations are highly variable reflecting the broad heterogeneity in the underlying pathophysiology of COPD as will be discussed below. Exacerbations play a key role in the progression of COPD. They accelerate the decline in lung function and impact on all cause mortality, which has been reported to be as high as 20% and 49% at 2 months and 2 years following an admission for hypercapnic respiratory failure.<sup>18</sup> The impact on lung function, symptoms and health status persist beyond the index events; Seemungal and colleagues prospectively followed a cohort of 101 patients with moderate to severe COPD for 2.5 years. At 35 days measures of lung function had returned to baseline in only 75.2% of subjects, with 14% remaining symptomatic. At 91 days 7.1% remain more flow limited compared to pre-exacerbation levels.<sup>19</sup>

Prevention and early treatment play a vital role in maintaining health in COPD, where a history of an exacerbation is the best predictor of developing future ones.<sup>20, 21</sup>

### **Dyspnoea: MRC score**

Dyspnoea is the most disabling symptom of COPD and is an important factor in the patient's perception of the illness. In the 1940's Fletcher and co-workers devised a short questionnaire that allowed a numeric value to be placed on each person's exercise capacity, first published in 1952.<sup>22</sup> The scale is still employed today, consisting of a five-point scale based on the patient's perception of dyspnoea while walking distances on the level or climbing. It does not quantify breathlessness itself rather the disability of it. There is good inter-observer agreement of up to 98% and it correlates well with other breathlessness and symptom scores, oxygen saturations, shuttle distance and measures of health related quality of life.<sup>23-25</sup> The scale is sufficiently sensitive to establish a treatment response to long-acting bronchodilators and pulmonary rehabilitation.<sup>26-28</sup> Furthermore, it predicts 5-year survival to a better extent than FEV<sub>1</sub> in isolation and has been incorporated into a highly validated composite index called the BODE index to help predict mortality in COPD.<sup>29, 30</sup>

### **Symptom score: CAT**

The CAT test was introduced and first validated in 2009 as a simple short, patient-completed instrument to assess symptoms and quality of life in patients with COPD. It comprises 8 questions, each scored between 0-5, giving a total maximum score of 40. Scores of 0-10, 11-20, 21-30 and 31-40 represent mild, moderate, severe and very severe clinical impact. It has been shown to have good internal consistency and reliability.<sup>31, 32</sup> It correlates well with other more established questionnaires such as the COPD specific St. Georges Respiratory Questionnaire (SGRQ) in the stable state. Furthermore, it can differentiate between the stable and exacerbating state, can differentiate mild from severe exacerbations and is sufficiently sensitive to identify improvements post exacerbation and post pulmonary rehabilitation in the short term where it correlates with Chronic Respiratory Questionnaire (CRQ) and SGRQ.<sup>33-35</sup> It shows similar changes than the more complex SGRQ and therefore arguably is a more simplistic and time efficient way of monitoring health status longitudinally.<sup>31, 36</sup>



## Inhaled pharmacological treatment of COPD

### Inhaled bronchodilators

Inhaled long-acting bronchodilators are central to the management of COPD and have been shown in large randomised controlled trials (TORCH, UPLIFT, POET, INSPIRE) to be effective at reducing symptoms and preventing further exacerbations.<sup>17, 37-40</sup> Furthermore, subgroup analyses of TORCH and UPLIFT have shown that as well as those with severe disease this also applies to those with moderate disease.<sup>41, 42</sup> Both long acting  $\beta$ 2-agonists (LABA) and long-acting muscarinic antagonists (LAMAs) are available in once daily and twice-daily forms, with newer combinations presently in development. Both classes act by relaxing airway smooth muscle tone. LABAs stimulate  $\beta$ 2-adrenergic receptors and provide functional antagonism to bronchoconstriction, whereas LAMAs prevent acetylcholine binding to muscarinic receptors that are involved in smooth muscle contractions.<sup>43</sup> Evidence indicates that once daily LABA and LAMAs have superior bronchodilation properties and clinical efficacy. An example of a once daily LABA or “ultra-LABA”, the first to be licensed in the UK, is Indacaterol. It has shown to be efficacious versus placebo, and other twice-daily LABAs.

### Inhaled corticosteroids (ICS) and fixed dose combination inhalers

The mechanism of action of inhaled corticosteroids is discussed on page 53 (Effects of inhaled COPD Therapies). Early studies looking at ICS in COPD showed no beneficial effect, although the studies contained small numbers of participants and were of short duration. The ICS in Obstructive Lung Disease in Europe (ISOLDE) study was the first large long-term, randomised, double-blind, placebo-controlled clinical trial that evaluated the effect of long term ICS on lung function, exacerbations, and health status in 751 patients with moderate-to-severe COPD which reported significant reduction in the median exacerbation rate by about 25%. A post-hoc analysis of ISOLDE suggested that this effect was seen predominantly in those patients with severe COPD ( $FEV_1 < 50\%$ ). However, ICS reduced the percentage of patients who had more than one exacerbation per year, indicating that ICS are effective in patients with mild COPD and frequent exacerbations.<sup>44</sup>

A number of studies have looked at fixed dose combinations (LABA and ICS) in

COPD. TRISTAN revealed that all active treatment arms (ICS/LABA and individual components) improved lung function, symptoms, and health status and reduced use of rescue medication and frequency of exacerbations compared to placebo, however combination therapy with fluticasone/salmeterol proved significantly more effective than salmeterol alone.<sup>45</sup> The TORCH study published in 2007 is the largest COPD trial of pharmacotherapy to-date. It randomised a total of 6112 COPD patients at 444 centers in 42 countries and investigated the effects of fixed dose ICS/LABA and its components with placebo on mortality, lung function, exacerbations and quality of life for a period of 3 years. Patients in the ICS/LABA group demonstrated reduced annual rate of exacerbations (0.85 95% CI 0.80, 0.90) compared to placebo (1.13 95% CI, 1.07, 1.20). The resulted rate ratio for exacerbations was 0.75 (95% CI, 0.69, 0.81; P<0.001), depicting a 25% reduction compared to placebo that corresponded to a number needed to treat of four to prevent one exacerbation in 1 year. As discussed above a post-hoc analysis by Jenkins et al supported the notion that those patients with milder disease may also benefit from inhaled corticosteroids.<sup>41</sup> Further evidence can be found in a recent Cochrane review and a meta-analysis on ICS and COPD where long-term use of ICS was found to significantly reduce the mean rate of exacerbations.<sup>46, 47</sup>

Concerns persist related to adverse events. Of particular concern is the number of the larger randomised controlled trials that report an increase risk of pneumonia, findings that have been confirmed in subsequent meta-analyses and Cochrane reviews.<sup>26, 37, 39, 48, 49</sup> Furthermore, a nested case control study involving 163,514 patients with COPD after adjustment for covariates has demonstrated that the use of ICS is associated with a 69% increase in the rate of serious pneumonia (RR 1.69; 95% CI 1.63, 1.75), which disappeared within a few months of stopping the therapy. Despite this, international guidelines continue to recommend treatment with an inhaled corticosteroid (ICS) on top of long-acting bronchodilators for severe/very severe chronic obstructive pulmonary disease (COPD) patients with a history of recurrent exacerbations. A number of different ultra-LABAS are now in development, some on which have been combined with inhaled corticosteroids with 24-hour duration.

### Fluticasone Furoate/Vilanterol (FF/VI)

One such example is Fluticasone Furoate/Vilanterol (FF/VI). Vilanterol (VI) is an inhaled LABA with 24-hour activity. Fluticasone furoate (FF) is an enhanced-affinity ICS with a pharmacologic profile that demonstrates greater retention in the lung and longer duration of action than fluticasone propionate (FP).<sup>50, 51</sup> In dose-ranging phase II studies it has shown to be effective in providing rapid and sustained improvement in FEV<sub>1</sub> in subjects with moderate to severe COPD with improvements in weighted mean FEV<sub>1</sub> of 173-214 ml and trough FEV<sub>1</sub> 115 - 144 ml respectively over 24 weeks.<sup>52, 53</sup> Further phase III studies have confirmed its effects are maintained throughout the 24-hour dosing period.<sup>54</sup> It appears safe in renal impairment, with no clinically relevant effects on pharmacokinetic, pharmacodynamics properties or tolerability of FF/VI. A 4-week study with safety among its primary endpoints has demonstrated that this therapy vs. placebo has no significant effects on heart rate, QTc interval, premature beats, ventricular ectopics or blood pressure. However, in patients with moderate to severe hepatic impairment there is a suggestion of increased systemic corticosteroid effects with evidence of reduced serum cortisol levels.<sup>55</sup>

### The complexity of COPD

The Global initiative for chronic lung diseases (GOLD) guidelines 2011 define COPD as a “common preventable and treatable disease, characterised by persistent airflow limitation that is usually progressive and associated with an enhanced chronic inflammatory response in the airways and the lung to noxious particles or gases”.<sup>17</sup> This definition is broad and as a result can be broadly applied to most people with COPD. However, it does not expose the complexity of the condition, which is made up of a number of different clinical phenotypes. The document does however attempt to make a fuller, more rounded assessment of the individual compared to previous documents. Prior to this, it has been argued that guideline development for COPD has been an oversimplification of a complex reality.<sup>56</sup> The one treatment fits all attitude led to the selection of pharmacological treatment based exclusively on the severity of airflow obstruction and was proposed as early as the 2001 GOLD guideline. There has been a paradigm shift in this most recent document proposing treatment guided by severity of symptoms and exercise capacity (as assessed by the MRC scale and CAT score discussed above), the risk of poor outcomes (assessed by airflow obstruction and frequency of exacerbations) in a 3-dimensional evaluation.

It has become evident that not all people respond in the same way to particular treatments irrespective of the above subdivisions, leading to the development of the term clinical phenotypes within COPD.

## Clinical phenotype

The term “clinical phenotype” has recently been proposed:<sup>57</sup> “A single or combination of disease attributes that describe differences between individuals as they relate to clinically meaningful outcomes, (symptoms, exacerbations, response to therapy, rate of disease progression, or death)”. This definition emphasises two key aspects: the attributes that define the clinical phenotype cannot occur in all patients with the disease of interest since they have to identify a subgroup of patients that differ in their prognosis or therapeutic needs; and the phenotype has to relate to clinically meaningful outcomes. Therefore any potential clinical phenotype must be validated longitudinally and prior to this these phenotypic traits should be considered mere descriptors of disease complexity.<sup>58</sup> Examples in COPD include the frequent exacerbator phenotype, defined as two or more exacerbations per year based on the findings of the ECLIPSE study, due to the potential for therapeutic interventions and the presence of systemic inflammation which is associated with high mortality.<sup>59 60, 61</sup>

## Lung hyperinflation

A further example of a clinical phenotype is lung hyperinflation, often associated with emphysema, and which can develop to varying degrees as a consequence of expiratory flow limitation (EFL). It impacts on mortality, was a predictor of exacerbations in the COPD Gene Study and the recent Spanish guidelines for COPD have acknowledged that these patients should follow a different treatment algorithm to those with chronic bronchitis predominant disease.<sup>62-64</sup>

## Assessment of lung volumes and the development of lung hyperinflation

Lung volumes can be divided into several compartments defined by the normal cycle of tidal breathing and the maximum capacity to inhale and exhale. During relaxed tidal breathing the lung tends to return to a basal level of inflation, which is termed the functional residual capacity (FRC) or end expiratory lung volume (EELV), which in normal lungs represents the point at which the outward recoil of the chest wall equals the inward recoil of the lungs.<sup>65</sup> Once this value is known all other values can be determined from spirometry including the total lung capacity (TLC; the maximum

volume of air that can be inhaled), the residual volume (RVol; volume of air remaining at the end of complete exhalation) and inspiratory capacity (IC; The difference between EELV and TLC - see Figure 3 and Box 1).

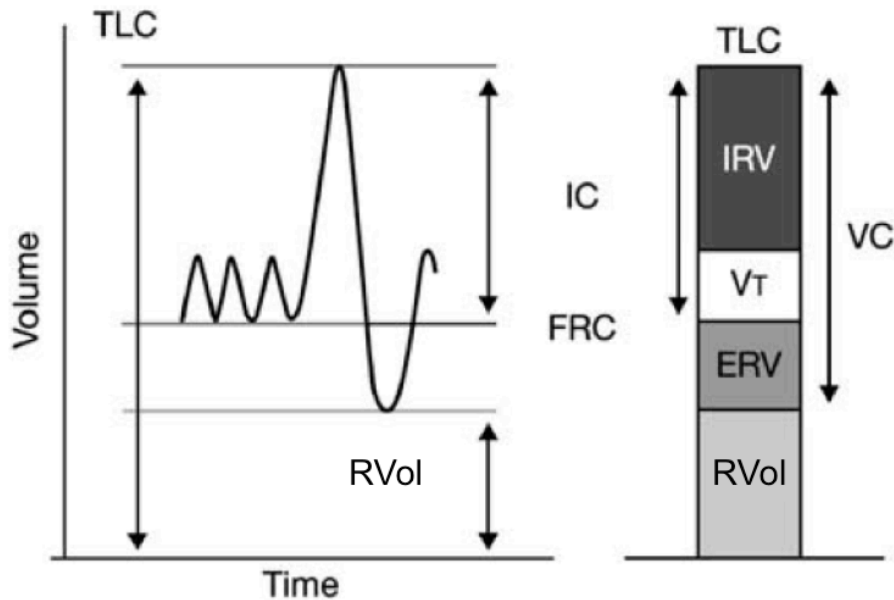


**Figure 3 Diagram of lung volumes** ERV: expiratory reserve volume; FRC: functional residual capacity; IC: inspiratory capacity; IRV: inspiratory reserve volume; RVol: residual volume TLC: total lung capacity; VT: tidal volume

Most COPD patients have some degree of lung hyperinflation, although this can remain undetected. Destruction of elastic tissue associated with emphysema alters the elastic recoil of the lung, adjusting the pressure volume of the curve so that a given lung volume produces less lung recoil than in healthy lung. Hence, the reduced lung recoil requires a greater volume to balance the chest wall recoil and over time this results in lung over-inflation, termed static lung hyperinflation.<sup>65</sup> Static lung hyperinflation increases functional residual capacity, RVol and TLC.

Cosio et al in 1978 first demonstrated that the RVol, reflecting early airway closure, is the first parameter to increase, followed by FRC and eventually TLC.<sup>66</sup> In this 4-year follow-up study they found no change in FEV<sub>1</sub> or FEV<sub>1</sub>/FVC, most probably as a result of increases in TLC that allowed VC to remain the same or increase and prevented the fall in FEV<sub>1</sub>. As the disease progresses airway narrowing, as a result of vagal tone, inflammation, mucus plugging and early collapse, causes a reduction in the time available for complete lung emptying during spontaneous breathing and insufficient lung emptying. This results in increases in (RVol) relative to the TLC with

a resultant fall in FEV<sub>1</sub> and FVC. The primary event therefore is gas trapping, the extent of which is a continuous variable, determined by expiratory flow limitation and ventilator demand at any one time.<sup>67, 68</sup>

### Measuring lung hyperinflation

The measurement of Total Lung Capacity (TLC) and its subdivisions provide detailed information concerning the functional status of the lung and are determined by its elastic properties. The value is mainly estimated through the use of plethysmographic and helium dilution techniques, although more recently the use of CT has also been employed. Significant differences in the measurement of TLC exist between these methods.<sup>69</sup> Regarding CT assessment is made at maximal inspiration in the supine position, which is not the case for other techniques.<sup>70</sup> Measurement at full inspiration is also in conflict with the clinical definition of lung hyperinflation which implies an abnormal increase in the volume of gas in the lungs at the end of tidal (functional residual capacity FRC) or maximal expiration (residual volume RVol).<sup>71</sup>

Important differences also exist between helium dilution and plethysmography. Over-estimation of lung volumes can occur during plethysmography when breathing frequencies greater than 2 Hz are employed, an error which has been shown to be corrected for if frequencies of less than 1 Hz are used.<sup>72-75</sup> In patients with significant airflow obstruction and poorly communicating areas of lung, helium dilution will result in underestimation of lung volumes owing to the helium not mixing with gas trapped in these under-ventilated areas.<sup>76</sup> Thus body plethysmography is considered the best modality for assessing patients with airflow obstruction for estimating the FRC, known as the thoracic gas volume TGV when calculated by this technique. The resulting TGV is combined with measurements of inspiratory capacity (IC) and slow vital capacity (SVC) to derive values for lung hyperinflation (see page 31) .

Indices used for estimating lung hyperinflation include TLC, RVol and the ratio of RVol/TLC. There is no consensus as to which value is the most robust although in COPD TLC varies as a function of the prevalent phenotype (it is increased in emphysema and often normal in chronic bronchitis) and it has been shown that RVol and RVol/TLC were more sensitive than TLC to the degree of airway obstruction.<sup>77</sup> Furthermore, a recent study by Deesomchok et al found that the RVol was increased in mild, moderate, and severe obstruction, and the greatest change in percent of predicted values following bronchodilators, as well as the largest frequency of a

positive response post bronchodilators, was seen in RVol.<sup>78</sup> Although there has been renewed interest in inspiratory capacity (IC) as a surrogate for hyperinflation, predominantly due to the ease at which it can be measured from simple spirometry, RVol is still presently considered to be the best way to evaluate therapies aimed at reducing air-trapping<sup>79</sup>. Despite suggestions in some reviews that the current RVol cut-off for hyperinflation of > 120% predicted of normal actually sits within the normal range of some individuals, they base this on unpublished personal communications which have not been the subject of peer review.<sup>79</sup> Accordingly for the purposes of this thesis we will consider an RVol value of >120% predicted as the cut-off to define lung hyperinflation.

#### Box 1: Calculating lung volume parameters

##### **Slow vital capacity (SVC)**

The maximum volume of gas which can be expired from the lungs during relaxed expiration from a position of full inspiration.

##### **Inspiratory capacity (IC)**

The maximum volume of gas which can be inspired from functional residual capacity.

##### **Thoracic gas volume (TGV)**

The volume of gas in the thorax at the end of tidal breathing.

These can be used to derive the following parameters:

##### **Total lung capacity (TLC) = TGV + IC (highest value)**

The volume of gas in the lungs and airways at full inspiration.

##### **Residual volume (RVOL) = TLC-SVC (highest value)**

The volume of gas in the lungs and airways at full expiration

### Clinical implications of lung hyperinflation

Lung hyperinflation has significant clinical implications. In lung hyperinflation tidal breathing takes place at a position closer to TLC. As a consequence, breathing takes place on a flatter part of the lung compliance curve, where progressive pressure increases generate smaller incremental volume changes - greater effort is required for a given change in volume. Furthermore, as a result of expiratory flow limitation, intrapulmonary pressures are positive at the end of expiration, termed intrinsic end expiratory pressure, which essentially acts as an inspiratory threshold load that must be overcome on top of the inward recoil of the lung before inspiration can occur. This has been measured to be as much as 6-9cm of H<sub>2</sub>O during quiet breathing in clinically stable hyperinflated COPD patients, and as a result of these mechanical limitations on ventilation work of breathing is increased.<sup>80, 81</sup> Activity related dyspnoea is one of the earliest symptoms of lung hyperinflation and may progress over time to incapacitating levels, particularly in situations where the ventilation system is under more stress such as during exercise or an exacerbation, and the drive to breathe is increased but the ability of the respiratory system to respond is hindered (neuro-mechanical dissociation).<sup>82, 83</sup> This has a major impact on the wellbeing of the patient where they develop symptoms of respiratory distress or possibly fear and panic which progresses with worsening COPD.<sup>20 84</sup>

As well as these mechanistic and symptomatic consequences, arguably most importantly it is predictive of mortality in clinical trials, whether assessed radiologically or by residual volume.<sup>85</sup> It acts as a marker of disease progression, where it correlates with the extent of oxygen desaturation on exercise and limitations in daily activity regardless of GOLD stage.<sup>86 87</sup> Through quantitative CT there is evidence that extent of emphysema may identify those whose FEV<sub>1</sub> may rapidly progress due to “active disease” despite having no significant airflow limitation at baseline.<sup>88</sup> In a prospective study by Ozgur et al lasting 47 months, lung hyperinflation significantly correlated with emergency visits and hospital admissions, although only weakly. This finding is further supported by a retrospective cohort study by Zaman et al where lung hyperinflation as measured by IC/TLC was able to identify a cohort with increased exacerbation frequency.<sup>89 90</sup>

### Change in paradigm

Spirometry has been used to physiologically stage the disease. Following seminal work by Fletcher and Peto an accelerated decline in FEV<sub>1</sub> has been universally accepted as the paradigm for the natural history of COPD. Subsequent to this it has



been shown that forced expiratory volume in 1s (FEV<sub>1</sub>) strongly predicts all-cause and cardiovascular mortality, the need for re-hospitalisation following an exacerbation and the likelihood for treatment failure or intensification of drug treatment<sup>91-93</sup>. However, its use as a surrogate is far from perfect. FEV<sub>1</sub> has a limited application in the assessment of response to bronchodilators or predicting other patient centred outcomes in terms of exercise ability or dyspnoea.<sup>94-96</sup> For example, in the National Emphysema Treatment Trial (NETT), a multicentre prospective randomised controlled trial that compared optimal medical treatment versus optimal medical treatment plus lung volume reduction surgery, a FEV<sub>1</sub> of 0.75 litres resulted in significant variation in maximum exercise capacity of between 10-80W and no meaningful relationship between FEV<sub>1</sub> and six-minute walk distance was identified.<sup>97</sup> It has become clear that the development of air trapping and dynamic hyperinflation through the mechanisms described above play a key role in a number of these processes. Paradigms have been proposed that focus on lung volumes rather than simple spirometry alone in the progression of the disease, thereby focussing therapeutic aims towards reducing air trapping, the primary event in the development of COPD, rather than simply focussing on airway calibre and flow limitation.<sup>68</sup>

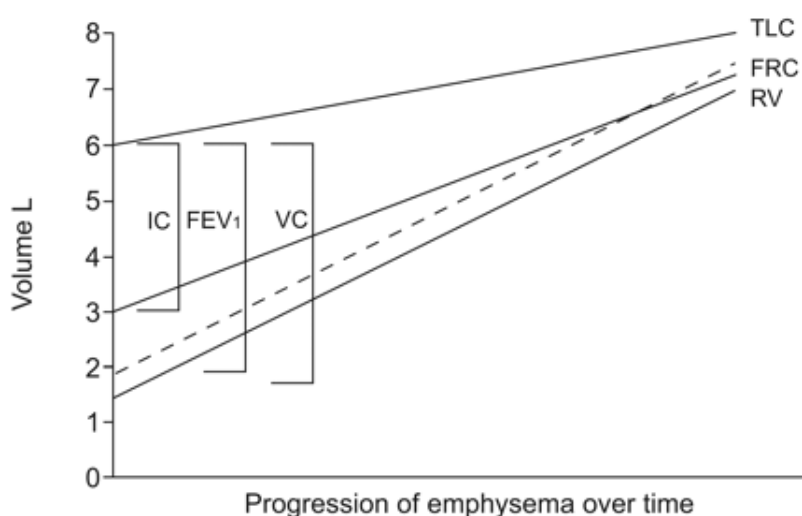


**Figure 4: The natural history of chronic obstructive pulmonary disease, characterised by a progressive increase in gas trapping measured by a progressive increase in residual volume (RV). A lesser increase in total lung capacity (TLC) leads to a progressive decline in vital capacity (VC) imposing a reduction in forced expiratory volume in 1 s (FEV<sub>1</sub>). FRC: functional residual capacity; IC: inspiratory capacity. (Reproduced with permission of the European Respiratory Society © Eur Respir J March 2010 35:676-680; doi:10.1183/09031936.00120609<sup>68</sup>)**

## Pharmacological treatment of lung hyperinflation: Bronchodilator therapy

Bronchodilator therapy is the mainstay of treatment for lung hyperinflation. Improvements in resting lung hyperinflation have been demonstrated in both short and longer term studies using all classes of bronchodilators.<sup>98</sup> A retrospective study of lung function databases demonstrated that the measurement of lung volumes may expose improvements that are not uncovered by the standard measurement of FEV<sub>1</sub>, with up to 75% being responsive to bronchodilator therapy, the largest difference being seen in RVol.<sup>99</sup> These findings have been replicated elsewhere: Tantucci et al conducted a single dose study using salbutamol in moderate to severe COPD and demonstrated improvements in IC and FRC in flow limited COPD patients despite no change in FEV<sub>1</sub>. O'Donnell et al have also demonstrated that plethysmography increases the sensitivity for identifying people that show bronchodilator response, that the RVol showed the greatest response and was most sensitive for detecting a significant reduction in air trapping, and that IC and VC underestimated changes in FRC and RVol respectively in 43% of patients due to small but consistent changes in the TLC. A reduction in hyperinflation post bronchodilation in both these studies seems to depend to some extent on the presence of expiratory flow limitation. Expected changes in lung volumes post bronchodilator in those considered to have irreversible lung function on simple spirometry have been reported as 18+/-2, -10+/-1, 8+/-1 % predicted for RVol, functional residual capacity (FRC), inspiratory capacity (IC) respectively. Long-acting bronchodilators improve dyspnoea relative to placebo and provide equivalent improvements in lung hyperinflation-related exercise dyspnoea ratings in the short term compared to shorter acting bronchodilators.<sup>100, 101</sup>

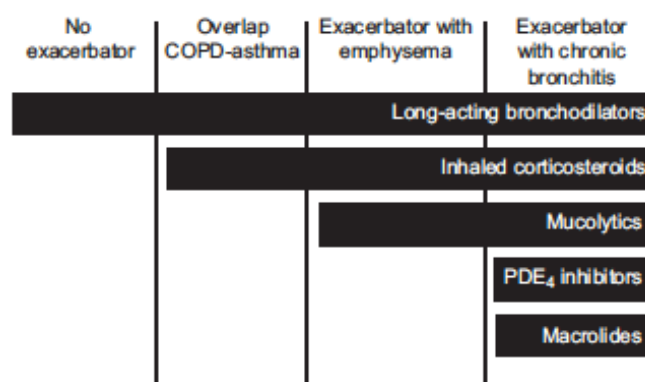


**Figure 5: Proposal of pharmacological treatment COPD according to clinical phenotypes** (Reproduced with permission of the European Respiratory Society © Eur Respir J June 2013 41:1252-1256; published ahead of print October 11, 2012, doi:10.1183/09031936.00118912).<sup>56</sup>

### Improvements in milder disease

Improvements in lung hyperinflation are not confined to the moderately severe end of the spectrum. Anticholinergic bronchodilation has also shown to have beneficial effects in patients with airflow obstruction and preserved FRC, IC and post-bronchodilator FEV<sub>1</sub>. Inhaled bronchodilation was associated with consistent improvements in forced expiratory flow rates, specific airways resistance and RVol, although to a lesser extent than the more severe patients.<sup>102</sup> These findings have been replicated in a retrospective analysis, which confirmed that RVol, FRC and TLC were significantly increased in GOLD Stage 1, whereas VC and IC were largely preserved.<sup>78</sup> It is felt that lung deflation reflects improvements in mechanical lung emptying through reduced airway resistance and increased functional strength of the respiratory muscles rather than increasing the static elastic recoil of the lung.<sup>103</sup>

### Sustained improvements in lung deflation

Initially the question remained as to whether acute volume reduction with SABA/SAMA could lead to sustained symptomatic and physiological benefits for people taking these medications on a regular basis. Studies have looked at responses over 2, 4 and 6 weeks and found consistent improvements in resting as well as exercise parameters of hyperinflation with salmeterol and tiotropium.<sup>104</sup> Computer tomography is increasingly used to assess emphysema and has also demonstrated radiological improvements in lung hyperinflation following long-acting anticholinergics over 1 year, which correlated with improvements in residual volume<sup>105-107</sup>. Magnussen et al have also shown that combining bronchodilating agents appears to have an additive effect which persist over a 2 month period compared to a single agent alone. The development of “ultra-LABAs”, 24 hour bronchodilation with once daily dosing, has the potential to further improve the ability to lung deflate through what some have described as “pharmacological stenting”.<sup>108</sup> One such compound indacaterol showed significant improvement in resting IC with differences of 140-200ml with placebo at 3 weeks, although this may simply reflect the potency of the bronchodilator it is likely the sustained bronchodilator effect plays a part. Surprisingly these were less than previous studies involving tiotropium (LAMA), probably due to severity differences between the studies and different study designs.<sup>109-111</sup>

### The impact of lung deflation

Lung deflation correlates with improvements in dyspnoea during exercise manoeuvres in mild to severe disease and 10% (0.39l) improvement in IC results in a 25-32% increase in exercise endurance time.<sup>94, 95, 112, 113</sup> Reduced inspiratory threshold load (intrinsic PEEP) as a result of lung deflation is thought to relieve dyspnoea by reducing the disparity between efferent motor output (sensed by corollary discharge) and afferent inputs from mechanosensors in the respiratory muscles, chest wall and lungs (improved neuro-mechanical coupling). This improved dyspnoea in combination with lung deflation is thought to result in the patient being less vulnerable to the triggers of an exacerbation resulting in the reduced exacerbation frequency described above.<sup>38, 114, 115</sup> Lung hyperinflation contributes to the co-morbidity associated with COPD and, as discussed later (page 58), its treatment may lead to improvements in other physiological systems.

# Chapter Two:

## Co-Morbidity And The COPD Cardiovascular Phenotype

*Sections of this Chapter have been published in Heart Journal as part of a Review Article and Editorial:*

**Chronic obstructive pulmonary disease: a modifiable risk factor for cardiovascular disease?** Ian S Stone, Neil C Barnes, Steffen E Petersen  
*Heart* 2012; **98**:14 1055-1062

**Raised troponin in COPD: clinical implications and possible mechanisms** Ian S Stone, Steffen E Petersen, Neil C Barnes *Heart* 2013; **99**:2 71-72

Dr. Ian Stone was first author and conceived the idea of the review article and drafted the manuscripts.

The phenotypic approach to managing COPD has the advantage that these “new” phenotypes are based on current knowledge making implementation into practice more feasible. There is however inherently a bias. An alternative approach involves the use of “hypothesis generating” or “discovery driven” techniques with the use of cluster analysis or principal component analysis based on standardised guideline directed approaches. A number of studies have begun utilising this approach although only one has longitudinally validated the identified “phenotypes” with clinically relevant outcomes such as mortality and hospitalisation. One such group consisted of patients with moderate COPD (FEV<sub>1</sub> 58%) but a predominant metabolic/cardiovascular phenotype. More recently Van Fleeteren et al have published a cluster analysis where 97.7 % of all patients had at least one co-morbidity, which was undiagnosed in a large proportion. They identified clusters which had markedly different health status despite having similar degrees of COPD severity where cardiovascular disease was once again found to play a key role.<sup>116</sup> These findings mirror a study by Barnett et al where multi-morbidity was found to predominate in a number of chronic disorders including COPD, emphasising the importance of multi-morbidity in COPD health-status and outcome, where cardiovascular co-morbidities appear to carry a particularly high weight.<sup>117</sup>

## **Increased cardiovascular morbidity and mortality in COPD**

Reduced pulmonary function, no matter what cause, is associated with increases in all-cause and cardiac mortality, myocardial infarction (MI) and arrhythmia.<sup>118-121</sup> Forced expiratory volume in 1s (FEV<sub>1</sub>) is ranked second to smoking and above blood pressure and cholesterol as a predictor of all-cause and cardiovascular mortality.<sup>93</sup> It has been suggested that a reduction in FEV<sub>1</sub> combined with a smoking history better predicts cardiovascular mortality than cholesterol.<sup>122</sup>

### **Cardiovascular mortality in COPD**

In COPD a large proportion of patients succumb to cardiovascular causes rather than respiratory failure, where cardiovascular causes of death have been reported in 12 and 37% of COPD patients.<sup>123</sup> Curkendall et al demonstrated a greater than two-fold increase in cardiovascular and all cause mortality in those with more severe COPD from a retrospective cohort study.<sup>124</sup> The HUNT lung study recruited 10,491 adults between 1995-1997, who were followed up for up to 12 years. Compared to normal airflow obstruction those with a FEV < 50% predicted had a HR of 3.8-6.85 for all

cause mortality. Although to a lesser degree, CV mortality was also increased: In men for every 10% decrease in percent predicted FEV<sub>1</sub> the adjusted HR for CV mortality was 1.24 (95% CI 1.10, 1.39).<sup>125</sup> Similarly the Lung Health Study revealed adjusted cardiovascular mortality rose by 28% for every 10% decrease in FEV<sub>1</sub>.<sup>122</sup> As well as severity, the “activity” of the disease is associated with cardiovascular mortality. As part of the 29 year follow up of the Buffalo Health Study cohort Schunemann et al have shown the rate of FEV<sub>1</sub> loss independently predicts coronary artery disease (CAD) mortality.<sup>126</sup> Furthermore, in the Baltimore Longitudinal study of ageing, patients with the greatest decline in FEV<sub>1</sub> over a 16 year period were three to five times more likely to die from a cardiac cause than those with the lowest decline, after adjusting for confounders. Importantly, this cardiovascular mortality risk associated with FEV<sub>1</sub> has been shown as part of a systematic review in a number of different cohorts to be independent of smoking.<sup>127</sup>

### **COPD morbidity in cardiovascular disease (CVD)**

With an ageing population it is perhaps unsurprising that a number of chronic diseases co-exist and are often not recognised and remain undiagnosed. As well as the high prevalence of cardiovascular disease in COPD populations (discussed below) it comes as little surprise that the reverse is also true; namely within those patients with known CAD, COPD is often found. Soriano et al found the prevalence of undiagnosed airflow limitation in community populations with CVD to be 19 % whereas in those hospitalised with CAD, the prevalence of COPD to be as high as 33.6 %.<sup>128</sup> Elsewhere the reported prevalence of COPD in patients hospitalised for ACS was 7 and 16%.<sup>129, 130</sup>

### **Cardiovascular morbidity in COPD**

A number of cross-sectional studies have looked at cardiovascular disease prevalence in COPD. In one such study looking at a large UK primary care records database of patients aged over 35 years by Feary et al, physician diagnosed COPD patients were five times more likely to have cardiovascular disease than those without the condition.<sup>131</sup> Johnson et al reported that the adjusted HR for incident CVD increased from 1.1(CI 0.9, 1.3) in GOLD stage 1 to 1.5 (CI 1.1, 2.0) in patients with GOLD stage III/IV as compared to patients without COPD.<sup>132</sup> A retrospective nested case-control study from Canada involving 11,493 individuals found that the prevalence of cardiovascular disease (MI, congestive heart failure (CHF) and arrhythmia) was higher in the COPD group than the controls even after adjustment for traditional cardiovascular risk factors. As well as pre-existing heart disease, this

study found an increased risk of hospitalisation due to cardiovascular disease in the COPD group.<sup>133</sup> Similarly, in a retrospective matched case control study involving COPD patients with a mean follow-up of 2.75 years, hospitalisation was higher in the COPD cohort for all cardiovascular hospitalisation endpoints with a relative risk of 2.09 (CI 1.99, 2.20) after adjusting for pre-existing cardiovascular disease and traditional risk factors.<sup>134</sup> The prospective Lung health study found cardiovascular events to be the leading cause of COPD hospitalisations, accounting for 50% of hospital admissions.<sup>135</sup> Even in moderate to severe COPD patients without pre-existing heart disease, 50% are at high risk of developing cardiovascular events within 10 years.<sup>136</sup> A recent systematic review of the literature supports the view that COPD is associated with increased risk of cardiovascular disease, with the risk of CVD increasing with the severity of airflow limitation.<sup>137</sup>

The outcome following hospitalisation for cardiovascular events appears to be worse for this population. The web-based REAL registry included 2032 COPD patients who were followed up for 3 years following MI. COPD was found to be an independent predictor of mortality and re-admissions for re-infarction, revascularisation and heart failure were significantly higher in those patients with COPD.<sup>138</sup> A multicentre outcome study following MI revealed after extensive adjustment for baseline differences that COPD patients have a two-fold mortality rate, increased re-hospitalisation rates and worse health-status 1 year following MI compared to those patients without COPD.<sup>129</sup> In a retrospective analysis by Wakabayashi et al COPD patients have higher rates of the composite endpoint of death or cardiogenic shock compared to patients without the condition following primary angioplasty or rescue PCI.<sup>139</sup> Following percutaneous coronary intervention, COPD patient experience significantly higher incidence of angina, arrhythmias and most importantly composite major cardiovascular events (MACE). Importantly, a relationship with COPD severity and MACE was also found.<sup>140</sup> A secondary prevention study for MI conducted between 1981 and 1988 demonstrated increased in-hospital (23.9%) and five-year (35.9%) mortality for those patients with COPD, although this was not independently associated in a multivariate analysis.<sup>130</sup>



Table 2: Proportion of deaths attributed to cardiac disease in patients with COPD

Author	Year	Sample size (N)	Mean Follow-up (years)	Mean Age (years)	No. of deaths	All Cardiac causes n/N	All Cardiac causes % of total	Specific Cardiac causes, if reported % of total
*Anthonisen <sup>135</sup> (RCT)	1994	5887	5	48	149	37/149	25	
*Anthonisen <sup>141</sup> (RCT)	2005	5887	14.5	48	731	163/731	22	IHD 10
+Calverly <sup>39</sup> (RCT)	2007	6112	3	65	875	137/875	16	Unknown/Other 10
+McGarvey <sup>142</sup> (RCT)	2007	6184	3	65	911	Not reported	27	CCF 3; MI 3; CVA 4; Sudden death 16
McGarvey <sup>143</sup> (RCT)	2011	5992	4	65	981	184/981	23	Cardiovascular 108 (11) Sudden cardiac 43 (4) Sudden death 33 (3)
Vilkman <sup>144</sup>	1997	2237	Not reported	67	1070		37	
Keistinen <sup>145</sup>	1998	2727	8.5	50-54	973	Not reported	Males 38 Females 26	CHD 27; CVA 4 CHD 26; CVA 8
Engstrom <sup>146</sup>	2001	200	14	68	181	91/181	50	IHD 29
Garcia-Aymerich <sup>92</sup>	2003	340	1.1	69	98	12/98	12	IHD 5
Celli <sup>30</sup>	2004	625	2.3	64-67	162	Not reported	14	
Stavem <sup>147</sup>	2005	405	26	50	196	89/196	45	IHD 20; CVA 5; Sudden death 14 Other 5
Curkendall <sup>133</sup>	2006	7575	4	Over 65	1975	Not reported	30	

RCT: randomised controlled trial; IHD: Ischaemic heart disease; CCF: congestive cardiac failure; MI: myocardial infarction; CVA: cerebrovascular accident; CHD: coronary heart disease

## COPD and troponin

Over the past decade it has become apparent that during an exacerbation of COPD, classically defined by the combination of worsening dyspnoea with increased sputum volume and/or purulence, there is subclinical myocardial damage typified by an increase in newer assays such as highly sensitive troponin as well as other biomarkers which predict mortality.<sup>148-151</sup> The key question relates to the mechanisms behind this rise, since without an understanding of the mechanisms the ability to identify an appropriate intervention that will improve outcome is hindered. Søyseth and colleagues have sought to further our understanding of this relationship.<sup>152</sup> Specifically, they addressed the important issue as to whether the raised levels of troponin found at exacerbation are chronically raised or are a phenomenon related to the exacerbation itself, and found that the troponin levels were significantly higher in the exacerbator group compared to stable patients from a pulmonary rehabilitation clinic. It is however questionable whether these groups really represent similar populations in the stable and exacerbating state, with significantly different modes of referral, smoking histories and spirometry readings when measured during periods of stability. In an ideal world these exacerbating COPD patients would be compared against their own baseline measures. Such a study has recently been undertaken and Patel et al have shown small (+ 0.005 µg/L) but significant increases in troponin during COPD exacerbations that did not require hospitalisation, the increase persisting up to 5 weeks post exacerbation, a higher rise being found in those with pre-existing heart disease.<sup>153</sup> Interestingly no relationship between exacerbation frequency and baseline troponin was found.

## Heart failure and COPD

A number of studies have looked at the prevalence of heart failure in COPD. Early population studies have focused on systolic failure with very low estimates (0-16%) in selected patients without concurrent disease and 10-46% in unselected COPD patients.<sup>154</sup> More recent prevalence estimates are similar, ranging from 7.1-31.3%.<sup>137</sup> The annual incidence rate of CHF in these populations has been reported as 3.7%.<sup>155</sup> In a long-term population study by Engstrom et al, a moderately reduced FEV<sub>1</sub> was associated with an increased incidence of hospitalisation due to heart failure, in the absence of previous history or concurrent MI.<sup>156</sup> The risk for hospitalisation is not just confined to those with moderately severe disease. In the Health ABC study FEV per cent predicted had a linear association with heart failure risk (HR 1.21; 95% CI 1.11, 1.32) as defined as treatment requiring hospitalisation which included those without overt lung disease.<sup>157</sup> As well as systolic dysfunction diastolic dysfunction also

contributes to the burden of heart failure, up to 50% of which may remain undiagnosed and contributes substantially to all-cause mortality whether mild or severe and is commonly found in patients with COPD. Of those patients with heart failure, the presence of COPD further increases their risk of death and hospitalisation.<sup>158, 159</sup>

## The impact of shared exposures

It may be that the relationship between COPD and cardiovascular disease (CVD) is solely due to shared common risk factors:

### Smoking

It is well accepted that smoking causes both COPD and cardiovascular disease. Passive smoke inhalation, in a dose-response manner, also increases the likelihood of fatal and non-fatal MI with an estimated pooled odds ratio (OR) from a meta-analysis of 1.22 (1.04-1.41) and 1.32 (1.04-1.67) respectively. Similarly, increased risks have been observed for COPD mortality with ORs related to spousal smoking of 1.67 in never-smoking males.<sup>160</sup>

### Smoke free legislation (SFL)

Recently, there has been a significant focus on international public health strategies to combat the adverse effects of smoking, and second-hand smoke in particular. Although the impact of SFL on respiratory symptoms is well studied, in normal individuals data on lung function are less robust since the changes noted were arguably of little clinical relevance, suffered from poor participant compliance and were confounded by seasonal variation in temperature.<sup>161-167</sup> The impact of SFL on COPD is unclear since the few studies that have assessed the rate of admissions for COPD exacerbations show conflicting results.<sup>168, 169</sup> This is in contrast to the data for CVD. A recent meta-analysis assessing the impact of SFL revealed a reduction of acute coronary syndrome risk in 30 of 35 estimates with a 10% (95%CI 6,14; p<0.001) pooled relative risk reduction, supporting the notion that smoke exposure has a significant independent role in cardiovascular morbidity, although whether those patients with concomitant COPD achieved equivalent improvements in coronary events is unclear.<sup>170</sup>

## Air pollution

The development of COPD as a result of damage caused by air pollution is well documented.<sup>171, 172</sup> Day-to-day changes in pollutant levels and longer term exposure also affect CVD risk, and all commonly measured pollutants are positively associated with increased mortality and hospital admissions for cardiovascular disease. Hypotheses relate to direct pollutant-effects of oxidative stress, pulmonary and systemic inflammation or pro-coagulant reactions that, as will be discussed later, have significant overlap with the postulated effects of COPD. Although observational studies have found associations between cardiac autonomic dysfunction and air pollution, this has not been borne out in controlled conditions and further mechanistic explanations are needed for this discrepancy.<sup>173-175</sup>

## The impact of differential prescribing practises

COPD patients have been excluded from clinical trials involving  $\beta$ -blockers due to historical concerns over bronchoconstriction.<sup>176</sup> Database studies persistently demonstrate a survival benefit for COPD patients receiving  $\beta$ -blockers in CAD and CCF. Furthermore, a Cochrane review has confirmed the safety of cardio-selective  $\beta$ -blockers in COPD of all severities and a recent study has also demonstrated a survival benefit of cardioselective  $\beta$ -blockers during COPD exacerbations.<sup>177</sup> The benefits of  $\beta$ -blocker use in heart failure extend to the use of non cardio-selective  $\beta$ -blockers, an assertion supported by a recent meta-analysis, although the authors stress the absence of any randomised controlled trials on the subject.<sup>178-180</sup> Despite the increasing awareness of the benefits of this class of drug in COPD, underuse persists due to lingering concerns over bronchoconstriction.<sup>181, 182</sup> The suboptimal management of cardiovascular disease in COPD patients goes beyond inadequate  $\beta$ -blocker prescribing; in one retrospective study 13% of patients with confirmed coronary artery disease were on neither a statin or anti-platelet therapy and a further 9% of the cohort had severe occult coronary artery disease. This sub-optimal management is ill placed since based on the above evidence, COPD patients arguably have the most to gain.

Although the under-prescribing of key medication contributes to cardiac risk, it is now appreciated that COPD is a multi-system disorder that exerts “systemic effects”.

Despite the aforementioned shared risk, the intriguing finding that increased cardiovascular morbidity and mortality in COPD is independent of smoking and other conventional cardiovascular risk factors, age, and gender is driving research into

understanding the underlying mechanisms of this increased risk and to what extent it is modifiable.<sup>123, 126, 127, 147, 179, 183-185</sup>

## **Models explaining the interaction between COPD and cardiovascular disease**

The hypotheses relating to why COPD patients are at increased risk of developing or succumbing to cardiovascular disease are best summarised through the following models:

**Inflammation model**

**Pulmonary hypertension model**

**Lung hyperinflation model**

**Shared genetics model**

### **Inflammation model**

Evidence is growing that COPD and cardiovascular disease may be linked through inflammatory processes contributing to atherosclerosis:

#### ***Inflammation and coronary artery disease***

The involvement of inflammation in the development of atheromatous plaques is well established.<sup>186, 187</sup> The majority of cells are monocytes which gain entry, along with T-cells and mast cells, via vessel adhesion molecules after exposure to irritative stimuli including cytokines, dyslipidaemia and hypertension.<sup>188, 189</sup> The monocytes develop into macrophages which themselves have an array of pro-inflammatory actions when studied in mice models.<sup>188</sup> Thrombotic complications are not always at the most severely narrowed site but at recently disrupted fibrous plaques, which typically contain macrophages, whose caps have been thinned by inflammatory and immune processes.<sup>189, 190</sup> Thus, the fate of an atherosclerotic lesion depends on the balance between pro-inflammatory and anti-inflammatory cytokines which in turn determines the magnitude of the inflammatory response.<sup>191</sup>

C-reactive protein (CRP) is an acute phase reactant and a marker of systemic inflammation. CRP and Interleukin (IL) 6, the pre-cursor to CRP, are increased during unstable angina and are markers of poor prognosis.<sup>194,192,195</sup> In situations of coronary vasospasm rather than plaque rupture CRP is normal, suggesting vessel

inflammation not myocardial ischaemia causes the inflammatory response.<sup>193</sup> CRP measured on a highly sensitive immunoassay (Hs-CRP) can predict MI and mortality in apparently healthy individuals.<sup>194, 195</sup> Although association does not prove causality, many are convinced that further investigation is warranted.

Hallmarks of atherosclerosis include endothelial dysfunction with reduced arterial compliance, increased central arterial pressure, left ventricular afterload and reduced diastolic coronary artery filling. A measure of arterial stiffness, known as aortic pulse wave velocity (PWV), can be measured non-invasively using applanation tonometry of the radial artery.<sup>196</sup> Repeatedly, aortic PWV has been shown to be an independent predictor of coronary artery disease in hypertensives, diabetics and the general population including the elderly.<sup>197-202</sup> PWV is also associated with disease duration, the presence of CRP and interleukin (IL) 6 (independent of atherosclerosis), and in rheumatoid arthritis and other chronic inflammatory conditions.<sup>203, 204</sup>

Statins have potent lipid lowering but also anti-inflammatory effects. The JUPITER trial, a randomised double blind placebo-controlled trial, demonstrated a 1.2% absolute risk reduction (RR) and a 44% relative risk reduction in combined cardiovascular endpoints in healthy individuals when treated with Rosuvastatin versus placebo. Significantly, participants had elevated HsCRP but lipid levels below treatment threshold, suggesting benefit due to anti-inflammatory rather than lipid lowering effects. Much controversy remains as to whether the population received care consistent with current standards and confounding lipid-lowering actions are hard to ignore.<sup>205</sup> Future studies involving methotrexate and canakinumab, potential cardiovascular therapeutic agents without confounding effects, are planned to help establish the contribution of inflammation. Respiratory therapeutics may also have a role to play.<sup>190, 206</sup>

### ***Inflammation and COPD***

COPD causes an airway inflammatory process, distinct from asthma, involving neutrophils, macrophages, T-lymphocytes and augmented concentrations of leukotriene B<sub>4</sub>, IL 1, 6 and 8b and tumour necrosis factor  $\alpha$  (TNF $\alpha$ ).<sup>207-212</sup> There is evidence suggesting inflammation may spill-over from the lungs to the systemic circulation, most likely caused by alveolar macrophages which clear inhaled particles and initiate local and systemic inflammation.<sup>213, 214</sup> Animal studies have shown movement of lung proteins to the systemic circulation is dependent on a number of

factors including lung inflammation, whereas human studies provide circumstantial evidence in the form of increased circulating levels of TNF- $\alpha$ , CRP and fibrinogen<sup>215-218</sup>. Furthermore, positron emission tomography studies have demonstrated excessive aortic inflammation in COPD, whose associated co-morbidities include skeletal muscle dysfunction, osteoporosis and diabetes which all have inflammatory aetiologies.<sup>212, 219-221</sup> The complex nature of inflammation within COPD has recently been elucidated, at least to some extent, as a result of data from the ECLIPSE (Evaluation of COPD Longitudinally to Identify Predictive Surrogate Endpoints) trial where it has been shown that in patients at risk of exacerbation, systemic inflammation defined according to a specific combination of several different inflammatory biomarkers persists during periods of stability.<sup>61</sup> Subsequent populations studies have shown the same three biomarkers, CRP, WCC and fibrinogen in COPD patients can predict the risk of IHD with a hazard ratio compared to those with no evidence of a raised inflammatory profile of 2.19 (95% CI 1.48, 3.23).<sup>222</sup>

This pro-inflammatory state and resultant spill-over of pulmonary inflammation may lead to down-stream effects such as arterial stiffness which could provide a mechanistic link between COPD, CAD and diastolic dysfunction.<sup>223-225</sup> Studies have indeed shown that arterial stiffness is raised in COPD and related to the extent of airflow obstruction and emphysema.<sup>226, 227</sup> Furthermore, Patel et al have shown that during COPD exacerbations there are increases in PWV which are associated with myocardial injury, although due to the short observational period of 5 weeks no stepwise deterioration in PWV was identified.<sup>153</sup> An alternative hypothesis has also been proposed which shifts the emphasis from left ventricular afterload excess to coronary microvascular inflammation.<sup>228</sup> These concepts support the findings of reduced myocardial perfusion reserve in COPD patients in the absence of either ischaemia or infarction.<sup>229</sup>

### **Pulmonary hypertension (PH) model**

Although PH is an established prognostic factor, its true prevalence in COPD is unknown due to selection bias in studies mainly assessing hospitalized patients.<sup>230</sup> The pathogenesis of pulmonary vascular disease is multifactorial, relating to alterations in vascular and pulmonary biology, gas exchange, structural changes in the pulmonary vasculature as well as mechanical factors.<sup>231</sup> Pulmonary artery pressure (PAP) depends on pulmonary artery wedge pressure, cardiac output and pulmonary vascular resistance (PVR). Many factors increase PVR in COPD (Box 2)

and alveolar hypoxia, which results in vascular remodelling and hypoxic vasoconstriction localised to the small pre-capillary arteries, is classically considered to be the most important.<sup>232</sup>

The development of pulmonary hypertension in COPD is classically attributed to severe hypoxia in end-stage disease causing raised pulmonary pressures, right ventricular hypertrophy, dilatation and systolic failure, or “chronic cor pulmonale” resulting in reduced exercise tolerance and survival. This simple hypothesis remains controversial;<sup>233</sup> vascular remodelling is seen in patients with milder forms of the disease and pulmonary endothelial dysfunction develops in COPD before the onset of hypoxaemia which is thought to be due to the combination of the direct effects of cigarette smoke and that of local inflammation, and is considered one of the initiating events in the progression to pulmonary hypertension.<sup>231, 234</sup>

It is argued that the severity of PH in most COPD patients cannot account for all the manifestations; although transient rises in PAP occur during nocturnal hypoxaemia and exacerbations, only 1-4% have a PAP >40 mmHg at rest, significantly lower than other forms of PH, and in sufficiently severe COPD to be considered for lung volume reduction surgery, the PAP may only be moderately elevated at baseline (26.3+/-5.2 mmHg).<sup>235-239</sup>

These observations have led to alternative explanations for the morbidity and a better appreciation of the contribution of diastolic dysfunction with the chronically pressure-overloaded right ventricle (RV) causing leftward septal shift, ventricular interdependence and LV diastolic dysfunction, despite normal LV systolic function.<sup>240, 241</sup> The impact of diastolic dysfunction should not be discounted; in a single-centre echocardiographic out-patient study, including patients with COPD, moderate to severe diastolic dysfunction independently predicted mortality in patients with normal systolic function.<sup>242</sup> Although PH associated diastolic dysfunction contributes to the cardiac morbidity of COPD, other mechanisms must also contribute since sub-clinical diastolic dysfunction exists in milder airflow obstruction without PH.<sup>243, 244</sup>



**Box 2: Confirmed and suspected factors leading to increased PVR in COPD<sup>245</sup>**

<b>Factors affecting PH in COPD</b>	<b>Impact on pulmonary vessels</b>
Airflow limitation	Pressure swings
Emphysema	Reduction of vascular bed
Alveolar hypoxia	Vasoconstriction/remodelling
Hypercapnic acidosis	Vasoconstriction
Polycythaemia	Hyperviscosity
Lung/systemic inflammation	Remodelling, including fibrosis

**Lung hyperinflation model**

Lung hyperinflation results from loss of elastic recoil combined with expiratory flow limitation, promoting increased expiratory lung volume (or “air trapping”) and intrinsic positive end-expiratory pressure (PEEPi) with significant clinical consequences in those with a more severe phenotype, including a two fold increase in all-cause mortality.<sup>62, 67</sup> It exerts its effects via 2 mechanisms:

***The mechanical effects of hyperinflation***

Lung hyperinflation increases mediastinal pressures through stiffening of the parietal pleura and cardiac fossa, with potentially significant cardiovascular physiological consequences including left and right diastolic dysfunction.<sup>246</sup> This assertion has been supported by a recent cross-sectional echocardiographic study which found sub-clinical diastolic dysfunction that was more severe in those with lung hyperinflation as assessed by static lung volumes.<sup>247</sup> The diastolic dysfunction described has generally occurred despite preservation of systolic function, which in the case of those with RV hypertrophy has been attributed to the flattening or leftward displacement of the interventricular septum in emphysematous patients<sup>248</sup> Although Lopez-Sanchez et al have recently found the prevalence of diastolic dysfunction in COPD to be as high 90% in consecutive hospital outpatients, they were unable to reproduce this association with lung hyperinflation and found no correlation with inflammation or right ventricular overload parameters.<sup>249</sup> They were however able to find an association with exercise tolerance which has been replicated elsewhere. Vassaux and colleagues have demonstrated that lung hyperinflation predicts a reduced oxygen pulse, a surrogate for cardiac performance during exercise.<sup>250</sup>

Observational echocardiographic studies have shown hyperinflation to independently predict cardiac chamber size. Watz et al have demonstrated that static lung hyperinflation is associated with a reduction in size of all 4 cardiac chambers over a whole spectrum of disease severity and confirmed associations with LV diastolic dysfunction. The increasing interest in COPD and cardiovascular disease has seen the introduction of a lung sub-study to the “Multi-ethnic study of atherosclerosis”, a large prospective cohort study designed to identify sub-clinical measures of CVD. Consistent with the study by Watz, in the 2816 participant lung sub-study significant associations were found between CT-quantified levels of emphysema and MRI measures of LV end-diastolic and end-systolic volumes.<sup>105</sup> Subsequent population studies from MESA have shown reduced RV volumes although, perhaps surprisingly, to a lesser degree than the left ventricle.<sup>107</sup>

The cause for reduced cardiac chamber volumes has also been investigated. The unaffected isovolumetric relaxation time suggests reduced pre-load conditions rather than a stiff myocardium as the cause for diastolic dysfunction, a concept supported by Jorgensen et al who found associations between decreased intrathoracic blood volume and LV performance in severe emphysema.<sup>251, 252</sup> This is also supported by a further COPD CT study from the MESA cohort showing reduced pulmonary vein dimensions, which were inversely associated with the extent of emphysema on CT.<sup>253</sup>

Further cardiac structural changes that occur in COPD that are as yet unexplained is the development of LVH in the absence of systolic dysfunction, hypertension or hypoxia with normal BNP levels, although lung hyperinflation may have a role, as recent associations have also been found with residual lung volume and RVol/TLC, although not with TLC or FRC.<sup>254</sup> The relationship was independent of blood pressure and other traditional cardiac risk factors among older smokers with predominantly mild to moderate COPD, the contribution to LVM being similar to that of systolic blood pressure.<sup>255</sup>

### *Neuro-humoral effects of hyperinflation*

Activation of the sympathetic nervous system (SNS) in normal individuals causes cardiovascular remodelling, with altered PWV, arterial compliance and diastolic dysfunction, which may occur through direct effects on tone, modulation of baro-receptor sensitivity or activation of the renin-angiotensin system.<sup>256-259</sup>

Heart rate variability (HRV) expresses cyclic fluctuations of heart rate (HR) and reflects autonomic modulation by sympathetic and parasympathetic efferent nervous impulses of heart rhythm. A sympathetic predominance is a predictor of mortality post-MI and in COPD there is evidence of a depressed HRV response to sympathetic and vagal stimuli which has also been shown to be related to static hyperinflation.<sup>260, 261</sup> As well as heart rate variability, SNS activation in COPD is demonstrated by the presence of increased noradrenaline turnover and increased plasma-renin activity.<sup>262</sup>

Hyperinflation, as well as its mechanical restrictions, may also impact on the SNS via a lung inflation reflex, increased hypoxia and neural-respiratory drive, which drives skeletal muscle contractility with the subsequent ischaemic release of free radicals.<sup>263</sup>

### **Shared genetics model**

#### *Genome wide association studies*

There may be more to the relationship between COPD and cardiovascular disease than simply sharing smoking as a risk factor. Parallel pathologic processes, as a result of shared genetics, may mediate the relationship between COPD and cardiovascular disease via gene-environment interactions causing connective tissue remodelling through modification of elastin content and proteolytic enzyme activity. There is extensive literature on the role of genomics and genome wide association studies in the understanding of the complex polygenic interactions of COPD and cardiovascular disease and the interested reader is referred to two well-written reviews on the subject.<sup>264, 265</sup> Two examples are provided here to illustrate this large area of research. Matrix metalloproteases (MMPs) are proteolytic enzymes that degrade collagen and elastin within the lung matrix and have other pro-inflammatory roles in smoking-induced emphysema models. MMPs also contribute to vascular remodelling in pulmonary hypertension (PH) and it is widely accepted that MMP polymorphisms are pivotal to non-pulmonary vascular remodelling in atherosclerosis.<sup>266-268</sup> Polymorphisms of epoxide hydrolase and glutathione-s-

transferase, involved in oxidative stress, are strongly associated with upper lobe emphysema and are risk factors for MI and atherosclerosis respectively.<sup>269, 270</sup>

### **Telomere function and the aging process**

“The senescence hypothesis” is the shortening of telomere length, a marker of cellular aging, caused by the failure to protect DNA against oxidative injury and reactive oxygen species.<sup>271</sup> Telomere shortening accelerates end-stage heart failure and several studies in diverse populations have shown an association, which exists before the development of clinical disease, between shorter telomeres in circulating leucocytes and both CAD and coronary artery calcification<sup>272-274</sup>. The oxidative damage and chronic inflammation in COPD, originating from environmental irritants such as cigarette smoking and air pollution, may reduce telomere length in circulating cells with important downstream effects on auto-immunity, potentially explaining the persistence of lung inflammation in COPD despite many years of smoking cessation, driving telomere attrition and increase cardiac risk over and above the risk associated with smoking.<sup>275-277</sup> Inflammation and oxidative stress are involved in virtually all cardiovascular and associated diseases which may explain the wide number of conditions associated with telomere length and the emerging evidence points towards the potential use of telomere length as a marker of both cardiovascular and obstructive airways disease or as a therapeutic target.<sup>278, 279</sup>

## **Evidence that COPD treatment reduces cardiovascular morbidity and mortality**

### **Effects of smoking cessation**

Smoking cessation results in an almost immediate improvement in blood pressure and heart rate, with the risk of stroke and CAD normalized to that of never smokers between 5 and 15 years after cessation. During the 5 years follow-up of The Lung Health Study (LHS), involving 5887 smokers with mild to moderate COPD, smoking cessation was associated with a 32% reduction in all-cause mortality, the trend persisting for 14.5 years of follow-up, and a 45% reduction in cardiovascular mortality likely through a direct reduction of cardiovascular events, but probably also through reducing the rate of COPD decline.<sup>280</sup>

### Effects of oxygen therapy

In the Nocturnal Oxygen Therapy Trial, 203 COPD patients with evidence of chronic hypoxaemia were randomised to receive oxygen supplementation. After a minimum follow-up of 12 months, the relative risk of death with nocturnal versus continuous oxygen was 1.94 (95% CI 1.17, 3.24).<sup>281</sup> This protective effect was also seen in the Medical Research Council study where 5-year mortality for those receiving oxygen was half that of the control group.<sup>282</sup> The benefit of oxygen in COPD patients with transient hypoxaemia related to sleep or exercise remains to be determined and is the subject of the “Long-term Oxygen Therapy Trial”.<sup>283</sup>

### Effects of pulmonary rehabilitation (PR)

It is unclear to what extent the reductions in hospital admissions, exacerbations and mortality seen following PR in COPD are a result of reduced cardiac morbidity. Endurance training results in adaptive responses of the heart including resting bradycardia, increasing end-diastolic dimensions, non-pathological cardiac hypertrophy, improved ventricular function and resistance to ischaemic insult.<sup>284, 285</sup> Significant improvements (10.3 +/- 0.7 to 9.2 +/- 0.8 m/s) in carotid-radial PWV occurred in an isolated exercise intervention. A case-control study of a seven week multidisciplinary PR course demonstrated significant reductions in PWV from 9.8 (+/- 3) to 9.3 (+/- 2.7) due to a reduction of 10mmHg in systolic blood pressure, the magnitude of which, if sustained, being sufficient to reduce cardiovascular morbidity and mortality by at least 13%.<sup>286, 287</sup> Improvements in dynamic hyperinflation (progressive air trapping during exercise), neuromuscular coupling or tolerance to dyspnoegenic stimuli may have contributed to PWV improvement.<sup>288</sup>

### Effects of inhaled COPD therapies

Two recent multi-centre, randomised, double-blind, parallel-group, placebo, controlled trials have raised the possibility that pharmacotherapy could affect survival. The 3-year TOWARDS a Revolution in COPD Health (TORCH) study was conducted at 444 centres in 42 countries and randomised 6184 patients. Comparing salmeterol (SAL), fluticasone propionate (FP) and salmeterol/fluticasone propionate (SFC) combination inhaler with placebo, a reduction in all-cause mortality, the primary efficacy endpoint, despite a large differential drop-out from the placebo arm would have reached statistical significance ( $p=0.04$ ) but for an interim analysis for safety resulting in a corrected  $p$ -value of 0.052.<sup>39</sup>

In the 4-year Understanding Potential Long-Term Impacts on Function with Tiotropium (UPLIFT) trial, 5993 patients were randomised to receive tiotropium or placebo. Hospitalisations and mortality one month following the completion of the trial (and cessation of study drug) was the pre-specified secondary outcome measure. Although a reduction in all-cause mortality versus placebo on an intention to treat basis was demonstrated, this did not reach statistical significance (HR 0.89, CI 0.79, 1.02). However, post-hoc, there was a significant reduction in all-cause mortality whilst on treatment after the protocol defined treatment period of 4 years (HR 0.84; CI 0.73, 0.97; p=0.016).<sup>40</sup>

Data on adverse events in these trials further raises the possibility of cardio-protective effects. A post-hoc analysis in TORCH showed fewer cardiovascular events within the SFC group after adjusting for smoking status and gender (SFC 11.3%, FP 13.8%, SAL 13.4%, placebo 14.6%). In UPLIFT a relative risk reduction in cardiac mortality (RR 0.86; 95% CI 0.75, 0.99), CHF (RR 0.59; 95% CI 0.37, 0.96) and MI (RR 0.71; 95% CI 0.52, 0.99) were observed.<sup>289, 290</sup>

## Could the COPD models explain the beneficial effects of COPD treatment?

### Inflammation model

#### *Effects of inhaled COPD therapies*

Inhaled fluticasone with or without long acting  $\beta_2$ -agonists reduce exacerbations and improve health status in COPD.<sup>39</sup> Observational studies as well as double-blind placebo controlled biopsy studies have confirmed modulation of inflammation within the airway following administration of inhaled corticosteroids.<sup>291-293</sup> Research data are conflicting with regards to whether inhaled therapies can reduce levels of systemic inflammation by reducing the spill-over of lung inflammation. Pinto-Plata et al found a significantly raised CRP level in COPD patients, which was 20% lower in those taking inhaled corticosteroids. An open label prospective study demonstrated that salmeterol and fluticasone significantly reduced circulating CRP levels compared to a combination of an anti-cholinergic and albuterol.<sup>294</sup> Furthermore, a proof of concept double-blind placebo controlled clinical trial by Sin et al found that withdrawing inhaled steroids increased CRP levels and re-introduction of inhaled fluticasone for 2 weeks resulted in 50% and 26% reductions in CRP and IL-6 respectively.<sup>295</sup>

However, when repeated as an 11 centre randomised, placebo-controlled, double blind trial, no significant changes in CRP or IL-6 were identified, which may be due to a higher proportion of smokers in the latter study or the use of long-term inhaled corticosteroids modifying inflammatory processes within the lung.<sup>296</sup> In any case, it is argued that lack of correlation between inflammatory biomarkers in the airway and the systemic circulation does not necessarily exclude the possibility of “spill over”, since many factors will influence concentrations in different body compartments; for example receptor binding influences the free concentrations of many cytokines, with potential downstream spill-over effects on the cardiovascular system without noticeable changes to the intermediary biomarkers.<sup>218</sup>

The effect of inhaled therapies on PWV in COPD has been investigated. 249 patients were randomised to receive fluticasone/salmeterol combination inhaler (Seretide) or placebo with a primary outcome measure of the change in PWV at 12 weeks, which did not reach statistical significance on an intention to treat basis. However, in those patients that remained on the study drug throughout the trial, a significant, although modest, reduction (0.4 m/s) in PWV was achieved, which was found in a post-hoc analysis to be more marked in those with a PWV of greater than 10.9 m/s at baseline. Although an increase in aortic PWV of 1 m/s corresponds to an adjusted increased risk of 15% in CV mortality, the reverse is less clear.<sup>297</sup> Clinically significant reductions are yet to be established and the effect of these reductions on cardiac structure and function are, until such studies are carried out, unknown.

#### *The effect of phosphodiesterase-4 (PDE4) inhibitors*

PDE4, a member of the PDE enzyme superfamily that inactivates cyclic adenosine monophosphate and cyclic guanosine monophosphate, is the main isoenzyme involved in inflammatory airway disease.<sup>298</sup> The PDE4 inhibitors are a new anti-inflammatory drug with efficacy and acceptable tolerability in pre-clinical studies in COPD with no effect on cardiac repolarization.<sup>299, 300</sup> A Cochrane review involving 23 RCTs, concluded that PDE4 inhibitors, including roflumilast and cilomilast, were associated with significant improvements in FEV over placebo regardless of severity or concomitant treatment, and reduced the likelihood of exacerbations.<sup>301</sup> Given that it is administered orally, it seems likely that it will exert a systemic effect on inflammation and thereby potentially having a dual benefit on the cardiovascular system. In-vitro studies have pointed towards a third cardio-protective effect through

prevention of nitric oxide induced myocyte apoptosis, potentially protecting against myocardial ischaemia and ischaemic reperfusion injury.<sup>302</sup>

### *Lung hyperinflation model: The effect of lung deflation*

Bronchodilators, whether beta-agonist or anticholinergic, improve air trapping in mild and more severe forms of COPD. Lung deflation results in improved exertional dyspnoea and exercise tolerance due to a combination of reduced inspiratory muscle loading and dynamic hyperinflation.<sup>99, 102</sup> Some of these improvements may also be due to an improvement in cardiovascular function. Jorgensen et al demonstrated increased left ventricular end-diastolic dimensions and filling with significant improvements in cardiac index following lung volume reduction surgery (LVRS). In the National Emphysema Treatment Trial cardiovascular sub-study there were improvements in capillary wedge pressure post LVRS. At 6 months there was improvement in “O<sub>2</sub> pulse”, the total oxygen consumed during maximal effort per heart beat and a surrogate for stroke volume, in a subsequent post-hoc analysis, which, interestingly, was also seen in a proportion of patients treated with medical therapy alone.<sup>303-305</sup> Although this offers an insight into how lung deflation may improve cardiac function, the impact and exact onset is unclear since prospective RCT data are lacking.



**Chapter Three:**

**Imaging And Assessment Of Cardiac  
Structure And Function**

## The aorta and aortic function

The term aorta is derived from the Greek word “aorter” which refers to an umbilical/belt used to hang up the “aor”, the word Homer used for sword. It was Aristotle who described the great vessel as an “aorte” something that hangs or carries (the heart). Different models have subsequently been applied to the arterial system. In the Windkessel model the arterial system is compared to a fire-house system where cushioning and conducting functions are separated: The large arteries cushioning the pulsations from the central pump, the wide bore hose acting as a conduit and the fire hose nozzle likened to the peripheral arterioles.<sup>306</sup> Limitations to this model include the fact that cushioning and conduit functions are not in reality separated, with a progressive loss of cushioning function and progressive increase in conduit function from the aorta to the peripheral arteries, whose stiffness is further modulated by vasomotor tone through involvement of the sympathetic nervous system, renin-angiotensin system and local endothelial function.<sup>256, 257</sup> A propagative model is therefore considered to more accurately reflect the nature of the circulatory system, the propagation (velocity) of the pressure wave being inversely related to the distensibility of the arterial tube. It is the collagen and elastin contained within the aorta, which makes up to 60% of intima media, which provides the elastic buffering capacity, transforming the pulsatile effect caused by ventricular ejection into continuous blood flow.<sup>307-309</sup> The elastin content and hence the elasticity reduces as one moves away from the heart.<sup>310</sup> The buffering capacity of the aorta also typically reduces with age and in certain pathological states, described as stiffening of the aorta, with important clinical consequences. The effects of arterial stiffness are wide-ranging and result in microvascular damage in both the brain and kidneys. The microvascular damage is caused by differential input impedance in these organs compared to other vascular beds. The low resistance to flow in these organs expose the small vessels to high-pressure fluctuations. In renal disease the presence of arterial stiffness is independently associated with reduced creatinine clearance and is independent of plasma glucose, cholesterol, obesity and smoking.<sup>311, 312</sup> Reduced distensibility has been shown to result in left ventricular dysfunction and reduced exercise capacity. Early identification may provide a means to identify subtle changes in function prior to the occurrence of remodelling and provide a target for therapeutic interventions.<sup>307, 313, 314</sup>

The assessment of aortic function can occur specifically at different locations along its path, known as regional assessment or via a global assessment:

## Regional assessment of aortic function

Aortic distensibility or compliance is defined as the relative change in area for a given pressure change and actually makes up 60-70% of the total systemic compliance. It has been used on a regional level to assess aortic stiffness where a reduction in compliance has been shown to reduce coronary and endocardial perfusion in animal models with and without coronary artery stenosis;<sup>309, 315, 316</sup> reduced compliance predicts reduced coronary flow velocity reserve in patients with suspected coronary artery disease, and it modestly correlates with the extent of CAD and was a predictor of left ventricular end-systolic volume index post MI<sup>317-319</sup>. Even in the absence of overt cardiovascular disease, increases in proximal aortic stiffness associated with ageing results in unfolding of the aortic arch and is associated with increased left ventricular mass and mass to volume ratio.<sup>320</sup>

## Measurement of regional arterial stiffness

CMR has compared favourably to ultrasound in the assessment of regional distensibility. It has a number of advantages over other modalities including a wider field of view, the ability to precisely delineate aortic anatomy, sufficient spatial and temporal resolution to detect rapid and small changes in the aorta which can be isolated to specific segments, a lack of ionizing radiation as well as the simultaneous assessment of cardiac structure and function in an integrated study.<sup>310, 321</sup> Typically cross-sectional images are acquired in the transverse plane at the location of interest, using a single breath-hold steady-state free precession (SSFP) technique that provides high temporal and spatial resolutions typically without respiratory motion artefacts. Phase contrast sequences have also been used although SSFP images appear to result in better inter-observer reproducibility.<sup>322</sup> Aortic contours are either manually drawn, segmented using semi-automated software or fully automated techniques, the latter techniques providing minimum and maximum cross-sectional area values for calculating the distensibility while avoiding the important inter-observer variation often associated with manual tracing.<sup>314, 323-326</sup>

Historically one of the difficulties in studying compliance has been the need for invasive monitoring, for example through cardiac catheterisation, to establish the

central pressure. In recent years the development of non-invasive devices, which use validated transfer functions to estimate aortic pressure, have been employed with some success. Peripheral waveform analysis with dedicated devices with an integrated invasively validated radial-to-aortic transfer function first enabled assessment of central systolic BP and are discussed further below. Although waveform analysis occurred at the wrist, typically these tonometric devices such as the SphygmoCor were calibrated against brachial BP, the fundamental assumption being that very little wave amplification takes place between the brachial and radial artery.<sup>327</sup> However, there is increasing evidence that this is not the case, which may significantly affect estimations of central pressure.<sup>328</sup> The Vicorder device is a commercially available non-invasive relatively operator independent device which determines brachial artery pressure waveforms using a volume displacement technique and central blood pressure via a previously described brachial to aortic transfer function.<sup>329</sup> Reliable estimates of central pressure have been demonstrated, where it was found to show better agreement and was highly correlated with invasive measures compared to the SphygmoCor.<sup>327</sup> It has the further advantage that measurements can be made simultaneously during the CMR image acquisition.

## Global assessment of aortic function

Global arterial stiffness is increasingly recognised as a surrogate for cardiovascular disease. Carotid-femoral pulse wave velocity (cfPWV) and Augmentation Index (AI) are commonly used methods for estimating global arterial stiffness.

## Pulse wave velocity (PWV)

PWV is calculated from measurements of pulse transit time and the distance travelled by the pulse between 2 recording sites ( $PWV = \text{Distance}/\text{transit time (TT)}$ ). Pulse wave velocity (PWV) has the advantage that it is a direct measurement of parameters which are strongly linked to wall stiffness and has been shown to be highly clinically relevant. It is associated with the presence of cardiovascular risk factors and atherosclerotic disease.<sup>330-332</sup> Aortic PWV has been shown to be an independent predictor of all cause and cardiovascular mortality in hypertensive and diabetic patients.<sup>197, 198</sup> Associations have also been found in well functioning older adults where in a cohort study 2488 participants that were followed up for 4.5 years there was a significant increase in relative risk of between 1.5-1.7 for total mortality and 2.1-3.0 for cardiovascular mortality in those patients in the upper quartiles of

PWV compared with the lower quartile.<sup>201</sup> As well as a predictor for fatal events, in other population studies it has also been shown to be a predictor of non-fatal cardiovascular events in the general population independent sex, age, BMI, MAP, smoking and alcohol intake, where for a 1SD increment in PWV the risk increased by 16-20%.<sup>202</sup> These associations continue to remain significant in later life; a longitudinal study of elderly patients recruited following a hospital admission has shown that PWV is a strong independent predictor of cardiovascular death in subjects aged 70-100 years.<sup>199</sup> Although numerous studies have given the general impression that PWV may have a predictive role in both cardiovascular and non-cardiovascular mortality endpoints many were within very contrasting populations, the sizes of which were diverse providing very dissimilar risk estimates and publication bias cannot be ruled out. The predictive value of pulse wave velocity has however been the subject of a systematic review and metanalysis which has demonstrated a stepwise increase in the relative risk of clinical events from the first to third tertile of aortic PWV and has estimated that a 1m/s increase corresponds to a 14-15% increase in total cardiovascular events and cardiovascular and all cause mortality.<sup>297</sup>

### **Measurement of PWV**

There is no universal agreement as to which particular technique or device is optimal. It is however generally agreed that external factors impact on pulse wave velocity and as a consequence recommendations exist to standardise conditions (the control of room temperature, the timing of measurements, the avoidance of caffeine and alcohol for 3 and 10 hours respectively and the maintenance of consistent position (supine recommended) for all measurements.<sup>333</sup>

### **Non-invasive bedside techniques**

A number of devices exist for the “bed-side” estimation of PWV and if the aforementioned external factors are controlled, variability in measurements remains between the devices and is dependent on: i) the site of measurement, ii) the algorithm used for timing of the pressure wave transit (TT) and iii) the method employed for calculating path length.

### **Site of measurement**

Pulse wave velocity may be a surrogate marker of plaque burden or arterial calcification.<sup>334, 335</sup> Studies have looked at its predictive value and it is clear that the site of measurement is important. In end-stage renal disease whereas the upper and

lower limb PWV have no predictive value, the aorto-iliac pathway measured via carotid-femoral PWV is a predictor of cardiovascular and all cause mortality<sup>336, 337</sup>. It is the carotid-femoral PWV (cfPWV) that is thought to be the most clinically relevant and robust measurement. Studies have confirmed cfPWV to be an independent predictor of coronary artery disease in hypertensives and diabetics as well as the general population including the elderly and it is at present considered the gold standard.<sup>197-202, 297, 338</sup>

### Measurement of transit time

The TT is the time delay of a waveform between two pulse points. Originally it was not clear which part of the pressure wave should be used as the point of reference. Options included the point of minimum diastolic pressure, the first systolic peak (the point at which the first derivative of pressure is maximum), the late systolic peak (the point at which the second derivative of pressure is maximum) and the foot of the wave (the point yielded by the intersecting tangent to the initial systolic upstroke of the pressure tracing and a horizontal line through the minimum point). The latter model, known as the “intersecting tangent model” is considered to be the most reproducible and there are theoretical reasons why this is likely to be the case; the foot of the wave is least likely to be influenced by distortion of the pressure waveform during its forward propagation through the arterial tree attributable, for example, to pressure wave reflections.<sup>339</sup>

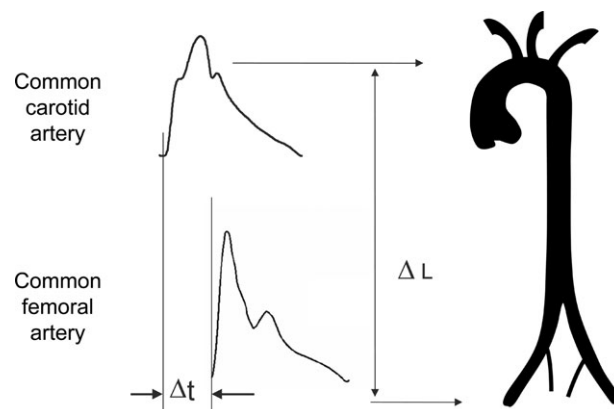


**Figure 6 Measurement of carotid-femoral PWV with the foot to foot method.** (reproduced with permission from the European Society of Cardiology © Eur Heart J. 2006; 27(21): 2588-605; Laurent S, Cockcroft J, Van Bortel L, Boutouyrie P, Giannattasio C, Hayoz D, et al<sup>338</sup>).

Currently available devices differ significantly with respect to measuring the TT. The Complior® device uses pressure transducers for simultaneous recording of the carotid and femoral pulses that then use a correlation algorithm between each simultaneously recorded wave to derive the transit time. The SphygmoCor (AtCor

Medical, USA) device uses a tonometric transducer in a two-step process recording the pressure waves sequentially. It then calculates the transit time between the 2 arterial sites determined in relation to the R wave of the ECG. A limitation of this method is that since measurements are performed sequentially and compared through ECG-gating, error is introduced in the presence of a variable heart rate, and patients with arrhythmias such as atrial fibrillation are as a consequence very hard to assess. A third device, Vicorder (Skidmore Medical, UK) simultaneously records the pulse waveform at the carotid and femoral site using inflatable cuffs and an oscillometric signal, which is digitally analysed to extract the pulse time delay in real time.

These devices have been compared in head to head studies with some conflicting results. In comparisons between SphygmoCor and Complior®, Rajzer et al showed that differences in PWV between devices were as a result of path length rather than transit time measurements, whereas Millaseau et al demonstrated that the SphygmoCor device had significantly shorter transit times compared to the Complior® device, which ceased to be the case when the intersecting tangent model was applied to the Complior® data, suggesting that the algorithms were responsible for the disparity. In these studies and others Complior® device has been shown to both overestimate and underestimate PWV compared to the SphygmoCor.<sup>340-342</sup> Improved reproducibility has been demonstrated in a more recent study containing increased numbers of patients for both these devices.<sup>342-345</sup>

Hickson et al revealed significant differences in transit times between the SphygmoCor and Vicorder devices, although there was good overall linear agreement. Further analysis confirmed that the differences in transit times were not due to the algorithms but path length differences. There was a suggestion that at higher PWVs there is an inherent bias toward lower Vicorder PWV values compared to the SphygmoCor, which may be due to fixed stiffness to the extra segment of femoral artery included in the Vicorder measurement. Alternatively, a low signal-sampling rate could potentially cause larger errors in transit time. The difference in sampling rates between The Vicorder (556Hz) and the SphygmoCor (acquired at 128Hz and analysed at 1KHz) is unlikely to explain the inherent bias seen.<sup>346</sup> Of the other studies that have compared these devices Kracht et al showed good reproducibility with comparable values for both devices but were studying younger people with PWVs whose values were lower than those where bias was identified by Hickson et al.<sup>347</sup> A third study found the Vicorder to be less reproducible than the

SphygmoCor in a sample size of 30, with limits of agreement of -4.24 to 4.72 m/s and -1.53 to 1.71m/s and co-efficient of variations of 22% and 7% respectively.<sup>348</sup> At present no published data exist on the reproducibility of these measurements in COPD, where large intrathoracic pressure swings may have a considerable effect.<sup>349</sup>

### Measurement of path length

The path length is estimated using a tape measure or callipers over the body surface between the carotid and femoral measuring sites. Different strategies of measurement have been employed by different investigators which can significantly affect the value of cfPWV derived, in some cases by up to 30%.<sup>340, 350, 351</sup> Despite these discrepancies some studies fail to identify which method has been used.<sup>352</sup> The lack of standardisation extends to manufacturers who recommend the use of different derivations. The “direct measurement” (A), from carotid pulse site to femoral pulse site results in an overestimation of path length and therefore PWV.<sup>353</sup> Other methods include suprasternal notch-to-femoral site (B), suprasternal notch-to-femoral site minus suprasternal notch-to-carotid site (C), carotid-to-femoral site minus suprasternal notch-to-carotid site. Invasive studies have suggested that the use of suprasternal notch-to-femoral site minus suprasternal notch-to-carotid site to calculate the distance during non-invasive measurements gives the best agreement with invasive data and predicts mortality in certain populations, although the invasive measurement in question only measured the PWV within the aorta and therefore does not necessarily equate to the real cfPWV which includes any additive effect that may arise in the iliac and carotid vessels.<sup>353, 354</sup>

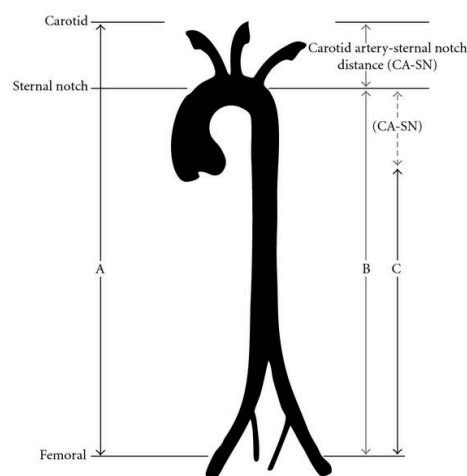


**Figure 7 Different measurement techniques for path length; A: direct method; B: suprasternal notch to femoral site; C: B - suprasternal notch to carotid site (reproduced with permission from the European Society of Cardiology © Eur Heart J. 2006; 27(21): 2588-605; Laurent S, Cockcroft J, Van Bortel L, Boutouyrie P, Giannattasio C, Hayoz D, et al)<sup>338</sup>.**



From a methodological point of view the precision of any particular measured distance is dependent on the accuracy of identifying the measurement site and the precision of the tape measure. For those techniques that involve 2 measurements the error is made twice, is cumulative, and in certain circumstances may be larger than the discrepancy between different path length techniques.<sup>351</sup> Furthermore, this study can only validate the specific device being tested (SphygmoCor) and further invasive studies are warranted involving different devices with the use of different path length measurements. Until such a time that this occurs, with the exception of the SphygmoCor device, it seems reasonable to follow the manufacturers recommendations for path length measurement. Despite this lack of standardisation, algorithms derived for the conversion of path length measurements has enabled the comparison and combination of values from different trials.<sup>251, 297, 351</sup>

### **Augmentation index: The assessment of wave reflections**

The arterial pressure waveform is created by a combination of the forward pressure wave created by ventricular contraction and reflected waves which are reflected in the periphery at branch points or sites of impedance mismatch. Whereas in elastic vessels with low PWV these reflected waves arrive in diastole, in stiff arteries the reflected wave may arrive in early systole, superimpose on the forward wave and boost systolic pressure (Figure 8). This phenomenon can be quantified through the augmentation index, defined as the difference between the first and second systolic peak, expressed as a percentage of the pulse pressure. Values of augmentation index are derived from a process called pulse wave analysis.<sup>338</sup> The nature of reflected waves in the periphery do not exactly mirror those centrally. Whereas in the upper limb the reflective wave returns between 90-130 ms after the initial systolic upstroke, in the aorta the later return of more distal reflections tend to result in the augmentation occurring after 150ms. It is however entirely impractical to use invasive techniques to assess central pressure waveforms in routine practice and the development of non-invasive devices which allow for measurement of arterial stiffness, including reliable and reproducible estimations of central pressures and augmentation index are therefore of significant scientific and clinical interest.

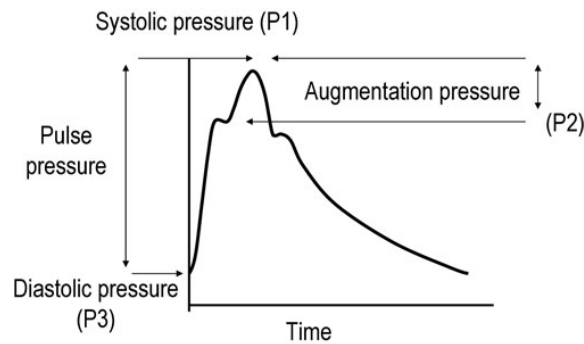


**Figure 8 Carotid pressure waveform as recorded by applanation tonometry.** The height of the late systolic peak (P1) above the inflection (P2) defines the augmentation pressure, and the ratio of augmentation pressure to PP defines the Alx (in percent). (reproduced with permission from the European Society of Cardiology © Eur Heart J. 2006; 27(21): 2588-605; Laurent S, Cockcroft J, Van Bortel L, Boutouyrie P, Giannattasio C, Hayoz D, et al<sup>338</sup>).

PWA studies have sought to estimate central aortic pulse wave morphology through the analysis of the radial artery waveform by applanation tonometry. Some have sought to estimate central pressures through the direct analysis of the radial artery morphology, through the temporal relationship to the aortic systolic peak and analysis of the late systolic shoulder. Although they provide reasonable estimates of central and pulse pressure they do not provide any information on central aortic augmentation index. Further limitations with these methods include the need for information on vessel diameter and significant inaccuracy in identifying the systolic shoulder when wave reflections are either very early, very late or when the pulse pressure is below 35 or above 85 mmHg.<sup>354</sup>

### Radial or brachial to aortic transfer functions

The employment of radial to aortic transfer functions, the mathematical process by which the central pulsatile phenomenon can be estimated from peripheral waveforms have been calculated for the radial artery and incorporated into commercial devices, although this was initially met with scepticism.<sup>355, 356</sup> Concerns included the accuracy of the transfer function and the fact that the original transfer function was based on invasive rather than non-invasive oscillometric estimations of blood pressure, while others argue that it is simply not possible to develop a single mathematical function that can accurately account for the many variables introduced by human variation and the impact of disease states.<sup>357-360</sup> Subsequent validation studies demonstrated that transfer functions do improve the fit between estimated and measured values by up to 96%.<sup>361</sup> Prospective validation studies showed that calculations of the aortic pressure wave (including augmentation) from the radial pressure wave agreed with measured aortic values to US Association for the Advancement of Medical

Instrumentation (AAMI) SP10 criteria.<sup>196</sup> Furthermore data presented to and accepted by regulatory bodies were obtained from over 600 subjects.<sup>362</sup>

As alluded to in the “measuring regional arterial stiffness” section (p61), it has recently been demonstrated that significant augmentation of the pulse wave occurs between the brachial and radial artery measuring points, which may result in inaccurate estimates of central pressure and augmentation index if radial artery readings are calibrated with brachial BP. Furthermore, the estimates obtained for central pressures are very dependent on which peripheral values are used for the calibration, no matter which device is used. Some devices such as the Vicorder partly overcome this by assessing the pulse wave at the level of the brachial artery. The classic calibration techniques employed by the commonly used SphygmoCor device have been shown to systematically underestimate central pressures compared to other commercially available devices which also employ transfer functions. These findings have been replicated by Pucci et al, who have recently shown that although when calibrated against invasive diastolic pressure the central systolic pressure estimates obtained fulfilled the standards set by the AAMI for non-invasive measures of blood pressure for both the Vicorder and SphygmoCor, this ceased to be the case when the devices were calibrated against non-invasive brachial measures of diastolic pressure. Of the devices measured, the Vicorder, which employs an oscillometric technique at the level of the brachial artery, was the most accurate. Weber et al have also confirmed the ability to measure the pulse wave and peripheral blood pressure with a brachial cuff on an alternative device to accurately estimate central blood pressure with the use of a transfer function.<sup>327, 328, 363, 364</sup>

Although employed, the use of the transfer function for the estimation of augmentation index is more challenging due to the dependency on higher frequency signals, where it has been shown the transfer function appears to be less accurate and to show greater between subject variability.<sup>196, 365</sup> Under-estimations of between 6 (+/-20) % and 7(+/-9) % compared to invasively measured central values have been demonstrated.<sup>361, 366</sup> Furthermore, many factors influence augmentation index, including the duration and pattern of ventricular ejection, exercise, time of day, age and medication.<sup>367-371</sup> It is estimated that for every 1 bpm increase in heart rate there is a 0.6% absolute decrease on augmentation index.<sup>372</sup> In population studies there appears to be a linear relationship between age and augmentation index up to approximately 60 years of age, where other factors such as changes to cardiac

output and LV ejection flow wave come into play.<sup>370, 373</sup> It is therefore important to standardise conditions as much as possible and when this strategy is employed the values obtained for augmentation index are reproducible in a number of different populations, with significant correlations between different devices and acceptable variation.<sup>342, 345</sup>

### **Predictive value of augmentation index**

Despite this variability the values obtained seem to have clinical relevance. Some longitudinal studies have shown AI to be a predictor of all cause and cardiovascular mortality and events in patients with coronary heart disease, end stage renal disease, and following cardiac intervention.<sup>200, 374-377</sup> Furthermore, a reduction in AI due to a reduction in the reflected wave, during therapeutic trials of hypertensive agents has resulted in favourable outcomes in both REASON (reduction in left ventricular mass) and CAFÉ (cardiovascular events).<sup>367, 378</sup> However, other studies including those with end-stage renal disease and elderly populations could find no independent association between augmentation index and cardiovascular endpoints.<sup>379, 380</sup> This topic has been subject to a recent systematic review and meta-analysis. There was significant heterogeneity amongst the studies for cardiovascular events but not total mortality. Overall there was a relative risk for an absolute increase of central augmentation index by 10% of 1.318 and 1.384 for total cardiovascular events and total mortality respectively which corresponded to a risk increase of 31.8% and 38.4%. These findings were independent of blood pressure and heart rate.<sup>381</sup>

## **Cardiac MRI**

Cardiovascular magnetic resonance (CMR) imaging has developed rapidly over the last two decades. CMR provides unparalleled image quality non-invasively, which is reflected in excellent accuracy and reproducibility. A major strength of CMR is the ability of multi-parametric imaging in one session. This versatility, the reproducibility and the non-invasiveness are key advantages of CMR over other advanced imaging modalities, such as echocardiography and cardiac CT.

## Cardiac volumes and function

Cardiovascular magnetic resonance (CMR) imaging is highly accurate and reproducible in measuring left ventricular (LV) volumes and mass and now established as the gold standard.<sup>382-384</sup> To this end, CMR is highly superior to 2D echocardiography, partly due to the excellent image quality, but very importantly due to the avoidance of geometric assumptions that may lead to inaccuracies. 3D echocardiography is a promising new modality, as it avoids geometric assumptions as well, but without echo contrast administration underestimates the LV volumes and sufficient image quality will not be achieved for both LV and RV.<sup>385</sup> This insufficient image quality may not be random, and thus may prevent acquisition of cardiac data in important subgroups of subjects (e.g. with chronic obstructive airways disease or obesity). Most importantly, 3D echocardiography has not got the capability of the multi-parametric approach, which makes CMR so powerful. For CMR, compared to cast volume displacement of the left ventricle, a correlation of 0.99 was found.<sup>386</sup> Inter-study reproducibility has been reported in the range of 5% for LV mass and volume parameters in single centre studies.<sup>387-390</sup> The accuracy and reproducibility of CMR in analysing cardiac volumes, function, and mass in heart failure compared to echocardiography allows for a substantial reduction in the number of patients needed in clinical trials.<sup>391</sup>

Left ventricular end-systolic volume is an important diagnostic and prognostic factor in heart disease.<sup>392</sup> Left ventricular hypertrophy and mass are powerful predictors of cardiovascular disease morbidity and mortality.<sup>393-396</sup> Both systolic and diastolic parameters can be derived from standard CMR cine volume studies, such as peak contraction and filling rates and time to peak contraction and filling rates.

LV ejection fraction is the most established endpoint in the medical community and has been extensively validated for diagnostic and prognostic purposes.<sup>397</sup> In the available consensus statements, EF is the only specified marker for the diagnosis and classification of heart failure, whereas for the RV this measure gets little mention, partly due to lack of validation in large multicentre trials and partly due to the variability of the measurements.<sup>398</sup> The shape of the RV is more complex than the LV and one cannot rely on one- or two-dimensional geometrical assumptions. Right ventricular volume and mass can be determined without geometric assumptions from the same CMR dataset used for the left ventricle and is considered the most accurate

and reproducible for RV assessment.<sup>399</sup> Many CMR publications found, as expected, similar left and right ventricular stroke volumes in healthy individuals but measurements remain more variable although still excellent given the complex shape of the RV.<sup>387, 400</sup> Caudron et al have looked at variability of measurements in acquired heart disease and found a number of factors contribute to the variability, including the observers' experience, choice of RV basal slice and processing time.<sup>401</sup>

## Tagging and other non-invasive measures of myocardial deformation

Assessment of myocardial regional wall motion plays a key role in many diagnostic and therapeutic decisions in current clinical practice. Regional wall motion quantification may be a powerful tool to detect sub-clinical cardiovascular disease. Semi-quantitative grading of regional wall motion is the most frequently applied technique, but it is highly subjective and has limited reproducibility. Tissue Doppler ultrasonography (US), strain imaging, and strain-rate imaging with echocardiography are highly dependent on transducer angulation and thus have inherent limitations in regard to complete three-dimensional myocardial coverage and reproducibility.<sup>402</sup>

Left ventricular strain measurement abnormalities detected by CMR have been demonstrated to be earlier and more sensitive markers of contractile dysfunction than global LV EF in hypertrophic and hypertensive cardiomyopathy and chemotherapy induced cardiotoxicity. Various techniques have been applied including displacement encoding with stimulated echoes and real-time myocardial strain encoding.<sup>403</sup> CMR tagging is currently considered the "reference" method for regional wall motion. It is used by a large number of centres and has been validated across different patient populations and showed good intra- and interobserver variability of both systolic and diastolic parameters in MESA.<sup>404-406</sup> Radiofrequency and gradient pulses are used to saturate lines in the myocardium in which the signal is destroyed, and the lines therefore appear black, in a process by the name of spatial modulation of magnetisation ("SPAMM"). The resultant tag-lines are used as non-invasive myocardial markers which are used to identify regional changes in deformation or strain during the cardiac cycle. The movement of these lines throughout the cardiac cycle can be analysed in a semi-automated way in order to calculate local myocardial strain, which can be derived in circumferential, radial or longitudinal directions. Limitations persist with this technique, including the loss of tag definition in diastole

as magnetisation recovers towards equilibrium. Efforts have been made to improve this with the use of complimentary SPAMM (CSPAMM). Other practical limitations exist including the need for further images to be acquired.

A novel–post processing technique called feature tracking has been developed which is a vector based analysis tool that uses a hierarchical algorithm to track in 2-dimensions certain myocardial voxel features on standard SSFP images, thus deriving measures of strain and velocity in a similar manner to speckle-tracking and negating the need for specialised tagged images (Figure 9).<sup>407</sup> A number of different parameters can be obtained directly or calculated from the raw data including endocardial velocity, which reflects the speed of the endocardium ( $\text{cm}\cdot\text{s}^{-1}$  for radial and longitudinal velocities and  $\text{deg}\cdot\text{s}^{-1}$  for circumferential velocities); strain, reflecting thickening/thinning in short-axis plane and shortening/lengthening in long-axis plane; endocardial strain rate, reflecting speed at which deformation occurs (measured in  $\text{deformation}\cdot\text{s}^{-1}$ ) and torsion, calculated by dividing the difference in absolute values of circumferential velocities of the basal and apical slice by their distance which reflecting the twist between the base and the apex of the LV.

Initial studies looked at global strain on individual short axis slices.<sup>408, 409</sup> It compared favourably with circumferential strain as measured by HARP in Duchene’s muscular dystrophy patients and has even allowed further clinical stratification that was otherwise may not have been possible.<sup>403</sup> Subsequent studies have looked at the segmental level where these non-invasive post-processing tools have been used to identify LV dyssynchrony through regional differences in radial strain, although other studies have found this parameter to be highly variable. At present it appears that circumferential strain is the most reproducible parameter with apical values tending to be the most variable for all types of strain measurement, a situation also noted with tagging.<sup>407</sup> An alternative algorithm has been developed for use on SSFP cine images which utilise a constrained deformable model.<sup>410</sup> At present there is no data available on its reproducibility.

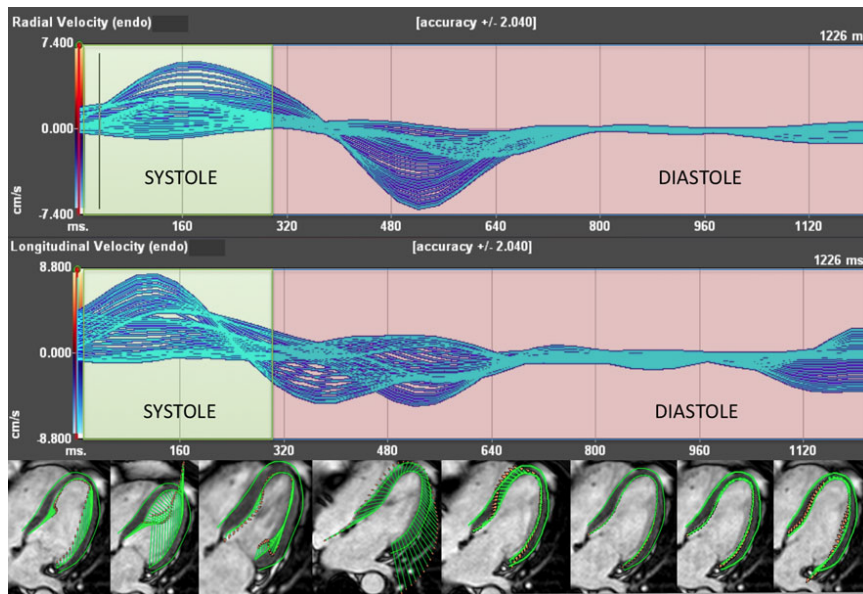


**Figure 9 Feature tracking analysis for radial and longitudinal velocities of the left ventricle.** The 48 blue lines represent tracking of the endocardial borders and the green vectors represent absolute values of the velocities.

## Imaging of pulmonary arteries

The imaging of the pulmonary outflow tract with CMR has been incorporated into the routine assessment and management of congenital heart disease and is being increasingly employed within the field of pulmonary vascular disease. Traditional methods within these fields have involved the use of invasive assessment through right heart catheterisation or non-invasive assessment with echocardiogram with its inherent limitations of inadequate acoustic windows, short ultrasound penetrating depth or insufficient tricuspid regurgitation to estimate pulmonary pressure, a situation which is noted in 10-25% of pulmonary hypertension patients.<sup>411 412</sup> The increasing number of conditions associated with pulmonary hypertension, including COPD, has led to an increased need for a less invasive assessment in the preliminary stages of the key endpoints that allow the close monitoring of those with less severe disease.<sup>413</sup>

## Pulmonary artery pulsatility

The highly distensible pulmonary artery plays a key role in dampening the pulsatile flow from the RV prior to its arrival at the capillary level.<sup>414</sup> This right ventricular–pulmonary artery coupling is essential for the preservation of right ventricular haemodynamics, and alterations in pulmonary artery compliance may result in



elevated RV pulsatile workload and reduced contractile performance as seen in pulmonary hypertension.<sup>415</sup> The changes in pulmonary artery compliance will precede any right ventricular remodelling that takes place and may represent a method by which early changes can be identified.

Compliance is defined as the absolute change in lumen area for a given change in pressure and direct measurement necessitates knowledge of pulmonary artery pressure which is mainly acquired through invasive monitoring with right heart catheterization, a procedure not without risk and which does not readily lend itself to screening or use in research.<sup>414</sup> Vessel wall stiffness (beta) can be calculated from the equation proposed by Hayashi et al and Kawasaki et al:<sup>416 417</sup>  $\beta = [\ln(PS/PD)] / (2\Delta A/A)$ , where PS/PD is the ratio to systolic and diastolic pressure and  $\Delta A/A$  is the relative cross-sectional area change. Previous research has shown that there is strong linear relation between systolic and diastolic pressure across a wide range of pulmonary artery pressures, thus implying that PS/PD is constant and  $\Delta A/A$  the relative area change or RAC is inversely proportional to the stiffness constant and represents pulmonary artery elasticity.<sup>418</sup> Given that the RAC (maxArea – minArea/min area) can be obtained non-invasively, CMR imaging therefore offers an attractive alternative by which non-invasive assessment may take place. RAC has been shown to be reduced in pulmonary hypertension and furthermore is a predictor of exercise capacity, mortality and predicts response to treatment in certain groups.<sup>415, 418-421</sup> Alterations in PA elasticity are observed in the course of the disease even before overt pressure alterations.<sup>414</sup> RAC has good sensitivity for the detection of early elevations in pulmonary vascular resistance (PVR), prior to the development of any RV abnormalities. Higher distending pressures therefore do not fully account for the increased stiffness suggesting a role of altered PA intrinsic elastic properties which may be particularly pertinent when considering pulmonary artery function in COPD. It is feasible that the postulated mechanisms that contribute to aortic stiffness, lung hyperinflation, neurohumoral activation and systemic inflammation<sup>422</sup>, may also be involved in pulmonary artery stiffening. One study has looked at pulmonary artery stiffness in COPD (SPAP 30  $\pm$  7.9) using echocardiography and has found stiffness to be increased compared to controls and related to NYHA functional class.<sup>423</sup> Limitations of this study was an incomplete data set due to poor acoustic windows, the method by which the RPA was measured was not by a standardised method with the potential for underestimation of area change due to oblique imaging or confusion with the superior wall of the left atrium.

## **Chapter 4:**

## **Methods**

## Ethics

All aspects of this thesis were conducted in accordance with the principles of the Declaration of Helsinki. The COPD and cardiovascular disease database study received a favourable ethical opinion from the NRES Committee London – South East (11/LO/0562). The Lung Deflation study (Eudract 2012-000927-42) received a favourable ethical opinion NRES Committee London – Chelsea (12/LO/0869). The HAPPY London study received a favourable ethical opinion from NRES Committee London Central (13/LO/0094).

## Patient selection

COPD patients were recruited from outpatient clinics at Bart's Health NHS Trust, via advertisement, from the affiliated University Cardio-Respiratory Research Centre and from local General Practitioners. The patients were identified by their primary care-provider.

Non-smoking and smoking controls for Chapter 5 were recruited from the HAPPY London cohort, an e-health cardiovascular primary prevention study for people with increased cardiovascular risk.

## Patient eligibility

The diagnosis of COPD was made according to published criteria:<sup>424</sup> A post bronchodilator FEV<sub>1</sub>/FVC ratio of <0.7 was required. Patients were over 40 years of age with at least 15 pack-year smoking history. For the lung deflation study further requirements included post bronchodilator FEV<sub>1</sub> of < 70%, evidence of lung hyperinflation (RVol ≥120 % predicted), demonstrating evidence of reversibility post bronchodilator of ≥ 7.5% predicted, and MRC score >1.

Patients were eligible to act as smoking control subjects if they were smokers with no history of underlying respiratory disease and no evidence of airflow obstruction or limitation on spirometry.

General exclusion criteria included the presence of significant respiratory problems other than COPD e.g. clinically significant bronchiectasis or fibrosis (a history of previous asthma was acceptable provided the predominant diagnosis is COPD) and if they were unable to undergo study procedures; in particular, if they had contraindications to CMR in the case of the MRI studies.

## Lung function measurements

All pulmonary function measurements were made after any cardiovascular assessments, after reliever therapies had been withheld for over 6 hours, refraining from exercising for 2 or more hours, smoking for 1 hour, exposure to cold air for 15 minutes and after refraining from drinks with high levels of caffeine such as tea and coffee.

### The measurement of lung volumes: Plethysmography

IC, SVC and TGV were measured before any other lung function measurements using whole body plethysmography (ZAN500, Germany) in a paired manoeuvre. Measurements were made as previously described in ATS/ERS guidelines.<sup>70</sup>

Briefly, body plethysmography, first described by DuBois in 1956, applies the principle of Boyle's Law which states at a constant temperature, the product of Pressure (P) and Volume (V) in a sealed vessel will be constant, ( $P_1V_1 = P_2V_2$ ). The plethysmograph contains a pneumatograph which allows measurement of airflow and transducers which measure the mouth and box pressure respectively. At the beginning of the test the subject has an unknown volume of gas in their chest. The subject is asked to breathe at their resting tidal volume. A shutter interrupts their breath and measures the mouth pressure at end expiration when, since there is no airflow, the pressure of the gas in the alveolus is known to be atmospheric. If his airway is then occluded so that no pulmonary gas can escape and he/she compresses the pulmonary gas through a voluntary respiratory manoeuvre, the pulmonary gas will have a new pressure and volume. The change in pulmonary gas pressure can be measured since mouth pressure equals alveolar pressure in a closed system. From knowledge of the original pulmonary gas pressure and of the change in pulmonary gas pressure and volume, the original volume of gas in the chest, the thoracic gas volume or TGV, can be calculated.<sup>425</sup> This is combined with IC and SVC values to calculate measures of lung hyperinflation (Box 1, Page 31).

### **Spirometry**

Three valid spirometry efforts were attempted (with no more than eight) using the ATS/ERS guidelines on automated pulmonary function testing equipment (CPL PFT, United States or Microlab 3500, Micromedical, UK).<sup>426</sup> Post bronchodilator-salbutamol FEV<sub>1</sub> and FVC were performed 15-20 minutes after the administration of 400mcg of salbutamol. Percentage predicted values were calculated according to NHANES III reference equations.<sup>427</sup>

### **Diffusion capacity**

TLCO is used to assess the gas-exchange ability of the lungs, specifically oxygenation of mixed venous blood. The most commonly used method is the single-breath method or breath-hold technique. The technique was performed on automated pulmonary function testing equipment (CPL PFT, United States) according to manufacturers' instructions and in accordance with ERS/ATS guidelines by a qualified respiratory physiologist with over 30 years experience.<sup>428</sup>

### **Bedside measurements of PWV and augmentation index**

All measurements were performed by a single investigator with 18 months experience in arterial stiffness measurements (IS). IS was blinded to all previous bedside measurements of arterial stiffness except in the Vicorder reproducibility study (chapter 5). The brachial blood pressure was used to calibrate both the Vicorder and SphygmoCor devices. In situations where both devices were employed (Vicorder Comparison Study; Chapter 5), the SphygmoCor measurements were performed first, followed by the Vicorder measurements.

All arterial stiffness measurements were in a temperature controlled room with the patient rested for 15 minutes in a supine position and awake. Patients were required to refrain from vasoactive medications for 2 hours, bronchodilator therapy for 6 hours, alcohol for 10 hours and smoking and caffeine for 3 hours prior to the measurements. Measurements were performed prior to CMR and lung function manoeuvres except during the estimation of central aortic pulse pressure while measuring aortic distensibility, which took place inside CMR scanner at the time of scanning. For those

measurements performed at the bedside, measurements were repeated 3 times and the mean value was derived.

## **Vicorder measurements**

### *Pulse wave velocity*

Measurements were obtained by placing a 10cm wide blood pressure cuff around the upper right thigh for measurement of the femoral pulse and a 3 cm wide partial cuff around the neck at the level of the carotid artery. The path-length was calculated according to manufacturers instructions, from the suprasternal notch to a defined point on the upper part of the femoral Cuff. The cuffs were inflated simultaneously to 65 mmHg and 2 high quality waveforms were simultaneously recorded for 3 seconds using a volume displacement method. The foot-to-foot transit time (TT) was measured as described previously and values for cfPWV were derived automatically.<sup>346</sup>

### *Pulse wave analysis*

Two brachial blood pressure readings were obtained using a manual sphygmomanometer used for calibrating peripheral waveforms and immediately afterwards a brachial pressure wave trace was digitally computed by the Vicorder with the cuff statically inflated to 70 mmHg using a volume displacement technique. A previously described brachial-to-aortic transfer function was then applied by the Vicorder software to calculate the waveform and values for central BP.<sup>329</sup> The first and second central systolic peaks were automatically identified by the software and used to calculate the augmentation index (difference in amplitude between first and second systolic peak/pulse pressure x 100).

## **SphygmoCor measurements**

### *Pulse wave velocity*

The SphygmoCor device (software version CvMS V9, Atcor Medical) employs applanation tonometry (Miller Instruments Inc. Houston TX, USA) to sequentially record ECG gated carotid and femoral artery waveforms. The system software calculated TT by the intersecting tangent method, using the R wave of a simultaneously recorded ECG as a reference frame. The path length was calculated according to the guidelines of the ARTERY society and manufacturers recommendation (supra-sternal notch to femoral artery recording site – suprasternal notch to carotid artery recording site) and the automated software derived the

cfPWV.<sup>429</sup>

### *Pulse wave analysis*

Two brachial blood pressure readings were obtained using a manual sphygmomanometer, used for calibrating radial artery waveforms, which were recorded using the same high-fidelity applanation tonometer described above. A previously validated radial-aortic transfer function was then automatically applied to the waveform to derive central BP.<sup>196</sup> The first and second central systolic peaks were automatically identified by the software and used to calculate the Augmentation index (difference in amplitude between first and second systolic peak/pulse pressure x 100).

## **CMR data acquisition**

### **CMR hardware**

CMR imaging was performed on a 1.5T CMR system (Achieva, Philips, Netherlands) using a Software release 3.2 and Cardiac package installed. The CMR machine has 32 receiver channels and a dedicated 32-channel cardiac coil. All subjects were asked to complete a separate safety consent form prior to the procedure on each occasion. This is a safety precaution to ensure that the patients have not been fitted with any ferromagnetic device.

### *CMR protocols*

CMR at 1.5T was performed for measurement of left and right ventricular volumes, function, mass and tagging, left atrial volumes and function and aortic and pulmonary artery distensibility. Black blood imaging was performed in the transverse, coronal and oblique sagittal planes (in the plane of the aorta).

### **Aortic sections, distensibility and total arterial compliance**

For the aorta sections planes were defined perpendicular to the thoracic aorta at the level of the pulmonary artery, and 10–14cm below this plane, immediately below the diaphragm at the level of the abdominal aorta. SSFP cine images were acquired at these image positions during end-expiration.

Peripheral blood pressure was measured using a MRI conditional oscillatory sphygmomanometer (Vicorder, Skidmore Medical, UK) and central blood pressure estimated using a validated transfer function used in calculating distensibility where

Distensibility (%/mmHg) = [(maximum Area– minimum Area)/PP x minimum Area] x 100.<sup>414</sup>

Minimum and maximum values were derived using an in-house validated automated endoluminal border-tracking programme written in MatLab (v.7.5). The section of interest (ascending, descending or abdominal aortic section) was selected and the centre of the lumen manually identified. The programme then tracks the endoluminal border through all phases of the cardiac cycle and calculates cross-sectional area for each phase. This is achieved by the radial detection of a signal change (thresholding technique) in comparison to a region of interest around the manually identified centre of the vessel. The automated detection was considered acceptable if within one pixel of where the investigator would have placed the contour.

Total arterial compliance (TAC) was calculated with the use of the central pulse pressure derived as described above and the stroke volume, described below:

TAC (ml/m<sup>2</sup>/mmHg) = Stroke volume Index / Central pulse pressure<sup>313</sup>

### **Pulmonary artery sections**

For the pulmonary artery sections, planes were defined perpendicularly to the main and also to right and left pulmonary arteries prior to any secondary branches and SSFP cine images were acquired at end expiration with a typical temporal resolution of 17 ms. For the purposes of this thesis no invasive monitoring of pulmonary artery pressures were performed and as such pulmonary artery distensibility or compliance could not be measured. However, pulsatility or relative area change (RAC) was measured and was calculated as follows:

Pulsatility (%) = (Maximum Area – Minimum Area) / Minimum Area x 100

The maximum and minimum areas were calculated as described above for the aortic sections.



### Ventricular volume, mass and function

Ventricular volumes and function data were acquired at 1.5 Tesla. After pilot imaging, a stack of 12 short axis SSFP cine slices was acquired from the atrio-ventricular groove to the cardiac apex, perpendicular to the ventricular long axes. Acquisitions were performed during held end-expiration, using retrospective electrocardiographic gating. Sequence settings were: echo time 1.44 ms, repetition time 2.9 ms, in-plane field of view 205x380 mm, acquired voxel size 1.9x2.04 mm (reconstructed to 1.46x1.48 mm), acquisition matrix 108x186 (frequency encoding x phase encoding), slice thickness 8 mm and a 2 mm gap between slices, 30 reconstructed frames per cardiac cycle (typical temporal resolution of 46 ms for a heart rate of 60 beats per minute), flip angle 60°.

7 mm slice thickness with 3mm slice gap has been validated for the LV volumes, ejection fraction and mass and has been shown to be comparable to 6mm thickness/4mm gap and 7mm thickness/no gap protocols and it reasonable to assume that 8mm with a 2mm gap is equally comparable.<sup>430-432</sup>

Left and right ventricular endocardial contours were manually segmented based on the short axis stack of cine images, at each slice position, at end-diastole and end-systole and summed for the whole ventricle using semi-automated software using CVI 42 (Circle Cardiovascular imaging Inc, Calgary, Canada). Basal slices were included in the LV segmentation if more than 50% of the lumen was surrounded by myocardium and a visual control of the short axis slice position on the 4-chamber view, as described previously. The identification of the basal slice within the RV is more challenging. Although some have advocated acquisition axial or perpendicular to the long axis of the RV, short-axis acquisitions have been chosen since it allows for assessment of ventricular wall morphology and function as well as being more validated.<sup>433-436,387</sup> Papillary muscles were included in the ventricular volume and excluded from the LV mass calculation.<sup>437, 438</sup> This segmentation was used to quantify left and right ventricular end-diastolic and end-systolic volumes, and to calculate ejection fraction, stroke volume and stroke volume difference. Epicardial contours were also manually segmented at end-diastole for the left ventricle. The final results represented the sum of the volumes for each individual slice based on Simpson's rule, while mass was derived from the myocardial volumes multiplied by the density of the myocardium (1.05g/ml). LV and RV parameters were indexed to body surface area (BSA) as determined by the Mosteller formula.<sup>439</sup>

### Atrial volumes and function

After pilot imaging, a stack of 14 to 16 short axis SSFP cine slices was acquired from the atrio-ventricular groove, perpendicular to the atrial long axis. Acquisitions were performed during held end-expiration, using retrospective electrocardiographic gating. Sequence settings were: echo time 1.4 ms, repetition time 2.8 ms, in-plane field of view 205x380 mm, acquired voxel size 1.9x2.04 mm (reconstructed to 1.46x1.48 mm), acquisition matrix 108x186 (frequency encoding x phase encoding), slice thickness 5 mm and a 0 mm gap between slices, 30 reconstructed frames per cardiac cycle (typical temporal resolution of 44 ms for a heart rate of 60 beats per minute), flip angle 60°. Left atrial endocardial contours were manually segmented based on the short axis stack of cine images, at each slice position, at end-diastole and end-systole using dedicated software, CVI 42 (Circle Cardiovascular imaging Inc., Calgary, Canada). This multiple slice method was the preferred option to the area length method, which leads to an underestimation of atrial volumes and overestimation of function in comparison.<sup>440</sup> Pulmonary veins were excluded at their ostia and the left atrial appendage was excluded at its base as described previously.<sup>441</sup> LA volume was automatically calculated from all the included slices. Slices were excluded in the segmentation if more than 50% of the lumen was surrounded by myocardium. This segmentation was used to quantify left atrial end-diastolic and end-systolic volumes, and to calculate the atrial ejection fraction (ejection fraction =  $100 \times (\text{EDV} - \text{ESV}) / \text{EDV}$ , where EDV is the end-diastolic and ESV the end-systolic volume.). Atrial parameters were indexed to body surface area (BSA) as determined by the Mosteller formula.<sup>439, 442</sup>

### Feature and tissue tracking

Feature tracking and tissue tracking analysis was performed using dedicated software (Image-Arena, Version 4.6, TomTec Imaging Systems GmbH, Unterschleissheim, Germany and CVI 42, Circle Cardiovascular imaging Inc, Calgary, Canada, respectively). Following uploading of the image the brightness is optimized to ensure optimal endocardial to blood pool discrimination. Both epi- and endocardial LV contours were drawn. All contours were tracked semi-automatically in all views. For a particular slice level, the first phase was used to draw a contour that was then automatically propagated by the software to all phases of the cardiac cycle for that slice. Manual image analysis correction was performed where the automated tracking visually seemed to be inaccurate. Poor tracking was considered

to be present when the movements of the points along the border deviated from the movement of the apparent endocardial border by more than 50% of the myocardial width, as described previously.<sup>407</sup> Tracking data were only saved when the contours seemed to be accurate. The 2- and 4-chamber views were used to determine all longitudinal parameters; radial parameters were derived from both short axis (SAX) and long axis views whereas circumferential values were derived from the SAX views. In the SAX views, three slices were analysed: basal, mid-ventricular and apical). The basal slice is identified as being the first slice without the presence of the outflow tract throughout the cardiac cycle. The mid-ventricular and apical slices were a further 2 cm and 4 cm respectively towards the apex.<sup>442</sup> Post-analysis processing in the case of feature tracking included averaging of the 48 (feature-tracking) software-created tracking points for each slice. In the case of tissue tracking the number of contour points depends on the length of the contour and varies from between 20-50 points. Unlike in feature tracking, these points are not directly used to calculate the strain values, rather inputted into the deformation model algorithm which calculates the values. The phase representing end-systole was identified by the smallest mid-ventricular volume. This allowed assessment of systolic and diastolic parameters separately.

## CSPAMM tagging

CSPAMM (complementary spatial modulation of magnetisation) imaging combines steady state free precession imaging with myocardial tagging as discussed above. 2D CSPAMM grid images (horizontal and vertical tags) were acquired at three levels (basal, mid-ventricular and apical), selected manually at the time of acquisition. The basal slice is identified as being the first slice without the presence of the out-flow tract throughout the cardiac cycle. The mid-ventricular and apical slices were a further 2 cm and 4cm respectively towards the apex.<sup>442</sup> Images were acquired in one slice per breath hold with good contrast to noise ratio such that the tag lines persisted throughout the cardiac cycle.<sup>443 444</sup> Typical parameters were as follows: Field of view 214 x 214 mm; reconstructed voxel size 1.11 x1.11 mm, echo time 11 ms, repetition time 25 ms, no parallel imaging, flip-angle 25°, maximum number of cardiac phases 33 (depending on heart rate) and a grid lines spacing of 7.5 mm in both horizontal and vertical directions. Each breath hold was typically 10-15 seconds. CIM Tag 2-D (v7.0, Auckland, NZ) post-processing tool was used to analyse the tagging acquisition as per manufacturers instructions (Auckland University Services, 2008).

## Statistical methods

### Descriptive statistics

Continuous parametric variables were expressed as means with standard deviations whereas non-parametric and categorical data as medians with interquartile ranges. The distribution of each variable was evaluated for symmetry using a histogram, and for normality using a normal plot.

### Parametric tests

Where all distributional assumptions necessary for the conduct of parametric tests were met, hypothesis testing for statistical significance was performed using independent samples two-tailed t-tests. T-tests were used in cases where a single observation was made in two groups. Where more than two sets of observations were made, the one-way analysis of variance (ANOVA) method was used. Where assumptions regarding equal variance between groups were violated, but data were otherwise suitable for parametric analysis, the Welch test (modified t-test for use with unequal variance) was used.

### Non-parametric tests

Where distributional assumptions necessary for the use of parametric tests were violated, non-parametric tests were used as follows: Mann-Whitney tests for independent samples; Wilcoxon matched pairs signed rank sum tests for paired samples; Kruskal-Wallis tests for more than 2 observations on the same individual. In all cases a (two-tailed) p value of  $<0.05$  was deemed statistically significant.

## Chapter Five:

# Reproducibility Of Arterial Stiffness And Wave Reflections In Chronic Obstructive Pulmonary Disease; The Contribution Of Lung Hyperinflation And A Comparison Of Techniques

This Chapter has been published in *Respiratory Medicine* Journal.

**Reproducibility of arterial stiffness and wave reflections in chronic obstructive pulmonary disease: The contribution of lung hyperinflation and a comparison of techniques.** Stone IS, John L, Petersen SE, Barnes NC. *Respir Med.*2013; **107**(11): 1700-8.

Dr Ian S Stone is the first author and designed the study, recruited the patients, analysed the data and drafted the manuscript.

## Abstract

**Introduction** Significant cardiovascular morbidity and mortality exists in chronic obstructive pulmonary disease (COPD). Arterial stiffness is raised in COPD and may be a mechanistic link. Non-invasive assessment of arterial stiffness has the potential to be a surrogate outcome measure, although no reproducibility data exists in COPD patients.

**Methods** Two studies (23 and 33 COPD patients) were undertaken to 1) assess the Vicorder reproducibility of carotid-femoral pulse wave velocity and Augmentation index in COPD; 2) compare it to SphygmoCor; and 3) assess the contribution of lung hyperinflation to measurement variability.

**Results** There were excellent correlations and good agreement between repeat Vicorder measurements for carotid-femoral pulse wave velocity ( $r=0.96$  ( $p<0.001$ ); mean difference  $\pm$ SD =  $-0.03\pm 0.36$ m/s ( $p=0.65$ ); co-efficient of reproducibility = 4.02%; limits of agreement =  $-0.68$ - $0.75$ m/s). Augmentation index significantly correlated ( $r=0.736$  ( $p<0.001$ ); mean difference  $\pm$ SD =  $0.72\pm 4.86$ % ( $p=0.48$ ), however limits of agreement were only 10.42-9.02%, with co-efficient of reproducibility of 27.93%. Comparing devices, Vicorder values were lower but there was satisfactory agreement. There was no correlation between lung hyperinflation (as measured by residual volume percent predicted, total lung capacity percent predicted or the ratio of inspiratory capacity to residual volume) and variability of measurements in either study.

**Conclusion** In COPD, measurement of carotid-femoral pulse wave velocity is highly reproducible, not affected by lung hyperinflation and suitable as a surrogate endpoint in research studies. Day-to-day variation in augmentation index highlights the importance of such studies prior to the planning and undertaking of clinical COPD research.

## Introduction

Significant cardiovascular morbidity and mortality exists in chronic obstructive pulmonary disease (COPD) which is independent of shared risk factors such as smoking.<sup>185</sup> Different mechanisms linking these two common conditions have been proposed, including arterial stiffness, a surrogate shown to be an independent predictor of cardiovascular disease in a number of other chronic inflammatory conditions.<sup>198, 203</sup> A spill over of inflammation from the pulmonary to the systemic circulation whose down-stream effects result in raised arterial stiffness could provide the mechanistic link between COPD and cardiovascular morbidity and mortality. Similarly neuro-humoral activation of the sympathetic nervous system as a result of lung hyperinflation may be a contributory factor.<sup>422</sup>

Carotid-femoral pulse wave velocity (cfPWV) and Augmentation Index (AI) are non-invasive measures by which arterial stiffness can be measured. The arterial pressure wave is formed by a composite of ventricular contraction and a reflected wave that arrives back early in stiff arteries, adding to the forward wave, augmenting systolic pressure and forming the second systolic peak. This phenomenon can be quantified as the AI, defined as the difference between the 2 systolic peaks expressed as a percentage of the pulse pressure. It is derived from pulse wave analysis (PWA) where peripheral artery waveforms are acquired and validated transfer functions are used to derive values of the Aortic AI. cfPWV is estimated by measuring the transit time of the pulse wave between two pulse points.<sup>338</sup>

A number of commercial devices exist for arterial stiffness measurement although at present no consensus exists as to which is the most accurate or reproducible. A novel relatively operator-independent device is now available which has potential advantages for screening programmes and use in intervention studies. It has compared favourably with the more established SphygmoCor device, considered by some to be the gold standard, in normal individuals, and those undergoing routine angiography.<sup>327, 346</sup> Although CfPWV has been found to be raised in COPD and related to disease severity and other studies report on pulse wave analysis (PWA), no data exist on the reproducibility of these devices in COPD patients, who due to their lung hyperinflation may have large intra-thoracic pressure swings with potentially significant breath-to-breath variation in the pulse wave. Such information is integral to the design and powering of longitudinal intervention studies.<sup>226, 227, 445</sup>

The aim of this study was: 1) To assess the reproducibility of the Vicorder Device in measuring cfPWV and AI in COPD patients; 2) to compare the measurements with those of the SphygmoCor device in a second separate cohort of COPD patients and; 3) assess the contribution of hyperinflation to the reproducibility of arterial stiffness measurements.

## Methods

### Patients

Patients were prospectively enrolled between October 2011 and August 2012. All patients were over 40 years of age, with a smoking history of at least 15 pack-years, and spirometric evidence of COPD according to ATS/ERS criteria. They were clinically stable with no history or recent exacerbations or long-term oxygen therapy use. Demographic data and a full medical and therapeutic history were collected on all participants. Furthermore, lung function (spirometry and body plethysmograph) was performed in all participants. For the Vicorder reproducibility study 23 consecutive patients had repeat measurements of cfPWV and PWA performed within 2 weeks of each other. For the comparison study with SphygmoCor a separate cohort of 33 consecutive COPD patients had cfPWV and PWA measurements performed on the same day with both devices. No patients in the Vicorder reproducibility cohort were included in the comparison study cohort. The study received a favourable review by the local research ethics committee and written informed consent was obtained from all patients.

### Measurement techniques

All measurements were performed by a single investigator with 18 months experience in arterial stiffness measurements (IS). IS was blinded to the previous results in the Vicorder reproducibility study (VRS) but not the Vicorder Comparison Study (VCS) since measures were collected on the same day for the latter study. Vicorder and SphygmoCor measurements of PWV and PWA and pulmonary function testing were performed as described in the Methods (Chapter 4).



## Statistical analysis

Statistical analysis was performed using SPSS 21.0 for Mac (SPSS Inc., Chicago, Illinois, USA). The distribution of the data was assessed visually. Continuous variables were expressed as mean $\pm$ SD for parametric variables and median (interquartile range) for non-parametric variables. Agreement between repeated Vicorder values in the case of the VRS, and SphygmoCor and Vicorder values in the case of the VCS for both cfPWV and AI were analysed with a student's paired t-test with further analysis performed using Bland-Altman Plots.<sup>446</sup> Pearson's correlation co-efficient was used to assess the strength of correlation between these values as well as the contribution of hyperinflation to the variability of PWV and AI. All analyses were 2 sided and a probability of less than 0.05 was considered significant.

## Results

### Vicorder reproducibility study

Demographic parameters for VRS are shown in Table 3. Haemodynamic parameters for both VRS visits are shown in Table 4. Good quality waveforms were available for all 23 patients. There was a strong significant correlation between repeat Vicorder measurements with respect to cfPWV ( $r=0.96$   $p<0.001$ ). The mean difference  $\pm$  SD between repeated cfPWV measurements was  $-0.03 \pm 0.36$  m/s ( $p= 0.65$ ) with a coefficient of reproducibility (COR) of 4.02 % and limits of agreement (LOA) of  $-0.68$ - $0.75$  m/s (Figure 10). Repeat path length and pulse transit time measurements were similar and strongly correlated with CORs of 3.6% and 4.77% respectively (Table 5). The repeat AI measurements were also strongly and significantly correlated ( $r=0.736$   $p<0.001$ ) with mean difference  $\pm$ SD of  $0.72 \pm 4.86\%$  ( $p = 0.48$ ), however LOA were only  $-10.42$  -  $9.02$  %, with COR of 27.93 % (Figure 11).

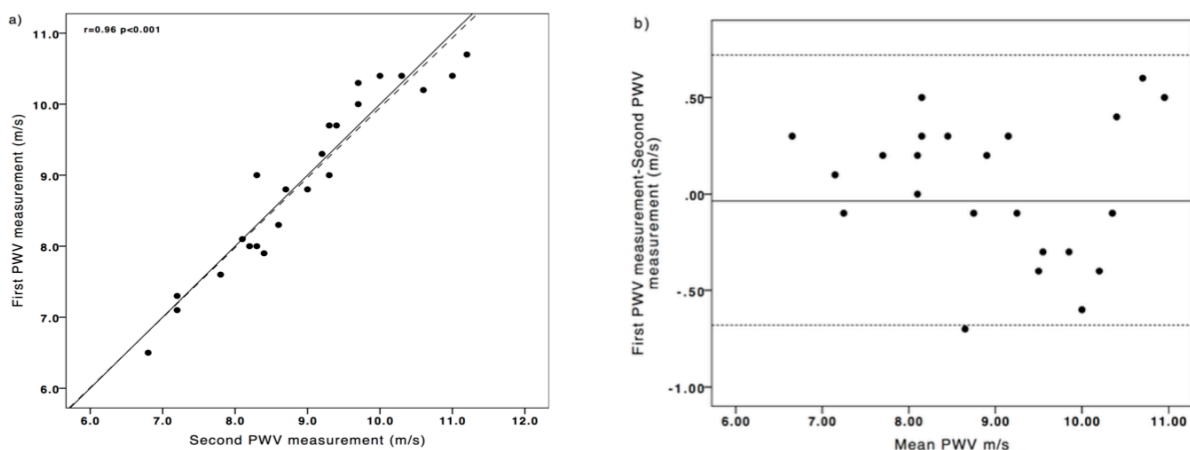


**Figure 10 a) Scatterplot of repeat Vicorder pulse wave velocity measurements.** Solid line: line of equality; dotted line: linear regression line. **b) Bland-Altman plot of the differences between repeat Vicorder pulse wave velocity measurements.** Solid line: mean value; dotted lines: Limits of Agreement (mean  $\pm$  2SD). PWV: pulse wave velocity

**Table 3: Demographic characteristics for Vicorder reproducibility study and Vicorder comparison study**

	<b>VRS Mean<math>\pm</math>SD or Median (25-75%)</b>	<b>VCS Mean<math>\pm</math>SD</b>
<b>Number of participants</b>	<b>23</b>	<b>33</b>
<b>Age (years)</b>	65.9 $\pm$ 7.9	67.5 $\pm$ 8.2
<b>FEV1%</b>	50.1 $\pm$ 18.9	52.9 $\pm$ 19.0
<b>FEV/FVC</b>	45.9 $\pm$ 15.4	45.6 $\pm$ 13.2
<b>RVol%</b>	163.9 $\pm$ 52.8	157.5 $\pm$ 47.7
<b>TLC%</b>	113.7 $\pm$ 22.6	116.2 $\pm$ 39.2
<b>IC/TLC</b>	33.4 $\pm$ 12.2	33.5 $\pm$ 9.4
<b>BMI (kg/m<sup>2</sup>)</b>	25.9 $\pm$ 5.8	25.0 $\pm$ 8.7
<b>Pack year history</b>	50(40-120)	56.9 $\pm$ 38.1
<b>Current smoker</b>	4/23	5/33
<b>Males: females</b>	12:11	19:14
<b>Statin</b>	12/23	15/33
<b>Aspirin</b>	8/23	8/33
<b>Anti-hypertensive</b>	11/23	13/33
<b>ICS</b>	1/23	3/33
<b>SABA</b>	22/23	27/33
<b>LABA</b>	1/23	2/33
<b>ICS/LABA</b>	19/23	20/33
<b>LAMA</b>	21/23	26/33
<b>Methylxanthines</b>	3/23	6/33

VRS: Vicorder reproducibility study; VCS: Vicorder comparison study; FEV1%: forced expiratory volume in one second per cent predicted of normal value; FEV/FVC: ratio of the forced expiratory volume/forced vital capacity; RVol%: residual volume per cent predicted of normal value; IC/TLC: ratio of inspiratory capacity to total lung capacity; TLC%: total lung capacity per cent predicted of normal value; BMI: body mass index; SBP: systolic blood pressure; DBP: diastolic blood pressure; ICS: inhaled corticosteroid; SABA: short-acting beta-agonist; LABA: long-acting beta-agonist; LAMA: long-acting muscarinic antagonist

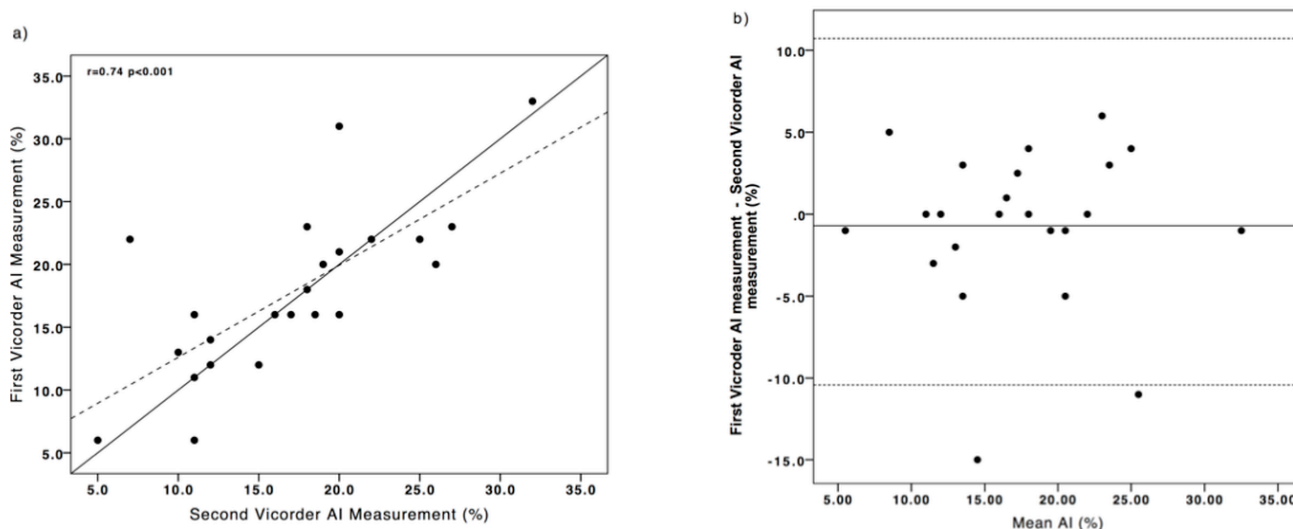


**Figure 11 a) Scatterplot of repeat Vicorder augmentation index measurements.** Solid line: line of equality; dotted line: linear regression line. **b) Bland-Altman plot of the differences between repeat Vicorder augmentation index measurements.** Solid line: mean value; dotted lines: Limits of Agreement (mean  $\pm$  2SD). AI: Augmentation index.

### Vicorder comparison study

Demographic parameters and haemodynamic parameters for VCS are shown in Table 3 and Table 4 respectively. Good quality waveforms were achieved for AI, however, 3 patients were unable to record SphygmoCor cfPWV readings due to a variable heart rate. There were statistically significant differences in the mean differences of cfPWV and AI between devices. Path length and pulse transit time differences were also significantly different between devices although strongly correlated (Table 5). The Vicorder device recorded lower values of both cfPWV and AI readings (mean difference  $\pm$  SD  $-0.64 \pm 1.00$  m/s  $p=0.002$  and mean difference  $\pm$  SD  $-4.53 \pm 7.8$   $p=0.002$ , respectively). There was, however, a strong linear relationship between Vicorder and SphygmoCor for cfPWV ( $r=0.76$   $P<0.001$ ) and AI ( $r=0.56$ ,  $p=0.01$ ) and Bland-Altman plots confirmed satisfactory agreement (Figure 12 and Figure 13).

### The contribution of lung hyperinflation to reproducibility

In order to assess the contribution of lung hyperinflation to the reproducibility of arterial stiffness correlations were performed between RVol%, TLC% and IC/TLC and the difference between repeated measurements of AI and PWV. There was no significant correlation between the extent of lung hyperinflation and the variability of PWV or AI measurements in either the VRS or VCS (Table 6).

**Table 4 Haemodynamic parameters for the Vicorder reproducibility study and comparison study**

	VRS		VCS	
N	23		33	
	Visit 1	Visit 2	Vicorder	SphygmoCor
Heart Rate (beats/min)	72.6 ± 11.5	73.1 ± 10.2	74.1 ± 11.6	75.3 ± 11.8
Brachial SBP (mmHg)	138.5 ± 13.9	136.8 ± 15.8	129.1 ± 16.5	
Brachial DBP (mmHg)	75.6 ± 6.3	74.3 ± 8.1	69.6 ± 11.7	
MAP (mmHg)	102.0 ± 9.0	101.3 ± 10.2	90 ± 11.3	
Central SBP (mmHg)	130.9 ± 13.7	130.8 ± 14.5	119.2 ± 24.7	115.9 ± 15.2
Central DBP (mmHg)	75.0 ± 6.9	74.1 ± 7.5	69.5 ± 10.9	70.6 ± 11.7
PWV (m/s)	8.94 ± 1.23	8.97 ± 1.19	8.93 ± 1.3	9.5 ± 1.5
AI (%)	17.8 ± 6.7	17.1 ± 6.7	21.9 ± 8.1	26.5 ± 8.6

VRS: Vicorder reproducibility study; VCS: Vicorder comparison study; SBP; systolic blood pressure; DBP: diastolic blood pressure; MAP: mean arterial blood pressure; PWV; pulse wave velocity; AI: augmentation index

**Table 5 Mean transit time and path length data**

Vicorder reproducibility study				
	Visit 1 Mean ± SD	Visit 2 Mean ± SD	Mean Difference ±SD	Correlation
Path length (cm)	66.4 ± 5.5	66.7 ± 5.0	0.3 ± 2.4 (p=0.61)	0.90 (p<0.001)
Transit time (ms)	77.1 ± 11.9	76.2 ± 11.0	0.96 ± 3.7 (p=0.23)	0.95 (p<0.001)
Vicorder comparison study				
	Vicorder Mean ± SD	SphygmoCor Mean ± SD	Mean Difference ±SD	Correlation
Path length (cm)	66.6 ± 5.3	47.9 ± 4.0	18.8 ± 3.7 (p<0.001)	0.72 (p<0.001)
Transit time (ms)	75.7 ± 11.4	50.6 ± 8.5	25.1 ± 9.0 (p<0.001)	0.63 (p=0.01)

SD: standard deviation

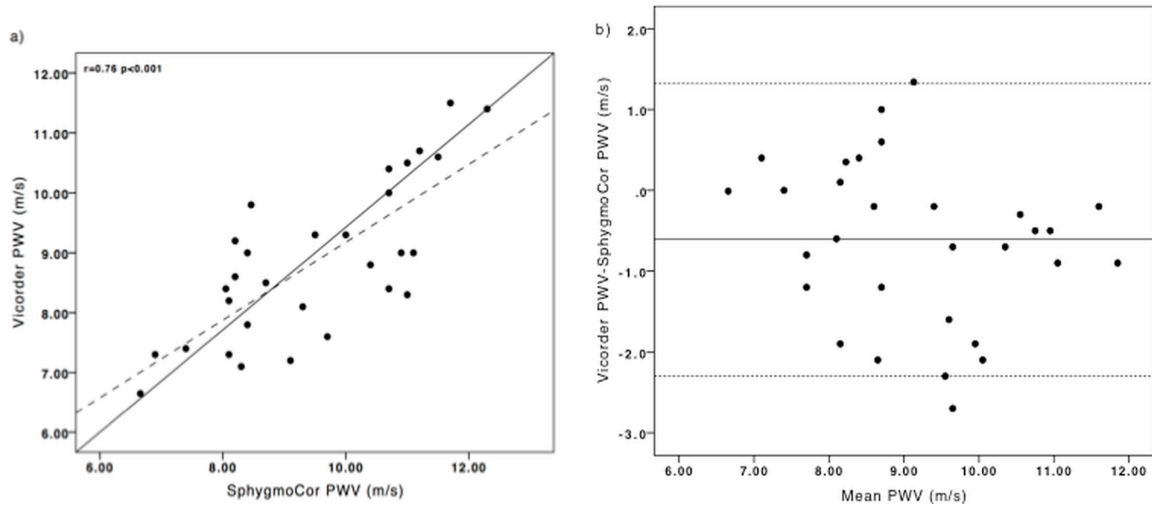


**Figure 12 a) Scatterplot of Vicorder and SphygmoCor pulse wave velocity.** Solid line: line of equality; dotted line: linear regression line. **b) Bland-Altman plot of the differences between Vicorder and SphygmoCor pulse wave velocity.** Solid line: mean value; dotted lines: Limits of Agreement (mean  $\pm$  2SD). PWV: pulse wave velocity.

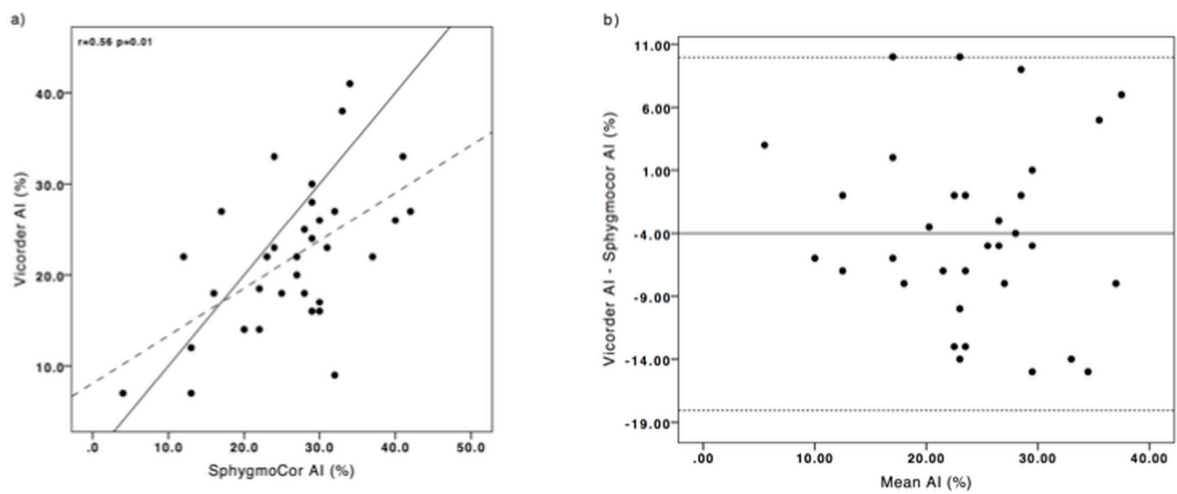


**Figure 13 a) Scatterplot of Vicorder and SphygmoCor augmentation index.** Solid line: line of equality; dotted line: linear regression line. **b) Bland-Altman plot of the differences between Vicorder and SphygmoCor augmentation index.** Solid line: mean value; dotted lines: Limits of Agreement (mean  $\pm$  2SD). PWV: pulse wave velocity; AI: Augmentation index

**Table 6 Correlation between measures of lung hyperinflation and the variability of repeat AI and PWV measurements in the Vicorder reproducibility study and the Vicorder comparison study**

		Difference between repeat haemodynamic measurements			
		Vicorder reproducibility study		Vicorder comparison study	
		AI	PWV	AI	PWV
<b>Measures of lung hyperinflation</b>	<b>RVol%</b>	0.34 (p = 0.12)	0.20 (p = 0.36)	0.10 (p = 0.61)	0.22 (p = 0.25)
	<b>TLC%</b>	0.21 (p = 0.35)	0.16 (p = 0.47)	-0.092 (p = 0.63)	0.11 (p = 0.59)
	<b>IC/TLC</b>	- 0.158 (p = 0.48)	- 0.32 (p = 0.15)	0.11 (p = 0.58)	-0.34 (p = 0.08)

AI: augmentation index; PWV: pulse wave velocity; RVol%: residual volume per cent predicted of normal value; IC/TLC; ratio of inspiratory capacity to total lung capacity; TLC%; total lung capacity per cent predicted of normal value

## Discussion

The contribution of arterial stiffness to the cardiovascular morbidity in COPD is a topic of considerable interest<sup>422, 445</sup>. This is the first study to report reproducibility of Vicorder measures of arterial stiffness and, furthermore, how they compare to SphygmoCor measurements in patients with COPD. The main finding of our study is that PWV measured by the Vicorder device is highly reproducible in COPD patients. The Vicorder reproducibility achieved in this study for PWV is better than some other published results including those in children and studies employing different commercially available devices.<sup>344, 347, 348, 447</sup> The second finding is that the reproducibility of PWV or Augmentation index does not appear to be affected by lung hyperinflation and thirdly, although significant statistical differences exist between the Vicorder and SphygmoCor devices the Bland-Altman plot showed satisfactory agreement and the values showed good linear agreement in this COPD cohort.

It is generally agreed that external factors impact on pulse wave velocity. A potential limitation of this study is that we are unable to gauge the impact of changes in

oxygenation, known to affect PWV and AI, since blood gas sampling was not performed.<sup>448</sup> However, efforts had been made to minimise its occurrence through the recruitment of only clinically stable patients who did not require any form of oxygen therapy as well as the implementation of existing recommendations to standardise conditions.<sup>333</sup> The value derived for PWV is also known to depend on the site of measurement, the algorithm used for timing of the pressure wave transit (TT) and the method employed for calculating path length.

The predictive value of PWV is dependent on the site of measurement. In end-stage renal disease whereas the upper and lower limb PWV have no predictive value, the aorto-iliac pathway measured via carotid-femoral PWV is a predictor of cardiovascular and all cause mortality.<sup>336, 337</sup> It is the carotid-femoral PWV (cfPWV) that is thought to be the most clinically relevant and robust measurement and it has been shown to be an independent predictor of coronary artery disease in the general population including the elderly and it is at present considered the gold standard.<sup>199, 201, 297, 338</sup> In line with the ARTERY society guidelines, both studies contained within this manuscript exclusively measured cfPWV.<sup>429</sup>

The impact of the algorithm used to calculate the transit time has been investigated with different commercially available devices with conflicting results, some attributing differences to the algorithm whereas others identify path length measurements as the main driver for differences between devices. This however is the first study to look at the contribution of lung hyperinflation to measurement variability.<sup>340, 341</sup> Lung hyperinflation can be defined according to the residual volume with RVol% >120 considered abnormal. The patients enrolled in the two studies had had a substantial degree of lung hyperinflation, with mean RVol% values of 163.9 % and 157.5 % respectively, but no significant correlation between the extent of lung hyperinflation and variability of arterial stiffness measurements was identified in either of the 2 studies regardless of which parameter for measuring lung hyperinflation was adopted (RVol, TLC or IC/TLC). Hence our results are closely aligned with other studies that compare Vicorder and SphygmoCor, demonstrating that methodological differences in the measurement of path length are contributing to the differences seen in PWV values between these two devices, although significant differences were demonstrated there was good linear agreement between devices, and there was a bias towards lower values with the Vicorder.<sup>346, 449</sup>

Measurement of the path length can result in a disparity between values derived for PWV of up to 30%.<sup>350</sup> We have shown that the path length is also the main driver for the variability of PWV measurements in both studies. In the VRS the COR for path length accounts for most of the variability seen in pulse transit time. In the VCS the situation is further complicated by different manufacturers recommending different methodologies to calculate the path length, as seen with the Vicorder and SphygmoCor devices. From a methodological perspective the precision of any particular measured distance is dependent on the accuracy of identifying the measurement site and the precision of the tape measure. For those techniques that involve 2 measurements, as in the case of the SphygmoCor, the error is made twice, is cumulative, and in certain circumstances may be larger than the discrepancy between different path length techniques.<sup>351</sup> It is currently not clear which path length is the most appropriate or which device is the more accurate since validation of pulse wave velocity with invasive studies has proven difficult, a problem acknowledged by the published guidelines on validation of haemodynamic non-invasive measurement devices.<sup>429</sup> The difficulty arises since the invasive measure chosen typically equates to the PWV within the aorta and does not take into account the additive effect that may arise from the iliac and carotid vessels.<sup>353, 450</sup> This lack of a comparable invasive measure for PWV as well as AI is a resultant limitation of this study. Screening tools to establish whether a subject has raised arterial stiffness require agreed normal ranges and a device which is both accurate and reproducible. Although there have been developments in this field, until an agreed methodology for path length measurements and further validation studies are available it seems the most likely use of PWV will be in assessing the impact of particular interventions within clinical trials.<sup>251</sup> In this setting accuracy is arguably less important than reproducibility; it not only impacts on the sample size but the mean bias, derived from such measures, is important for trial comparison in the context of systematic reviews and meta-analyses. Reproducibility of a particular test is therefore paramount, and the Vicorder device has shown itself to be a highly plausible option in COPD studies looking to utilise cfPWV as a surrogate endpoint.

Augmentation index is a measure of the augmentation of central blood pressure in systole by reflected pressure waves from the small peripheral arteries.<sup>338</sup> It is dependent on ventricular ejection, the timing of reflected waves (and hence PWV) and the extent of reflection (determined by arterial tone). In the VRS although the Bland-Altman plot showed reasonable agreement and the SD of differences were similar to previously published studies of different devices, the larger LOA and COV



associated with AI and resultant loss of statistical power would require far larger sample sizes to demonstrate any significant treatment effects.<sup>344</sup> However a limitation of this study is that the repeat measurements were not performed on the same day for the VRS which, given the number of factors that contribute to augmentation, may have resulted in the differences observed. The notion is supported by a study in chronic kidney disease that looked at day to day variations in AI which showed even greater variability in measures with a mean difference (SD) of 2.6 (5.6).<sup>345</sup> Furthermore, validation studies, which are more feasible for PWA due to the relative ease of acquiring invasive central blood pressures, have demonstrated that the Vicorder device is accurate. Vicorder measures of central blood pressure, estimated using the same transfer function as AI, showed better agreement with invasive measures than the SphygmoCor and was highly correlated to the invasive measure.<sup>327</sup> Despite this, in COPD the utility of AI in the elderly remains in question; although Janner et al showed a significant association between AI and COPD this was only for males less than 60 years of age once mild cases had been excluded.<sup>451</sup>

In conclusion, this study highlights the highly reproducible nature of Vicorder PWV measurements in COPD patients, including those with lung hyperinflation, which offers a feasible alternative to traditional tonometry techniques that is ideally suited for use as a surrogate marker in intervention studies. The wide day-to-day variation in repeat AI measurements highlights the importance of such calculations prior to the planning and undertaking of clinical research in COPD.

## **Chapter Six**

# **Feature Tracking, Tissue Tracking And Tagging Assessment Of Myocardial Function In Stable Hyperinflated COPD: A Validation Study**

## Abstract

**Introduction** Alterations to cardiovascular structure and function occur in COPD often with preservation of the ejection fraction. Global measures such as EF may not be sensitive enough to detect subtle changes in ventricular function. Myocardial strain imaging, a non-invasive measure of cardiac deformation, can identify subtle changes in myocardial function although reproducibility in COPD has not previously been assessed. The aims of this study were to establish inter-study reproducibility of myocardial tagging and newer CMR strain-imaging techniques in COPD patients and, secondly, to establish the extent of inherent bias between the newer techniques and the “gold standard” in the most reproducible parameters.

**Methods** This study utilised the CMR scans of the 45 hyperinflated COPD patients randomised into the clinical trial detailed in Chapter 8. The trial took place from November 2012 to August 2014. Tagging, feature tracking (FT) and tissue tracking (TT) analysis was undertaken on the baseline CMR and the scan following the placebo period.

**Results** All 40 who completed the placebo arm of the study were included in the analysis. The inter-study reproducibility for global measures of tagging, FT and TT ranged from an ICC 0.002-0.659, 0.012-0.56 and 0.253-0.593, respectively. Circumferential strain was the most consistent and Bland-Altman plots confirmed acceptable agreement. FT-derived circumferential strain rate was consistent for diastolic parameters with moderate agreement (ICC 0.57). Diastolic parameters for longitudinal strain rate showed moderate agreement with best results in the 4-chamber view (ICC 0.641). The best agreement with tagging was found with mid-ventricular circumferential strain (FT mean difference  $+1.07 \pm 3.17$  %; ICC 0.402; 95% CI 0.11, 0.63; TT mean difference  $-2.17 \pm 2.23$  %; ICC 0.424; 95 % CI 0.132, 0.649). Bland Altman plots confirmed acceptable agreement. Acceptable agreement was found between FT and tagging for the diastolic parameter of mid-ventricular peak circumferential strain rate (ICC 0.581 95% CI 0.33, 0.76)

**Conclusion** The inter-study reproducibility of feature tracking and tissue tracking are comparable to tagging. The assessment of intrinsic diastolic function in hyperinflated COPD shows promise. The data we have provided here will allow for accurate powering of future COPD studies which may in turn allow a better understanding of the natural history of cardiac disease in COPD.

## Introduction

Alterations to cardiovascular structure and function occur in COPD often with preservation of the ejection fraction (Chapter 7). It is however well recognised that global measures such as EF may not be sensitive enough to detect subtle changes in ventricular function.<sup>105, 405</sup>

Strain is a sensitive measure of cardiac deformation. It can be measured non-invasively through the use of advanced imaging techniques and is therefore attractive for use in clinical trials to assess the effect of an intervention. Echocardiographic Doppler imaging has its own inherent limitations of operator dependency, noise interference, angle dependency and the use of geometric assumptions.<sup>452-454</sup> Speckle tracking has difficulties related to image quality, which is worsened by the poor echocardiographic windows secondary to lung hyperinflation in COPD.<sup>455, 456</sup> The development of cardiac magnetic resonance imaging based strain analysis is therefore a particularly attractive option in this cohort.

Tagging, the present 'gold standard' for CMR systolic strain imaging, is not without its limitations and has never been validated in COPD. Low signal to noise ratio, tag fading and the need for prolonged breath holds are of particular concern when considering the assessment of diastole in a dyspnoeic population such as COPD. Furthermore, it requires further image acquisitions, thus increases scanning time and requires complex and laborious post-processing. A number of commercially available systems have a number of advantages over the 'gold standard'. Before they can be applied to clinical trial settings, an understanding of the inter-study reproducibility in patients with COPD is necessary.

The aims of this study were to establish the inter-study reproducibility of myocardial tagging and newer CMR strain-imaging techniques in COPD patients with evidence of lung hyperinflation to inform the powering of future studies and, secondly, to establish the extent of inherent bias between the newer techniques and the "gold standard" in the most reproducible parameters.

## Methods

### Study population

This study utilised the CMR scans of the 45 hyperinflated COPD patients randomised into the clinical trial detailed in Chapter 8. The trial took place from November 2012 to August 2014.

### Image acquisition

The details regarding SSFP and myocardial tagging image acquisition can be found in the Methods section (Chapter 4). All images were acquired by ISS on the same scanner between 0800-1300 hrs. Due to the nature of the crossover study design the time interval between baseline and placebo-period scans varied from 1 - 4 weeks.

### Image analysis

Details regarding the performing of the strain and strain rate analysis for tagging (CIM Tag 2-D v7.0, Auckland, NZ), tissue tracking (CVI 42, Circle Cardiovascular Imaging Inc., Calgary, Canada) and feature tracking (Image-Arena, Version 4.6, TomTec Imaging Systems GmbH, Unterschleissheim) can be found in the Methods section (Chapter 4). Offline analysis of the tagged and SSFP scans were performed by one blinded observer in a random order (ISS - 2 years experience), on all scans. Scans were excluded from the analysis if post-processing software was unable to track the myocardium. A schematic representation of how peak and reverse peak strain and strain rate values are derived can be found in Figure 14.

For tissue tracking and tagging, global (transmural) strain and strain rate values were used. For feature tracking, the means of the extracted endocardial and epicardial values were derived for circumferential and longitudinal strain and strain rates. The feature tracking output includes the transmural radial strain and strain rate values since radial strain is a representation of myocardial thickening and thinning and thus requires both endocardial and epicardial data for its calculation.

### Statistics

Statistical analysis was performed using R 3.2.1 (R Foundation for statistical Computing, Vienna, Austria) and SPSS 21.0 for Mac (SPSS Inc., Chicago, Illinois, USA).<sup>457</sup> The distribution of the data was assessed visually. Continuous variables

were expressed as mean ( $\pm$ SD) for parametric variables and median (interquartile range) for non-parametric variables. Baseline and placebo period scans were compared to assess the inter-study reproducibility of tagging, tissue tracking and feature tracking. Baseline imaging was used to assess the extent of inherent bias between the different modalities. The differences in strain variables between 2 exams were represented by mean difference and standard deviation of the mean difference. Agreement was assessed through the intra-class correlation co-efficient (ICC) with a model of absolute agreement. Agreement was classed as weak (ICC 0.10 - 0.39), moderate (ICC 0.40-0.69) or strong (ICC 0.70-0.99).<sup>458</sup> Bland-Altman analysis was performed to visualise agreement and measurement error between studies.<sup>446</sup>

## Results

Of the 45 patients randomised in the original study, the 40 who completed baseline and placebo assessments were included in the analysis. Whilst 11 baseline and 7 placebo images of the 200 acquired could not be analysed due to poor image quality for tagging, all images were of sufficient quality from feature tracking and tissue tracking. For their full demographic characteristics please refer to Table 7.

### Inter-study reproducibility

For full breakdown of the results please refer to the supplementary appendix (pages 157, 159, 161, 163).

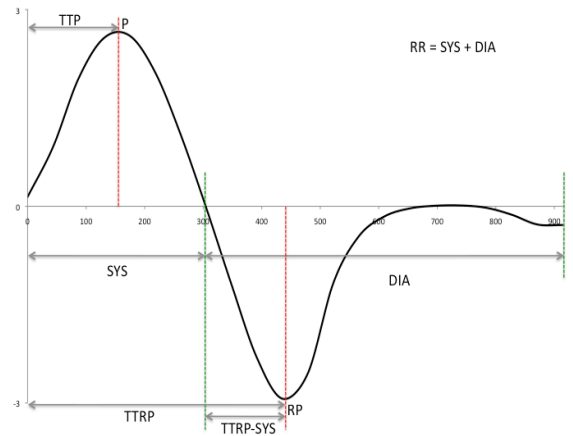
### Tagging

Overall the inter-study reproducibility for global measures of tagging ranged from an ICC of 0.002 to 0.659 with radial strain being the least reproducible and mid-ventricular circumferential strain having the highest reproducibility. The Bland-Altman plots confirm acceptable agreement between measurements (Figure 15). For longitudinal strain the 2-chamber was more reproducible than the 4-chamber with moderate agreement.

All measures of systolic strain rate performed poorly apart from mid-ventricular circumferential strain rate (ICC 0.430; 95% CI 0.116, 0.667) and the 4-chamber longitudinal reverse peak strain-rate (ICC 0.377 95% CI 0.03, 0.645).

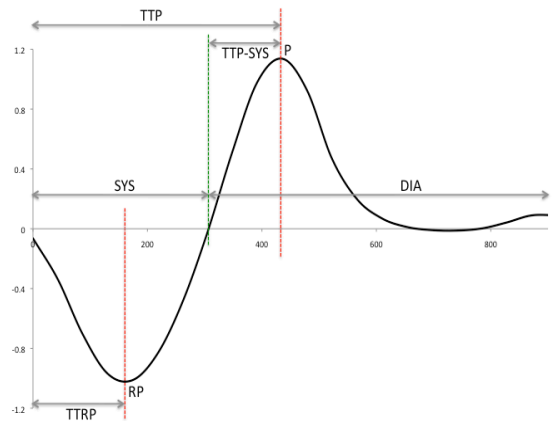
### 1. Parameters with peak before reverse peak

Parameters with strain rate curves of this morphology have systolic peaks and diastolic reverse peaks e.g. radial strain rate:



### 2. Parameters with reverse peak before peak

Parameters with strain rate curves of this morphology have systolic reverse peaks and diastolic peaks e.g. circumferential and longitudinal strain rate



### 3. Parameters with reverse peak only

Parameters with strain curves of this morphology have reverse peaks only e.g. circumferential and longitudinal Strain.

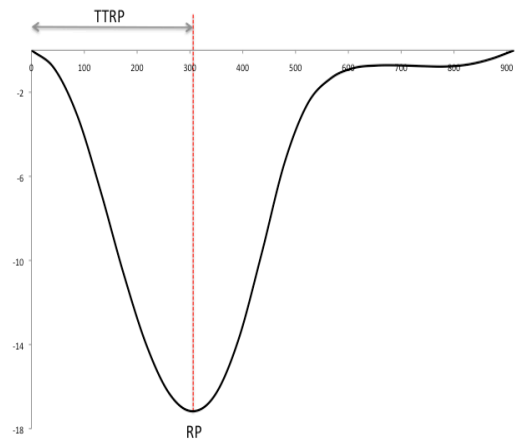


**Figure 14 A schematic diagram explaining the derivation of parameters for strain and strain rate analysis.** SYS: systole; DIA: Diastole; P: peak; RP: reverse peak; TTRP: time to reverse peak; TTP: time to peak. In this analysis we have only utilized peak and reverse peak.

**Table 7 Baseline demographics**

No of subjects	40
Age, years	64.8±9.1
Male, %	65%
COPD assessment Test Score	17.5±8.6
Smoking, Pack years	48.3±31.3
Forced Expiratory Volume in 1 second, L	1.4±0.5
FEV1 per cent predicted, %	49.7±15.5
Residual Volume, L	3.7±0.9
Residual Volume per cent predicted, %	164.9±33.8
Pulse, beats/min	73±12
Left Ventricular Mass Index, g/m <sup>2</sup>	95.3±25.3
Left Ventricle End Diastolic Volume Index, ml/m <sup>2</sup>	66.1±12.9
Left Ventricle End Stroke Volume Index, ml/m <sup>2</sup>	27.0±8.0
Left Ventricle Ejection Fraction, %	59.7±6.6

Circumferential strain rate also performed best within the diastolic parameters (mid-ventricular peak circumferential strain rate ICC 0.673 (95% CI 0.44, 0.822). Mid-ventricular reverse peak radial strain rate was the only reproducible radial parameter from the tagging analysis (ICC 0.596, 95% CI 0.331,0.775). The diastolic longitudinal strain rate parameter performed best in the 2-chamber view (ICC 0.727, 95% CI 0.504, 0.859).

#### **Feature tracking**

Overall the inter-study reproducibility for global measures of feature tracking ranged from an ICC 0.012 to 0.56. Circumferential strain was the most consistent (ICC 0.51-0.56). The Bland-Altman plots confirm acceptable agreement between measurements (Figure 15). Although more reproducible than tagging, the radial strain was variable with best results in mid-ventricular (ICC 0.451) and 4-chamber views (ICC 0.443). For global longitudinal strain, the 4-chamber gave better results than the 2-chamber (ICC 0.419 vs. 0.378).



Table 8 Inter-study reproducibility of global, systolic and diastolic end-points for tagging, feature tracking and tissue tracking.

Variable	Tagging				Feature tracking				Tissue tracking			
	Mean	Mean diff (SD)	LoA	ICC (95% CI)	Mean	Mean diff (SD)	LoA	ICC (95% CI)	Mean	Mean diff (SD)	LoA	ICC (95% CI)
Global parameters												
Mid-ventricular reverse peak circumferential strain, %	-16.41	0.13 (2.56)	-5.00, 4.73	0.659 (0.42, 0.813)	-17.23	0.75 (4.03)	- 6.90, 8.39	0.531 (0.269, 0.721)	-13.97	0.80 (2.59)	-4.13, 5.72	0.546 (0.281, 0.734)
Mid-ventricular peak radial strain, %	35.71	6.12 (15.58)	-35.72, 23.49	0.321 (-0.011, 0.59)	37.57	-4.32 (14.91)	-32.66, 24.02	0.451 (0.168, 0.665)	22.55	-2.03 (5.11)	-11.73, 7.68	0.541 (0.274, 0.731)
2-chamber reverse peak longitudinal strain, %	-12.39	-0.81 (3.00)	-6.51, 4.90	0.396 (0.052, 0.657)	-14.41	0.43 (4.69)	-8.48, 9.34	0.378 (0.082, 0.614)	-14.14	0.11 (2.45)	-4.54, 4.77	0.51 (0.235, 0.711)
4-chamber reverse peak longitudinal strain, %	-13.65	0.64 (3.21)	-5.45, 6.73	0.337 (-0.016, 0.617)	-12.39	0.28 (5.32)	-10.38, 9.83	0.419 (0.13, 0.643)	-14.56	0.75 (2.83)	-4.63, 6.13	0.253 (-0.066, 0.525)
Systolic parameters												
Mid-ventricular reverse peak circumferential strain rate, %/s	-83.79	-2.91 (16.16)	-33.61, 27.79	0.430 (0.116, 0.667)	-110.53	7.97 (27.85)	-44.95, 60.89	0.467 (0.189, 0.677)	-97.56	-18.23 (152.51)	-308.01, 271.56	-0.049 (-0.357, 0.270)
Basal reverse peak circumferential strain rate, %/s	-74.00	-4.29 (14.68)	-32.19, 23.60	0.453 (0.144, 0.683)	-109.22	2.99 (27.62)	-49.48, 55.47	0.526 (0.262, 0.717)	-168.06	21.54 (50.21)	-73.87, 116.95	0.597 (0.349, 0.768)
Basal peak radial strain rate, %/s	328.73	-114.02 (465.97)	-999.36, 771.32	0.054 (-0.282, 0.380)	165.15	-8.23 (63.62)	-129.11, 112.65	0.277 (-0.032, 0.538)	294.69	-41.91 (129.02)	-287.05, 203.23	0.492 (0.211, 0.698)
2-chamber reverse peak longitudinal	-70.45	-6.25 (17.83)	-40.14, 27.63	0.284 (-0.074, 0.570)	-94.15	4.05 (32.51)	-57.71, 65.82	0.315 (0.01, 0.567)	-91.09	2.48 (28.78)	-52.20, 57.16	0.368 (0.062, 0.612)

strain rate, %/s												
4-chamber reverse peak longitudinal strain rate, %/s	-77.43	0.18 (15.95)	-30.12, 30.49	0.377 (0.03, 0.645)	82.10	-3.77 (41.91)	-83.41, 75.86	0.195 (-0.118, 0.473)	-125.36	19.98 (61.23)	-96.37, 136.32	0.291 (-0.025, 0.555)
Diastolic parameters												
Mid-ventricular peak circumferential strain rate, %/s	75.67	-3.81 (21.83)	-45.30, 37.68	0.673 (0.44, 0.82)	87.71	-0.17 (27.53)	-52.48, 52.13	0.57 (0.321, 0.747)	96.90	16.19 (149.56)	-267.97, 300.35	0.064 (-0.254, 0.372)
Basal peak circumferential strain rate, %/s	68.71	-2.68 (18.35)	-37.54, 32.18	0.588 (0.320, 0.77)	103.12	-8.53 (32.54)	-70.35, 53.30	0.549 (0.293, 0.733)	136.90	-16.04 (46.71)	-104.78, 72.70	0.644 (0.414, 0.797)
Mid-ventricular reverse peak radial strain rate, %/s	-195.20	3.69 (74.48)	-137.82, 145.20	0.596 (0.331, 0.775)	-149.69	1.78 (44.15)	-82.11, 85.67	0.604 (0.366, 0.769)	-136.83	1.22 (53.57)	100.56, 103.01	0.363 (0.056, 0.608)
basal reverse peak radial strain rate, %/s	-339.49	138.94 (614.47)	-1028.55, 1306.42	0.010 (0.322, 0.341)	-140.56	9.60 (54.81)	-94.53, 113.73	0.291 (-0.016, 0.549)	-264.78	40.18 (130.54)	-207.85, 288.20	0.579 (0.324, 0.756)
2-chamber peak longitudinal strain rate, %/s	56.45	- 1.08 (14.71)	-29.02, 26.86	0.727 (0.504, 0.859)	83.42	-7.76 (31.00)	-66.65, 51.14	0.405 (0.114, 0.633)	98.32	-16.34 (35.84)	-84.44, 51.76	0.322 (0.009, 0.578)
4-chamber peak longitudinal strain rate, %/s	62.61	3.45 (20.24)	-35.00, 41.90	0.486 (0.162, 0.716)	84.30	-4.04 (31.24)	-63.40, 55.31	0.641 (0.416, 0.792)	113.91	-17.79 (60.21)	-132.19, 96.60	0.242 (-0.078, 0.517)

CI: confidence interval; Diff: difference; ICC: intra-class correlation co-efficient; LoA: limits of agreement; SD: standard deviation.

Circumferential strain rate was consistent for systolic parameters, showing moderate agreement. Peak radial strain rate remained variable, with best results in 4-chamber (ICC 0.437). Systolic measures of longitudinal strain performed poorly.

Circumferential strain rate was consistent for diastolic parameters with moderate agreement. Unlike systolic strain rate the diastolic short axis radial strain performed better, with best results in mid-ventricle (ICC 0.604). Diastolic parameters for longitudinal strain rate showed moderate agreement with best results in the 4-chamber view (ICC 0.641).

### *Tissue tracking*

Overall tissue tracking inter-study reproducibility for global measures ranged from an ICC of 0.253 to 0.593. Circumferential strain was the most consistent (ICC 0.523-0.593). The Bland-Altman plots confirm acceptable agreement between measurements (Figure 15). Radial strain performed best in mid-ventricular slice (ICC 0.541) and 2-chamber views (ICC 0.593). For global longitudinal strain the 2-chamber gave better results than the 4-chamber, with moderate agreement.

Systolic parameters generally performed poorly for circumferential and radial strain rate except the basal slice in short axis (0.597 and 0.492 respectively). In the long axis the 2-chamber view was most reproducible for systolic radial strain rate (ICC 0.542) and longitudinal strain rate parameters (ICC 0.368).

Tissue tracking diastolic parameters also performed poorly apart from the short axis basal slice for radial (0.579) and circumferential strain rate (0.644). The 2-chamber outperformed the 4-chamber for both longitudinal and radial strain rate diastolic parameters.

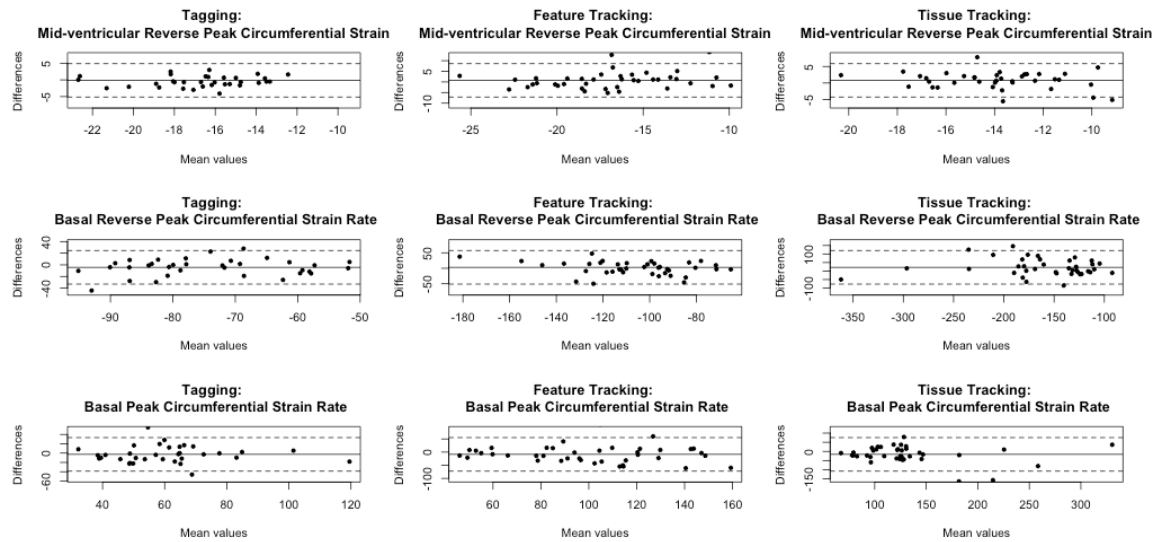


**Figure 15 Bland-Altman plots showing inter-study reproducibility for global, systolic and diastolic strain and strain rate parameters derived from tagging, feature tracking and tissue tracking analysis.** Units: Strain parameters %; Strain Rate %/s. Global parameters in top panel; systolic parameters in middle panel and diastolic parameters in bottom panel.

### Comparing techniques: Inherent bias

The global value of mid ventricular circumferential strain showed the best agreement between techniques with a mean difference of  $+1.07 \pm 3.17$  % for feature tracking and  $-2.17 \pm 2.23$  % for tissue tracking. Bland Altman plots confirmed acceptable agreement and a significant moderate interclass correlation was confirmed statistically (Table 9).

There was also acceptable agreement for the diastolic parameter of mid-ventricular peak circumferential strain rate (Figure 16). The mean difference was  $-4.06 \pm 26.3$  %/s for feature tracking and  $-22.69 \pm 32.86$  %/s for tissue tracking. The inter-class correlation was statistically significant for feature tracking (ICC 0.581; 95% CI 0.33, 0.76) but only of borderline significance for tissue tracking (ICC 0.264; 95% CI -0.049, 0.531).

Overall no significant ICC was found between tagging values of radial strain and strain rate and those derived from feature tracking or tissue tracking.

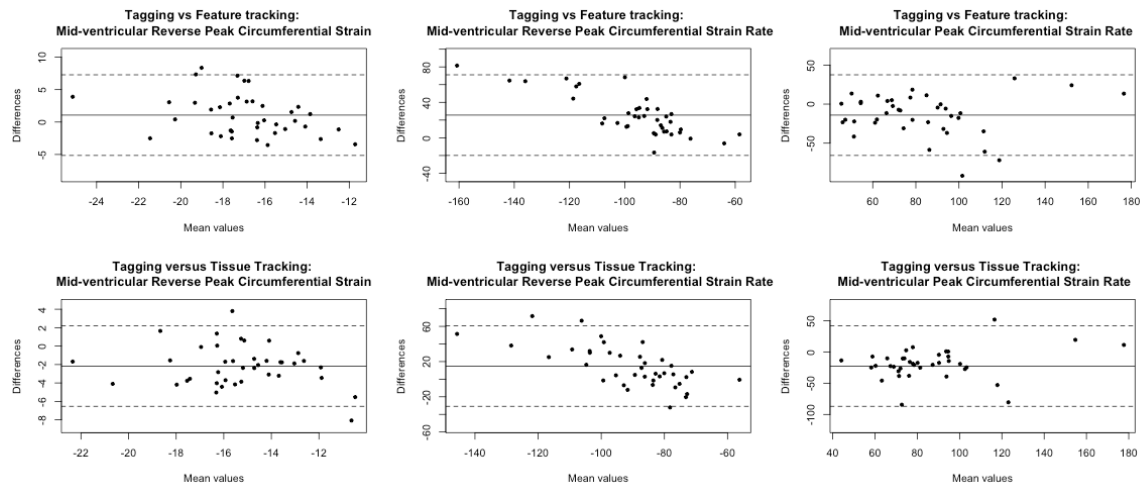


**Figure 16 Bland-Altman plots showing extent of agreement between feature tracking and tissue tracking versus tagging for mid-ventricular global strain (%) and diastolic and systolic strain rate (%/s) measurements.**

## Discussion

This is the first study to demonstrate the inter-study reproducibility of CMR-derived strain and strain-rate parameters in COPD patients with lung hyperinflation and the extent of inherent bias compared to the current CMR gold standard of myocardial tagging.

We have demonstrated that both feature tracking and tissue tracking demonstrate similar degrees of inter-study reproducibility compared to tagging, with circumferential values being the most consistently reproducible. We have also demonstrated that acceptable agreement exists with those values derived from myocardial tagging in the circumferential but not radial direction; and furthermore feature tracking appears to be a legitimate option for assessing diastolic function in hyperinflated COPD.

As per previously published data, the inter-study reproducibility measured in this COPD cohort demonstrates moderate ICC.<sup>459</sup> Factors that affect the reproducibility of CMR strain imaging include the strength of the magnetic field, image acquisition, image orientation, slice location and quality of tags.<sup>460</sup> In an effort to avoid this variability, studies were obtained at the same site, on the same scanner with the use

Table 9: Agreement between different strain measurement techniques. SD; standard deviation: ICC; interclass correlation co-efficient: CI; confidence interval

Variable, units	Tagging	Feature tracking					Tissue tracking				
	Mean Value	Mean difference	SD	Limits of Agreement	ICC	95% CI	Mean difference	SD	Limits of Agreement	ICC	95% CI
Global											
Mid-ventricular reverse peak circumferential strain, %	-16.41	1.07	3.17	-4.95, 7.09	0.402	0.11, 0.63	-2.17	2.23	-6.41, 2.07	0.424	0.132, 0.649
Mid-ventricular peak radial strain, %	35.71	-2.34	23.52	-47.016, 42.34	-0.022	-0.33, 0.29	12.93	17.27	-19.89, 45.74	-0.215	-0.492, 0.102
2-chamber reverse peak longitudinal strain, %	-12.39	1.77	3.87	-5.58, 9.12	0.175	-0.16, 0.47	1.67	2.70	-3.46, 6.81	0.215	-0.114, 0.503
Systolic											
Mid-ventricular reverse peak circumferential strain rate, %/s	-83.79	25.60	23.20	-18.49, 69.70	0.142	-0.18, 0.43	14.85	23.36	-29.53, 59.23	0.234	-0.082, 0.508
2-chamber reverse peak longitudinal strain rate %/s	-70.45	19.82	26.81	-31.11, 70.76	-0.031	-0.35, 0.30	20.64	24.64	-26.17, 67.46	0.210	-0.12, 0.499
Diastolic											
Mid-ventricular peak circumferential strain rate, %/s	75.67	-14.06	26.33	-64.10, 35.96	0.581	0.33, 0.76	-22.69	32.86	-85.12, 39.74	0.264	-0.049, 0.531
Mid-ventricular reverse peak radial strain rate, %/s	-195.20	-44.18	97.44	-229.33, 140.97	-0.066	-0.37, 0.25	-57.05	89.95	-227.95, 113.88	-0.102	-0.399, 0.216
2-chamber peak longitudinal strain rate, %/s	56.45	-25.94	30.26	-83.43, 31.55	0.146	-0.185, 0.448	-40.67	30.93	-99.44, 18.10	0.020	-3.04, 0.34

of standardised prospectively gated protocols and imaging protocols for the selection of the short-axis slices performed by the same technician (IS). In the case of feature tracking and tissue tracking analysis, these were performed on the same images, whereas the tagging images were acquired at the same sitting. In an effort to mirror a real life scenario, in all cases the technician was blinded to the previously chosen slices.

The differences in strain reproducibility can be explained by myocardial geometry. Strain accuracy is related to the number of tags or points of interest in a particular segment. Since more points of interest are contained within a segment's arc than its radius, circumferential strain, particularly at the level of the mid-ventricle is more reproducible than radial strain, a situation echoed in previous studies.<sup>460-462</sup> The reduced circumferential strain reproducibility at the base in both feature tracking and tagging may be a result of the relative increase in through plane motion typically observed here. Longitudinal strain data is also generally less reproducible than the short axis circumferential strain, possibly as a result of a tendency to track the mitral valve apparatus.

Myocardial strain appears to have better inter-study reproducibility compared to myocardial strain rate. This, and the better reproducibility in diastolic strain rate parameters compared to systolic strain rate may be explained by temporal resolution. In systole the change in strain will occur over a shorter period of time and therefore to accurately capture the change in strain (strain rate) a higher temporal resolution may be necessary. The temporal resolution of CMR strain imaging is a known limitation and may account for these discrepancies.<sup>459</sup>

For technical reasons the breath holds for tagging needed to be longer than those for the standard SSFP images, which may have had implications for the image quality at the end of diastole, particularly in this dyspnoeic COPD population. Although our study demonstrated similar agreement with tagging for peak and reverse peak diastolic strain rates compared with other published studies, this may explain why the values for feature tracking and tissue tracking were more closely aligned with each other, demonstrating a consistent direction of inherent bias for diastolic parameters, compared to tagging.<sup>463</sup> Validation of both feature tracking and tissue tracking is still lacking and until such data is available the ability to compare values across studies and vendors will be limited. Despite this the ability of the newer imaging modalities, particularly feature tracking, to provide reproducible diastolic function data is

particularly pertinent. Recent studies have suggested that identification of diastolic dysfunction through non-invasive strain imaging predicts the development of atrial fibrillation and heart failure independent of established risk factors and markers of subclinical CVD.<sup>464</sup> COPD patients often develop diastolic dysfunction with a preserved ejection fraction and have a high incidence of arrhythmias.<sup>158, 422</sup> Echocardiography is technically difficult in patients with lung hyperinflation and hence CMR-strain imaging may provide a modality whereby interventions that alter diastolic function prior to the onset of clinical manifestations can be identified, thus providing the tools to alter the natural history of cardiac disease in COPD. These newer modalities have the added advantage of not needing further image acquisitions since they utilise the standard SSFP cines. Furthermore, they can reduce the time needed to analyse strain imaging four fold, which may make the use of such techniques more viable in the clinical setting.<sup>465</sup>

A number of limitations to this study deserve a mention. Our study utilised two-dimensional strain calculations to derive strain and strain rate parameters and the effect of through plane motion was not determined. Furthermore, due to the nature of the RCT from which the data was used, the baseline and CMR scans were taken up to 4 weeks apart. Despite every effort being made to ensure that the scans are comparable, minor variations in physiological state of those taking part cannot completely be excluded and may contribute to the inter-study reproducibility demonstrated.

In conclusion, the inter-study reproducibility of feature tracking and tissue tracking are comparable to tagging. The assessment of intrinsic diastolic function with these parameters in hyperinflated COPD shows real promise. The data we have provided here will allow for accurate powering of future COPD studies which may in turn allow a better understanding of the natural history of cardiac disease in COPD.



**Chapter Seven:**

**The Applicability Of Current  
Cardiovascular Risk Scores And  
Cardiovascular Surrogates In COPD: A  
Case-Control Study**

## Abstract

**Introduction** COPD is a complex multi-morbid disorder with significant cardiac mortality. Despite this, current cardiovascular scoring systems do not include COPD in their risk prediction models. The aims of this study were to assess whether differences in cardiovascular surrogate markers exist in COPD and to further our understanding of the relationship of COPD to cardiovascular structure and function.

**Methods** This post-hoc cross-sectional analysis utilised baseline data from two randomised controlled trials (n=36 and 54, 90 patients in total). Patients underwent cardiac magnetic resonance imaging, arterial stiffness and lung function measurements. Of the 36 COPD patients, 26 were matched for global cardiovascular risk with 26 controls with normal lung function. Regression analysis was performed on all 90 to look at associations in those surrogates that showed differences.

**Results** Pulse wave velocity (PWV) (mean difference +1.0 m/s, 95% CI 0.1, 1.9; p=0.033), and total arterial compliance (TAC) (mean difference -0.27 mL/m<sup>2</sup>/mmHg, 95% CI -0.4, -0.2; p<0.001) were adversely affected in COPD compared to the control group matched for cardiovascular risk. In the 90-patient cohort QRISK2 ( $\beta$ = 0.046, p=0.017) and FEV1 ( $\beta$ =-0.013, p=0.022) were associated with PWV in multivariate analysis. The relationship between QRISK2 and PWV appeared to be modified by COPD, where the interaction term reached borderline significance (p=0.060). FEV1 ( $\beta$ =0.005, p=0.004) was also associated with TAC in multivariate analysis. Cardiac chamber size and stroke volume was decreased in COPD compared to controls. The mean difference in left ventricle stroke volume index (LVSVI) and left and right end diastolic volume index was -10.3 ml/m<sup>2</sup> (95% CI -15.4, -5.3, p<0.001), -14.1 ml/m<sup>2</sup> (95% CI -22.1, -6.1, p<0.001) and -13.0 ml/m<sup>2</sup> (95% CI -23.9, -2.0, p<0.022) respectively, which were shown to be associated with airflow limitation in multivariate models. In the COPD group (n=36) associations were found with lung hyperinflation (LVSVI:  $\beta$ =-0.075, p=0.032; Left atrial size:  $\beta$ =-0.129, p=0.047) and fibrinogen (TAC:  $\beta$ = 0.716, p=0.030).

**Conclusions** Surrogates for cardiovascular outcomes are adversely affected in COPD compared to a group matched for global cardiovascular risk, suggesting that current scoring systems may be suboptimal in risk prediction in COPD.

## Introduction

Chronic obstructive pulmonary disease (COPD) is predicted to be the third leading cause of death worldwide by 2020.<sup>466</sup> It is a complex multi-morbid disorder in which up to 37% succumb to cardiovascular causes rather than respiratory failure<sup>123</sup>. The precise mechanisms contributing to cardiovascular risk in COPD are not yet fully elucidated but lung hyperinflation and systemic inflammation are postulated as possible mechanisms.<sup>422</sup>

Predicting prognosis in COPD has proven to be difficult.<sup>467</sup> Airflow limitation as measured by the FEV<sub>1</sub> is the hallmark of COPD and was traditionally used for predicting all cause mortality. However, when used in isolation it only shows a weak association with all cause mortality in COPD and has therefore been combined in multi-dimensional risk assessments to improve its predictive value.<sup>30, 468</sup> Regarding cardiovascular mortality it has been suggested that a reduction in forced expiratory volume in one second (FEV<sub>1</sub>), combined with a smoking history is a better predictor than cholesterol.<sup>122</sup> Despite this, current accepted global cardiovascular risk scores do not factor in COPD severity which raises the possibility that risk estimation in this cohort may be suboptimal.<sup>469, 470</sup>

A number of algorithms for estimating cardiovascular risk have been developed and are advocated by national cardiovascular prevention guidelines to communicate risk and facilitate treatment decisions. QRISK, a multifactor cardiovascular disease risk prediction algorithm, was developed and validated for use in the United Kingdom. QRISK predicts the likelihood of a myocardial infarction or cerebrovascular accident in the next 10 years based on routinely collected data from National Health Service general practitioner databases in the United Kingdom. QRISK includes traditional cardiovascular disease risk factors (age, sex, systolic blood pressure, smoking status, and serum cholesterol:high density lipoprotein ratio) that are incorporated in the long established Framingham risk equations. Its most recent incarnation, QRisk 2 2011, also includes self-assigned ethnicity (white or not recorded, Indian, Pakistani, Bangladeshi, other Asian, black African, black Caribbean, Chinese, other including mixed race), body mass index (kg/m<sup>2</sup>), family history of coronary heart disease in first degree relative, Townsend deprivation score, treated hypertension, and diagnosis of rheumatoid arthritis, atrial fibrillation, type 2 diabetes, and chronic renal disease.<sup>469, 471, 472</sup>

Aortic distensibility, total arterial compliance and left ventricular mass (LVM) have been identified as cardiac magnetic resonance (CMR) surrogates of cardiovascular risk, a modality which provides unparalleled image quality non-invasively with excellent accuracy and reproducibility.<sup>197, 473-475</sup> Carotid-femoral pulse wave velocity (PWV), a non-invasive bedside measure of global arterial stiffness, is also an independent predictor of coronary artery disease.<sup>197, 200, 202</sup>

The aim of this study was to assess whether there are differences in cardiovascular surrogate markers in COPD compared to controls with normal lung function matched for global cardiovascular risk and to further our understanding of the relationship of COPD to cardiovascular structure and function.

We hypothesised that: 1) Established non-invasive surrogates of cardiovascular risk would be adversely affected in hyperinflated COPD compared to a control group with equivalent global cardiovascular risk scores and 2) These differences will relate to the extent of hyperinflation, airflow limitation and markers of systemic inflammation.

## Methods

### Patients

This post-hoc cross-sectional analysis utilised baseline data from two randomised controlled trials that have been undertaken at our centre.

### COPD group

The COPD group consisted of the 45 consecutive stable hyperinflated patients as described in the main methods section. All patients with a prior history of cardiovascular disease (7) or atrial fibrillation (2) were excluded, leaving 36 evaluable hyperinflated COPD patients.

### Control group with known cardiovascular risk

The control group was drawn from 96 participants with a global 10-year cardiovascular risk score > 10% who were recruited to the Heart Attack Prevention Programme for You (HAPPY) London (clinicaltrials.gov, NCT01911910), a primary prevention randomised controlled study (RCT) aiming to reduce cardiovascular risk

in a cohort free of pre-existing cardiovascular disease. Only those patients that underwent CMR imaging with normal spirometry and an absence of respiratory disease or atrial fibrillation were included, leaving 54 evaluable subjects. Thus overall there were 90 evaluable subjects, 36 from the COPD cohort and 54 from the control group prior to matching.

### Cardiac parameters

Please refer to Methods section (Chapter 4) detailing the acquisition of cardiac structure and function, aortic distensibility, pulse wave velocity and total arterial compliance.

### Statistics

The matching of the groups was performed using SAS (SAS Institute Inc., Cary, NC, US, Version 9.3). Patients were matched by QRISK2 score  $\pm$  2% to test the initial hypothesis. Statistical analysis was performed using SPSS 21.0 for Mac (SPSS Inc., Chicago, Illinois, USA). The distribution of the data was assessed visually. Continuous variables were expressed as mean  $\pm$  SD for parametric variables and median (interquartile range) for non-parametric variables. Differences between the matched COPD and controls were assessed using paired t-tests.

Univariate followed by multivariate linear regression analysis was performed on all 90 evaluable subjects to evaluate associations between lung function parameters and the surrogate endpoints that showed differences between the groups. Where an association was found further regression analyses were performed on the interaction terms to establish whether the presence or absence of COPD as a binary variable had any impact on the relationship between QRISK2 and the cardiovascular surrogates. Univariate followed by multivariate linear regression analysis was performed on all 36 evaluable COPD subjects to evaluate associations between lung hyperinflation and systemic inflammation and surrogate endpoints that showed differences between the groups.

The extent of intra-observer agreement was assessed via the Bland-Altman method on 20 randomly selected patients (10 from each cohort) for the CMR measures and on 16 of the HAPPY London cohort with respect to the Vicorder measures of PWV and aortic pulse pressure.<sup>446</sup> Statistical significance was defined as a two-sided  $p < 0.05$ .

## Results

Of the 36 eligible COPD patients 26 were successfully matched for 10-year global cardiovascular risk  $\pm$  2% based on the QRISK2 scoring system with 26 out of the 54 HAPPY London participants having normal lung function. Baseline demographics and pulmonary function of the 52 matched individuals are shown in Table 10. As expected, there were no differences in QRISK2 score ( $p=0.693$ ), age ( $p=0.447$ ), gender ( $p=0.161$ ), blood pressure ( $p=0.447$ ), renal function ( $p=0.055$ ) or cholesterol treatment ( $p=0.449$ ) between the groups. However, the control group had a higher prevalence of diabetes than the COPD group, whilst the COPD group had more impaired pulmonary function and significant smoking history. The baseline demographics and pulmonary function for the COPD and Control groups making up the 90 patient cohort are shown in Table 11.

### Inter-observer agreement

The Bland Altman plots (Figure 17) confirmed acceptable agreement between ISS and MYK measurements of PWV (bias 0.43 m/s, limits of agreement (LOA) -0.91-1.76, Intra-class correlation coefficient (ICC) 90.5 %), aortic pulse pressure (bias -1.14 mmHg, LOA -22.9-23.2, ICC 86.4 %), aortic relative area change (Thoracic ascending aorta (TAA) bias 0.0093, LOA -0.0634-0.820, ICC 80.2 %; thoracic descending aorta (TDA) bias 0.0014, LOA 0.0185-0.0213, ICC 97.9 %; abdominal aorta (ABA) bias -0.0029 LOA -0.0190-0.02774, 99.2 %) left ventricle end-diastolic volume index (LVEDVI) (bias -3.6 ml/m<sup>2</sup> LOA-12.5-5.8, ICC 96.6 %), left ventricular mass index (LVMI) (bias -2.9 g/m<sup>2</sup>, LOA -13.65-7.83, ICC 87.5 %) and LVSVI (bias 2.0 ml/m<sup>2</sup> LOA -2.5-8.5, ICC 92.5 %).

### Global arterial stiffness: Total arterial compliance and PWV

PWV and total arterial compliance were adversely affected in COPD compared to the control group matched for cardiovascular risk. PWV was increased in the COPD group compared to the matched controls with a mean difference of +1.0 m/s (95% CI 0.1, 1.9;  $p=0.033$ ), whereas TAC was reduced by -0.27 mL/m<sup>2</sup>/mmHg (95% CI -0.4, -0.2;  $p<0.001$ ). (Table 12; Figure 18).

**Table 10: Demographic and pulmonary function characteristics of COPD and control groups matched for global cardiovascular risk**

Variable	Control group matched for cardiovascular risk (n=26)	COPD (n=26)	P
10-year global cardiovascular risk (QRisk2) score <sup>†</sup> , %	19.3±6.9	18.6±7.0	0.693
Age, yrs	63.7±5.1	64.9±7	0.447
Male n (%)	21 (81)	17 (65)	0.161
Pulse, beats/min	63±11	76±14	0.001*
eGFR, mL/min/1.73m <sup>2</sup>	89±18	78±20	0.055
Brachial SBP, mmHg	134±12	138±23	0.447
Brachial DBP, mmHg	82±10	79±11	0.221
HT treatment, n (%)	16 (61)	9 (35)	0.050
Cholesterol treatment, n (%)	15 (58)	12 (46)	0.449
Diabetes, n (%)	7 (27)	0 (0)	0.006*
Smoking, pack years	5±10	44±36	<0.001*
FEV <sub>1</sub> , mL	3204±743	1419±597	<0.001*
FEV <sub>1</sub> % predicted	103±14	49±15	<0.001*
FEV/FVC, %	75±5	47±14	<0.001*
Residual Volume, mL	-	3852±956	-
Residual Volume, % predicted	-	170±37	-

DBP: diastolic blood pressure; eGFR: estimated glomerular filtration rate; FEV<sub>1</sub>: forced expiratory volume in 1 second; FVC: forced vital capacity; HT: hypertension; SBP: systolic blood pressure, SD: standard deviation. Plus-minus values are means ± SD. \* Denotes p-value of <0.05 † The QRisk2 score is a validated global cardiovascular risk score which predicts the likelihood of a myocardial infarction or cerebrovascular accident in the next 10 years based on routinely collected data from National Health Service general practitioner databases in the United Kingdom.

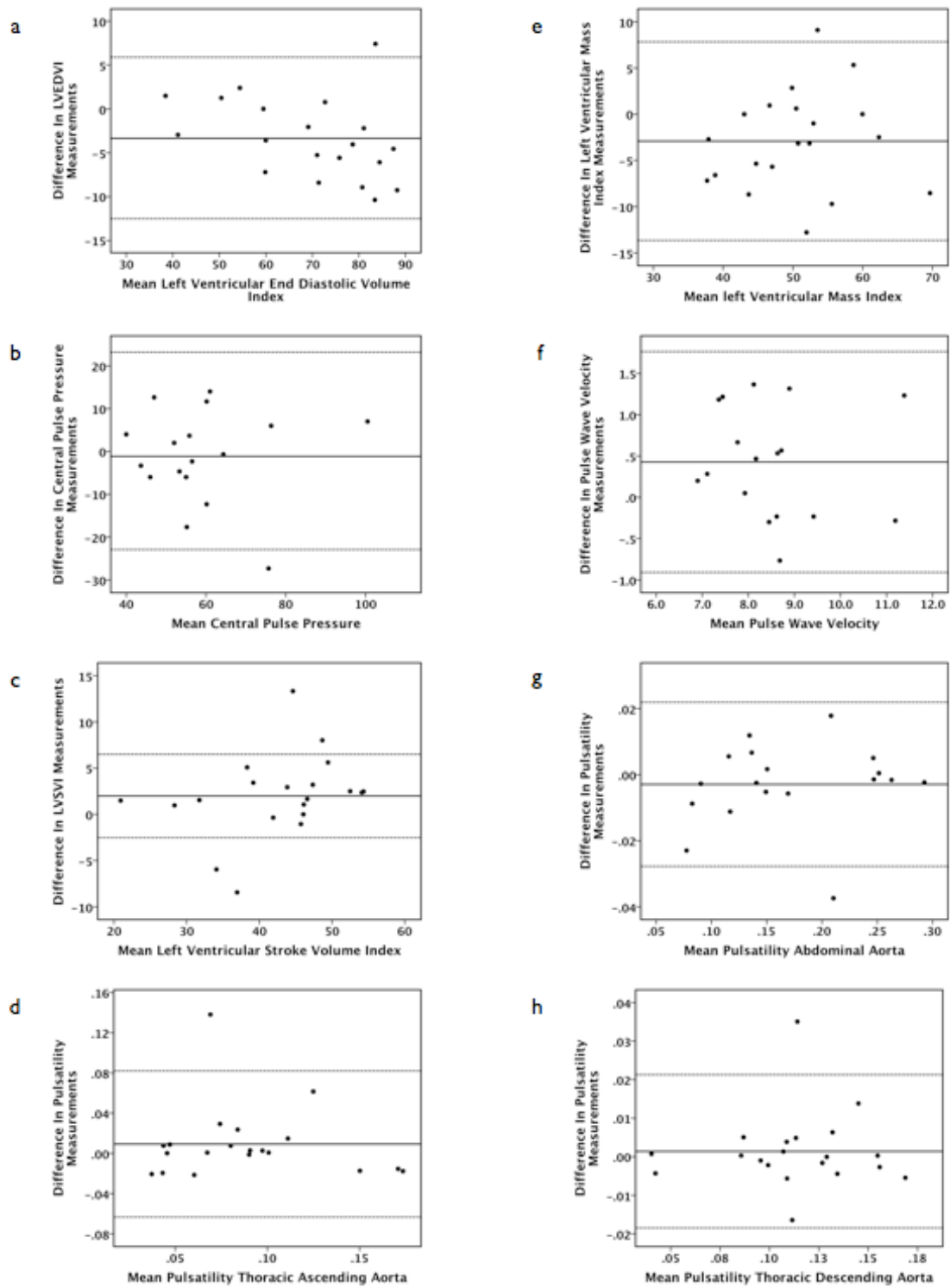


Figure 17 Bland-Altman plots showing agreement between measurements a) Left ventricular end diastolic volume index (LVEDVI), b) Central pulse pressure, c) Left ventricular stroke volume index (LVSVI), d) Thoracic ascending aorta pulsatility, e) Left ventricular mass index, f) Pulse wave velocity, g) Abdominal aorta pulsatility and h) Thoracic descending aorta pulsatility.



### **Local arterial stiffness: Aortic distensibility**

Although numerically reduced in the COPD group compared to controls in all 3 regions analysed, no statistical differences were identified in aortic distensibility (mean difference TAA:  $-0.41 \text{ \%/mmHg} \times 10^{-3}$  95% CI  $-0.9, 0.1$ ,  $p=0.088$ ; TDA  $-0.29 \text{ \%/mmHg} \times 10^{-3}$  95% CI  $-0.8, 0.2$   $p=0.216$ ; ABA  $-0.27 \text{ \%/mmHg} \times 10^{-3}$  95% CI  $-1.2, 0.6$ ,  $p=0.536$ ).

### **Left ventricular mass**

No differences in LVMI were identified between the matched groups (mean difference  $2.8 \text{ g/m}^2$ ; 95% CI  $-2.5, 8.1$ ,  $p=0.291$ ) (Table 12).

### **Ventricular size and function**

Chamber size was decreased in the COPD group compared to the control group with mean differences in LVEDVI and RVEDVI of  $-14.1 \text{ ml/m}^2$  (95%  $-22.1, -6.1$   $p<0.001$ ) and  $-13.0$  (95% CI  $-23.9, -2.0$   $p<0.022$  respectively. There was a corresponding reduction in LVSVI (mean difference  $-10.3 \text{ ml/m}^2$  95% CI  $-15.4, -5.3$ ,  $p<0.001$ ) but no differences in LV ejection fraction, which was preserved in both groups. Despite a reduction in stroke volume, cardiac index was maintained as a consequence of an increased heart rate in the COPD group ( $76 \pm 14$  vs.  $63 \pm 11$  beats/min,  $p=0.001$ ).

### **Univariate and multivariate analysis for the 90 patient cohort**

The baseline demographics and pulmonary function for the COPD and Control groups making up the 90 patient cohort are shown in Table 11.

### **Pulse wave velocity**

The results of the univariate and multivariate analyses for the whole 90 patient cohort are shown in Table 13. QRISK2 and  $FEV_1$  were associated with PWV in the multivariate analysis. A 10 % worsening of  $FEV_1$  percent predicted was associated with a 0.1 m/s increase in PWV when adjusting for other co-variables in the model. Whereas a 10% increase in QRISK2 was associated with 0.4 m/s increase in PWV when adjusting for other co-variables in the model. However, the relationship between QRISK2 and PWV appears to differ when stratified according to the presence or absence of COPD (COPD group  $r^2=0.26$ ; control group  $r^2=0.0031$ ) which approached significance on formal stepwise regression analysis of the interaction term ( $p=0.060$ ) (Figure 18).

### *Total arterial compliance*

Male gender and FEV<sub>1</sub> were positively associated with TAC, whereas age, pulse, systolic BP were negatively correlated in multivariate analyses. For every 20% decrease in FEV<sub>1</sub> there is 0.1 mL/m<sup>2</sup>/mmHg decrease in TAC across both cohorts when adjusting for other co-variables in the model. The relationships between QRISK2 and TAC for the COPD and matched controls are shown in Figure 18. For both the COPD and the control group there was only a very weak relationship between QRISK2 and TAC (COPD,  $r^2=0.35$ ; Control group  $r^2 = 0.25$ ). Stratifying according to the presence or absence of COPD revealed no significant interaction.

### *Cardiac volumes*

The results of the univariate and multivariate analyses for LVEDVI, LVSVI and RVEDVI for all 90 participants are shown in Table 14. Both pulse and FEV<sub>1</sub> were independent predictors of LVEDVI and SVI.

## **The contribution of lung hyperinflation and systemic inflammation to cardiovascular structure and function in COPD**

### *Pulse wave velocity and total arterial compliance*

The univariate and multivariate analysis of TAC and PWV for the 36 COPD group is shown in the lower panel of Table 12. There did not appear to be a relationship with lung hyperinflation or total white cell count. For TAC both fibrinogen and FEV<sub>1</sub> were only associated in the univariate analysis; whereas Q-risk, fibrinogen and dyspnoea scores were related to PWV in the multivariate analysis.

### *Cardiac Volumes*

Information on hyperinflation, levels of systemic inflammation and atrial size were available for the COPD cohort (n=36). Increasing plasma fibrinogen levels and worsening airflow limitation and lung hyperinflation were associated with smaller LVEDVI and RVEDVI in the univariate analyses (Table 14). Worsening airflow limitation and hyperinflation were also associated with reduced LVSVI, whilst worsening airflow limitation, airflow obstruction and lung hyperinflation were associated with decreased maximal left atrial size (size of the left atrium just prior to mitral valve opening at the end of ventricular systole). Two different multivariate models were analysed. In Model 1 all parameters with a p-value of <0.1 in the univariate analysis were included. The relationship between worsening airflow limitation and reduced LVSVI was stronger in the COPD group compared to the aforementioned analysis of all 90 participants ( $\beta$  0.202 vs. 0.129).

**Table 11 Demographic and pulmonary function characteristics of all eligible patients from the COPD cohort and HAPPY London cohort used in univariate and multivariate analyses**

variable	COPD group	Control group
n	36	54
10-year global cardiovascular risk (QRisk2) score <sup>†</sup> , %	17.0±10.2	19.2±7.0
Age, yrs	63±9	64±6
Male n (%)	21(58)	41 (76)
Pulse, beats/min	72±16	62±11
eGFR, mL/min/1.73m <sup>2</sup>	80±20	85±19
Brachial SBP, mmHg	133±22	132±12
Brachial DBP, mmHg	77±11	79±9
HT treatment, n (%)	(25)	29(54)
Cholesterol treatment, n (%)	13±36	33(61)
Diabetes, n (%)	0(0)	13(24)
Smoking, pack years	47±33	7±10
FEV <sub>1</sub> , mL	1393±616	3158±808
FEV <sub>1</sub> % predicted	49±16	101±13
FEV/FVC, %	45±13	74±4
Residual Volume, mL	3763±900	-
Residual Volume, % predicted	172±37	-

DBP: diastolic blood pressure; eGFR: estimated glomerular filtration rate; FEV<sub>1</sub>: forced expiratory volume in 1 second; FVC: forced vital capacity; HT: hypertension; SBP: systolic blood pressure, SD: standard deviation. Plus-minus values are means ± SD. † The QRisk2 score is a validated global cardiovascular risk score which predicts the likelihood of a myocardial infarction or cerebrovascular accident in the next 10 years based on routinely collected data from National Health Service general practitioner databases in the United Kingdom.

Similar relationships were also seen for RVEDVI but not for LVEDVI. There were no multivariate relationships between any of the parameters with left atrial size in Model 1. Following the exclusion of FEV<sub>1</sub> from the analysis (Model 2) a 10% increase in residual volume percent predicted resulted in a 1.3 ml and 0.75 ml volume reduction of LAESVI and LVSVI respectively.

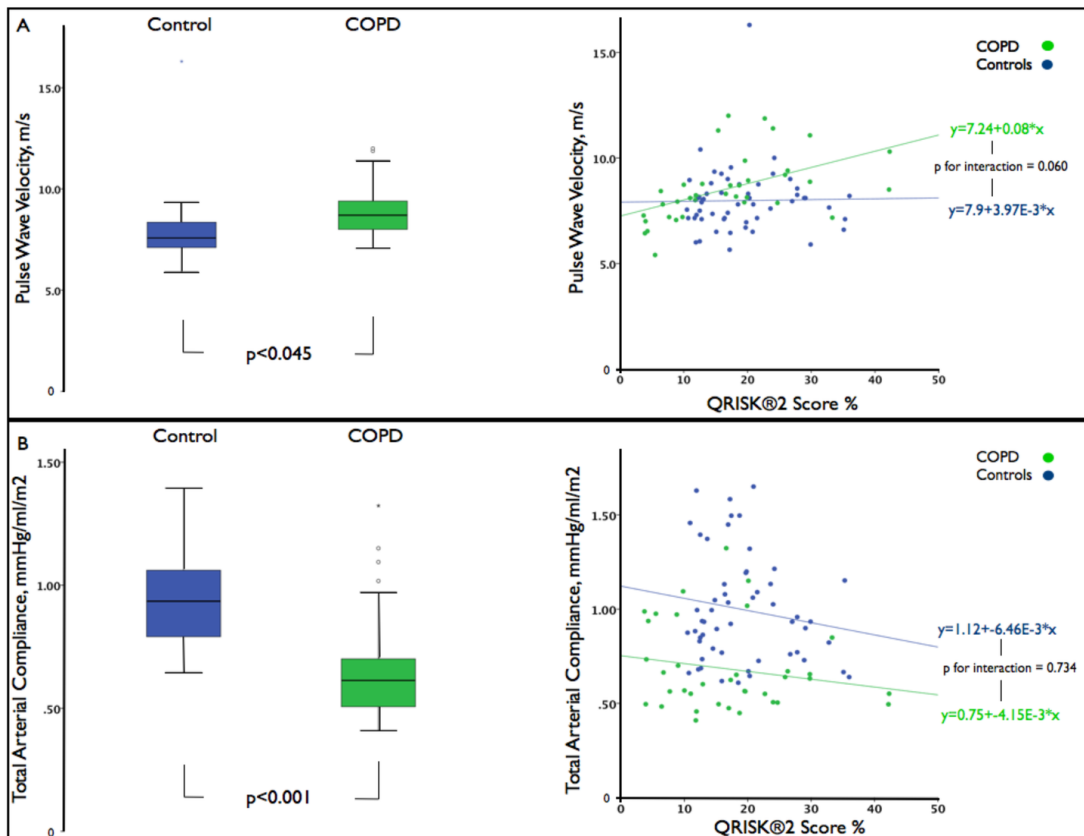


**Figure 18** Differences in pulse wave velocity, total arterial compliance and their relationship to QRISK®2 in COPD compared to controls matched for cardiovascular risk.

## Discussion

The principle novel findings of our study are 1) PWV and TAC, two known independent predictors of cardiovascular disease, are adversely affected in stable hyperinflated COPD over and above a cohort considered to have equivalent global cardiovascular risk but normal lung function. 2) There appears to be an interaction between COPD and QRISK2 with regard to its relationship to PWV 3) Fibrinogen levels are related to PWV in COPD.

Concerns have recently been raised about the accuracy of a number of different scoring systems and over-estimation of risk in the general population.<sup>476</sup> However, the 1.0 m/s increase in PWV presented in the COPD cohort, a disease with an estimated UK prevalence 13.5% in those over 35 years of age, equates to an age, sex and risk-factor adjusted increase in relative risk of cardiovascular events and mortality of 14 and 15 %, respectively.<sup>297, 477</sup> This raises the possibility that the

presence of smoking status alone in current cardiovascular scoring systems may be insufficient to predict cardiovascular risk in this common disease.

The novel finding in this preliminary data that an interaction appears to exist between COPD and the QRISK2 in relation to PWV has potential clinical implications. Whilst it has been shown that the addition of Framingham risk score to FEV1 improves risk stratification for cardiovascular events compared to FEV1 alone, our findings importantly allude to the opposite scenario; that the inclusion of COPD may improve the predictive ability of cardiovascular risk scores themselves and should be further confirmed in larger population studies.<sup>136</sup> Secondly, this interaction implies that COPD could potentially act as a modifiable risk factor. This is a concept supported by previous post-hoc analyses of large randomised controlled trials and two more recent randomised controlled trials where the treatment of COPD with conventional therapies have led to a reduction in pulse wave velocity.<sup>289, 290, 478, 479</sup>

Consistent with other studies we have found a relationship between FEV1 and PWV.<sup>226</sup> Mechanisms proposed for the association between PWV and COPD include systemic inflammation and the effects of hyperinflation on neurohumoral activation.<sup>422</sup> CT defined emphysema has been associated with PWV whilst reports linking systemic inflammation to PWV in COPD have been inconsistent.<sup>227</sup> Sabit et al found relationships with Interleukin (IL)-6, whereas a more recent study found no relationship with leukocytes, C-reactive protein, IL-6, IL-8 or soluble tumour necrosis factor receptor pathway 2. Whilst we also found no relationship with leucocytes, we have found a relationship between PWV and fibrinogen, a marker of systemic inflammation in both COPD and cardiovascular disease.<sup>226, 480, 481</sup> An accurate understanding of the role of fibrinogen in the relationship between COPD and cardiovascular disease is lacking and is the subject of the ERICA project (Evaluation of the Role of Inflammation In Non-pulmonary Disease Manifestations in Chronic Airways Disease) and related studies, but if confirmed could act as a potential therapeutic target.<sup>482</sup>

Table 12 Comparison of cardiovascular endpoints between COPD and control group matched for global cardiovascular risk

Variable	Control group matched for cardiovascular risk (n=26)	COPD (n=26)	Mean Difference of COPD vs Control group (SE)	95% CI	P
<b>Cardiac Volumes, Mass and Function</b>					
LVEDVI, mL/m <sup>2</sup>	77.7±12.2	63.6±15.7	-14.1(3.9)	-22.1, -6.1	0.001*
LVESVI, mL/m <sup>2</sup>	28.7±7.7	24.9±7.5	-3.8(1.9)	-7.9, 0.2	0.062
LVSVI, mL/m <sup>2</sup>	49.0±6.9	38.7±10.1	-10.3(2.5)	-15.4, -5.3	<0.001*
Cardiac Index mL/min/m <sup>2</sup>	3079±607	2868±610	-211(170)	-560.5, 138.4	0.225
LVEF, %	63.4±5.4	61.0±6.5	-2.5(1.5)	-5.6, 0.6	0.115
LVMI, g/m <sup>2</sup>	50.0±7.9	52.7±8.5	2.8(2.6)	-2.5, 8.1	0.291
RVEDVI mL/m <sup>2</sup>	90.5±17.6	77.5±19.5	-13.0(5.3)	-23.9, -2.0	0.022*
<b>Vascular Function</b>					
<b>Global Measures</b>					
PWV, m/s	8.0±1.9	9.0±1.4	1.0(0.4)	0.1, 1.9	0.033*
Total Arterial Compliance, mmHg/ml/m <sup>2</sup>	0.950±0.19	0.680±0.24	-0.27(0.1)	-0.4, -0.2	<0.001*
<b>Local Measures</b>					
<b>Aortic Distensibility, %/mmHg x10<sup>-3</sup></b>					
Thoracic Ascending	2.01±0.9	1.59±1.0	-0.41(0.2)	-0.9, 0.1	0.088
Thoracic Descending	2.24±1.0	1.95±0.8	-0.29(0.2)	-0.8, 0.2	0.216
Abdominal	3.27±1.2	3.00±1.8	-0.27(0.4)	-1.2, 0.6	0.536

CI: confidence interval; COPD: chronic obstructive pulmonary disease; LVEDVI: left ventricle end diastolic volume index; LVEF: left ventricle ejection fraction; LVESVI: left ventricle end systolic volume index; LVMI, left ventricle mass index; LVSVI: left ventricle stroke volume index; PWV: carotid-femoral pulse wave velocity; RVEDVI: right ventricle end diastolic volume index; SE: standard error.

Data expressed as mean±SD.

Indexed values are calculated as raw values divided by body surface area. \*Denotes p-value of <0.05

Table 13: Univariate and multivariate predictors of pulse wave velocity

Variable	Pulse Wave velocity m/s				Total Arterial Compliance mmHg/ml/m <sup>2</sup>			
	Univariate**		Multivariate†		Univariate**		Multivariate <sup>  </sup>	
Whole Cohort n=90								
	β	P-value	β	P-value	β	P-value	β	P-value
Age, yrs	0.095	<0.001*			-0.010	0.022*	-0.007	0.045*
Gender (male)	-0.195	0.589			0.263	<0.001*	0.136	0.012*
QRisk2, %	0.042	0.033*	0.046	0.017*	-0.003	0.490		
Pulse, bts/min	0.012	0.299			-0.010	<0.001*	-0.005	0.013*
Systolic blood pressure, mmHg	0.045	<0.001*			-0.005	0.008*	-0.002	0.253
eGFR, mL/min/1.73m <sup>2</sup>	0.007	0.443			0.002	0.148		
FEV <sub>1</sub> , % predicted	-0.011	0.044*	-0.013	0.022*	0.006	<0.001*	0.005	0.004*
FEV/FVC, %	-0.016	0.11			0.008	<0.001*	<0.001	0.904
COPD Cohort n=36								
Age, yrs	0.117	<0.001*			-0.011	0.010*	-0.006	0.145
Gender (male)	-0.215	0.689			0.152	0.047*	0.142	0.051
QRisk2, %	0.077	0.002*	0.062	0.021*	-0.004	0.277		
Pulse, bts/min	0.005	0.776			-0.005	0.067	-0.003	0.235
Systolic blood pressure, mmHg	0.050	<0.001*			-0.004	0.020*	-0.001	0.713
eGFR, mL/min/1.73m <sup>2</sup>	-0.010	0.453			0.001	0.703		
FEV <sub>1</sub> , % predicted	-0.005	0.783			0.005	0.041*	0.003	0.156
FEV/FVC, %	0.001	0.979			0.002	0.569		
Residual Volume, % predicted <sup>‡</sup>	-0.003	0.717			-0.001	0.220		
IC/TLC, %‡	-0.568	0.844			0.972	0.125		
Fibrinogen, g/l <sup>‡</sup>	0.823	0.026*	0.716	0.030*	-0.137	0.010*	-0.060	0.286
Wcc, x10 <sup>9</sup> /l‡	0.012	0.912			0.006	0.711		
Oxygen saturations %‡	-0.045	0.478			<0.001	0.998		
CAT score <sup>‡</sup>	-0.059	0.052*	-0.044	0.140	0.001	0.888		
MRC score <sup>‡</sup>	0.236	0.022*	0.188	0.027*	-0.011	0.494		
Smoking history, pack years	0.005	0.539			-0.001	0.273		

β: unstandardised beta co-efficient; eGFR: estimated glomerular filtration rate; FEV<sub>1</sub>: forced expiratory volume in 1 second; FVC: forced vital capacity \*Denotes p-value of <0.05\*\*; Univariable predictors with p < 0.1 were entered into multivariate model; †Age and systolic BP excluded from multivariate analysis since adjusted for in the composite global QRisk2 score; ‡ Measurements only available in COPD group

Table 14: Univariate and multivariate predictors of cardiac chamber size and stroke volume

Total cohort n=90	LVEDVI ml/m <sup>2</sup>				LVSVI ml/m <sup>2</sup>				RVEDVI ml/m <sup>2</sup>			
	Univariate**		Multivariate		Univariate**		Multivariate		Univariate**		Multivariate	
	β	P-value	β	P-value	β	P-value	β	P-value	β	P-value	β	P-value
Age, yrs	-0.302	0.2			0.027	0.867			-0.358	0.219		
Gender (male)	10.46	0.005*	5.430	0.069	7.169	0.005*	3.121	0.118	21.3	<0.001*	15.137	<0.001
Pulse, bts/min	-0.713	<0.001*	-0.528	<0.001*	-0.46	<0.001*	-3.12	<0.001*	-0.768	<0.001*	-0.512	<0.001
Systolic blood pressure, mmHg	-0.165	0.113			-0.023	0.749			-0.025	0.050*	-0.043	0.663
Pulse wave velocity m/s	-2.7	0.046*	-0.576	0.575	-1.582	0.087*	0.065	0.924	-0.070	0.132		
FEV <sub>1</sub> , % predicted	0.293	<0.001*	0.219	0.033*	0.241	<0.001*	0.129	0.042*	0.341	<0.001*	0.192	0.096
FEV <sub>1</sub> /FVC, %	0.382	<0.001*	-0.080	0.640	0.361	<0.001*	0.886	0.412	0.436	0.001*	-0.019	0.923
COPD cohort n=36	LVEDVI ml/m <sup>2</sup>						LVSVI ml/m <sup>2</sup>					
	Univariate**		Multivariate				Univariate**		Multivariate			
	β	P-value	Model 1		Model 2		β	P-value	Model 1		Model 2	
Age, yrs	-0.223	0.413					0.088	0.598				
Gender (male)	2.323	0.636					1.073	0.720				
Pulse, bts/min	-0.533	<0.001*	-0.438	0.001*	-0.458	0.001*	-0.286	0.001*	-0.235	0.004*	-0.253	0.003
Systolic blood pressure, mmHg	-0.164	0.130					0.021	0.749				
Pulse wave velocity m/s	-1.509	0.337					0.501	0.603				
FEV <sub>1</sub> , % predicted	0.431	0.003*	0.276	0.073		-	0.282	0.001*	0.202	0.036*		-
FEV <sub>1</sub> /FVC, %	0.189	0.308					0.163	0.145				
Residual volume % predicted	-0.137	0.035*	-0.011	0.866	-0.079	0.149	-0.095	0.016*	-0.023	0.560	-0.075	0.032*
White cell count	-0.154	0.880					0.315	0.611				
Fibrinogen	-8.000	0.017*	-4.559	0.094	-5.22	0.064	-2.436	0.246				
Smoking history, pack	-0.024	0.751					-0.012	0.797				



years												
Oxygen saturations, %	-0.251	0.657					-0.061	0.859				
LV ejection fraction	-0.514	0.155					0.336	0.126				
<b>COPD cohort n=36</b>	<b>RVEDVI ml/m<sup>2</sup></b>						<b>LAESVI ml/m<sup>2</sup></b>					
	Univariate**		Multivariate				Univariate**		Multivariate			
			Model 1		Model 2				Model 1		Model 2	
	$\beta$	P-value	$\beta$	P-value	$\beta$	P-value	$\beta$	P-value	$\beta$	P-value	$\beta$	P-value
Age, yrs	-0.225	0.521					0.631	0.003*	0.486	0.101	0.395	0.146
Gender (male)	12.818	0.036*	10.8	0.035*	11.66	0.034*	-4.454	0.271				
Pulse, bts/min	-0.452	0.021*	-0.354	0.035*	-3.89	0.030*	-0.19	0.142				
Systolic blood pressure, mmHg	-0.200	0.151					0.081	0.377				
Pulse wave velocity m/s	-1.274	0.529					2.184	0.090	-0.221	0.881	-0.002	0.999
FEV <sub>1</sub> , % predicted	0.585	0.002*	0.451	0.027*		-	0.247	0.050*	0.134	0.411		-
FEV <sub>1</sub> /FVC, %	0.258	0.276					0.297	0.048*	-0.043	0.818	0.026	0.877
Residual volume % predicted	-0.154	0.067	0.023	0.786	-0.089	0.072	-0.17	0.001*	-0.105	0.137	-0.129	0.047*
White cell count	0.551	0.671					0.151	0.858				
Fibrinogen	-10.868	0.010*	-0.249	0.083	-7.22	0.060	-2.303	0.429				
Smoking history, pack years	0.036	0.716					0.017	0.787				
Oxygen saturations, %	0.569	0.426					0.167	0.721				
LV ejection fraction	-0.555	0.233					0.312	0.300				
RV ejection fraction	-0.076	0.866					0.618	0.029*	0.339	0.101	0.369	0.143

$\beta$ : unstandardised beta co-efficient; FEV<sub>1</sub>: forced expiratory volume in 1 second; FVC: forced vital capacity; LAESVI: left atrium end systolic volume index; LV: Left Ventricle; LVEDVI: left ventricle end diastolic volume index; LVSVI: left ventricle stroke volume index; RV: right ventricle RVEDVI: right ventricle end diastolic volume index.

\*Denotes p-value of <0.05

\*\* Univariable predictors with p < 0.1 were entered into multivariate Model 1. FEV<sub>1</sub> excluded from Model 2.

Total arterial compliance as measured by PP/SVI is accurate over a wide range of aortic pressures, heart rates and extents of wave reflections.<sup>483</sup> TAC has been shown to be a predictor of cardiovascular events, in normal individuals free from cardiovascular disease, hypertensives and the elderly.<sup>484-486</sup> However, unlike PWV we found no relationship with QRISK2 in univariate or multivariate analysis. Arterial stiffness measures are surrogate measures of end-organ disease representing an index of the summed effects of aging and exposure. However, these surrogate measures have varying abilities to predict particular types of cardiovascular events. Whilst the QRISK2 score is designed to predict both the risk of myocardial infarction and stroke, TAC when measured using MRI has recently been shown to be independently associated with non-fatal cardiac events only, including hospitalisation for congestive heart failure and arrhythmia.<sup>474</sup> This may in part explain the lack of relationship.

Although numerically reduced compared to controls, there were no statistical differences in distensibility between groups. Whilst not supportive of the hypothesis, the successful matching of large conduit arterial function in this cohort suggests that the differences in PWV and TAC shown may relate to differences in more distal, smaller arteries. Lower arterial compliance is associated with cardiac events in the general population after adjustment for demographic, anthropometric and traditional cardiac risk factors.<sup>487</sup> Endothelial dysfunction has been implicated in COPD, where microalbuminuria, an indirect measure of it, is associated with all cause mortality. Many causes have been implicated in COPD and include sympathetic smooth muscle activity, hypoxia, systemic inflammation, oxidative stress, and physical activity.<sup>257, 488, 489</sup>

We have confirmed the findings of previous studies, which were limited by lacking suitable control groups and/or the inclusion of more severe patient populations, that COPD patients have smaller cardiac chambers and stroke volumes, and maintain cardiac output through a compensatory increase in heart rate<sup>105, 107, 251, 490</sup>. The cause of the reduced cardiac chamber size is thought to be a pre-load effect.<sup>105, 251-253</sup> As presented in chapter 8, lung deflation in the short-term results in at least partial reversal of these effects, with decompression of the cardiac chambers, improvements in stroke volume, cardiac output and atrial ejection fraction. The long term implications of these findings on heart failure and arrhythmia, both known to be increased in COPD, are as yet unknown, but may identify another therapeutic target in the prevention of cardiac co-morbidity.<sup>137</sup> At present COPD remains a risk factor

for heart failure mortality and has been incorporated into risk scores accordingly.<sup>491</sup> The findings presented here add weight to the belief that the same should be done for cardiovascular risk. COPD prevalence is higher than rheumatoid arthritis, a condition which is already included in QRISK score. An estimated 1 million COPD patients in the UK are undiagnosed.<sup>477</sup> The inclusion of COPD terms would not only potentially improve risk estimation but would also promote the early diagnosis of COPD through increased usage of pulmonary function testing and the availability of pulmonary function data on primary and secondary care databases.

The results have to be interpreted in the context of the study design. This is a post-hoc cross sectional analysis so we are only able to establish association but not causation. The groups were matched for overall cardiovascular risk but there were disparities between the groups, particularly in relation to prevalence of diabetes and extent of smoking. Given the relatively small sample size these findings should be interpreted with caution and replicated on a larger scale; the absence of a relationship does not necessarily mean that it does not exist. The COPD cohort in our study were all hyperinflated, thus further research is required to see if the results can be generalised to patients with milder COPD or those with differing clinical phenotypes. Our primary purpose was to investigate the applicability of cardiovascular risk scores to patients with COPD by way of assessing surrogates of cardiac risk and as such our investigation regarding the proposed mechanisms surrounding increased risk have not been exhaustive.

In summary, PWV and TAC are adversely affected in hyperinflated COPD compared to a group matched for global cardiovascular risk. The relationship between cardiovascular risk scores and PWV appears to be modified by COPD, suggesting that current scoring systems may be inadequate in risk prediction in COPD.

## Chapter Eight:

# The Effect Of Pharmacological Lung Deflation On Cardiovascular Structure And Function In Stable Hyperinflated COPD: A Single-Centre Randomised Controlled Crossover Trial

This Chapter has been published (in-press) in the *American Journal of Respiratory and Critical Care Medicine*:

**Lung deflation and cardiovascular structure and function in COPD: A randomized controlled trial.** Am J Respir Crit Care Med. 2015 Nov 9. [Epub ahead of print]

Dr Ian S Stone is the first author and designed the study, was involved in patient recruitment, data analysis and drafted the manuscript.

## Abstract

**Introduction** COPD patients develop increased cardiovascular morbidity with alterations in cardiac structure. Postulated mechanisms include the deleterious effect of lung hyperinflation. The effect of reducing lung hyperinflation by pharmacological treatment on cardiac function has not previously been studied.

**Methods** This single-centre, randomised, double-blind placebo-controlled study investigated the effects of reducing lung hyperinflation with seven days of the inhaled corticosteroid/long-acting  $\beta_2$ -agonist (ICS/LABA) fluticasone furoate/vilanterol (FF/VI) 100/25mcg on cardiac structure, function and arterial stiffness assessed by cardiac magnetic resonance in 45 hyperinflated COPD patients. Patients were randomly assigned 1:1 to the two-period complete-block crossover design, with a seven-day minimum washout. The primary outcome was change from baseline in right ventricular (RV) end diastolic volume indexed to body surface area (EDVI) versus placebo. (ClinicalTrials.gov:NCT01691885).

**Results** FF/VI treatment resulted in a 5.8ml/m<sup>2</sup> (CI 2.74, 8.91; p<0.001) increase from baseline in RVEDVI versus placebo, and a 429ml (p<0.001) reduction in residual lung volume. Left ventricular (LV) end-diastolic and left atrial end-systolic volumes increased by 3.63ml/m<sup>2</sup> (p=0.002) and 2.33ml/m<sup>2</sup> (p=0.002). A post-hoc analysis showed an increase of 4.87ml/m<sup>2</sup> in RV stroke volume (p=0.003) and an unchanged RV ejection fraction (EF). The LV showed similar adaptation, whereas the left atrial EF improved by +3.17% (p<0.001). There were no changes to intrinsic myocardial function or systemic vasculature, but pulmonary artery pulsatility increased in two of three locations studied (Main +2.9% p=0.001; Left +2.67% p=0.030). FF/VI safety profile was similar to placebo.

**Conclusion** Pharmacological treatment of chronic obstructive pulmonary disease has consistent beneficial and physiologically plausible effects on cardiac function and the pulmonary vasculature that may contribute to the favourable effects of ICS/LABA treatment in COPD. Whether intrinsic myocardial function can be modulated through prolonged lung deflation should be the focus of future trials.

## Introduction

Chronic obstructive pulmonary disease (COPD) is a complex multi-morbid condition in which patients often succumb to cardiovascular causes rather than respiratory failure, the incidence of which has been reported as high as 50%. It is now apparent that this relationship is independent of smoking and other common shared risk factors. Explanations proposed include the contribution of lung hyperinflation, caused by the loss of elastic recoil combined with expiratory flow limitation, which is associated with a two-fold increase in all-cause mortality.<sup>62, 63, 422</sup>

In cross-sectional studies, increased levels of static lung hyperinflation and emphysema are associated with reduced cardiac chamber size and function.<sup>105, 107, 251, 252</sup> The extent to which these structural alterations could potentially be modified through pharmacological treatment of lung hyperinflation has never been studied in a prospective manner.

Studies investigating cardiac function in COPD have traditionally used echocardiography, thermodilution or cardio-pulmonary exercise testing, which have their own inherent limitations of poor acoustic windowing in hyperinflated lungs, being highly invasive and representing surrogates of cardiac function respectively. Cardiac magnetic resonance (CMR) provides unparalleled image quality non-invasively, with excellent accuracy and reproducibility of cardiac structure and function<sup>433</sup>. Furthermore, novel imaging techniques allow tracking of myocardial deformation providing information on intrinsic function.

The primary objective of the study was to test the hypothesis that the cardiac structural and functional alterations seen in stable hyperinflated COPD are modifiable through pharmacological lung deflation

## Methods

### Study design and participants

This study was a single-centre, Phase IIIb, randomised, double-blind, placebo-controlled, crossover study (ClinicalTrials.gov:NCT01691885; HZC116601). From November 2012 to August 2014, 96 non-hypoxic COPD patients with at least a 15

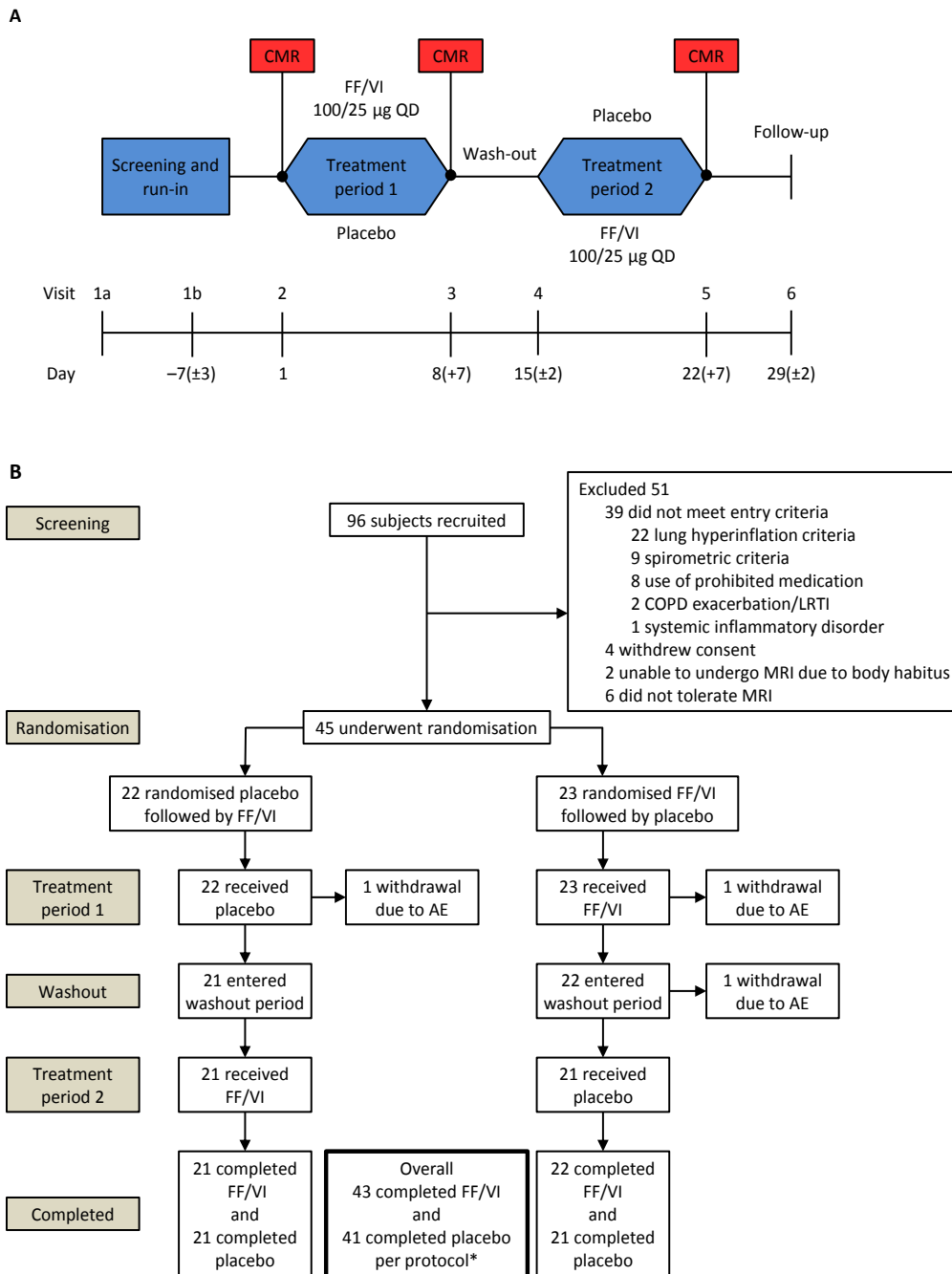


**Figure 19 Study design enrolment and outcome** Panel A shows the design of the study. Each patient, in two separate treatment periods, received 7-14 days of treatment and matching placebo separated by a 1-week washout period. Panel B shows the screening, randomisation, treatment and follow-up of patients. AE: adverse event; CMR: cardiac magnetic resonance; COPD: chronic obstructive pulmonary disease; FF: fluticasone furoate; LRTI: lower respiratory tract infection; MRI: magnetic resonance imaging; QD: once daily; VI: vilanterol.

pack-year history of smoking were recruited from the outpatients departments of an inner-city teaching hospital and the affiliated clinical research centre (Figure 19).

Eligible patients were >40 years of age, demonstrating post-bronchodilator forced expiratory volume in 1 second (FEV<sub>1</sub>) percent-predicted and FEV<sub>1</sub>/forced vital capacity (FVC) ratio < 70%, and a Medical Research Council score of >1. Furthermore evidence of lung hyperinflation as defined by a residual volume (RVol) >120 percent-predicted, was required, which improved by ≥7.5% following 400mcg of inhaled salbutamol. For a full list of the exclusion criteria, please refer to the Appendix Section 2. All patients gave written informed consent. The study was approved by a local ethics review committee and conducted in accordance with the Declaration of Helsinki.

All long-acting bronchodilators, inhaled corticosteroids (ICS) and oral COPD medications were stopped prior to screening after which participants entered a 7(±3) day run-in period where they received short-acting bronchodilators only. Subsequent visits occurred at the beginning and end of each treatment period and one week following trial completion, where trial procedures were carried out and any unscheduled visits to a healthcare provider or the occurrence of any adverse events (AEs) were noted (Figure 19).

## Randomisation and masking

Randomisation occurred at visit 2 following baseline CMR. The central randomisation schedule was generated by the GlaxoSmithKline statistics group, using a validated computerised system (RandAll; GlaxoSmithKline, London, UK), and treatment assignment was masked until database freeze. An interactive telephone system (RAMOS; GlaxoSmithKline, London, UK) was used for randomisation and drug-supply management. Eligible patients were randomly assigned 1:1 to the two-period complete-block crossover, receiving FF/VI 100/25mcg followed by placebo or placebo followed by FF/VI 100/25mcg once daily over two 7-day (maximum 14) treatment periods separated by a 7(±2) day washout period. The masking of the study drug was such that the treatments were indistinguishable.

## Study Procedures

1.5T CMR imaging (Achieva, Philips, Netherlands) was performed at baseline and



following each treatment period to acquire 2-chamber, 4-chamber and short axis cardiac views as well as cross-sections of the aorta and pulmonary arteries. Measures of regional and global arterial stiffness and measures of cardiac volumes, mass, function and feature-tracking derived measures of deformation were acquired as described in the methods section (Chapter 4).

Following screening, patients performed spirometry body plethysmography manoeuvres at baseline and following each treatment period as described in the methods section (Chapter 4).

### **Outcomes**

The primary outcome was change in right ventricular end diastolic volume index (RVEDVI) from baseline versus placebo after seven (maximum fourteen) days of treatment. Other pre-specified outcomes included structural, volumetric and functional changes compared to placebo of the RV, LV and LA as well measures of intrinsic myocardial function of the right and left ventricle, local and regional measures of aortic stiffness, pulmonary pulsatility, and spirometric and lung volume measurements.

### **Statistical analysis**

Analysis was performed using the per-protocol population, defined as those who received at least one dose of study-drug without any deviations that were considered to impact on the primary efficacy analysis.

Due to a lack of data relating to the cardiovascular effects of pharmacological lung deflation, the effect size chosen was extrapolated from studies of lung-volume reduction surgery.<sup>492</sup> An effect size of 5ml/m<sup>2</sup> was selected since it was hypothesized that the changes following pharmacological lung deflation would be of a smaller magnitude to those seen following lung volume reduction surgery.

Sample size calculations are based on the primary outcome and use Hudsmith and colleagues' estimate of between subject standard deviation (SD) of 16 and assumed a 0.75 correlation between same-subject measurements.<sup>433</sup> Using the resulting within subject SD of 8.13 and two-period crossover design, a total of 44 subjects with evaluable data from both periods provides 80% power to detect 5ml/m<sup>2</sup> change in RVEDVI at a two-sided significance level of 0.05.

Change from baseline in RVEDVI was analysed using mixed model analysis, with period, treatment group, and baseline RVEDVI fitted as fixed effects and subject as a random effect. All other pre-specified outcomes and post hoc analyses of SV and RV EF were similarly assessed. The relationship between change in RVol and RVEDVI, and the treatment effect once patients with a history of cardiovascular disease were excluded, was explored post hoc. All programming was performed with SAS (version 9.3).

## Results

Of the 96 patients who were screened, 45 underwent randomisation. The per-protocol population consisted of 43 (96%) who completed FF/VI treatment and 42 (93%) patients who completed treatment with placebo. Demographic and clinical characteristics are provided in Table 14 and Table 15. The order in which patients received treatment and placebo had no impact on the primary efficacy outcome. Following treatment with FF/VI for 7 (maximum 14) days, there was a mean increase from baseline in the primary efficacy outcome RVEDVI of 5.8ml/m<sup>2</sup> (95% CI 2.74, 8.91, p<0.001) compared with placebo (Figure 20; Table 16), an increase of 7.4% relative to the placebo adjusted-mean. There were corresponding improvements in all measures of lung hyperinflation and airflow limitation from baseline, with a 429 ml RVol reduction and increases of 261 ml, 4.6%, 220 ml and 350 ml in inspiratory capacity (IC), IC/total lung capacity (TLC), FEV<sub>1</sub> and FVC, respectively (Table 17)

Following increases in RVEDVI, there was an adaptive RV stroke volume increase (+4.87ml/m<sup>2</sup> 95% CI 1.81, 7.93; p=0.003), resulting in a maintained RVESVI (+0.95 ml/m<sup>2</sup> 95% CI -0.66, 2.57; p=0.240) and RVEF (+1.28% 95% CI -0.72, 3.28; p=0.203). Consistent with the primary outcome LV and atrial volumes were increased from baseline versus placebo (LVEDVI +3.63 ml/m<sup>2</sup> 95% CI 1.39, 5.88; p=0.002; LAESVI +2.33 ml/m<sup>2</sup> 95% CI 0.88, 3.77; p=0.002). The increased SV without alterations in pulse resulted in an improvement in cardiac index by +0.203 l/min/m<sup>2</sup> (95% CI 0.069, 0.337, p=0.004). The LA also demonstrated small but significant improvements in EF (+3.17% 95% CI 1.65, 4.68; p<0.001). The unchanged LV mass over the treatment duration described was expected and confirms the high reproducibility of CMR (Table 16; Figure 21)

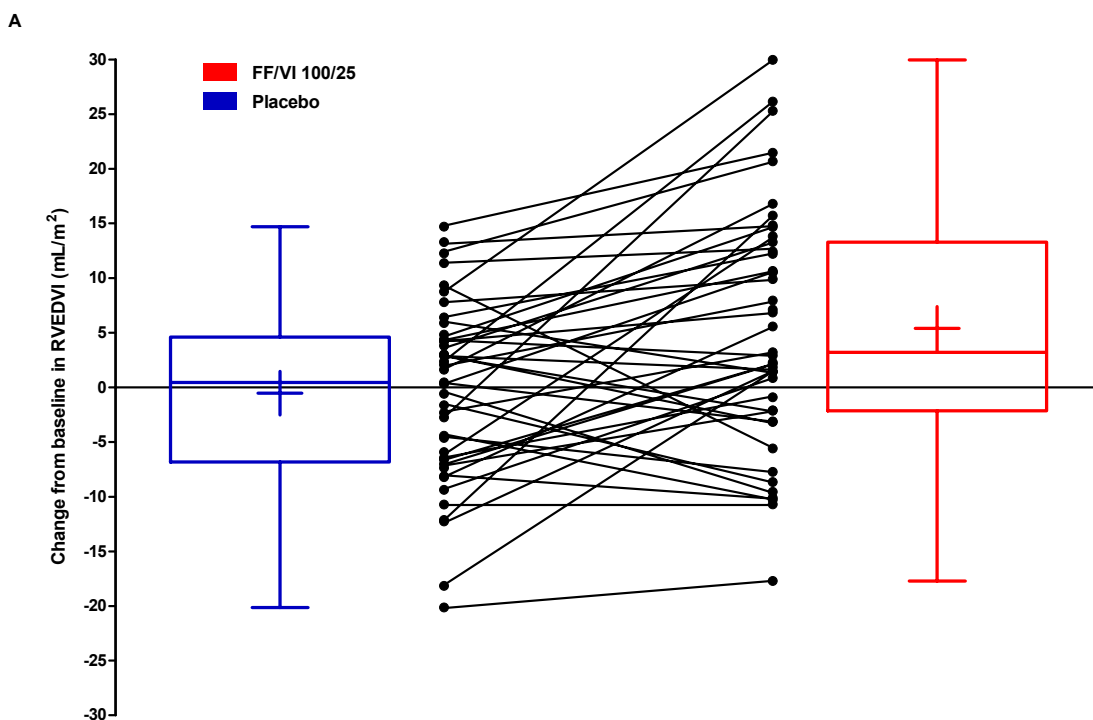


**Figure 20** Box-plot of change from baseline in right ventricular end diastolic volume index for fluticasone furoate/vilanterol 100/25 µg once daily versus placebo following 7–14 days of treatment. Baseline is the assessment taken at pre-dose on Day 1. FF: fluticasone furoate; VI : vilanterol; RVEDVI: Right ventricle end diastolic volume index

There were no differences in any of the 6 strain or strain-rate parameters involved in assessing the intrinsic myocardial function of the RV compared with placebo (Table 16). In the LV there was an improvement compared to baseline in the reverse-peak value of mid-ventricular circumferential strain by -1.5% (95% CI -2.92, -0.02;  $p=0.047$ ) compared with placebo. All of the other 8 parameters assessing the LV global, systolic or diastolic intrinsic myocardial function were unchanged

There were no alterations to systemic arterial stiffness on a local or regional level, with no changes in PWV, AI or distensibility at three aortic locations versus placebo. However, the change from baseline pulsatility was numerically increased in the pulmonary circulation compared to placebo in all 3 regions analysed, reaching statistical significance in the MPA and LPA (MPA +2.9% 95% CI 1.20, 4.59;  $p=0.001$  LPA +2.67% 95% CI 0.28, 5.06;  $p=0.030$ ) (Table 16; Figure 21)

There were no significant treatment interactions affecting change from baseline RVEDVI by any of the pre-specified categorical or continuous subgroups. Post hoc, no relationship was found between change from baseline in RVol and RVEDVI. Excluding patients with a history of cardiovascular disease, totalling 7 from placebo and 8 from the FF/VI periods, did not effect the primary outcome measure (+ 5.62 ml/m<sup>2</sup> 95% CI 2.27, 8.98;  $p=0.002$ ).

**Table 15 Demographic baseline clinical characteristics of patients in the efficacy population. (n = 45)**

<b>Variable</b>	
Age at enrolment, yr	64.4±9.0
Male sex – no. (%)	28 (62)
Body-mass index, kg/m <sup>2</sup> †	25.1±4.4
Body surface area, m <sup>2</sup> ††	1.8±0.2
Race – no. (%)	
Caucasian	39 (87)
African American/African heritage	6 (13)
Current smoker - no. (%)	21 (47)
Smoking history, Pack yr	48.5±30.9
Pre-study COPD therapy no. (%)	
Inhaled corticosteroid	3 (6)
Long acting beta-agonist	1 (2)
Inhaled corticosteroids/ long acting beta-agonist combination	23 (51)
Long acting muscarinic antagonist	25 (56)
Exacerbation in last 3 years – no. (%)	
Requiring antibiotics or oral corticosteroids at home	
0	8 (18)
1	7 (16)
2	9 (20)
>2	21 (47)
Requiring hospitalisation	
0	34 (76)
1	8 (18)
2	2 (4)
>2	1 (2)
Lung function parameters <sup>§</sup>	
Pre bronchodilator FEV <sub>1</sub> , litres	1.26±0.55
Post bronchodilator FEV <sub>1</sub> , litres	1.47±0.55
Post bronchodilator FEV <sub>1</sub> % of predicted	52.5±12.2
Post bronchodilator FEV <sub>1</sub> /FVC, %	45.3±10.3
Pre bronchodilator IC, litres	2.10±0.70
Pre bronchodilator IC/TLC, %	30.0±6.75
Pre bronchodilator RVol, litres	3.80±0.99

Pre bronchodilator RVol % of predicted	168.8±37.0
Reversibility RVol, litres <sup>††</sup>	-0.53 ± 0.30
Reversibility % of predicted RVol <sup>††</sup>	-23.8 ±11.2
DLCO, mmol/min/kPa	4.9±2.0
DLCO% of predicted	56.48±18.74
KCO, mmol/min/kPa/litre	1.0±0.3
KCO % of predicted	67.66±20.78
Symptom scores	
MRC dyspnoea scale — no. (%)	
1	0
2	26 (58)
3	14 (31)
4	5 (11)
5	0
Total score at baseline on COPD assessment test*, units	18±8
Cardiovascular background	
Ischaemic heart disease/angina– no. (%)	8 (18)
Atrial fibrillation– no. (%)	2 (4)
Cerebrovascular disease – no. (%)	1 (2)
Hypertension – no. (%)	16 (36)
Statin therapy no. (%)	14 (33)
Diabetes – no. (%)	1 (2)
Family history no. (%)	4 (9)

Plus–minus values are means ±SD.

<sup>†</sup> The body-mass index is the weight in kilograms divided by the square of the height in meters.

<sup>††</sup> The body surface area is calculated according to the Mostellar method: Height (cm) x Weight (kg) / 3600 )<sup>½</sup>

<sup>‡</sup> Exacerbations during the 3 years before screening were self-reported.

<sup>§</sup> Clinical data are from the screening visit except DLCO and KCO which are from baseline visit. FEV1: forced expiratory volume in 1 second; FVC: forced vital capacity; IC: inspiratory capacity; TLC: total lung capacity; Rvol: residual volume; DLCO: carbon monoxide diffusion capacity; KCO: carbon monoxide transfer coefficient

<sup>¶</sup> Reversibility denotes the change in the Rvol after the administration of 400 µg of salbutamol

\*Scores on the COPD assessment test are based on a scale of 0 to 40, with lower scores indicating less impact; a change of 2 units is considered clinically relevant.

Table 16 Baseline data of cardiovascular efficacy endpoint

Variable	N	Placebo	N	FF/VI
<b>Cardiac structure CMR</b>				
<b>Right ventricle</b>				
EDVI, ml/m <sup>2</sup>	43	79.4±17.4	44	78.6±18.0
ESVI, ml/m <sup>2</sup>	43	29.3±8.7	44	29.2±8.6
SVI, ml/m <sup>2</sup>	43	50.0±12.3	44	49.4±12.8
EF, %	43	63.1±6.8	44	62.8±6.8
<b>Left ventricle</b>				
EDVI, ml/m <sup>2</sup>	43	65.6±13.3	44	65.3±13.5
ESVI, ml/m <sup>2</sup>	43	26.9±7.8	44	26.8±7.8
SVI, ml/m <sup>2</sup>	43	38.6±7.8	44	38.5±8.0
EF, %	43	59.4±6.4	44	59.4±6.4
LVMl, g/m <sup>2</sup>	43	53.5±11.7	44	53.4±11.7
<b>Left atrium</b>				
EDVI, ml/m <sup>2</sup>	43	24.0±18.2	44	24.2±18.0
ESVI, ml/m <sup>2</sup>	43	40.3±17.9	44	39.9±18.0
SVI, ml/m <sup>2</sup>	43	16.3±5.4	44	15.7±6.4
EF, %	43	43.4±11.2	44	40.9±17.5
<b>Regional arterial stiffness</b>				
<b>Vicorder</b>				
PWV, m/s	43	8.8±1.6	44	8.8±1.6
Augmentation index, %	43	22.1±10.4	44	21.5±10.6
<b>Local aortic stiffness<sup>s</sup></b>				
<b>CMR distensibility, %/mmHg</b>				
Thoracic ascending aorta	42	0.167±0.11	43	0.165±0.11
Thoracic descending aorta	42	0.205±0.11	43	0.206±0.11
Abdominal aorta	42	0.333±0.19	43	0.331±0.19
<b>Pulmonary artery stiffness<sup>s</sup></b>				
<b>CMR pulsatility, %</b>				
Main pulmonary artery	42	24.9±8.4	43	24.7±8.5
Right pulmonary artery	42	34.2±8.4	43	33.8±8.1
Left pulmonary artery	41	29.6±9.5	42	28.9±9.1
<b>Intrinsic myocardial function<sup>s</sup></b>				
<b>Right ventricle feature tracking analysis</b>				
Global parameters, %				

Longitudinal strain RP	42	-19.0±8.2	43	-18.9±8.2
Radial strain P	42	31.0±12.2	43	31.0±12.1
<b>Systolic parameters, 1/s</b>				
Radial strain rate SP	42	1.5±0.5	43	1.5±0.5
Longitudinal strain rate SRP	42	-1.3±0.6	43	-1.3±0.6
<b>Diastolic parameters, 1/s</b>				
Radial strain rate DRP	42	-1.0±0.5	43	-1.0±0.5
Longitudinal strain rate DP	42	1.1±0.6	43	1.1±0.6

Data expressed as mean±SD.

Indexed values are calculated as raw values divided by body surface area

EDVI: End diastolic volume index; ESVI: End-systolic volume index; SVI: Stroke Volume Index; EF: Ejection Fraction; PWV: carotid-femoral pulse wave velocity; RP: reverse peak; P: Peak; SP: systolic peak; SRP: systolic reverse peak; DRP: diastolic reverse peak; DP: diastolic peak.

LAEDVI is the volume of the left atrium at the end-of ventricular diastole; LAESVI is the volume of the left atrium at the end of ventricular systole just prior to mitral valve opening

<sup>§</sup> Reduced patient numbers for particular endpoint since data excluded on basis of poor image quality

The incidence of on-treatment adverse events in placebo and FF/VI 100/25. There was one reported drug-related event in each treatment group. All withdrawals were due to COPD exacerbations (FF/VI 100/25, 2 (5%); placebo, 1 (2%)). No serious AEs were reported (Table 18).

## Discussion

To our knowledge, this is the first randomised, placebo-controlled study to demonstrate that changes in cardiac structure and function can be achieved following the pharmacological treatment of lung hyperinflation. In stable hyperinflated COPD, lung deflation with FF/VI results in structural alterations to both sides of the heart, improved biventricular stroke volume, left atrial function and pulsatility within the pulmonary circulation.

Lung deflation in this short-term study had no effect on systemic vascular function, intrinsic systolic or diastolic myocardial function, or ejection fraction of either ventricle. We have shown in hyperinflated COPD that reduced cardiac chamber size exists due to a reduced pre-load effect, and that lung deflation in the short-term results in decompression of the heart and associated pulmonary vasculature. This

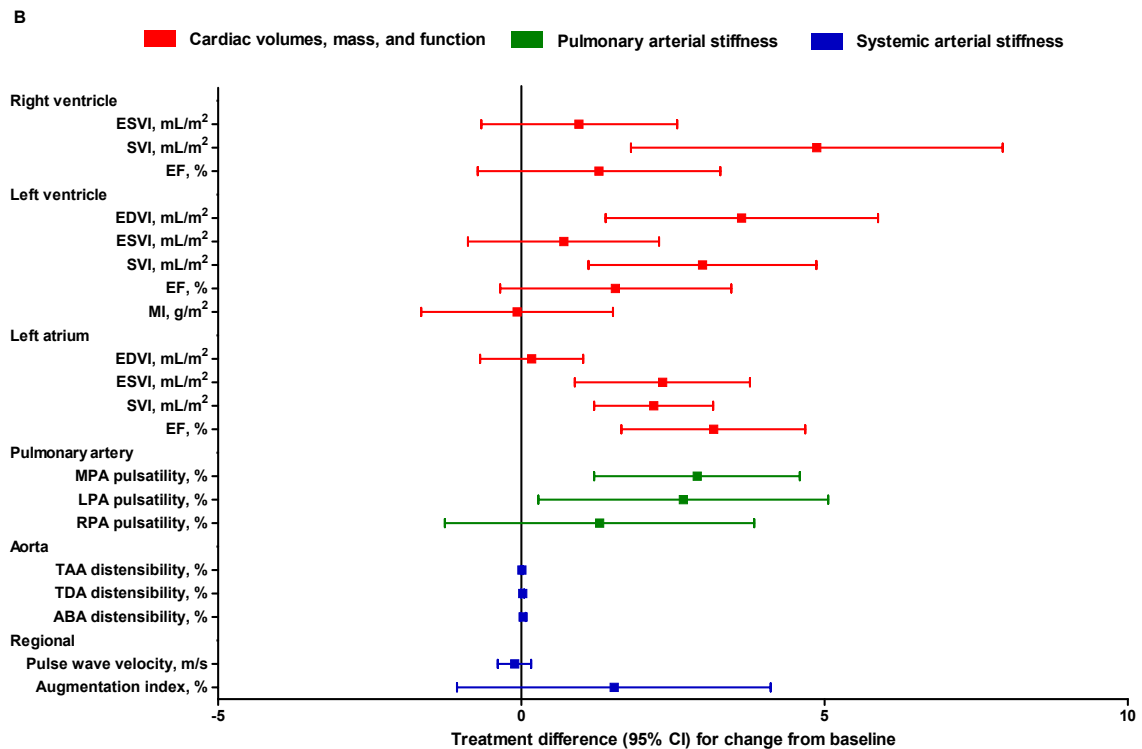


**Figure 21 Forest plot of other cardiovascular efficacy outcomes.** ABA: abdominal aorta; CI: confidence interval; EDVI: end diastolic volume index; EF: ejection fraction; ESVI: end systolic volume index; FF: fluticasone furoate; LPA: left pulmonary artery; MI: mass index; MPA; main pulmonary artery; RPA: right pulmonary artery; RVEDVI: right ventricular end diastolic volume; SVI: stroke volume index; TAA: thoracic ascending aorta; TDA: thoracic descending aorta; VI = vilanterol

leads to relative normalisation of end diastolic volumes and subsequent improvement in stroke volume.

Reduced RV size in hyperinflated COPD has been a consistent finding in recent CMR studies. RVEDV indexed to BSA, the primary end point in this study, has been shown to be reduced in volume by 18ml/m<sup>2</sup> compared to age, gender and body-size matched controls in those patients with severe emphysema.<sup>252</sup> In a prospective, multicentre cohort study of over 6000 participants involving two subgroups from the Multi-Ethnic Study of Atherosclerosis (MESA), a 10% increase in CT-defined emphysema was associated with a reduction in RVEDV by 2.43 ml (95% CI 0.7, 4.16) and 3.25 (95% CI 2.29, 4.20) for current and ex-smokers respectively.<sup>107</sup> Given that CT-emphysema values of 40% can be seen, based on the BSA of our study, up to a 7.22ml/m<sup>2</sup> reduction in RVEDVI may be attributed to emphysema. RVEDVI was selected as the primary endpoint for this study since the thin-walled RV was considered most sensitive to changes in pre-load conditions. We have demonstrated a 5.8ml/m<sup>2</sup> change from baseline compared to placebo suggesting partial reversal of the changes attributed to lung hyperinflation.



Table 17 Results of cardiovascular efficacy outcomes of FF/VI 100/25 versus placebo

Variable	Placebo		FFVI		Difference of FFVI 100/25 from placebo	95 % confidence interval	p-value
	N	Least squares mean change from baseline (SE)	N	Least squares mean change from baseline (SE)			
<b>Cardiac volumes and function</b>							
<b>Right ventricle</b>							
<b>Primary efficacy outcome</b>							
EDVI, ml/m <sup>2</sup>	41	-0.47 (1.39)	43	5.35 (1.37)	5.83	2.74, 8.91	<0.001*
<b>Other efficacy outcomes</b>							
ESVI, ml/m <sup>2</sup>	41	0.28 (0.77)	43	1.23 (0.76)	0.95	-0.66, 2.57	0.240
SVI, ml/m <sup>2</sup>	41	-0.76 (1.24)	43	4.11 (1.21)	4.87	1.81, 7.93	0.003*
EF, %	41	-0.44(0.85)	43	0.85 (0.84)	1.28	-0.72, 3.28	0.203
<b>Left ventricle</b>							
EDVI, ml/m <sup>2</sup>	41	0.03 (1.01)	43	3.66 (0.99)	3.63	1.39, 5.88	0.002*
ESVI, ml/m <sup>2</sup>	41	0.60 (0.63)	43	1.29 (0.62)	0.70	-0.88, 2.27	0.375
SVI, ml/m <sup>2</sup>	41	-0.62 (0.85)	43	2.37 (0.84)	2.99	1.11, 4.87	0.003*
EF, %	41	-1.36 (0.82)	43	0.20 (0.80)	1.55	-0.35, 3.46	0.107
LVMI, g/ m <sup>2</sup>	41	-1.27 (0.68)	43	-1.35 (0.67)	-0.07	-1.65, 1.51	0.927
<b>Left Atrium¶</b>							
EDVI, ml/m <sup>2</sup>	41	0.51 (0.49)	43	0.68(0.48)	0.17	-0.68, 1.02	0.690
ESVI, ml/m <sup>2</sup>	41	0.8 (0.87)	43	3.12 (0.86)	2.33	0.88, 3.77	0.002*
SVI, ml/m <sup>2</sup>	41	0.27 (0.54)	43	2.45 (0.53)	2.18	1.20, 3.16	<0.001*
EF, %	41	-0.65 (0.86)	43	2.51 (0.85)	3.17	1.65, 4.68	<0.001*
<b>Regional arterial stiffness Vicorder</b>							
PWV, m/s	42	-0.03 (0.14)	43	-0.14 (0.13)	-0.11	-0.39, 0.16	0.405
AI, %	42	1.66 (1.17)	43	3.18 (1.163)	1.53	-1.06, 4.11	0.241
<b>Local aortic stiffness<sup>§</sup> CMR distensibility, %</b>							
Thoracic ascending aorta	39	-0.014 (0.009)	41	-0.005 (0.009)	0.009	-0.009, 0.027	0.326
Thoracic descending aorta	39	-0.012 (0.011)	41	0.010 (0.012)	0.023	-0.001, 0.046	0.056
Abdominal aorta	39	-0.015 (0.020)	41	0.013 (0.019)	0.028	-0.015, 0.071	0.189
<b>Pulmonary artery stiffness<sup>§</sup> CMR pulsatility, %</b>							
Main pulmonary artery	39	-0.33 (0.98)	40	2.56 (0.97)	2.90	1.20, 4.59	0.001*
Left pulmonary artery	38	-0.30 (0.92)	40	2.37 (0.89)	2.67	0.28, 5.06	0.030*

Right pulmonary artery	39	0.93 (1.13)	41	2.22 (1.10)	1.29	-1.26, 3.84	0.313
<b>Intrinsic myocardial function<sup>§</sup></b>							
<b>Right ventricle feature tracking analysis</b>							
<b>Global parameters, %</b>							
Longitudinal strain RP	40	-0.47	42	-0.36	0.12	-2.70, 2.93	0.934
Radial strain P	40	4.25	42	5.64	1.40	-8.12, 10.91	0.768
<b>Systolic parameters, 1/s</b>							
Radial strain rate SP	40	0.09 (0.12)	42	0.14 (0.12)	0.05	-0.25, 0.35	0.742
Longitudinal strain rate SRP	40	0.00 (0.07)	42	0.13 (0.07)	0.13	-0.04, 0.30	0.120
<b>Diastolic Parameters, 1/s</b>							
Radial strain rate DRP	40	0.21 (0.09)	42	0.12 (0.09)	-0.09	-0.34, 0.158	0.466
Longitudinal strain rate DP	40	-0.08 (0.07)	42	-0.10 (0.07)	-0.01	-0.16, 0.14	0.876

Analysis performed using an ANCOVA model with covariates of treatment, baseline, period and subject as a random effect. EDVI ; End diastolic volume index; ESVI: End-systolic volume index; SVI: Stroke Volume Index; EF: Ejection Fraction; PWV: carotid femoral pulse wave velocity. RP: reverse peak; P : Peak; SP : systolic peak; SRP: systolic reverse peak; DRP : diastolic reverse peak; DP: diastolic peak.

Indexed values are calculated as raw values divided by body surface area;

¶Left Atrium EDVI is the volume of the left atrium at the end-of ventricular diastole ;

¶Left Atrium ESVI is the volume of the left atrium at the end of ventricular systole just prior to mitral valve opening

\* Denotes p-value of < 0.05;

§ Reduced patient numbers compared to primary efficacy endpoint since some data excluded on basis of poor image quality

Table 18 Results of pulmonary efficacy outcomes of FF/VI 100/25 versus placebo

Variable	N	Placebo		FF/VI		95 % Confidence Interval	p-value
		Least squares mean change from baseline (SE)	N	Least squares mean change from baseline (SE)	Diff of FFVI 100/25 from placebo		
<b>Spirometry</b>							
FEV <sub>1</sub> , l	43	0.00 (0.052)	44	0.22 (0.052)	0.220	0.12, 0.31	<0.001*
FVC, l	43	0.11 (0.071)	44	0.46 (0.071)	0.350	0.21, 0.49	<0.001*
FEV <sub>1</sub> /FVC, %	43	-0.9 (1.10)	44	1.1 (1.09)	2.02	-0.3, 4.3	0.092
<b>Body Plethysmograph</b>							
Rvol, l	42	0.028 (0.074)	43	-0.401 (0.074)	-0.429	-0.59, -0.27	<0.001*
IC, l	42	-0.012 (0.044)	43	0.249 (0.044)	0.261	0.17, 0.35	<0.001*
IC/TLC, %	42	-0.5 (0.54)	43	4.1 (0.54)	4.6	3.1, 6.0	<0.001*

Analysis performed using an ANCOVA model with covariates of treatment, baseline, period and subject as a random effect. CI: Confidence Interval; FEV<sub>1</sub>: forced expiratory volume in 1 second; FVC: forced vital capacity; Rvol: residual volume; IC: inspiratory capacity; TLC: total lung capacity.

\* Denotes p-value of < 0.05

Table 19 Summary of on-treatment adverse events

	Placebo	FF/VI 100/25
N	43	44
<b>Serious adverse events</b>	<b>0</b>	<b>0</b>
<b>Any on-treatment event</b>	<b>5 (12)</b>	<b>6 (14)</b>
Headache	2 (5)	2 (5)
Fatigue	1 (2)	1 (2)
Pain in extremity	1 (2)	1 (2)
Chest pain	1 (2)	0
COPD exacerbations	1 (2)	0
Contusion	1 (2)	0
Dizziness	1 (2)	0
Influenza	0	1 (2)
Joint swelling	1 (2)	0
Local swelling	1 (2)	0
Muscle spasms	1 (2)	0
Nausea	0	1 (2)
Neck pain	1 (2)	0
Pruritus	0	1 (2)
Rhinitis	0	1 (2)
Toothache	0	1 (2)
Urinary tract infection	1 (2)	0

Data presented as numbers of patients (percent)

Reduced cardiac chamber size in COPD has been attributed to the stiffening of the mediastinum or, alternatively decreased ventricular pre-load through vascular remodelling in emphysema or increased intrathoracic pressure due to gas trapping and airflow obstruction.<sup>62, 105, 251, 422</sup> Given the irreversible nature of emphysema, alterations to airways resistance and increased functional strength are likely to be responsible for the lung deflation and subsequent cardiac decompression presented here.<sup>103</sup>

The long-term clinical consequences of the changes in cardiac size and function presented here are not fully determined. Subclinical changes in RV morphology have recently been shown to affect patient centred outcomes and may be an early marker of cardiopulmonary dysfunction. On a population level, one SD decrement (11ml/m<sup>2</sup>) in RVEDVI has been associated with a 12% increase in the risk of dyspnoea after adjustment for spirometric measurements and CT-defined emphysema.<sup>493</sup> Furthermore, increases in cardiac output are associated with improvements in walking intensity across all severities of COPD, and reduced atrial ejection fraction, independent of atrial size, predicts the development of atrial fibrillation in dyspnoeic patients.<sup>494-496</sup> Thus, the ability to modify cardiac morphology

and function does therefore appear to independently impact on relevant clinical and patient-centred outcomes, and highlights the importance of identifying and optimally treating this “lung-deflator” clinical phenotype.<sup>497</sup>

The ability to alter ventricular size and SV through lung deflation has also been seen following lung volume reduction surgery (LVRS). Mineo and colleagues using thermodilution demonstrated an increase of 9 and 3ml/m<sup>2</sup> in RVEDVI and RVSVI, respectively. Post-hoc data from the National Emphysema Treatment Trial (NETT) demonstrated improvements in O<sub>2</sub>-pulse, an exercise-testing surrogate for SV, following LVRS in surgical “lung-deflators”. The modalities used to measure cardiac volumes are not directly comparable. Despite this, the direction of RVEDVI changes shown here are in line with those following LVRS, but given the volume reductions typically achieved post-surgery are of a smaller magnitude.<sup>492, 498, 499</sup>

The proposed mechanisms causing alterations to the heart following short-term changes in lung volume are corroborated by changes in the opposite direction observed in patients receiving ventilator support in critical care. Incremental increases in positive end-expiratory pressure and RVol decreased the RVEDVI by 4–5ml/m<sup>2</sup> in those patients with a non-dilated RV without affecting transmural pressure; while a second study demonstrated that reduced cardiac output was due to a decreased pre-load rather than contractility.<sup>500, 501</sup>

As well as its effects on the chambers of the heart, the intriguing finding that lung deflation results in improved PA pulsatility warrants further consideration. There is a scarcity of published data on PA stiffness in COPD. The MESA-COPD study has shown that in COPD patients free from cardiovascular disease, pulsatility was reduced compared to smoking controls in adjusted models.<sup>502</sup> A second echocardiographic study utilised Doppler flows and maximal systolic frequency shift to estimate PA stiffness and found it to be reduced in COPD compared age and sex-matched non-smoking controls. Although these changes may have been a result of raised PA pressures (30+/-7.9mmHg), Hilde and colleagues have demonstrated a disparity between PA pressures and RV remodelling in COPD.<sup>423, 503</sup> They identified a cohort of patients with reduced PA compliance, rather than raised pulmonary pressures, with echocardiographic appearances typically associated with pulmonary hypertension. This suggests a role for altered PA intrinsic elastic properties in RV adaptation. An altered inflammatory profile from cigarette smoke leading to endothelial dysfunction has been implicated.<sup>504, 505</sup> It is unlikely that the PA

inflammatory profile during this short-term study will have been altered sufficiently by the ICS component of FF/VI to modify the intrinsic elastic properties. Increased pulsatility may be caused by increased SV and subsequent PA distension. Alternatively lung deflation may have altered the elastic properties through decompression of the PA. Such alterations have been known to occur earlier than changes in RV performance and early work by Milnor and colleagues demonstrated that 30% of RV power is spent generating the oscillatory component of flow.<sup>506, 507</sup> Therefore improvements in stiffness could have potentially clinically important long-term benefits in reducing afterload, increasing ventricular efficiency and potentially attenuating the RV adaptation seen in COPD.

There are several limitations of this study. Firstly, it is a single-centre study within a predominantly Caucasian cohort of COPD patients, and as such may not apply to other populations. Secondly, we have included all patients with evidence of lung hyperinflation based on RVol, which is still considered to be the best way to evaluate therapies aimed at reducing air-trapping<sup>79</sup>. As a consequence, participants have not been clinico-radiographically separated, according to emphysematous versus chronic bronchitic phenotypes, and we are unable to establish a differential treatment effect. Thirdly, we have used novel cardiac imaging techniques to help understand the impact of lung deflation on cardiac deformation and vascular function, but for practical and ethical reasons have not employed invasive pressure monitoring. Finally, due to the brevity of this study there were no significant safety findings.

In summary, our study confirms that through pharmacological treatment of COPD, consistent and physiologically plausible beneficial effects on cardiac structure, function and the pulmonary vasculature can be achieved in the short term. Whether intrinsic myocardial function can be modulated through prolonged periods of lung deflation is as yet unverified and should be the focus of future clinical trials.

**Chapter Nine:**

**Summary of Thesis and Future  
Prospects**

The focus of this thesis was to establish the utility of non-invasive cardiovascular physiological measurements and imaging modalities in COPD, and to better understand the relationship between COPD, lung hyperinflation and its treatment on cardiovascular structure and function.

I have demonstrated for the first time that a novel, relatively operator-independent, device for the assessment of arterial stiffness is reproducible and not affected by lung hyperinflation. It is therefore an acceptable alternative to the more validated but more time-consuming SphygmoCor for use in longitudinal clinical studies involving hyperinflated COPD patients. With an increasing number of devices being developed, difficulties will persist until there is consensus regarding the specific site of measurement and path length estimation. Either invasive validation studies, or non-invasive studies utilising CMR are needed to identify the most accurate devices and allow their employment in clinical practice.

I have established for the first time the interstudy reproducibility of 3 separate cardiac deformation analysis techniques in COPD. I have highlighted the often unpublished variation in reproducibility that exists depending on which particular strain parameter is being considered. Progress in their development would be greatly accelerated if we are able to establish which of the newer modalities and algorithms produce the most accurate information. This could be achieved through the modelling of cardiac deformation and applying the algorithms to such a model. Despite their current limitations, some parameters have sufficient reproducibility to be employed in clinical studies and these parameters are particularly attractive for use in COPD due to difficulties with echocardiography in lung hyperinflation. A full understanding of the relative importance of these strain parameters to cardiac function and dysfunction is lacking. Future work needs to focus on the identification of particular groups of deformation parameters which define, as well as help predict, different aspects of systolic and diastolic myocardial performance in COPD. Understanding cardiac strain data in this way would thereby elucidate distinct prognostic indicators of cardiac dysfunction. This can potentially be achieved through the use of statistical dimensionality reduction techniques, such as principle component analysis or Bayesian principle component analysis. These are quantitative methods for data reduction and classification to develop simplified patterns from correlated multi-item



data, thereby identifying a smaller number of independent underlying components which best explains the variation in the dataset.

I have confirmed that cardiac chamber size is reduced and that these reductions relate to airflow limitation. Furthermore, I have found that cardiovascular prognostic markers are adversely affected in COPD compared to a group with normal lung function, considered to have equivalent cardiac risk according to validated scoring systems, and the relationship between the QRisk2 prediction model and pulse wave velocity appears to be modified by the presence or absence of COPD. It may therefore be that we are underestimating cardiac risk in COPD, and the presence or absence of COPD as a binary variable, or FEV1 per cent predicted, should be incorporated into these risk prediction models to increase their predictive value. The beneficial knock-on effect of this implementation may be the early pick up of COPD in primary care, allowing potentially life-prolonging early interventions. The high levels of cardiovascular co-morbidity in COPD is well accepted within the respiratory world, but less so outside of it so large cohort or population studies with “harder” cardiovascular endpoints emphasising the suboptimal risk prediction in COPD may be needed to drive this change.

Furthermore, I have demonstrated relationships between cardiovascular surrogates, cardiac structure, airflow limitation and systemic inflammation in COPD patients. This highlights the possibility that adapting the COPD phenotype or systemic inflammation in some way may enable cardiac structure and prognosis to be modified. Chapter Eight sheds some light on this as will the results of the recently completed, but as yet unpublished, “Study to Understand Mortality and Morbidity in COPD” (SUMMIT).<sup>508</sup>

I have demonstrated for the first time in a RCT that the pharmacological reduction of lung hyperinflation results in structural alterations to both sides of the heart, improved biventricular stroke volume, left atrial function and pulsatility within the pulmonary circulation. This study has opened up a number of avenues for further research: The effects of prolonged lung deflation are still unknown. Further studies would need to confirm that the changes demonstrated persist over the longer term. Other key areas for further research would be to establish, with a sufficiently powered study based on the reproducibility data from Chapter Six, whether COPD treatment can indeed alter intrinsic myocardial function.

Alternative directions include investigating what impact the ICS component has on vascular function within the systemic circulation and whether the ICS would further enhance the effects seen in the pulmonary circulation. On a public health level the priority remains to investigate the effect of the early identification of smokers to encourage cessation and thereby prevent the development of COPD. The hope would be that if we are able case-find at an early enough stage we may be able to alter its natural history and prevent the ensuing heart failure and cardiac arrhythmias. The development of closer relationships between primary and secondary care through an integrated care system, such as that being developed in the UK for the management of COPD, will hopefully provide the infrastructure to undertake such research.

In summary, I have demonstrated that cardiac imaging modalities exist that can be utilised in COPD to help us better understand the vital role the disease and its treatment plays in the development of cardiac structural and functional alterations, morbidity and mortality, and I have given credence to the suggestion that this relationship may be modifiable. A great deal of exciting work is still needed to better understand this complex interaction.

## Unrelated published manuscripts arising during my PHD period

**Moving from the Oslerian paradigm to the post-genomic era: are asthma and COPD outdated terms?** *Thorax* 2013 Louis E Vanfleteren, Jan-Willem Kocks, Ian S Stone, Robab Breyer-Kohansal, Timm Greulich, Donato Lacedonia et al.<sup>59</sup>

**Reporting standards in cardiac MRI, CT and SPECT diagnostic accuracy studies: Analysis of the impact of STARD criteria** *European Heart Journal of Cardiovascular Imaging* 2014 Edd N Maclean, Ian S Stone, Felix Ceelen, Xabier Garcia-Albeniz, Wieland H Sommer, Steffen E Petersen.<sup>509</sup>

# APPENDIX

## Section one

The following tables contain all the inter-study and agreement analysis performed for Chapter 6:

**Table 20 Tagging inter-study reproducibility.** SD; standard deviation; ICC; inter-class correlation coefficient; CI; Confidence interval n=34: Green= global value; red = systolic value, blue = diastolic value

Variable	Mean	Mean difference	SD of mean difference	Limits of Agreement	ICC	95% CI
Apical Peak Radial Strain, %	49.91	157.27	920.26	-1591.24, 1905.77	0.003	-0.348, 0.345
Apical Peak Radial Strain Rate, %/s	322.90	1178.03	6703.59	-11558.79, 3914.87	0.002	-0.347, 0.346
Apical Reverse Peak Radial Strain Rate, %/s	-303.90	-946.43	5568.83	-11527.21, 634.37	-0.00	-0.346, 0.347
Apical Reverse Peak Circumferential Strain, %/s	17.77	0.07	3.14	-5.90, 6.03	0.547	0.249, 0.752
Apical Peak Circumferential Strain Rate, %/s	94.58	-10.80	39.22	-85.32, 63.73	0.504	0.191, 0.725
Apical Reverse Peak Circumferential Strain rate, %/s	-106.18	3.00	29.38	-52.83, 58.82	0.143	-0.214, 0.467
Mid-ventricular Peak Radial Strain, %	35.71	6.12	15.58	-35.72, 23.49	0.321	-0.011, 0.59
Mid-ventricular Peak Radial Strain Rate, %/s	221.61	-33.39	98.59	-220.72, 53.93	0.186	-0.154, 0.488
Mid-ventricular Reverse Peak Radial Strain Rate, %/s	-195.20	3.69	74.48	-137.82, 145.20	0.596	0.331, 0.775
Mid-ventricular Reverse Peak Circumferential Strain, %	-16.41	-0.13	2.56	-5.00, 4.73	0.659	0.42, 0.813
Mid-ventricular Peak Circumferential Strain Rate, %/s	75.67	-3.81	21.83	-45.30, 37.68	0.673	0.44, 0.822
Mid-ventricular Reverse Peak Circumferential Strain Rate, %/s	-83.79	-2.91	16.16	-33.61, 27.79	0.430	0.116, 0.667
Basal Peak Radial Strain, %	50.40	-21.27	78.85	-171.09, 128.56	0.004	-0.334, 0.329
Basal Peak Radial Strain Rate, %/s	328.73	-114.02	465.97	-999.36, 771.32	0.054	-0.282, 0.380
Basal	-339.49	138.94	614.47	-1028.55, 1306.42	0.010	-0.322, 0.341

Reverse Peak Radial Strain Rate, %/s						
Basal Reverse Peak Circumferential Strain, %	-14.21	-0.23	3.74	-7.33, 6.86	0.241	-0.097, 0.531
Basal Peak Circumferential Strain Rate, %/s	68.71	-2.68	18.35	-37.54, 32.18	0.588	0.320, 0.77
Basal Reverse Peak Circumferential Strain Rate, %/s	-74.00	-4.29	14.68	-32.19, 23.60	0.453	0.144, 0.683
2-chamber Peak Radial Strain, %	24.25	-0.73	14.24	-27.78, 26.32	0.304	-0.053, 0.594
2-chamber Peak Radial Strain Rate, %/s	161.89	-9.63	102.48	-204.33, 185.07	0.039	-0.316, 0.387
2-chamber Reverse Peak Radial Strain Rate, %/s	-148.09	16.79	87.032	-148.56, 182.15	0.217	-0.145, 0.530
2-chamber Reverse Peak Longitudinal Strain, %	-12.39	-0.81	3.00	-6.51, 4.90	0.396	0.052, 0.657
2-chamber Peak Longitudinal Strain Rate, %/s	56.45	-1.08	14.71	-29.02, 26.86	0.727	0.504, 0.859
2-chamber Reverse Peak Longitudinal Strain Rate, %/s	-70.45	-6.25	17.83	-40.14, 27.63	0.284	-0.074, 0.570
4-chamber Peak Radial Strain, %	17.80	-1.50	12.38	-25.03, 22.03	0.306	-0.051, 0.595
4-chamber Peak Radial Strain Rate, %/s	147.20	-23.42	103.09	-219.30, 172.45	0.132	-0.23, 0.463
4-chamber Reverse Peak Radial Strain Rate, %/s	-123.55	-8.99	73.42	-148.50, 130.52	0.283	-0.076, 0.57
4-chamber Reverse Peak Longitudinal Strain, %	-13.65	0.64	3.21	-5.45, 6.73	0.337	-0.016, 0.617
4-chamber Peak Longitudinal Strain Rate, %/s	62.61	3.45	20.24	-35.00, 41.90	0.486	0.162, 0.716
4-chamber Reverse Peak Longitudinal Strain Rate, %/s	-77.43	0.18	15.95	-30.12, 30.49	0.377	0.03, 0.645

**Table 21 Feature tracking inter-study reproducibility:** SD; standard deviation: ICC; inter-class correlation coefficient: CI; Confidence interval: Green= global value; red = systolic value, blue = diastolic value

Variable	Mean	Mean diff	SD of mean diff	Limits of Agreement	ICC	95% CI
Apical Peak Radial Strain, %	24.90	1.60	19.21	-34.90, 38.11	0.359	0.06, 0.60
Apical Peak Radial Strain Rate, %/s	142.76	-1.01	64.33	-123.25, 121.23	0.402	0.11, 0.631
Apical Reverse Peak Radial Strain Rate, %/s	157.67	13.44	69.23	-118.10, 144.984	0.54	0.28, 0.726
Apical Reverse Peak Circumferential Strain, %	-24.20	2.00	6.33	-10.02, 14.01	0.56	0.307, 0.74
Apical Peak Circumferential Strain Rate, %/s	151.76	24.65	75.50	-168.11, 118.81	0.484	0.209, 0.689
Apical Reverse Peak Circumferential Strain rate, %/s	-177.56	18.45	65.43	-105.87, 142.77	0.488	0.215, 0.692
Mid-ventricular Peak Radial Strain, %	37.57	-4.32	14.91	-32.66, 24.02	0.451	0.168, 0.665
Mid-ventricular Peak Radial Strain Rate, %/s	178.30	-17.10	57.67	-126.67, 92.46	0.344	0.043, 0.589
Mid-ventricular Reverse Peak Radial Strain Rate, %/s	-149.69	1.78	44.15	-82.11, 85.67	0.604	0.366, 0.769
Mid-ventricular Reverse Peak Circumferential Strain, %	-17.23	0.75	4.03	- 6.90, 8.39	0.531	0.269, 0.721
Mid-ventricular Peak Circumferential Strain Rate, %/s	87.71	-0.17	27.53	-52.48, 52.13	0.57	0.321, 0.747
Mid-ventricular Reverse Peak Circumferential Strain Rate, %/s	-110.53	7.97	27.85	-44.95, 60.89	0.467	0.189, 0.677
Basal Peak Radial Strain, %	35.86	-2.51	18.41	-37.50, 32.48	0.059	-0.252, 0.359
Basal Peak Radial Strain Rate, %/s	165.15	-8.23	63.62	-129.11, 112.65	0.277	-0.032, 0.538
Basal Reverse Peak Radial Strain Rate, %/s	-140.56	9.60	54.81	-94.53, 113.73	0.291	-0.016, 0.549
Basal Reverse Peak Circumferential Strain, %	-17.74	0.65	4.44	-7.78, 9.08	0.51	0.242, 0.706
Basal Peak Circumferential Strain Rate, %/s	103.12	-8.53	32.54	-70.35, 53.30	0.549	0.293, 0.733
Basal Reverse Peak	-109.22	2.99	27.62	-49.48, 55.47	0.526	0.262, 0.717

Circumferential Strain Rate, %/s						
2-chamber Peak Radial Strain, %	37.79	-3.07	21.64	-44.18, 38.03	0.0127	-0.294, 0.318
2-chamber Peak Radial Strain Rate, %/s	169.06	7.68	97.35	-177.29, 192.65	0.0827	-0.379, 0.23
2-chamber Reverse Peak Radial Strain Rate, %/s	-149.76	4.76	68.58	-125.55, 135.07	0.24	-0.071, 0.51
2-chamber Reverse Peak Longitudinal Strain, %	-14.41	0.43	4.69	-8.48, 9.34	0.378	0.082, 0.614
2-chamber Peak Longitudinal Strain Rate, %/s	83.42	-7.76	31.00	-66.65, 51.14	0.405	0.114, 0.633
2-chamber Reverse Peak Longitudinal Strain Rate, %/s	-94.15	4.05	32.51	-57.71, 65.82	0.315	0.01, 0.567
4-chamber Peak Radial Strain, %	30.65	-0.67	13.01	25.39, 24.06	0.443	0.158, 0.66
4-chamber Peak Radial Strain Rate, %/s	148.76	-1.70	57.55	-111.06, 107.66	0.437	0.152, 0.656
4-chamber Reverse Peak Radial Strain Rate, %/s	-130.82	-0.31	49.74	-94.81, 94.19	0.378	0.082, 0.614
4-chamber Reverse Peak Longitudinal Strain, %	-12.39	0.28	5.32	-10.38, 9.83	0.419	0.13, 0.643
4-chamber Peak Longitudinal Strain Rate, %/s	84.30	-4.04	31.24	-63.40, 55.31	0.641	0.416, 0.792
4-chamber Reverse Peak Longitudinal Strain Rate, %/s	-82.10	-3.77	41.91	-83.41, 75.86	0.195	-0.118, 0.473
Right Ventricle Peak Radial Strain, %	30.96	4.09	20.88	-35.58, 43.76	0.169	-0.144, 0.453
Right Ventricle Peak Radial Strain Rate, %/s	147.97	10.20	57.88	-99.77, 120.17	0.362	0.064, 0.602
Right Ventricle Reverse Peak Radial Strain Rate, %/s	-127.19	-4.92	59.33	-117.65, 107.81	0.369	0.071, 0.607
Right Ventricle Reverse Peak Longitudinal Strain, %	-15.61	-0.17	6.00	-11.58, 11.23	0.606	0.369, 0.77
Right Ventricle Peak Longitudinal Strain Rate, %/s	99.65	-6.34	45.48	92.76, 80.09	0.412	0.121, 0.638
Right Ventricle Reverse Peak Longitudinal Strain Rate, %/s	-105.74	1.30	44.18	-82.63, 85.23	0.572	0.323, 0.748

**Table 22 Tissue tracking inter-study reproducibility:** SD; standard deviation: ICC; inter-class correlation coefficient: diff; difference: CI; confidence Interval: Green= global value; red = systolic value, blue = diastolic value

Variable	Mean	Mean diff	SD of mean diff	Limits Agreement of	ICC	95% CI
Apical Peak Radial Strain, %	23.42	-1.33	8.08	-16.67, 14.01	0.314	0, 0.572
Apical Peak Radial Strain Rate, %/s	166.75	-37.94	172.31	-365.35, 289.46	-0.000	-0.314, 0.314
Apical Reverse Peak Radial Strain Rate, %/s	-181.60	36.85	192.58	-329.04, 402.75	-0.0746	-0.379, 0.246
Apical Reverse Peak Circumferential Strain, %	-14.18	0.41	2.74	-4.80, 5.62	0.593	0.343, 0.765
Apical Peak Circumferential Strain Rate, %/s	132.23	-50.11	242.65	-511.15, 410.94	-0.0263	-0.337, 0.291
Apical Reverse Peak Circumferential Strain rate, %/s	125.06	45.38	240.92	-412.37, 503.13	0.0179	-0.297, 0.331
Mid-ventricular Peak Radial Strain, %	22.55	-2.03	5.11	-11.73, 7.68	0.541	0.274, 0.731
Mid-ventricular Peak Radial Strain Rate, %/s	151.76	-14.78	62.82	-134.14, 104.59	0.17	-0.151, 0.46
Mid-ventricular Reverse Peak Radial Strain Rate, %/s	-136.83	1.22	53.57	-100.56, 103.01	0.363	0.056, 0.608
Mid-ventricular Reverse Peak Circumferential Strain, %	-13.97	0.80	2.59	-4.13, 5.72	0.546	0.281, 0.734
Mid-ventricular Peak Circumferential Strain Rate, %/s	96.90	16.19	149.56	-267.97, 300.35	0.0644	-0.254, 0.372
Mid-ventricular Reverse Peak Circumferential Strain Rate, %/s	-97.56	-18.23	152.51	-308.01, 271.56	-0.0486	-0.357, 0.27
Basal Peak Radial Strain, %	39.28	-1.62	14.37	-28.93, 25.69	0.523	0.251, 0.719
Basal Peak Radial Strain Rate, %/s	294.69	-41.91	129.02	-287.05, 203.23	0.492	0.211, 0.698
Basal Reverse Peak Radial Strain Rate, %/s	-264.78	40.18	130.54	-207.85, 288.20	0.579	0.324, 0.756
Basal	-20.046	0.53	4.31	-7.68, 8.74	0.469	0.183, 0.683



Reverse Peak Circumferential Strain, %						
Basal Peak Circumferential Strain Rate, %/s	136.90	-16.04	46.71	-104.78, 72.70	0.644	0.414, 0.797
Basal Reverse Peak Circumferential Strain Rate, %/s	-168.06	21.54	50.21	-73.87, 116.95	0.597	0.349, 0.768
2-chamber Peak Radial Strain, %	25.83	-1.27	5.10	-10.96, 8.42	0.593	0.343, 0.765
2-chamber Peak Radial Strain Rate, %/s	158.16	-6.34	44.08	-90.10, 77.42	0.542	0.276, 0.732
2-chamber Reverse Peak Radial Strain Rate, %/s	-163.68	27.20	65.60	-97.44, 151.84	0.366	0.059, 0.61
2-chamber Reverse Peak Longitudinal Strain, %	-14.14	0.11	2.45	-4.54, 4.77	0.51	0.235, 0.711
2-chamber Peak Longitudinal Strain Rate, %/s	98.32	-16.34	35.84	-84.44, 51.76	0.322	0.009, 0.578
2-chamber Reverse Peak Longitudinal Strain Rate, %/s	-91.09	2.48	28.78	-52.20, 57.16	0.368	0.062, 0.612
4-chamber Peak Radial Strain, %	28.67	-2.67	8.05	-17.96, 12.62	0.343	0.033, 0.594
4-chamber Peak Radial Strain Rate, %/s	204.61	-30.02	81.10	-184.11, 124.06	0.399	0.098, 0.634
4-chamber Reverse Peak Radial Strain Rate, %/s	-171.12	30.02	85.03	-131.53, 191.56	0.181	-0.14, 0.46
4-chamber Reverse Peak Longitudinal Strain, %	-14.56	0.75	2.83	-4.63, 6.13	0.253	-0.066, 0.525
4-chamber Peak Longitudinal Strain Rate, %/s	113.91	-17.79	60.21	-132.19, 96.60	0.242	-0.078, 0.517
4-chamber Reverse Peak Longitudinal Strain Rate, %/s	-125.36	19.98	61.23	-96.37, 136.32	0.291	-0.025, 0.555

**Table 23 Agreement between different strain measurement techniques.** SD; standard deviation; ICC; interclass correlation co-efficient; CI; confidence interval; LoA; Limits of agreement

Variable	Tagging	Feature tracking					Tissue tracking				
	Mean Value	Mean difference	SD	LoA	ICC	95% CI	Mean difference	SD	LoA	ICC	95% CI
Apical Peak Radial Strain, %	49.91	24.72	79.84	-126.98, 176.41	-0.022	-0.33, 0.30	26.53	78.32	-122.29, 175.35	-0.020	-0.335, 0.301
Apical Peak Radial Strain Rate, %/s	322.90	182.98	513.72	-793.09, 1159.05	-0.064	-0.37, 0.26	152.60	548.73	-889.99, 1195.19	-0.074	-0.382, 0.251
Apical Reverse Peak Radial Strain Rate, %/s	-303.90	-156.98	442.40	-997.54, 683.58	0.047	-0.36, 0.28	-122.46	478.77	-1032.13, 787.21	-0.039	-0.352, 0.283
Apical Reverse Peak Circumferential Strain, %	17.77	6.12	6.51	-6.24, 18.48	0.026	-0.29, 0.34	-3.68	4.22	-11.70, 4.34	0.101	-0.224, 0.407
Apical Peak Circumferential Strain Rate, %/s	94.58	-50.38	71.42	-186.08, 85.32	0.286	-0.04, 0.55	-40.46	253.86	-522.78, 441.87	-0.036	-0.349, 0.286
Apical Reverse Peak Circumferential Strain rate, %/s	-106.18	66.52	89.85	-104.19, 237.23	-0.182	-0.47, 0.14	22.83	253.95	-459.68, 505.33	-0.008	-0.324, 0.312
Mid-ventricular Peak Radial Strain, %	35.71	-2.34	23.52	-47.016, 42.34	-0.022	-0.33, 0.29	12.93	17.27	-19.89, 45.74	-0.215	-0.492, 0.102
Mid-ventricular Peak Radial Strain Rate, %/s	221.61	41.62	112.96	-173.01, 256.26	-0.051	-0.36, 0.26	68.55	112.18	-144.59, 281.69	-0.184	-0.467, 0.135
Mid-ventricular Reverse Peak Radial Strain Rate, %/s	-195.20	-44.18	97.44	-229.33, 140.97	-0.066	-0.37, 0.25	-57.05	89.95	-227.95, 113.88	-0.102	-0.399, 0.216
Mid-ventricular Reverse Peak Circumferential	-16.41	1.07	3.17	-4.95, 7.09	0.402	0.11, 0.63	-2.17	2.23	-6.41, 2.07	0.424	0.132, 0.649

Strain, %											
Mid-ventricular Peak Circumferential Strain Rate, %/s	75.67	-14.06	26.33	-64.10, 35.96	0.581	0.33, 0.76	-22.69	32.86	-85.12, 39.74	0.264	-0.049, 0.531
Mid-ventricular Reverse Peak Circumferential Strain Rate, %/s	-83.79	25.60	23.20	-18.49, 69.70	0.142	-0.18, 0.43	14.85	23.36	-29.53, 59.23	0.234	-0.082, 0.508
Basal Peak Radial Strain, %	50.40	15.01	75.36	-28.16, 158.19	-0.047	-0.35, 0.27	11.11	75.14	-131.67, 153.88	-0.027	-0.333, 0.287
Basal Peak Radial Strain Rate, %/s	328.73	165.37	459.66	-707.97, 1038.72	-0.074	-0.38, 0.24	36.92	476.12	-867.71, 941.55	-0.023	-0.33, 0.29
Basal Reverse Peak Radial Strain Rate, %/s	-339.49	-201.56	584.22	-1311.59, 908.46	-0.070	-0.37, 0.25	-68.36	595.14	-1199.12, 1062.40	-0.000	-0.31, 0.31
Basal Reverse Peak Circumferential Strain, %	-14.1	3.78	4.28	4.35, 11.91	-0.3	-0.31, 0.31	6.04	3.83	-1.23, 13.31	0.340	0.032, 0.587
Basal Peak Circumferential Strain Rate, %/s	68.71	-34.51	41.25	-112.89, 43.86	0.036	-0.34, 0.28	-71.06	56.92	-179.21, 37.10	-0.157	-0.445, 0.162
Basal Reverse Peak Circumferential Strain Rate, %/s	-74.00	36.30	29.38	-19.51, 92.12	-0.190	-0.47, 0.13	95.35	59.03	-16.81, 207.52	-0.487	-0.692, 0.208
2-chamber Peak Radial Strain, %	24.25	-11.77	18.49	-46.91, 23.36	-0.230	-0.51, 0.10	-1.38	11.63	-23.48, 20.72	0.324	0.002, 0.586
2-chamber Peak Radial Strain Rate, %/s	161.89	-2.74	97.48	-187.96, 182.48	-0.027	-0.35, 0.30	3.00	70.04	130.07, 136.07	0.346	0.028, 0.602
2-chamber Reverse Peak Radial Strain Rate, %/s	-148.09	-0.16	66.52	-126.55, 126.24	0.370	0.06, 0.62	17.62	60.67	-97.66, 132.90	0.589	0.33, 0.766
2-chamber	-12.39	1.77	3.87	-5.58,	0.175	-0.16, 0.47	1.67	2.70	-3.46,	0.215	-0.114, 0.503

Reverse Peak Longitudinal Strain, %				9.12					6.81		
2-chamber Peak Longitudinal Strain Rate, %/s	56.45	-25.94	30.26	-83.43, 31.55	0.146	-0.185, 0.448	-40.67	30.93	-99.44, 18.10	0.020	-3.04, 0.34
2-chamber Reverse Peak Longitudinal Strain Rate, %/s	-70.45	19.82	26.81	-31.11, 70.76	-0.031	-0.35, 0.30	20.64	24.64	-26.17, 67.46	0.210	-0.12, 0.499
4-chamber Peak Radial Strain, %	17.80	-11.42	19.07	-47.64, 24.81	-0.43	-0.67, -0.11	-10.94	14.90	-39.26, 17.37	-0.312	-0.583, 0.022
4-chamber Peak Radial Strain Rate, %/s	147.20	10.83	108.79	-195.87, 217.52	-0.205	-0.50, 0.14	-59.15	139.27	-323.77, 205.46	0.148	-0.456, 0.194
4-chamber Reverse Peak Radial Strain Rate, %/s	-123.55	-0.94	60.28	-115.47, 113.58	0.052	0.28, 0.38	45.05	92.72	-131.13, 221.22	-0.215	-0.509, 0.127
4-chamber Reverse Peak Longitudinal Strain, %	-13.65	-1.36	4.68	-10.25, 7.52	0.225	-0.11, 0.52	1.11	2.63	-3.89, 6.11	0.427	0.112, 0.665
4-chamber Peak Longitudinal Strain Rate, %/s	62.61	-18.81	28.80	-73.54, 35.90	0.309	-0.02, 0.58	-52.26	127.33	-294.19, 189.67	-0.051	0.375, 0.286
4-chamber Reverse Peak Longitudinal Strain Rate, %/s	-77.43	-2.19	25.57	-50.78, 46.40	0.192	-0.15, 0.49	46.67	109.70	-161.76, 255.11	0.044	-0.291, 0.371

## Section two

### Exclusion criteria for the randomised controlled trial detailed in Chapter 8

Subjects meeting any of the following criteria were not be enrolled in the study:

1. Pregnancy: Women who are pregnant or lactating.
2. Asthma: Subjects with a current diagnosis of asthma. (Subjects with a prior history of asthma are eligible if they also have a current diagnosis of COPD).
3.  $\alpha$ 1-antitrypsin deficiency: Subjects with known  $\alpha$ -1 antitrypsin deficiency as the underlying cause of COPD
4. Other respiratory disorders: Subjects with active tuberculosis or lung cancer as well as clinically significant bronchiectasis, sarcoidosis, pulmonary fibrosis, interstitial lung diseases or other active pulmonary diseases. Pulmonary hypertension from causes other than COPD.
5. Lung resection or transplantation: Subjects with lung volume reduction surgery within the 12 months prior to Screening or having had a lung transplant or pneumonectomy.
6. A moderate/severe COPD exacerbation that has not resolved at least 14 days prior to screening and at least 30 days following the last dose of oral corticosteroids (if applicable).
7. Lower respiratory tract infection: Subjects with lower respiratory tract infection that required the use of antibiotics within 30 days prior to screening.
8. Pulmonary Rehabilitation: Patients to be excluded if they have been in the acute phase of pulmonary rehabilitation in the 4 weeks prior to screening
9. Current severe heart failure (New York Heart Association class IV). Subjects will also be excluded if they have a known ejection fraction of <30%.
10. Abnormal and clinically significant 12-lead ECG
11. Other systemic inflammatory conditions associated with chronic inflammation in the opinion of the investigator (e.g. rheumatoid arthritis, connective tissue disorders and Inflammatory Bowel Disease)
12. Other significant diseases / abnormalities: Any life-threatening condition with life expectancy <1 year, other than vascular disease or COPD, that might prevent the subject from completing the study.
13. Coronary Artery Bypass Grafting (CABG) in the 6months prior to screening.
14. Myocardial infarction, cerebrovascular event or coronary artery intervention other than CABG in the 1 month prior to screening.

15. History of malignancy within the past 5years, other than non-melanoma skin cancer.
16. End stage chronic renal disease: Subjects will be excluded if on renal replacement therapy (haemodialysis or peritoneal).
17. Drug/food allergy: Subjects with a history of hypersensitivity to any of the study medications (e.g. beta-agonists, corticosteroid) or components of the inhalation powder (e.g. lactose, magnesium stearate). In addition, patients with a history of severe milk protein allergy that, in the opinion of the study physician, contraindicates the subject's participation will also be excluded.
18. Drug/alcohol abuse: Subjects with a known or suspected history of alcohol or drug abuse within the last 2 years.
19. Oxygen therapy: Subjects receiving treatment with long-term oxygen therapy (LTOT) or nocturnal oxygen therapy required for greater than 12 hours a day. Oxygen should not be initiated during the trial.
20. Questionable validity of consent: Subjects with a history of psychiatric disease, intellectual deficiency, poor motivation or other conditions that will limit the validity of informed consent to participate in the study or the potential compliance to study procedures.
21. Additional medication: Use of an investigational device or investigational drug within 30 days or 5 half-lives (whichever is longer) preceding the first dose of study medication.
22. Use of the following medications is not permitted within the following time frames
  - Depot corticosteroids: 12 weeks
  - \*Cytochrome P450 3A4 strong inhibitors including but not limited to antiretrovirals (protease inhibitors) (e.g., indinavir, nelfinavir, ritonavir, saquinavir, atazanavir); imidazole and triazole anti- fungals (e.g., ketaconazole, itraconazole, voriconazole); clarithromycin, telithromycin, troleandomycin, mibefradil, cyclosporin, nefazodone: 6 weeks
  - Grapefruit is allowed up to Visit 1, then limited to no more than one glass of grapefruit juice (250 mL/8 ounces) or one grapefruit per day
  - Systemic, oral, parenteral (intra-articular) corticosteroids: 30 days
  - Antibiotics: 30 days
  - Inhaled corticosteroids: 2 weeks
  - Inhaled ICS/LABA combination products: 2 weeks
  - Long-acting anticholinergics (e.g., tiotropium): 4 days

- PDE-4 inhibitors (e.g., roflumilast): 1 week
- Oral leukotriene inhibitors (e.g., zafirlukast, montelukast, zileuton): 48 hours
- Inhaled long acting  $\beta_2$ -agonists (e.g., salmeterol): 48 hours
- Oral beta-agonists: 48 hours
- Inhaled sodium cromoglycate or nedocromil sodium: 24 hours
- Ipratropium/albuterol (salbutamol) combination product: 6 hours
- Oral Theophylline preparations 48 hours
- Short-acting anti-cholinergics (e.g., ipratropium bromide): 6 hours (ipratropium will be supplied for rescue) during the study, in inhaled or nebulized form)
- Inhaled short-acting  $\beta_2$ -agonists: 6 hours (albuterol/salbutamol was supplied for rescue during the study)

## References

1. Stone IS, Barnes NC, James WY, Midwinter D, Boubertakh R, Follows R, et al. Lung Deflation and Cardiovascular Structure and Function in COPD: A Randomized Controlled Trial. *Am J Respir Crit Care Med*. 2015.
2. NICE, . Chronic Obstructive Pulmonary Disease. NICE Guideline (Update). London: National Institute for Health and Clinical Excellence; 2011.
3. Mannino DM, Gagnon RC, Petty TL, Lydick E. Obstructive lung disease and low lung function in adults in the United States: data from the National Health and Nutrition Examination Survey, 1988-1994. *Arch Intern Med*. 2000; **160**(11): 1683-9.
4. Hubbard R. The burden of lung disease. *Thorax*. 2006; **61**(7): 557-8.
5. Soriano JB, Maier WC, Egger P, Visick G, Thakrar B, Sykes J, et al. Recent trends in physician diagnosed COPD in women and men in the UK. *Thorax*. 2000; **55**(9): 789-94.
6. Hansell AL, Walk JA, Soriano JB. What do chronic obstructive pulmonary disease patients die from? A multiple cause coding analysis. *Eur Respir J*. 2003; **22**(5): 809-14.
7. Health Statistics Quarterly In: Statistics OfN, editor.: HMSO; 2000.
8. Barnes PJ. Genetics and pulmonary medicine. 9. Molecular genetics of chronic obstructive pulmonary disease. *Thorax*. 1999; **54**(3): 245-52.
9. Hogg JC, Chu F, Utokaparch S, Woods R, Elliott WM, Buzatu L, et al. The nature of small-airway obstruction in chronic obstructive pulmonary disease. *N Engl J Med*. 2004; **350**(26): 2645-53.
10. Turato G, Zuin R, Saetta M. Pathogenesis and pathology of COPD. *Respiration*. 2001; **68**(2): 117-28.
11. O'Shaughnessy TC, Ansari TW, Barnes NC, Jeffery PK. Inflammation in bronchial biopsies of subjects with chronic bronchitis: inverse relationship of CD8+ T lymphocytes with FEV1. *Am J Respir Crit Care Med*. 1997; **155**(3): 852-7.
12. Saetta M, Di Stefano A, Turato G, Facchini FM, Corbino L, Mapp CE, et al. CD8+ T-lymphocytes in peripheral airways of smokers with chronic obstructive pulmonary disease. *Am J Respir Crit Care Med*. 1998; **157**(3 Pt 1): 822-6.
13. Stanescu D, Sanna A, Veriter C, Kostianev S, Calcagni PG, Fabbri LM, et al. Airways obstruction, chronic expectoration, and rapid decline of FEV1 in smokers are associated with increased levels of sputum neutrophils. *Thorax*. 1996; **51**(3): 267-71.
14. Pizzichini E, Pizzichini MM, Gibson P, Parameswaran K, Gleich GJ, Berman L, et al. Sputum eosinophilia predicts benefit from prednisone in smokers with chronic obstructive bronchitis. *Am J Respir Crit Care Med*. 1998; **158**(5 Pt 1): 1511-7.
15. Saetta M, Di Stefano A, Maestrelli P, Turato G, Ruggieri MP, Roggeri A, et al. Airway eosinophilia in chronic bronchitis during exacerbations. *Am J Respir Crit Care Med*. 1994; **150**(6 Pt 1): 1646-52.
16. Saetta M, Turato G, Maestrelli P, Mapp CE, Fabbri LM. Cellular and structural bases of chronic obstructive pulmonary disease. *Am J Respir Crit Care Med*. 2001; **163**(6): 1304-9.
17. Vestbo J, Hurd SS, Agusti AG, Jones PW, Vogelmeier C, Anzueto A, et al. Global strategy for the diagnosis, management, and prevention of chronic obstructive pulmonary disease: GOLD executive summary. *Am J Respir Crit Care Med*. 2013; **187**(4): 347-65.
18. Donaldson GC, Seemungal TA, Bhowmik A, Wedzicha JA. Relationship between exacerbation frequency and lung function decline in chronic obstructive pulmonary disease. *Thorax*. 2002; **57**(10): 847-52.
19. Seemungal TA, Donaldson GC, Paul EA, Bestall JC, Jeffries DJ, Wedzicha JA. Effect of exacerbation on quality of life in patients with chronic obstructive pulmonary disease. *Am J Respir Crit Care Med*. 1998; **157**(5 Pt 1): 1418-22.



20. Wilkinson TM, Donaldson GC, Hurst JR, Seemungal TA, Wedzicha JA. Early therapy improves outcomes of exacerbations of chronic obstructive pulmonary disease. *Am J Respir Crit Care Med*. 2004; **169**(12): 1298-303.
21. Hurst JR, Vestbo J, Anzueto A, Locantore N, Mullerova H, Tal-Singer R, et al. Susceptibility to exacerbation in chronic obstructive pulmonary disease. *N Engl J Med*. 2010; **363**(12): 1128-38.
22. Fletcher CM. The clinical diagnosis of pulmonary emphysema; an experimental study. *Proceedings of the Royal Society of Medicine*. 1952; **45**(9): 577-84.
23. Hajiro T, Nishimura K, Tsukino M, Ikeda A, Koyama H, Izumi T. Comparison of discriminative properties among disease-specific questionnaires for measuring health-related quality of life in patients with chronic obstructive pulmonary disease. *Am J Respir Crit Care Med*. 1998; **157**(3 Pt 1): 785-90.
24. Mahler DA, Weinberg DH, Wells CK, Feinstein AR. The measurement of dyspnea. Contents, interobserver agreement, and physiologic correlates of two new clinical indexes. *Chest*. 1984; **85**(6): 751-8.
25. Bestall JC, Paul EA, Garrod R, Garnham R, Jones PW, Wedzicha JA. Usefulness of the Medical Research Council (MRC) dyspnoea scale as a measure of disability in patients with chronic obstructive pulmonary disease. *Thorax*. 1999; **54**(7): 581-6.
26. Kardos P, Wencker M, Glaab T, Vogelmeier C. Impact of salmeterol/fluticasone propionate versus salmeterol on exacerbations in severe chronic obstructive pulmonary disease. *Am J Respir Crit Care Med*. 2007; **175**(2): 144-9.
27. Akamatsu K, Yamagata T, Takahashi T, Miura K, Maeda S, Yamagata Y, et al. Improvement of pulmonary function and dyspnea by tiotropium in COPD patients using a transdermal beta(2)-agonist. *Pulmonary pharmacology & therapeutics*. 2007; **20**(6): 701-7.
28. Wedzicha JA, Bestall JC, Garrod R, Garnham R, Paul EA, Jones PW. Randomized controlled trial of pulmonary rehabilitation in severe chronic obstructive pulmonary disease patients, stratified with the MRC dyspnoea scale. *Eur Respir J*. 1998; **12**(2): 363-9.
29. Nishimura K, Izumi T, Tsukino M, Oga T. Dyspnea is a better predictor of 5-year survival than airway obstruction in patients with COPD. *Chest*. 2002; **121**(5): 1434-40.
30. Celli BR, Cote CG, Marin JM, Casanova C, Montes de Oca M, Mendez RA, et al. The body-mass index, airflow obstruction, dyspnea, and exercise capacity index in chronic obstructive pulmonary disease. *N Engl J Med*. 2004; **350**(10): 1005-12.
31. Dodd JW, Marns PL, Clark AL, Ingram KA, Fowler RP, Canavan JL, et al. The COPD Assessment Test (CAT): short- and medium-term response to pulmonary rehabilitation. *Copd*. 2012; **9**(4): 390-4.
32. Jones PW, Harding G, Berry P, Wiklund I, Chen WH, Kline Leidy N. Development and first validation of the COPD Assessment Test. *Eur Respir J*. 2009; **34**(3): 648-54.
33. Agusti A, Soler JJ, Molina J, Munoz MJ, Garcia-Losa M, Roset M, et al. Is the CAT questionnaire sensitive to changes in health status in patients with severe COPD exacerbations? *Copd*. 2012; **9**(5): 492-8.
34. Mackay AJ, Donaldson GC, Patel AR, Jones PW, Hurst JR, Wedzicha JA. Usefulness of the Chronic Obstructive Pulmonary Disease Assessment Test to evaluate severity of COPD exacerbations. *Am J Respir Crit Care Med*. 2012; **185**(11): 1218-24.
35. Jones PW, Harding G, Wiklund I, Berry P, Tabberer M, Yu R, et al. Tests of the responsiveness of the COPD assessment test following acute exacerbation and pulmonary rehabilitation. *Chest*. 2012; **142**(1): 134-40.

36. Ringbaek T, Martinez G, Lange P. A comparison of the assessment of quality of life with CAT, CCQ, and SGRQ in COPD patients participating in pulmonary rehabilitation. *Copd*. 2012; **9**(1): 12-5.
37. Wedzicha JA, Calverley PM, Seemungal TA, Hagan G, Ansari Z, Stockley RA. The prevention of chronic obstructive pulmonary disease exacerbations by salmeterol/fluticasone propionate or tiotropium bromide. *American journal of respiratory and critical care medicine*. 2008; **177**(1): 19-26.
38. Vogelmeier C, Hederer B, Glaab T, Schmidt H, Rutten-van Molken MP, Beeh KM, et al. Tiotropium versus salmeterol for the prevention of exacerbations of COPD. *N Engl J Med*. 2011; **364**(12): 1093-103.
39. Calverley PM, Anderson JA, Celli B, Ferguson GT, Jenkins C, Jones PW, et al. Salmeterol and fluticasone propionate and survival in chronic obstructive pulmonary disease. *N Engl J Med*. 2007; **356**(8): 775-89.
40. Tashkin DP, Celli B, Senn S, Burkhart D, Kesten S, Menjoge S, et al. A 4-year trial of tiotropium in chronic obstructive pulmonary disease. *N Engl J Med*. 2008; **359**(15): 1543-54.
41. Jenkins CR, Jones PW, Calverley PM, Celli B, Anderson JA, Ferguson GT, et al. Efficacy of salmeterol/fluticasone propionate by GOLD stage of chronic obstructive pulmonary disease: analysis from the randomised, placebo-controlled TORCH study. *Respir Res*. 2009; **10**: 59.
42. Decramer M, Celli B, Kesten S, Lystig T, Mehra S, Tashkin DP. Effect of tiotropium on outcomes in patients with moderate chronic obstructive pulmonary disease (UPLIFT): a prespecified subgroup analysis of a randomised controlled trial. *Lancet*. 2009; **374**(9696): 1171-8.
43. Barnes PJ. Distribution of receptor targets in the lung. *Proc Am Thorac Soc*. 2004; **1**(4): 345-51.
44. Burge PS, Calverley PM, Jones PW, Spencer S, Anderson JA, Maslen TK. Randomised, double blind, placebo controlled study of fluticasone propionate in patients with moderate to severe chronic obstructive pulmonary disease: the ISOLDE trial. *BMJ*. 2000; **320**(7245): 1297-303.
45. Calverley P, Pauwels R, Vestbo J, Jones P, Pride N, Gulsvik A, et al. Combined salmeterol and fluticasone in the treatment of chronic obstructive pulmonary disease: a randomised controlled trial. *Lancet*. 2003; **361**(9356): 449-56.
46. Yang IA, Clarke MS, Sim EH, Fong KM. Inhaled corticosteroids for stable chronic obstructive pulmonary disease. *Cochrane Database Syst Rev*. 2012; **7**: CD002991.
47. Zervas E, Samitas K, Gaga M, Beghe B, Fabbri LM. Inhaled corticosteroids in COPD: pros and cons. *Curr Drug Targets*. 2013; **14**(2): 192-224.
48. Nannini LJ, Lasserson TJ, Poole P. Combined corticosteroid and long-acting beta(2)-agonist in one inhaler versus long-acting beta(2)-agonists for chronic obstructive pulmonary disease. *Cochrane Database Syst Rev*. 2012; **9**: CD006829.
49. Drummond MB, Dasenbrook EC, Pitz MW, Murphy DJ, Fan E. Inhaled corticosteroids in patients with stable chronic obstructive pulmonary disease: a systematic review and meta-analysis. *JAMA*. 2008; **300**(20): 2407-16.
50. Salter M, Biggadike K, Matthews JL, West MR, Haase MV, Farrow SN, et al. Pharmacological properties of the enhanced-affinity glucocorticoid fluticasone furoate in vitro and in an in vivo model of respiratory inflammatory disease. *Am J Physiol Lung Cell Mol Physiol*. 2007; **293**(3): L660-7.
51. Biggadike K. Fluticasone furoate/fluticasone propionate - different drugs with different properties. *Clin Respir J*. 2011; **5**(3): 183-4.
52. Martinez FJ, Boscia J, Feldman G, Scott-Wilson C, Kilbride S, Fabbri L, et al. Fluticasone furoate/vilanterol (100/25; 200/25 mug) improves lung function in COPD: a randomised trial. *Respir Med*. 2013; **107**(4): 550-9.

53. Kerwin EM, Scott-Wilson C, Sanford L, Rennard S, Agusti A, Barnes N, et al. A randomised trial of fluticasone furoate/vilanterol (50/25 mug; 100/25 mug) on lung function in COPD. *Respir Med*. 2013; **107**(4): 560-9.
54. Boscia JA, Pudi KK, Zvarich MT, Sanford L, Siederer SK, Crim C. Effect of once-daily fluticasone furoate/vilanterol on 24-hour pulmonary function in patients with chronic obstructive pulmonary disease: a randomized, three-way, incomplete block, crossover study. *Clin Ther*. 2012; **34**(8): 1655-66 e5.
55. Allen A, Davis A, Hards K, Tombs L, Kempford R. Influence of renal and hepatic impairment on the pharmacokinetic and pharmacodynamic properties and tolerability of fluticasone furoate and vilanterol in combination. *Clin Ther*. 2012; **34**(12): 2316-32.
56. Miravittles M, Soler-Cataluna JJ, Calle M, Soriano JB. Treatment of COPD by clinical phenotypes: putting old evidence into clinical practice. *Eur Respir J*. 2013; **41**(6): 1252-6.
57. Han MK, Agusti A, Calverley PM, Celli BR, Criner G, Curtis JL, et al. Chronic obstructive pulmonary disease phenotypes: the future of COPD. *Am J Respir Crit Care Med*. 2010; **182**(5): 598-604.
58. Wenzel SE. Asthma phenotypes: the evolution from clinical to molecular approaches. *Nat Med*. 2012; **18**(5): 716-25.
59. Vanfleteren LE, Kocks JW, Stone IS, Breyer-Kohansal R, Greulich T, Lacedonia D, et al. Moving from the Oslerian paradigm to the post-genomic era: are asthma and COPD outdated terms? *Thorax*. 2013.
60. Rennard SI, Calverley PM, Goehring UM, Bredenbroeker D, Martinez FJ. Reduction of exacerbations by the PDE4 inhibitor roflumilast--the importance of defining different subsets of patients with COPD. *Respir Res*. 2011; **12**: 18.
61. Agusti A, Edwards LD, Rennard SI, MacNee W, Tal-Singer R, Miller BE, et al. Persistent systemic inflammation is associated with poor clinical outcomes in COPD: a novel phenotype. *PLoS One*. 2012; **7**(5): e37483.
62. Casanova C, Cote C, de Torres JP, Aguirre-Jaime A, Marin JM, Pinto-Plata V, et al. Inspiratory-to-total lung capacity ratio predicts mortality in patients with chronic obstructive pulmonary disease. *American journal of respiratory and critical care medicine*. 2005; **171**(6): 591-7.
63. Han MK, Kazerooni EA, Lynch DA, Liu LX, Murray S, Curtis JL, et al. Chronic obstructive pulmonary disease exacerbations in the COPD Gene study: associated radiologic phenotypes. *Radiology*. 2011; **261**(1): 274-82.
64. Miravittles M, Calle M, Soler-Cataluna JJ. Clinical phenotypes of COPD: identification, definition and implications for guidelines. *Arch Bronconeumol*. 2012; **48**(3): 86-98.
65. Leith DE, Brown R. Human lung volumes and the mechanisms that set them. *Eur Respir J*. 1999; **13**(2): 468-72.
66. Cosio M, Ghezzo H, Hogg JC, Corbin R, Loveland M, Dosman J, et al. The relations between structural changes in small airways and pulmonary-function tests. *N Engl J Med*. 1978; **298**(23): 1277-81.
67. Ferguson GT. Why does the lung hyperinflate? *Proc Am Thorac Soc*. 2006; **3**(2): 176-9.
68. Macklem PT. Therapeutic implications of the pathophysiology of COPD. *Eur Respir J*. 2010; **35**(3): 676-80.
69. O'Donnell CR, Bankier AA, Stiebellehner L, Reilly JJ, Brown R, Loring SH. Comparison of plethysmographic and helium dilution lung volumes: which is best for COPD? *Chest*. 2010; **137**(5): 1108-15.
70. Wanger J, Clausen JL, Coates A, Pedersen OF, Brusasco V, Burgos F, et al. Standardisation of the measurement of lung volumes. *Eur Respir J*. 2005; **26**(3): 511-22.
71. Gibson GJ. Pulmonary hyperinflation a clinical overview. *Eur Respir J*. 1996; **9**(12): 2640-9.

72. Rodenstein DO, Stanescu DC. Reassessment of lung volume measurement by helium dilution and by body plethysmography in chronic air-flow obstruction. *Am Rev Respir Dis.* 1982; **126**(6): 1040-4.
73. Rodenstein DO, Stanescu DC, Francis C. Demonstration of failure of body plethysmography in airway obstruction. *J Appl Physiol.* 1982; **52**(4): 949-54.
74. Rodenstein DO, Francis C, Stanescu DC. Airway closure in humans does not result in overestimation of plethysmographic lung volume. *Journal of applied physiology: respiratory, environmental and exercise physiology.* 1983; **55**(6): 1784-9.
75. Shore SA, Huk O, Mannix S, Martin JG. Effect of panting frequency on the plethysmographic determination of thoracic gas volume in chronic obstructive pulmonary disease. *Am Rev Respir Dis.* 1983; **128**(1): 54-9.
76. Clayton N. Lung function made easy: assessing lung size. *Chron Respir Dis.* 2007; **4**(3): 151-7.
77. Dykstra BJ, Scanlon PD, Kester MM, Beck KC, Enright PL. Lung volumes in 4,774 patients with obstructive lung disease. *Chest.* 1999; **115**(1): 68-74.
78. Deesomchok A, Webb KA, Forkert L, Lam YM, Ofir D, Jensen D, et al. Lung hyperinflation and its reversibility in patients with airway obstruction of varying severity. *Copd.* 2010; **7**(6): 428-37.
79. Ruppel GL. What is the clinical value of lung volumes? *Respiratory care.* 2012; **57**(1): 26-35; discussion -8.
80. Pare PD, Brooks LA, Bates J, Lawson LM, Nelems JM, Wright JL, et al. Exponential analysis of the lung pressure-volume curve as a predictor of pulmonary emphysema. *Am Rev Respir Dis.* 1982; **126**(1): 54-61.
81. Haluszka J, Chartrand DA, Grassino AE, Milic-Emili J. Intrinsic PEEP and arterial PCO<sub>2</sub> in stable patients with chronic obstructive pulmonary disease. *Am Rev Respir Dis.* 1990; **141**(5 Pt 1): 1194-7.
82. Thomas M, Decramer M, O'Donnell DE. No room to breathe: the importance of lung hyperinflation in COPD. *Primary care respiratory journal : journal of the General Practice Airways Group.* 2013; **22**(1): 101-11.
83. O'Donnell DE, Ora J, Webb KA, Laveneziana P, Jensen D. Mechanisms of activity-related dyspnea in pulmonary diseases. *Respiratory physiology & neurobiology.* 2009; **167**(1): 116-32.
84. Williams M, Cafarella P, Olds T, Petkov J, Frith P. Affective descriptors of the sensation of breathlessness are more highly associated with severity of impairment than physical descriptors in people with COPD. *Chest.* 2010; **138**(2): 315-22.
85. Martinez FJ, Foster G, Curtis JL, Criner G, Weinmann G, Fishman A, et al. Predictors of mortality in patients with emphysema and severe airflow obstruction. *Am J Respir Crit Care Med.* 2006; **173**(12): 1326-34.
86. Zafar MA, Tsuang W, Lach L, Eschenbacher W, Panos RJ. Dynamic hyperinflation correlates with exertional oxygen desaturation in patients with chronic obstructive pulmonary disease. *Lung.* 2013; **191**(2): 177-82.
87. Garcia-Rio F, Lores V, Mediano O, Rojo B, Hernanz A, Lopez-Collazo E, et al. Daily physical activity in patients with chronic obstructive pulmonary disease is mainly associated with dynamic hyperinflation. *Am J Respir Crit Care Med.* 2009; **180**(6): 506-12.
88. Yuan R, Hogg JC, Pare PD, Sin DD, Wong JC, Nakano Y, et al. Prediction of the rate of decline in FEV<sub>1</sub> in smokers using quantitative Computed Tomography. *Thorax.* 2009; **64**(11): 944-9.
89. Ozgur ES, Nayci SA, Ozge C, Tasdelen B. An integrated index combined by dynamic hyperinflation and exercise capacity in the prediction of morbidity and mortality in COPD. *Respiratory care.* 2012; **57**(9): 1452-9.
90. Zaman M, Mahmood S, Altayeh A. Low inspiratory capacity to total lung capacity ratio is a risk factor for chronic obstructive pulmonary disease exacerbation. *The American journal of the medical sciences.* 2010; **339**(5): 411-4.

91. Niewoehner DE, Collins D, Erbland ML. Relation of FEV(1) to clinical outcomes during exacerbations of chronic obstructive pulmonary disease. Department of Veterans Affairs Cooperative Study Group. *Am J Respir Crit Care Med*. 2000; **161**(4 Pt 1): 1201-5.
92. Garcia-Aymerich J, Farrero E, Felez MA, Izquierdo J, Marrades RM, Anto JM. Risk factors of readmission to hospital for a COPD exacerbation: a prospective study. *Thorax*. 2003; **58**(2): 100-5.
93. Mannino DM, Watt G, Hole D, Gillis C, Hart C, McConnachie A, et al. The natural history of chronic obstructive pulmonary disease. *Eur Respir J*. 2006; **27**(3): 627-43.
94. Boni E, Corda L, Franchini D, Chirolu P, Damiani GP, Pini L, et al. Volume effect and exertional dyspnoea after bronchodilator in patients with COPD with and without expiratory flow limitation at rest. *Thorax*. 2002; **57**(6): 528-32.
95. Man WD, Mustafa N, Nikolettou D, Kaul S, Hart N, Rafferty GF, et al. Effect of salmeterol on respiratory muscle activity during exercise in poorly reversible COPD. *Thorax*. 2004; **59**(6): 471-6.
96. Maltais F, Hamilton A, Marciniuk D, Hernandez P, Scirba FC, Richter K, et al. Improvements in symptom-limited exercise performance over 8 h with once-daily tiotropium in patients with COPD. *Chest*. 2005; **128**(3): 1168-78.
97. Cooper CB. The connection between chronic obstructive pulmonary disease symptoms and hyperinflation and its impact on exercise and function. *The American journal of medicine*. 2006; **119**(10 Suppl 1): 21-31.
98. O'Donnell DE, Parker CM. COPD exacerbations . 3: Pathophysiology. *Thorax*. 2006; **61**(4): 354-61.
99. Newton MF. Response of Lung Volumes to Inhaled Salbutamol in a Large Population of Patients With Severe Hyperinflation\*. *Chest*. 2002; **121**(4): 1042-50.
100. Mahler DA, Donohue JF, Barbee RA, Goldman MD, Gross NJ, Wisniewski ME, et al. Efficacy of salmeterol xinafoate in the treatment of COPD. *Chest*. 1999; **115**(4): 957-65.
101. Ayers ML, Mejia R, Ward J, Lentine T, Mahler DA. Effectiveness of salmeterol versus ipratropium bromide on exertional dyspnoea in COPD. *Eur Respir J*. 2001; **17**(6): 1132-7.
102. O'Donnell DE, Laveneziana P, Ora J, Webb KA, Lam YM, Ofir D. Evaluation of acute bronchodilator reversibility in patients with symptoms of GOLD stage I COPD. *Thorax*. 2009; **64**(3): 216-23.
103. O'Donnell DE, Scirba F, Celli B, Mahler DA, Webb KA, Kalberg CJ, et al. Effect of fluticasone propionate/salmeterol on lung hyperinflation and exercise endurance in COPD. *Chest*. 2006; **130**(3): 647-56.
104. Puente-Maestu L, Stringer WW. Hyperinflation and its management in COPD. *Int J Chron Obstruct Pulmon Dis*. 2006; **1**(4): 381-400.
105. Barr RG, Bluemke DA, Ahmed FS, Carr JJ, Enright PL, Hoffman EA, et al. Percent emphysema, airflow obstruction, and impaired left ventricular filling. *N Engl J Med*. 2010; **362**(3): 217-27.
106. Tanabe N, Muro S, Oguma T, Sato S, Kiyokawa H, Takahashi T, et al. Computed tomography assessment of pharmacological lung volume reduction induced by bronchodilators in COPD. *Copd*. 2012; **9**(4): 401-8.
107. Grau M, Barr RG, Lima JA, Hoffman EA, Bluemke DA, Carr JJ, et al. Percent emphysema and right ventricular structure and function: the multi-ethnic study of atherosclerosis-lung and multi-ethnic study of atherosclerosis-right ventricle studies. *Chest*. 2013; **144**(1): 136-44.
108. Rossi A, Polese G. Indacaterol: a comprehensive review. *Int J Chron Obstruct Pulmon Dis*. 2013; **8**: 353-63.
109. Beeh KM, Beier J. The short, the long and the "ultra-long": why duration of bronchodilator action matters in chronic obstructive pulmonary disease. *Adv Ther*. 2010; **27**(3): 150-9.

110. Wedzicha JA, Decramer M, Seemungal TA. The role of bronchodilator treatment in the prevention of exacerbations of COPD. *Eur Respir J*. 2012; **40**(6): 1545-54.
111. Wedzicha JA. Choice of bronchodilator therapy for patients with COPD. *N Engl J Med*. 2011; **364**(12): 1167-8.
112. O'Donnell DE, Lam M, Webb KA. Spirometric correlates of improvement in exercise performance after anticholinergic therapy in chronic obstructive pulmonary disease. *American journal of respiratory and critical care medicine*. 1999; **160**(2): 542-9.
113. O'Donnell DE, Lam M, Webb KA. Measurement of symptoms, lung hyperinflation, and endurance during exercise in chronic obstructive pulmonary disease. *Am J Respir Crit Care Med*. 1998; **158**(5 Pt 1): 1557-65.
114. Dusser D, Bravo ML, Iacono P. The effect of tiotropium on exacerbations and airflow in patients with COPD. *Eur Respir J*. 2006; **27**(3): 547-55.
115. Tashkin DP. Preventing and managing exacerbations in COPD--critical appraisal of the role of tiotropium. *Int J Chron Obstruct Pulmon Dis*. 2010; **5**: 41-53.
116. Vanfleteren LE, Spruit MA, Groenen M, Gaffron S, van Empel VP, Bruijnzeel PL, et al. Clusters of comorbidities based on validated objective measurements and systemic inflammation in patients with chronic obstructive pulmonary disease. *Am J Respir Crit Care Med*. 2013; **187**(7): 728-35.
117. Clini EM, Beghe B, Fabbri LM. Chronic obstructive pulmonary disease is just one component of the complex multimorbidities in patients with COPD. *Am J Respir Crit Care Med*. 2013; **187**(7): 668-71.
118. Friedman GD, Klatsky AL, Siegelaub AB. Lung function and risk of myocardial infarction and sudden cardiac death. *N Engl J Med*. 1976; **294**(20): 1071-5.
119. Ebi-Kryston KL, Hawthorne VM, Rose G, Shipley MJ, Gillis CR, Hole DJ, et al. Breathlessness, chronic bronchitis and reduced pulmonary function as predictors of cardiovascular disease mortality among men in England, Scotland and the United States. *Int J Epidemiol*. 1989; **18**(1): 84-8.
120. Ebi-Kryston KL. Respiratory symptoms and pulmonary function as predictors of 10-year mortality from respiratory disease, cardiovascular disease, and all causes in the Whitehall Study. *J Clin Epidemiol*. 1988; **41**(3): 251-60.
121. Gulsvik A, Hansteen V, Sivertssen E. Cardiac arrhythmias in patients with serious pulmonary diseases. *Scand J Respir Dis*. 1978; **59**(3): 154-9.
122. Hole DJ, Watt GC, Davey-Smith G, Hart CL, Gillis CR, Hawthorne VM. Impaired lung function and mortality risk in men and women: findings from the Renfrew and Paisley prospective population study. *BMJ*. 1996; **313**(7059): 711-5; discussion 5-6.
123. Sin DD, Anthonisen NR, Soriano JB, Agusti AG. Mortality in COPD: Role of comorbidities. *Eur Respir J*. 2006; **28**(6): 1245-57.
124. Curkendall SM, Lanes S, de Luise C, Stang MR, Jones JK, She D, et al. Chronic obstructive pulmonary disease severity and cardiovascular outcomes. *Eur J Epidemiol*. 2006; **21**(11): 803-13.
125. Leivseth L, Nilsen TI, Mai XM, Johnsen R, Langhammer A. Lung Function and Respiratory Symptoms in Association with Mortality: The HUNT Study. *Copd*. 2013.
126. Schunemann HJ, Dorn J, Grant BJ, Winkelstein W, Jr., Trevisan M. Pulmonary function is a long-term predictor of mortality in the general population: 29-year follow-up of the Buffalo Health Study. *Chest*. 2000; **118**(3): 656-64.
127. Sin DD, Wu L, Man SF. The relationship between reduced lung function and cardiovascular mortality: a population-based study and a systematic review of the literature. *Chest*. 2005; **127**(6): 1952-9.

128. Soriano JB, Rigo F, Guerrero D, Yanez A, Forteza JF, Frontera G, et al. High prevalence of undiagnosed airflow limitation in patients with cardiovascular disease. *Chest*. 2010; **137**(2): 333-40.
129. Salisbury AC, Reid KJ, Spertus JA. Impact of chronic obstructive pulmonary disease on post-myocardial infarction outcomes. *Am J Cardiol*. 2007; **99**(5): 636-41.
130. Behar S, Panosh A, Reicher-Reiss H, Zion M, Schlesinger Z, Goldbourt U. Prevalence and prognosis of chronic obstructive pulmonary disease among 5,839 consecutive patients with acute myocardial infarction. SPRINT Study Group. *Am J Med*. 1992; **93**(6): 637-41.
131. Feary JR, Rodrigues LC, Smith CJ, Hubbard RB, Gibson JE. Prevalence of major comorbidities in subjects with COPD and incidence of myocardial infarction and stroke: a comprehensive analysis using data from primary care. *Thorax*. 2010; **65**(11): 956-62.
132. Johnston AK, Mannino DM, Hagan GW, Davis KJ, Kiri VA. Relationship between lung function impairment and incidence or recurrence of cardiovascular events in a middle-aged cohort. *Thorax*. 2008; **63**(7): 599-605.
133. Curkendall SM, DeLuise C, Jones JK, Lanes S, Stang MR, Goehring E, Jr., et al. Cardiovascular disease in patients with chronic obstructive pulmonary disease, Saskatchewan Canada cardiovascular disease in COPD patients. *Ann Epidemiol*. 2006; **16**(1): 63-70.
134. Sidney S, Sorel M, Quesenberry CP, Jr., DeLuise C, Lanes S, Eisner MD. COPD and incident cardiovascular disease hospitalizations and mortality: Kaiser Permanente Medical Care Program. *Chest*. 2005; **128**(4): 2068-75.
135. Anthonisen NR, Connett JE, Kiley JP, Altose MD, Bailey WC, Buist AS, et al. Effects of smoking intervention and the use of an inhaled anticholinergic bronchodilator on the rate of decline of FEV1. The Lung Health Study. *JAMA*. 1994; **272**(19): 1497-505.
136. Lee HM, Lee J, Lee K, Luo Y, Sin DD, Wong ND. Relation between COPD severity and global cardiovascular risk in US adults. *Chest*. 2012; **142**(5): 1118-25.
137. Mullerova H, Agusti A, Erqou S, Mapel DW. Cardiovascular Comorbidity in Chronic Obstructive Pulmonary Disease: Systematic Literature Review. *Chest*. 2013.
138. Campo G, Guastaroba P, Marzocchi A, Santarelli A, Varani E, Vignali L, et al. Impact of Chronic Obstructive Pulmonary Disease on Long-Term Outcome after ST-segment elevation Myocardial Infarction receiving primary Percutaneous Coronary Intervention. *Chest*. 2013.
139. Wakabayashi K, Gonzalez MA, Delhaye C, Ben-Dor I, Maluenda G, Collins SD, et al. Impact of chronic obstructive pulmonary disease on acute-phase outcome of myocardial infarction. *Am J Cardiol*. 2010; **106**(3): 305-9.
140. Zhang JW, Zhou YJ, Yang Q, Yang SW, Nie B, Xu XH. Impact of chronic obstructive pulmonary diseases on outcomes and hospital days after percutaneous coronary intervention. *Angiology*. 2013; **64**(6): 430-4.
141. Anthonisen NR, Skeans MA, Wise RA, Manfreda J, Kanner RE, Connett JE. The effects of a smoking cessation intervention on 14.5-year mortality: a randomized clinical trial. *Ann Intern Med*. 2005; **142**(4): 233-9.
142. McGarvey LP, John M, Anderson JA, Zvarich M, Wise RA. Ascertainment of cause-specific mortality in COPD: operations of the TORCH Clinical Endpoint Committee. *Thorax*. 2007; **62**(5): 411-5.
143. McGarvey LP, Magder S, Burkhart D, Kesten S, Liu D, Manuel RC, et al. Cause-specific mortality adjudication in the UPLIFT((R)) COPD trial: Findings and recommendations. *Respir Med*. 2011.
144. Vilkmann S, Keistinen T, Tuuponen T, Kivela SL. Survival and cause of death among elderly chronic obstructive pulmonary disease patients after first admission to hospital. *Respiration*. 1997; **64**(4): 281-4.

145. Keistinen T, Tuuponen T, Kivela SL. Survival experience of the population needing hospital treatment for asthma or COPD at age 50-54 years. *Respir Med.* 1998; **92**(3): 568-72.
146. Engstrom G, Wollmer P, Hedblad B, Juul-Moller S, Valind S, Janzon L. Occurrence and prognostic significance of ventricular arrhythmia is related to pulmonary function: a study from "men born in 1914," Malmo, Sweden. *Circulation.* 2001; **103**(25): 3086-91.
147. Stavem K, Aaser E, Sandvik L, Bjornholt JV, Erikssen G, Thaulow E, et al. Lung function, smoking and mortality in a 26-year follow-up of healthy middle-aged males. *Eur Respir J.* 2005; **25**(4): 618-25.
148. Baillard C, Boussarsar M, Fosse JP, Girou E, Le Toumelin P, Cracco C, et al. Cardiac troponin I in patients with severe exacerbation of chronic obstructive pulmonary disease. *Intensive Care Med.* 2003; **29**(4): 584-9.
149. Chang CL, Robinson SC, Mills GD, Sullivan GD, Karalus NC, McLachlan JD, et al. Biochemical markers of cardiac dysfunction predict mortality in acute exacerbations of COPD. *Thorax.* 2011; **66**(9): 764-8.
150. Marcun R, Sustic A, Brguljan PM, Kadivec S, Farkas J, Kosnik M, et al. Cardiac biomarkers predict outcome after hospitalisation for an acute exacerbation of chronic obstructive pulmonary disease. *Int J Cardiol.* 2012.
151. Hoiseth AD, Neukamm A, Karlsson BD, Omland T, Brekke PH, Soyseth V. Elevated high-sensitivity cardiac troponin T is associated with increased mortality after acute exacerbation of chronic obstructive pulmonary disease. *Thorax.* 2011; **66**(9): 775-81.
152. Soyseth V, Bhatnagar R, Holmedahl NH, Neukamm A, Hoiseth AD, Hagve TA, et al. Acute exacerbation of COPD is associated with fourfold elevation of cardiac troponin T. *Heart.* 2012.
153. Patel AR, Kowlessar BS, Donaldson GC, Mackay AJ, Singh R, George SN, et al. Cardiovascular Risk, Myocardial Injury and Exacerbations of Chronic Obstructive Pulmonary Disease. *Am J Respir Crit Care Med.* 2013.
154. Rutten FH, Cramer MJ, Lammers JW, Grobbee DE, Hoes AW. Heart failure and chronic obstructive pulmonary disease: An ignored combination? *European journal of heart failure.* 2006; **8**(7): 706-11.
155. Mapel DW, Dedrick D, Davis K. Trends and cardiovascular co-morbidities of COPD patients in the Veterans Administration Medical System, 1991-1999. *Copd.* 2005; **2**(1): 35-41.
156. Engstrom G, Melander O, Hedblad B. Population-based study of lung function and incidence of heart failure hospitalisations. *Thorax.* 2010; **65**(7): 633-8.
157. Georgiopoulou VV, Kalogeropoulos AP, Psaty BM, Rodondi N, Bauer DC, Butler AB, et al. Lung function and risk for heart failure among older adults: the Health ABC Study. *Am J Med.* 2011; **124**(4): 334-41.
158. Redfield MM, Jacobsen SJ, Burnett JC, Jr., Mahoney DW, Bailey KR, Rodeheffer RJ. Burden of systolic and diastolic ventricular dysfunction in the community: appreciating the scope of the heart failure epidemic. *JAMA.* 2003; **289**(2): 194-202.
159. Hawkins NM, Petrie MC, Jhund PS, Chalmers GW, Dunn FG, McMurray JJ. Heart failure and chronic obstructive pulmonary disease: diagnostic pitfalls and epidemiology. *European journal of heart failure.* 2009; **11**(2): 130-9.
160. Jaakkola MS, Jaakkola JJ. Impact of smoke-free workplace legislation on exposures and health: possibilities for prevention. *Eur Respir J.* 2006; **28**(2): 397-408.
161. Eisner MD, Smith AK, Blanc PD. Bartenders' respiratory health after establishment of smoke-free bars and taverns. *JAMA.* 1998; **280**(22): 1909-14.
162. Goodman P, Agnew M, McCaffrey M, Paul G, Clancy L. Effects of the Irish smoking ban on respiratory health of bar workers and air quality in Dublin pubs. *Am J Respir Crit Care Med.* 2007; **175**(8): 840-5.



163. Ayres JG, Semple S, MacCalman L, Dempsey S, Hilton S, Hurley JF, et al. Bar workers' health and environmental tobacco smoke exposure (BHETSE): symptomatic improvement in bar staff following smoke-free legislation in Scotland. *Occup Environ Med*. 2009; **66**(5): 339-46.
164. Schoj V, Alderete M, Ruiz E, Hasdeu S, Linetzky B, Ferrante D. The impact of a 100% smoke-free law on the health of hospitality workers from the city of Neuquen, Argentina. *Tob Control*. 2010; **19**(2): 134-7.
165. Reijula JP, Johnsson TS, Kaleva PS, Reijula KE. Exposure to tobacco smoke and prevalence of symptoms decreased among Finnish restaurant workers after the smoke-free law. *Am J Ind Med*. 2012; **55**(1): 37-43.
166. Zheng P, Li W, Chapman S, Zhang Z, Gao J, Fu H. Workplace exposure to secondhand smoke and its association with respiratory symptoms--a cross-sectional study among workers in Shanghai. *Tob Control*. 2011; **20**(1): 58-63.
167. Menzies D, Nair A, Williamson PA, Schembri S, Al-Khairalla MZ, Barnes M, et al. Respiratory symptoms, pulmonary function, and markers of inflammation among bar workers before and after a legislative ban on smoking in public places. *JAMA*. 2006; **296**(14): 1742-8.
168. Naiman A, Glazier RH, Moineddin R. Association of anti-smoking legislation with rates of hospital admission for cardiovascular and respiratory conditions. *CMAJ*. 2010; **182**(8): 761-7.
169. Kent BD, Sulaiman I, Nicholson TT, Lane SJ, Moloney ED. Acute Pulmonary Admissions Following Implementation of a National Workplace Smoking Ban. *Chest*. 2012.
170. Mackay DF, Irfan MO, Haw S, Pell JP. Meta-analysis of the effect of comprehensive smoke-free legislation on acute coronary events. *Heart*. 2010; **96**(19): 1525-30.
171. McDonnell WF, Stewart PW, Smith MV, Pan WK, Pan J. Ozone-induced respiratory symptoms: exposure-response models and association with lung function. *Eur Respir J*. 1999; **14**(4): 845-53.
172. Eisner MD, Anthonisen N, Coultas D, Kuenzli N, Perez-Padilla R, Postma D, et al. An official American Thoracic Society public policy statement: Novel risk factors and the global burden of chronic obstructive pulmonary disease. *Am J Respir Crit Care Med*. 2010; **182**(5): 693-718.
173. Henrotin JB, Zeller M, Lorgis L, Cottin Y, Giroud M, Bejot Y. Evidence of the role of short-term exposure to ozone on ischaemic cerebral and cardiac events: the Dijon Vascular Project (DIVA). *Heart*. 2010; **96**(24): 1990-6.
174. Bhaskaran K, Wilkinson P, Smeeth L. Cardiovascular consequences of air pollution: what are the mechanisms? *Heart*. 2011; **97**(7): 519-20.
175. Brook RD, Franklin B, Cascio W, Hong Y, Howard G, Lipsett M, et al. Air pollution and cardiovascular disease: a statement for healthcare professionals from the Expert Panel on Population and Prevention Science of the American Heart Association. *Circulation*. 2004; **109**(21): 2655-71.
176. Hawkins NM, Petrie MC, Macdonald MR, Jhund PS, Fabbri LM, Wikstrand J, et al. Heart failure and chronic obstructive pulmonary disease the quandary of Beta-blockers and Beta-agonists. *J Am Coll Cardiol*. 2011; **57**(21): 2127-38.
177. Rutten FH, Groenwold RH, Sachs AP, Grobbee DE, Hoes AW. beta-Blockers and All-Cause Mortality in Adults with Episodes of Acute Bronchitis: An Observational Study. *PLoS One*. 2013; **8**(6): e67122.
178. Etminan M, Jafari S, Carleton B, FitzGerald JM. Beta-blocker use and COPD mortality: a systematic review and meta-analysis. *BMC Pulm Med*. 2012; **12**: 48.
179. Salpeter S, Ormiston T, Salpeter E. Cardioselective beta-blockers for chronic obstructive pulmonary disease. *Cochrane Database Syst Rev*. 2005; (4): CD003566.
180. Mentz RJ, Wojdyla D, Fiuzat M, Chiswell K, Fonarow GC, O'Connor CM. Association of beta-blocker use and selectivity with outcomes in patients with heart

- failure and chronic obstructive pulmonary disease (from OPTIMIZE-HF). *Am J Cardiol.* 2013; **111**(4): 582-7.
181. Olenchock BA, Fonarow GG, Pan W, Hernandez A, Cannon CP. Current use of beta blockers in patients with reactive airway disease who are hospitalized with acute coronary syndromes. *Am J Cardiol.* 2009; **103**(3): 295-300.
182. Reed RM, Eberlein M, Girgis RE, Hashmi S, Iacono A, Jones S, et al. Coronary artery disease is under-diagnosed and under-treated in advanced lung disease. *Am J Med.* 2012; **125**(12): 1228 e13- e22.
183. Bang KM, Gergen PJ, Kramer R, Cohen B. The effect of pulmonary impairment on all-cause mortality in a national cohort. *Chest.* 1993; **103**(2): 536-40.
184. Tockman MS, Pearson JD, Fleg JL, Metter EJ, Kao SY, Rampal KG, et al. Rapid decline in FEV1. A new risk factor for coronary heart disease mortality. *American journal of respiratory and critical care medicine.* 1995; **151**(2 Pt 1): 390-8.
185. Nussbaumer-Ochsner Y, Rabe KF. Systemic manifestations of COPD. *Chest.* 2011; **139**(1): 165-73.
186. Alexander RW. Inflammation and coronary artery disease. *N Engl J Med.* 1994; **331**(7): 468-9.
187. Ross R. The pathogenesis of atherosclerosis: a perspective for the 1990s. *Nature.* 1993; **362**(6423): 801-9.
188. Tacke F, Alvarez D, Kaplan TJ, Jakubzick C, Spanbroek R, Llodra J, et al. Monocyte subsets differentially employ CCR2, CCR5, and CX3CR1 to accumulate within atherosclerotic plaques. *J Clin Invest.* 2007; **117**(1): 185-94.
189. van der Wal AC, Becker AE, van der Loos CM, Das PK. Site of intimal rupture or erosion of thrombosed coronary atherosclerotic plaques is characterized by an inflammatory process irrespective of the dominant plaque morphology. *Circulation.* 1994; **89**(1): 36-44.
190. Libby P, Ridker PM, Hansson GK. Progress and challenges in translating the biology of atherosclerosis. *Nature.* 2011; **473**(7347): 317-25.
191. Andersson J, Libby P, Hansson GK. Adaptive immunity and atherosclerosis. *Clin Immunol.* 2010; **134**(1): 33-46.
192. Liuzzo G, Biasucci LM, Gallimore JR, Grillo RL, Rebuffi AG, Pepys MB, et al. The prognostic value of C-reactive protein and serum amyloid a protein in severe unstable angina. *N Engl J Med.* 1994; **331**(7): 417-24.
193. Liuzzo G, Biasucci LM, Rebuffi AG, Gallimore JR, Caligiuri G, Lanza GA, et al. Plasma protein acute-phase response in unstable angina is not induced by ischemic injury. *Circulation.* 1996; **94**(10): 2373-80.
194. Ridker PM, Cushman M, Stampfer MJ, Tracy RP, Hennekens CH. Inflammation, aspirin, and the risk of cardiovascular disease in apparently healthy men. *N Engl J Med.* 1997; **336**(14): 973-9.
195. Kuller LH, Tracy RP, Shaten J, Meilahn EN. Relation of C-reactive protein and coronary heart disease in the MRFIT nested case-control study. Multiple Risk Factor Intervention Trial. *Am J Epidemiol.* 1996; **144**(6): 537-47.
196. Pauca AL, O'Rourke MF, Kon ND. Prospective Evaluation of a Method for Estimating Ascending Aortic Pressure From the Radial Artery Pressure Waveform. *Hypertension.* 2001; **38**(4): 932-7.
197. Laurent S, Boutouyrie P, Asmar R, Gautier I, Laloux B, Guize L, et al. Aortic stiffness is an independent predictor of all-cause and cardiovascular mortality in hypertensive patients. *Hypertension.* 2001; **37**(5): 1236-41.
198. Cruickshank K. Aortic Pulse-Wave Velocity and Its Relationship to Mortality in Diabetes and Glucose Intolerance: An Integrated Index of Vascular Function? *Circulation.* 2002; **106**(16): 2085-90.
199. Meaume S, Benetos A, Henry OF, Rudnichi A, Safar ME. Aortic pulse wave velocity predicts cardiovascular mortality in subjects >70 years of age. *Arterioscler Thromb Vasc Biol.* 2001; **21**(12): 2046-50.

200. Weber T, Auer J, O'Rourke MF, Kvas E, Lassnig E, Berent R, et al. Arterial stiffness, wave reflections, and the risk of coronary artery disease. *Circulation*. 2004; **109**(2): 184-9.
201. Sutton-Tyrrell K, Najjar SS, Boudreau RM, Venkitachalam L, Kupelian V, Simonsick EM, et al. Elevated aortic pulse wave velocity, a marker of arterial stiffness, predicts cardiovascular events in well-functioning older adults. *Circulation*. 2005; **111**(25): 3384-90.
202. Willum-Hansen T, Staessen JA, Torp-Pedersen C, Rasmussen S, Thijs L, Ibsen H, et al. Prognostic value of aortic pulse wave velocity as index of arterial stiffness in the general population. *Circulation*. 2006; **113**(5): 664-70.
203. Roman MJ, Devereux RB, Schwartz JE, Lockshin MD, Paget SA, Davis A, et al. Arterial stiffness in chronic inflammatory diseases. *Hypertension*. 2005; **46**(1): 194-9.
204. Selzer F, Sutton-Tyrrell K, Fitzgerald S, Tracy R, Kuller L, Manzi S. Vascular stiffness in women with systemic lupus erythematosus. *Hypertension*. 2001; **37**(4): 1075-82.
205. Kappagoda CT, Amsterdam EA. Another look at the results of the JUPITER trial. *Am J Cardiol*. 2009; **104**(11): 1603-5.
206. Ridker PM. Testing the inflammatory hypothesis of atherothrombosis: scientific rationale for the cardiovascular inflammation reduction trial (CIRT). *J Thromb Haemost*. 2009; **7 Suppl 1**: 332-9.
207. Fabbri LM, Romagnoli M, Corbetta L, Casoni G, Busljetic K, Turato G, et al. Differences in airway inflammation in patients with fixed airflow obstruction due to asthma or chronic obstructive pulmonary disease. *American journal of respiratory and critical care medicine*. 2003; **167**(3): 418-24.
208. Keatings VM, Barnes PJ. Granulocyte activation markers in induced sputum: comparison between chronic obstructive pulmonary disease, asthma, and normal subjects. *American journal of respiratory and critical care medicine*. 1997; **155**(2): 449-53.
209. Eid AA, Ionescu AA, Nixon LS, Lewis-Jenkins V, Matthews SB, Griffiths TL, et al. Inflammatory response and body composition in chronic obstructive pulmonary disease. *American journal of respiratory and critical care medicine*. 2001; **164**(8 Pt 1): 1414-8.
210. Broekhuizen R, Wouters EF, Creutzberg EC, Schols AM. Raised CRP levels mark metabolic and functional impairment in advanced COPD. *Thorax*. 2006; **61**(1): 17-22.
211. Saetta M, Di Stefano A, Maestrelli P, Ferrareso A, Drigo R, Potena A, et al. Activated T-lymphocytes and macrophages in bronchial mucosa of subjects with chronic bronchitis. *Am Rev Respir Dis*. 1993; **147**(2): 301-6.
212. Schmidt MI, Duncan BB, Sharrett AR, Lindberg G, Savage PJ, Offenbacher S, et al. Markers of inflammation and prediction of diabetes mellitus in adults (Atherosclerosis Risk in Communities study): a cohort study. *Lancet*. 1999; **353**(9165): 1649-52.
213. van Eeden SF, Tan WC, Suwa T, Mukae H, Terashima T, Fujii T, et al. Cytokines involved in the systemic inflammatory response induced by exposure to particulate matter air pollutants (PM<sub>10</sub>). *American journal of respiratory and critical care medicine*. 2001; **164**(5): 826-30.
214. Terashima T, Wiggs B, English D, Hogg JC, van Eeden SF. Phagocytosis of small carbon particles (PM<sub>10</sub>) by alveolar macrophages stimulates the release of polymorphonuclear leukocytes from bone marrow. *American journal of respiratory and critical care medicine*. 1997; **155**(4): 1441-7.
215. Smith RM, Traber LD, Traber DL, Spragg RG. Pulmonary deposition and clearance of aerosolized alpha-1-proteinase inhibitor administered to dogs and to sheep. *J Clin Invest*. 1989; **84**(4): 1145-54.

216. Hubbard RC, Brantly ML, Sellers SE, Mitchell ME, Crystal RG. Anti-neutrophil-elastase defenses of the lower respiratory tract in alpha 1-antitrypsin deficiency directly augmented with an aerosol of alpha 1-antitrypsin. *Ann Intern Med.* 1989; **111**(3): 206-12.
217. Stockley RA, Mistry M, Bradwell AR, Burnett D. A study of plasma proteins in the sol phase of sputum from patients with chronic bronchitis. *Thorax.* 1979; **34**(6): 777-82.
218. Sinden NJ, Stockley RA. Systemic inflammation and comorbidity in COPD: a result of 'overspill' of inflammatory mediators from the lungs? Review of the evidence. *Thorax.* 2010; **65**(10): 930-6.
219. Coulson JM, Rudd JH, Duckers JM, Rees JI, Shale DJ, Bolton CE, et al. Excessive aortic inflammation in chronic obstructive pulmonary disease: an 18F-FDG PET pilot study. *J Nucl Med.* 2010; **51**(9): 1357-60.
220. Skeletal muscle dysfunction in chronic obstructive pulmonary disease. A statement of the American Thoracic Society and European Respiratory Society. *Am J Respir Crit Care Med.* 1999; **159**(4 Pt 2): S1-40.
221. Bolton CE, Ionescu AA, Shiels KM, Pettit RJ, Edwards PH, Stone MD, et al. Associated loss of fat-free mass and bone mineral density in chronic obstructive pulmonary disease. *Am J Respir Crit Care Med.* 2004; **170**(12): 1286-93.
222. Thomsen M, Dahl M, Lange P, Vestbo J, Nordestgaard BG. Inflammatory biomarkers and comorbidities in chronic obstructive pulmonary disease. *Am J Respir Crit Care Med.* 2012; **186**(10): 982-8.
223. Mills NL, Miller JJ, Anand A, Robinson SD, Frazer GA, Anderson D, et al. Increased arterial stiffness in patients with chronic obstructive pulmonary disease: a mechanism for increased cardiovascular risk. *Thorax.* 2008; **63**(4): 306-11.
224. Zureik M, Benetos A, Neukirch C, Courbon D, Bean K, Thomas F, et al. Reduced pulmonary function is associated with central arterial stiffness in men. *American journal of respiratory and critical care medicine.* 2001; **164**(12): 2181-5.
225. Mottram PM, Haluska BA, Leano R, Carlier S, Case C, Marwick TH. Relation of arterial stiffness to diastolic dysfunction in hypertensive heart disease. *Heart.* 2005; **91**(12): 1551-6.
226. Sabit R, Bolton CE, Edwards PH, Pettit RJ, Evans WD, McEniery CM, et al. Arterial stiffness and osteoporosis in chronic obstructive pulmonary disease. *Am J Respir Crit Care Med.* 2007; **175**(12): 1259-65.
227. McAllister DA, Maclay JD, Mills NL, Mair G, Miller J, Anderson D, et al. Arterial stiffness is independently associated with emphysema severity in patients with chronic obstructive pulmonary disease. *American journal of respiratory and critical care medicine.* 2007; **176**(12): 1208-14.
228. Paulus WJ, Tschope C. A novel paradigm for heart failure with preserved ejection fraction: comorbidities drive myocardial dysfunction and remodeling through coronary microvascular endothelial inflammation. *J Am Coll Cardiol.* 2013; **62**(4): 263-71.
229. Nakamori S, Onishi K, Ishida M, Nakajima H, Yamada T, Nagata M, et al. Myocardial perfusion reserve is impaired in patients with chronic obstructive pulmonary disease: a comparison to current smokers. *European heart journal cardiovascular Imaging.* 2013.
230. Oswald-Mammosser M, Weitzenblum E, Quoix E, Moser G, Chaouat A, Charpentier C, et al. Prognostic factors in COPD patients receiving long-term oxygen therapy. Importance of pulmonary artery pressure. *Chest.* 1995; **107**(5): 1193-8.
231. Falk JA, Kadiev S, Criner GJ, Scharf SM, Minai OA, Diaz P. Cardiac disease in chronic obstructive pulmonary disease. *Proc Am Thorac Soc.* 2008; **5**(4): 543-8.
232. Fishman AP. Hypoxia on the pulmonary circulation. How and where it acts. *Circ Res.* 1976; **38**(4): 221-31.
233. Macnee W. Right heart function in COPD. *Semin Respir Crit Care Med.* 2010; **31**(3): 295-312.

234. Peinado VI, Pizarro S, Barbera JA. Pulmonary vascular involvement in COPD. *Chest*. 2008; **134**(4): 808-14.
235. Scharf SM. Hemodynamic Characterization of Patients with Severe Emphysema. *American journal of respiratory and critical care medicine*. 2002; **166**(3): 314-22.
236. Chaouat A, Bugnet AS, Kadaoui N, Schott R, Enache I, Ducolone A, et al. Severe pulmonary hypertension and chronic obstructive pulmonary disease. *Am J Respir Crit Care Med*. 2005; **172**(2): 189-94.
237. Fletcher EC, Levin DC. Cardiopulmonary hemodynamics during sleep in subjects with chronic obstructive pulmonary disease. The effect of short- and long-term oxygen. *Chest*. 1984; **85**(1): 6-14.
238. Abraham AS, Cole RB, Green ID, Hedworth-Whitty RB, Clarke SW, Bishop JM. Factors contributing to the reversible pulmonary hypertension of patients with acute respiratory failure studies by serial observations during recovery. *Circ Res*. 1969; **24**(1): 51-60.
239. Zakyntinos E, Daniil Z, Papanikolaou J, Makris D. Pulmonary hypertension in COPD: pathophysiology and therapeutic targets. *Curr Drug Targets*. 2011; **12**(4): 501-13.
240. Weitzenblum E. Chronic cor pulmonale. *Heart*. 2003; **89**(2): 225-30.
241. Boussuges A, Pinet C, Molenat F, Burnet H, Ambrosi P, Badier M, et al. Left atrial and ventricular filling in chronic obstructive pulmonary disease. An echocardiographic and Doppler study. *American journal of respiratory and critical care medicine*. 2000; **162**(2 Pt 1): 670-5.
242. Halley CM, Houghtaling PL, Khalil MK, Thomas JD, Jaber WA. Mortality rate in patients with diastolic dysfunction and normal systolic function. *Arch Intern Med*. 2011; **171**(12): 1082-7.
243. Sabit R, Bolton CE, Fraser AG, Edwards JM, Edwards PH, Ionescu AA, et al. Sub-clinical left and right ventricular dysfunction in patients with COPD. *Respir Med*. 2010; **104**(8): 1171-8.
244. Funk GC, Lang I, Schenk P, Valipour A, Hartl S, Burghuber OC. Left ventricular diastolic dysfunction in patients with COPD in the presence and absence of elevated pulmonary arterial pressure. *Chest*. 2008; **133**(6): 1354-9.
245. Chaouat A, Naeije R, Weitzenblum E. Pulmonary hypertension in COPD. *Eur Respir J*. 2008; **32**(5): 1371-85.
246. Butler J. The heart is not always in good hands. *Chest*. 1990; **97**(2): 453-60.
247. Malerba M, Ragnoli B, Salameh M, Sennino G, Sorlini ML, Radaeli A, et al. Sub-clinical left ventricular diastolic dysfunction in early stage of chronic obstructive pulmonary disease. *Journal of biological regulators and homeostatic agents*. 2011; **25**(3): 443-51.
248. Vonk Noordegraaf A, Marcus JT, Roseboom B, Postmus PE, Faes TJ, de Vries PM. The effect of right ventricular hypertrophy on left ventricular ejection fraction in pulmonary emphysema. *Chest*. 1997; **112**(3): 640-5.
249. Lopez-Sanchez M, Munoz-Esquerre M, Huertas D, Gonzalez-Costello J, Ribas J, Manresa F, et al. High Prevalence of Left Ventricle Diastolic Dysfunction in Severe COPD Associated with A Low Exercise Capacity: A Cross-Sectional Study. *PLoS One*. 2013; **8**(6): e68034.
250. Vassaux C, Torre-Bouscoulet L, Zeineldine S, Cortopassi F, Paz-Diaz H, Celli BR, et al. Effects of hyperinflation on the oxygen pulse as a marker of cardiac performance in COPD. *Eur Respir J*. 2008; **32**(5): 1275-82.
251. Watz H, Waschki B, Meyer T, Kretschmar G, Kirsten A, Claussen M, et al. Decreasing cardiac chamber sizes and associated heart dysfunction in COPD: role of hyperinflation. *Chest*. 2010; **138**(1): 32-8.
252. Jorgensen K, Muller MF, Nel J, Upton RN, Houtz E, Ricksten SE. Reduced intrathoracic blood volume and left and right ventricular dimensions in patients with severe emphysema: an MRI study. *Chest*. 2007; **131**(4): 1050-7.

253. Smith BM, Prince MR, Hoffman EA, Bluemke DA, Liu CY, Rabinowitz D, et al. Impaired Left Ventricular Filling in COPD and Emphysema: Is it the heart or the lungs?: The Multi-Ethnic Study of Atherosclerosis (MESA) COPD Study. *Chest*. 2013.
254. Anderson WJ, Lipworth BJ, Rekhraj S, Struthers AD, George J. Left ventricular hypertrophy in COPD without hypoxemia: the elephant in the room? *Chest*. 2013; **143**(1): 91-7.
255. Smith BM, Kawut SM, Bluemke DA, Basner RC, Gomes AS, Hoffman E, et al. Pulmonary hyperinflation and left ventricular mass: the Multi-Ethnic Study of Atherosclerosis COPD Study. *Circulation*. 2013; **127**(14): 1503-11, 11e1-6.
256. Mancia G, Dell'Oro R, Quarti-Trevano F, Scopelliti F, Grassi G. Angiotensin-sympathetic system interactions in cardiovascular and metabolic disease. *J Hypertens Suppl*. 2006; **24**(1): S51-6.
257. Boutouyrie P, Lacolley P, Girerd X, Beck L, Safar M, Laurent S. Sympathetic activation decreases medium-sized arterial compliance in humans. *Am J Physiol*. 1994; **267**(4 Pt 2): H1368-76.
258. Swierblewska E, Hering D, Kara T, Kunicka K, Kruszewski P, Bieniaszewski L, et al. An independent relationship between muscle sympathetic nerve activity and pulse wave velocity in normal humans. *J Hypertens*. 2010; **28**(5): 979-84.
259. Grassi G. Sympathetic overdrive as an independent predictor of left ventricular hypertrophy: prospective evidence. *J Hypertens*. 2006; **24**(5): 815-7.
260. Corbo GM, Inchingolo R, Sgueglia GA, Lanza G, Valente S. C-reactive protein, lung hyperinflation and heart rate variability in chronic obstructive pulmonary disease --a pilot study. *Copd*. 2013; **10**(2): 200-7.
261. Volterrani M, Scalvini S, Mazzuero G, Lanfranchi P, Colombo R, Clark AL, et al. Decreased heart rate variability in patients with chronic obstructive pulmonary disease. *Chest*. 1994; **106**(5): 1432-7.
262. Andreas S, Anker SD, Scanlon PD, Somers VK. Neurohumoral activation as a link to systemic manifestations of chronic lung disease. *Chest*. 2005; **128**(5): 3618-24.
263. Jolley CJ, Luo YM, Steier J, Reilly C, Seymour J, Lunt A, et al. Neural respiratory drive in healthy subjects and in COPD. *Eur Respir J*. 2009; **33**(2): 289-97.
264. O'Donnell CJ, Nabel EG. Genomics of cardiovascular disease. *N Engl J Med*. 2011; **365**(22): 2098-109.
265. Todd JL, Goldstein DB, Ge D, Christie J, Palmer SM. The state of genome-wide association studies in pulmonary disease: a new perspective. *Am J Respir Crit Care Med*. 2011; **184**(8): 873-80.
266. Churg A, Zhou S, Wright JL. Matrix Metalloproteases in COPD. *Eur Respir J*. 2011.
267. Abilleira S, Bevan S, Markus HS. The role of genetic variants of matrix metalloproteinases in coronary and carotid atherosclerosis. *J Med Genet*. 2006; **43**(12): 897-901.
268. Wang J, Xu D, Wu X, Zhou C, Wang H, Guo Y, et al. Polymorphisms of matrix metalloproteinases in myocardial infarction: a meta-analysis. *Heart*. 2011; **97**(19): 1542-6.
269. Singh N, Sinha N, Kumar S, Pandey CM, Agrawal S. Glutathione S-transferase gene polymorphism as a susceptibility factor for acute myocardial infarction and smoking in the North Indian population. *Cardiology*. 2011; **118**(1): 16-21.
270. Wang YX, Ulu A, Zhang LN, Hammock B. Soluble epoxide hydrolase in atherosclerosis. *Curr Atheroscler Rep*. 2010; **12**(3): 174-83.
271. Harman D. Free radical theory of aging: an update: increasing the functional life span. *Ann N Y Acad Sci*. 2006; **1067**: 10-21.
272. Samani NJ, van der Harst P. Biological ageing and cardiovascular disease. *Heart*. 2008; **94**(5): 537-9.

273. Mainous AG, 3rd, Codd V, Diaz VA, Schoepf UJ, Everett CJ, Player MS, et al. Leukocyte telomere length and coronary artery calcification. *Atherosclerosis*. 2010; **210**(1): 262-7.
274. Oh H, Wang SC, Prahash A, Sano M, Moravec CS, Taffet GE, et al. Telomere attrition and Chk2 activation in human heart failure. *Proc Natl Acad Sci U S A*. 2003; **100**(9): 5378-83.
275. Savale L, Chaouat A, Bastuji-Garin S, Marcos E, Boyer L, Maitre B, et al. Shortened telomeres in circulating leukocytes of patients with chronic obstructive pulmonary disease. *Am J Respir Crit Care Med*. 2009; **179**(7): 566-71.
276. Tsuji T, Aoshiba K, Nagai A. Alveolar cell senescence in patients with pulmonary emphysema. *Am J Respir Crit Care Med*. 2006; **174**(8): 886-93.
277. Lee SH, Goswami S, Grudo A, Song LZ, Bandi V, Goodnight-White S, et al. Antielastin autoimmunity in tobacco smoking-induced emphysema. *Nat Med*. 2007; **13**(5): 567-9.
278. De Meyer T, Rietzschel ER, De Buyzere ML, Van Criekinge W, Bekaert S. Telomere length and cardiovascular aging: the means to the ends? *Ageing Res Rev*. 2011; **10**(2): 297-303.
279. Madonna R, De Caterina R, Willerson JT, Geng YJ. Biologic function and clinical potential of telomerase and associated proteins in cardiovascular tissue repair and regeneration. *Eur Heart J*. 2011; **32**(10): 1190-6.
280. Wu J, Sin DD. Improved patient outcome with smoking cessation: when is it too late? *Int J Chron Obstruct Pulmon Dis*. 2011; **6**: 259-67.
281. Continuous or nocturnal oxygen therapy in hypoxemic chronic obstructive lung disease: a clinical trial. Nocturnal Oxygen Therapy Trial Group. *Ann Intern Med*. 1980; **93**(3): 391-8.
282. Long term domiciliary oxygen therapy in chronic hypoxic cor pulmonale complicating chronic bronchitis and emphysema. Report of the Medical Research Council Working Party. *Lancet*. 1981; **1**(8222): 681-6.
283. Stoller JK, Panos RJ, Krachman S, Doherty DE, Make B. Oxygen therapy for patients with COPD: current evidence and the long-term oxygen treatment trial. *Chest*. 2010; **138**(1): 179-87.
284. Puhan M, Scharplatz M, Troosters T, Walters EH, Steurer J. Pulmonary rehabilitation following exacerbations of chronic obstructive pulmonary disease. *Cochrane Database Syst Rev*. 2009; (1): CD005305.
285. Moore RL. Cellular adaptations of the heart muscle to exercise training. *Ann Med*. 1998; **30 Suppl 1**: 46-53.
286. Gale NS, Duckers JM, Enright S, Cockcroft JR, Shale DJ, Bolton CE. Does pulmonary rehabilitation address cardiovascular risk factors in patients with COPD? *BMC Pulm Med*. 2011; **11**: 20.
287. Verdecchia P, Gentile G, Angeli F, Mazzotta G, Mancia G, Reboldi G. Influence of blood pressure reduction on composite cardiovascular endpoints in clinical trials. *J Hypertens*. 2010; **28**(7): 1356-65.
288. Gigliotti F, Coli C, Bianchi R, Romagnoli I, Lanini B, Binazzi B, et al. Exercise training improves exertional dyspnea in patients with COPD: evidence of the role of mechanical factors. *Chest*. 2003; **123**(6): 1794-802.
289. Calverley PM, Anderson JA, Celli B, Ferguson GT, Jenkins C, Jones PW, et al. Cardiovascular events in patients with COPD: TORCH study results. *Thorax*. 2010; **65**(8): 719-25.
290. Celli B, Decramer M, Kesten S, Liu D, Mehra S, Tashkin DP. Mortality in the 4-year trial of tiotropium (UPLIFT) in patients with chronic obstructive pulmonary disease. *Am J Respir Crit Care Med*. 2009; **180**(10): 948-55.
291. Gizycki MJ, Hattotuwa KL, Barnes N, Jeffery PK. Effects of fluticasone propionate on inflammatory cells in COPD: an ultrastructural examination of endobronchial biopsy tissue. *Thorax*. 2002; **57**(9): 799-803.

292. Hattotuwa KL, Gizycki MJ, Ansari TW, Jeffery PK, Barnes NC. The effects of inhaled fluticasone on airway inflammation in chronic obstructive pulmonary disease: a double-blind, placebo-controlled biopsy study. *Am J Respir Crit Care Med*. 2002; **165**(12): 1592-6.
293. Confalonieri M, Mainardi E, Della Porta R, Bernorio S, Gandola L, Beghe B, et al. Inhaled corticosteroids reduce neutrophilic bronchial inflammation in patients with chronic obstructive pulmonary disease. *Thorax*. 1998; **53**(7): 583-5.
294. Tang YJ, Wang K, Yuan T, Qiu T, Xiao J, Yi Q, et al. Salmeterol/fluticasone treatment reduces circulating C-reactive protein level in patients with stable chronic obstructive pulmonary disease. *Chin Med J (Engl)*. 2010; **123**(13): 1652-7.
295. Man SF, Sin DD. Effects of corticosteroids on systemic inflammation in chronic obstructive pulmonary disease. *Proc Am Thorac Soc*. 2005; **2**(1): 78-82.
296. Sin DD, Man SF, Marciniuk DD, Ford G, FitzGerald M, Wong E, et al. The effects of fluticasone with or without salmeterol on systemic biomarkers of inflammation in chronic obstructive pulmonary disease. *Am J Respir Crit Care Med*. 2008; **177**(11): 1207-14.
297. Vlachopoulos C, Aznaouridis K, Stefanadis C. Prediction of cardiovascular events and all-cause mortality with arterial stiffness: a systematic review and meta-analysis. *Journal of the American College of Cardiology*. 2010; **55**(13): 1318-27.
298. Rabe KF. Update on roflumilast, a phosphodiesterase 4 inhibitor for the treatment of chronic obstructive pulmonary disease. *Br J Pharmacol*. 2011; **163**(1): 53-67.
299. Huennemeyer A, Nassr N, Bredenbroker D, Lahu G. Supra-therapeutic doses of roflumilast have no effect on cardiac repolarization in healthy subjects. *Expert Opin Drug Saf*. 2011; **10**(4): 509-19.
300. Lipworth BJ. Phosphodiesterase-4 inhibitors for asthma and chronic obstructive pulmonary disease. *Lancet*. 2005; **365**(9454): 167-75.
301. Chong J, Poole P, Leung B, Black PN. Phosphodiesterase 4 inhibitors for chronic obstructive pulmonary disease. *Cochrane Database Syst Rev*. 2011; (5): CD002309.
302. Kwak HJ, Park KM, Choi HE, Chung KS, Lim HJ, Park HY. PDE4 inhibitor, roflumilast protects cardiomyocytes against NO-induced apoptosis via activation of PKA and Epac dual pathways. *Cell Signal*. 2008; **20**(5): 803-14.
303. Jorgensen K. Effects of Lung Volume Reduction Surgery on Left Ventricular Diastolic Filling and Dimensions in Patients With Severe Emphysema. *Chest*. 2003; **124**(5): 1863-70.
304. Criner GJ, Scharf SM, Falk JA, Gaughan JP, Sternberg AL, Patel NB, et al. Effect of lung volume reduction surgery on resting pulmonary hemodynamics in severe emphysema. *American journal of respiratory and critical care medicine*. 2007; **176**(3): 253-60.
305. Come CE, Divo MJ, San Jose Estepar R, Sciruba FC, Criner GJ, Marchetti N, et al. Lung deflation and oxygen pulse in COPD: Results from the NETT randomized trial. *Respir Med*. 2011.
306. Nichols WW, McDonald DA. Wave-velocity in the proximal aorta. *Med Biol Eng*. 1972; **10**(3): 327-35.
307. Metafratzi ZM, Efremidis SC, Skopelitou AS, De Roos A. The clinical significance of aortic compliance and its assessment with magnetic resonance imaging. *J Cardiovasc Magn Reson*. 2002; **4**(4): 481-91.
308. London GM, Guerin AP. Influence of arterial pulse and reflected waves on blood pressure and cardiac function. *Am Heart J*. 1999; **138**(3 Pt 2): 220-4.
309. Vulliemoz S, Stergiopoulos N, Meuli R. Estimation of local aortic elastic properties with MRI. *Magnetic resonance in medicine : official journal of the Society of Magnetic Resonance in Medicine / Society of Magnetic Resonance in Medicine*. 2002; **47**(4): 649-54.



310. Boudoulas KD, Vlachopoulos C, Raman SV, Sparks EA, Triposciadis F, Stefanadis C, et al. Aortic function: from the research laboratory to the clinic. *Cardiology*. 2012; **121**(1): 31-42.
311. O'Rourke MF, Safar ME. Relationship between aortic stiffening and microvascular disease in brain and kidney: cause and logic of therapy. *Hypertension*. 2005; **46**(1): 200-4.
312. Safar ME, London GM, Plante GE. Arterial stiffness and kidney function. *Hypertension*. 2004; **43**(2): 163-8.
313. Mohiaddin RH, Underwood SR, Bogren HG, Firmin DN, Klipstein RH, Rees RS, et al. Regional aortic compliance studied by magnetic resonance imaging: the effects of age, training, and coronary artery disease. *British heart journal*. 1989; **62**(2): 90-6.
314. Rerkpattanapipat P, Hundley WG, Link KM, Brubaker PH, Hamilton CA, Darty SN, et al. Relation of aortic distensibility determined by magnetic resonance imaging in patients > or =60 years of age to systolic heart failure and exercise capacity. *Am J Cardiol*. 2002; **90**(11): 1221-5.
315. Watanabe H, Ohtsuka S, Kakihana M, Sugishita Y. Coronary circulation in dogs with an experimental decrease in aortic compliance. *J Am Coll Cardiol*. 1993; **21**(6): 1497-506.
316. Ohtsuka S, Kakihana M, Watanabe H, Sugishita Y. Chronically decreased aortic distensibility causes deterioration of coronary perfusion during increased left ventricular contraction. *J Am Coll Cardiol*. 1994; **24**(5): 1406-14.
317. Kyliantreas I, Shirodaria C, Lee JM, Cunnington C, Lindsay A, Francis J, et al. Multimodal cardiovascular magnetic resonance quantifies regional variation in vascular structure and function in patients with coronary artery disease: relationships with coronary disease severity. *J Cardiovasc Magn Reson*. 2011; **13**: 61.
318. Hirsch GA, Ingkanisorn WP, Schulman SP, Gerstenblith G, Dyke CK, Rhoads KL, et al. Age-related vascular stiffness and left ventricular size after myocardial infarction. *Am J Geriatr Cardiol*. 2007; **16**(4): 222-8.
319. Nemes A, Csanady M, Forster T. Does increased aortic stiffness predict reduced coronary flow velocity reserve in patients with suspected coronary artery disease? *Acta physiologica Hungarica*. 2012; **99**(3): 271-8.
320. Redheuil A, Yu WC, Mousseaux E, Harouni AA, Kachenoura N, Wu CO, et al. Age-related changes in aortic arch geometry: relationship with proximal aortic function and left ventricular mass and remodeling. *J Am Coll Cardiol*. 2011; **58**(12): 1262-70.
321. Leeson CP, Robinson M, Francis JM, Robson MD, Channon KM, Neubauer S, et al. Cardiovascular magnetic resonance imaging for non-invasive assessment of vascular function: validation against ultrasound. *J Cardiovasc Magn Reson*. 2006; **8**(2): 381-7.
322. Herment A, Lefort M, Kachenoura N, De Cesare A, Taviani V, Graves MJ, et al. Automated estimation of aortic strain from steady-state free-precession and phase contrast MR images. *Magn Reson Med*. 2011; **65**(4): 986-93.
323. van der Meer RW, Diamant M, Westenberg JJ, Doornbos J, Bax JJ, de Roos A, et al. Magnetic resonance assessment of aortic pulse wave velocity, aortic distensibility, and cardiac function in uncomplicated type 2 diabetes mellitus. *J Cardiovasc Magn Reson*. 2007; **9**(4): 645-51.
324. Lalande A, Khau van Kien P, Salve N, Ben Salem D, Legrand L, Walker PM, et al. Automatic determination of aortic compliance with cine-magnetic resonance imaging: an application of fuzzy logic theory. *Invest Radiol*. 2002; **37**(12): 685-91.
325. Krug R, Boese JM, Schad LR. Determination of aortic compliance from magnetic resonance images using an automatic active contour model. *Phys Med Biol*. 2003; **48**(15): 2391-404.

326. Rose JL, Lalonde A, Bouchot O, Bourennane el B, Walker PM, Ugolini P, et al. Influence of age and sex on aortic distensibility assessed by MRI in healthy subjects. *Magnetic resonance imaging*. 2010; **28**(2): 255-63.
327. Pucci G, Cheriyan J, Hubsch A, Hickson SS, Gajendragadkar PR, Watson T, et al. Evaluation of the Vicorder, a novel cuff-based device for the noninvasive estimation of central blood pressure. *J Hypertens*. 2012.
328. Segers P, Mahieu D, Kips J, Rietzschel E, De Buyzere M, De Bacquer D, et al. Amplification of the pressure pulse in the upper limb in healthy, middle-aged men and women. *Hypertension*. 2009; **54**(2): 414-20.
329. O'Rourke MF. Influence of ventricular ejection on the relationship between central aortic and brachial pressure pulse in man. *Cardiovasc Res*. 1970; **4**(3): 291-300.
330. O'Rourke MF, Staessen JA, Vlachopoulos C, Duprez D, Plante GE. Clinical applications of arterial stiffness; definitions and reference values. *Am J Hypertens*. 2002; **15**(5): 426-44.
331. Ziemann SJ, Melenovsky V, Kass DA. Mechanisms, pathophysiology, and therapy of arterial stiffness. *Arterioscler Thromb Vasc Biol*. 2005; **25**(5): 932-43.
332. Kullo IJ, Malik AR. Arterial ultrasonography and tonometry as adjuncts to cardiovascular risk stratification. *J Am Coll Cardiol*. 2007; **49**(13): 1413-26.
333. Van Bortel LM, Duprez D, Starmans-Kool MJ, Safar ME, Giannattasio C, Cockcroft J, et al. Clinical applications of arterial stiffness, Task Force III: recommendations for user procedures. *Am J Hypertens*. 2002; **15**(5): 445-52.
334. van Popele NM, Mattace-Raso FU, Vliegenthart R, Grobbee DE, Asmar R, van der Kuip DA, et al. Aortic stiffness is associated with atherosclerosis of the coronary arteries in older adults: the Rotterdam Study. *J Hypertens*. 2006; **24**(12): 2371-6.
335. Cecelja M, Hussain T, Greil G, Botnar R, Preston R, Moayeri A, et al. Multimodality imaging of subclinical aortic atherosclerosis: relation of aortic stiffness to calcification and plaque in female twins. *Hypertension*. 2013; **61**(3): 609-14.
336. Pannier B, Guerin AP, Marchais SJ, Safar ME, London GM. Stiffness of capacitive and conduit arteries: prognostic significance for end-stage renal disease patients. *Hypertension*. 2005; **45**(4): 592-6.
337. Shoji T, Emoto M, Shinohara K, Kakiya R, Tsujimoto Y, Kishimoto H, et al. Diabetes mellitus, aortic stiffness, and cardiovascular mortality in end-stage renal disease. *J Am Soc Nephrol*. 2001; **12**(10): 2117-24.
338. Laurent S, Cockcroft J, Van Bortel L, Boutouyrie P, Giannattasio C, Hayoz D, et al. Expert consensus document on arterial stiffness: methodological issues and clinical applications. *Eur Heart J*. 2006; **27**(21): 2588-605.
339. Chiu YC, Arand PW, Shroff SG, Feldman T, Carroll JD. Determination of pulse wave velocities with computerized algorithms. *Am Heart J*. 1991; **121**(5): 1460-70.
340. Millasseau SC, Stewart AD, Patel SJ, Redwood SR, Chowienczyk PJ. Evaluation of carotid-femoral pulse wave velocity: influence of timing algorithm and heart rate. *Hypertension*. 2005; **45**(2): 222-6.
341. Rajzer MW, Wojciechowska W, Klocek M, Palka I, Brzozowska-Kiszka M, Kawecka-Jaszcz K. Comparison of aortic pulse wave velocity measured by three techniques: Complior, SphygmoCor and Arteriograph. *J Hypertens*. 2008; **26**(10): 2001-7.
342. Baulmann J, Schillings U, Rickert S, Uen S, Dusing R, Illyes M, et al. A new oscillometric method for assessment of arterial stiffness: comparison with tonometric and piezo-electronic methods. *J Hypertens*. 2008; **26**(3): 523-8.
343. Pannier BM, Avolio AP, Hoeks A, Mancia G, Takazawa K. Methods and devices for measuring arterial compliance in humans. *Am J Hypertens*. 2002; **15**(8): 743-53.

344. Wilkinson IB, Fuchs SA, Jansen IM, Spratt JC, Murray GD, Cockcroft JR, et al. Reproducibility of pulse wave velocity and augmentation index measured by pulse wave analysis. *J Hypertens*. 1998; **16**(12 Pt 2): 2079-84.
345. Frimodt-Moller M, Nielsen AH, Kamper AL, Strandgaard S. Reproducibility of pulse-wave analysis and pulse-wave velocity determination in chronic kidney disease. *Nephrol Dial Transplant*. 2008; **23**(2): 594-600.
346. Hickson SS, Butlin M, Broad J, Avolio AP, Wilkinson IB, McEniery CM. Validity and repeatability of the Vicorder apparatus: a comparison with the SphygmoCor device. *Hypertens Res*. 2009; **32**(12): 1079-85.
347. Kracht D, Shroff R, Baig S, Doyon A, Jacobi C, Zeller R, et al. Validating a new oscillometric device for aortic pulse wave velocity measurements in children and adolescents. *Am J Hypertens*. 2011; **24**(12): 1294-9.
348. van Leeuwen-Segarceanu EM, Tromp WF, Bos WJ, Vogels OJ, Groothoff JW, van der Lee JH. Comparison of two instruments measuring carotid-femoral pulse wave velocity: Vicorder versus SphygmoCor. *J Hypertens*. 2010; **28**(8): 1687-91.
349. Stone IS, John L, Petersen SE, Barnes NC. Reproducibility of arterial stiffness and wave reflections in chronic obstructive pulmonary disease: The contribution of lung hyperinflation and a comparison of techniques. *Respir Med*. 2013.
350. Sugawara J, Hayashi K, Yokoi T, Tanaka H. Carotid-Femoral Pulse Wave Velocity: Impact of Different Arterial Path Length Measurements. *Artery Res*. 2010; **4**(1): 27-31.
351. Vermeersch SJ, Rietzschel ER, De Buyzere ML, Van Bortel LM, Gillebert TC, Verdonck PR, et al. Distance measurements for the assessment of carotid to femoral pulse wave velocity. *J Hypertens*. 2009; **27**(12): 2377-85.
352. Stewart AD, Millasseau SC, Kearney MT, Ritter JM, Chowienczyk PJ. Effects of inhibition of basal nitric oxide synthesis on carotid-femoral pulse wave velocity and augmentation index in humans. *Hypertension*. 2003; **42**(5): 915-8.
353. Weber T, Ammer M, Rammer M, Adji A, O'Rourke MF, Wassertheurer S, et al. Noninvasive determination of carotid-femoral pulse wave velocity depends critically on assessment of travel distance: a comparison with invasive measurement. *J Hypertens*. 2009; **27**(8): 1624-30.
354. Adji A, O'Rourke MF. Determination of central aortic systolic and pulse pressure from the radial artery pressure waveform. *Blood Press Monit*. 2004; **9**(3): 115-21.
355. Fetcs B, Nevo E, Chen CH, Kass DA. Parametric model derivation of transfer function for noninvasive estimation of aortic pressure by radial tonometry. *IEEE Trans Biomed Eng*. 1999; **46**(6): 698-706.
356. Rezai MR, Goudot G, Winters C, Finn JD, Wu FC, Cruickshank JK. Calibration mode influences central blood pressure differences between SphygmoCor and two newer devices, the Arteriograph and Omron HEM-9000. *Hypertens Res*. 2011; **34**(9): 1046-51.
357. McVeigh GE. Pulse waveform analysis and arterial wall properties. *Hypertension*. 2003; **41**(5): 1010-1.
358. Hoeks AP, Meinders JM, Dammers R. Applicability and benefit of arterial transfer functions. *J Hypertens*. 2003; **21**(7): 1241-3.
359. Davies JI, Band MM, Pringle S, Ogston S, Struthers AD. Peripheral blood pressure measurement is as good as applanation tonometry at predicting ascending aortic blood pressure. *J Hypertens*. 2003; **21**(3): 571-6.
360. Hope SA, Tay DB, Meredith IT, Cameron JD. Use of arterial transfer functions for the derivation of aortic waveform characteristics. *J Hypertens*. 2003; **21**(7): 1299-305.
361. Chen CH, Nevo E, Fetcs B, Pak PH, Yin FC, Maughan WL, et al. Estimation of central aortic pressure waveform by mathematical transformation of radial

- tonometry pressure. Validation of generalized transfer function. *Circulation*. 1997; **95**(7): 1827-36.
362. O'Rourke MF, Nichols WW. Use of arterial transfer function for the derivation of aortic waveform characteristics. *J Hypertens*. 2003; **21**(11): 2195-7; author reply 7-9.
363. Mahieu D, Kips J, Rietzschel ER, De Buyzere ML, Verbeke F, Gillebert TC, et al. Noninvasive assessment of central and peripheral arterial pressure (waveforms): implications of calibration methods. *J Hypertens*. 2010; **28**(2): 300-5.
364. Weber T, Wassertheurer S, Rammer M, Maurer E, Hametner B, Mayer CC, et al. Validation of a brachial cuff-based method for estimating central systolic blood pressure. *Hypertension*. 2011; **58**(5): 825-32.
365. Millasseau SC, Patel SJ, Redwood SR, Ritter JM, Chowienczyk PJ. Pressure wave reflection assessed from the peripheral pulse: is a transfer function necessary? *Hypertension*. 2003; **41**(5): 1016-20.
366. Hope SA, Antonis P, Adam D, Cameron JD, Meredith IT. Arterial pulse wave velocity but not augmentation index is associated with coronary artery disease extent and severity: implications for arterial transfer function applicability. *J Hypertens*. 2007; **25**(10): 2105-9.
367. de Luca N, Asmar RG, London GM, O'Rourke MF, Safar ME. Selective reduction of cardiac mass and central blood pressure on low-dose combination perindopril/indapamide in hypertensive subjects. *J Hypertens*. 2004; **22**(8): 1623-30.
368. Hirata K, Vlachopoulos C, Adji A, O'Rourke MF. Benefits from angiotensin-converting enzyme inhibitor 'beyond blood pressure lowering': beyond blood pressure or beyond the brachial artery? *J Hypertens*. 2005; **23**(3): 551-6.
369. Papaioannou TG, Karatzis EN, Karatzi KN, Gialafos EJ, Protogerou AD, Stamatelopoulos KS, et al. Hour-to-hour and week-to-week variability and reproducibility of wave reflection indices derived by aortic pulse wave analysis: implications for studies with repeated measurements. *J Hypertens*. 2007; **25**(8): 1678-86.
370. Wojciechowska W, Staessen JA, Nawrot T, Cwynar M, Seidlerova J, Stolarz K, et al. Reference values in white Europeans for the arterial pulse wave recorded by means of the SphygmoCor device. *Hypertens Res*. 2006; **29**(7): 475-83.
371. O'Rourke MF, Nichols WW, Safar ME. Pulse waveform analysis and arterial stiffness: realism can replace evangelism and scepticism. *J Hypertens*. 2004; **22**(8): 1633-4; author reply 4.
372. Lemogoum D, Flores G, Van den Abeele W, Ciarka A, Leeman M, Degaute JP, et al. Validity of pulse pressure and augmentation index as surrogate measures of arterial stiffness during beta-adrenergic stimulation. *J Hypertens*. 2004; **22**(3): 511-7.
373. McEniery CM, Yasmin, Hall IR, Qasem A, Wilkinson IB, Cockcroft JR. Normal vascular aging: differential effects on wave reflection and aortic pulse wave velocity: the Anglo-Cardiff Collaborative Trial (ACCT). *J Am Coll Cardiol*. 2005; **46**(9): 1753-60.
374. London GM, Blacher J, Pannier B, Guerin AP, Marchais SJ, Safar ME. Arterial wave reflections and survival in end-stage renal failure. *Hypertension*. 2001; **38**(3): 434-8.
375. Ueda H, Hayashi T, Tsumura K, Yoshimaru K, Nakayama Y, Yoshikawa J. The timing of the reflected wave in the ascending aortic pressure predicts restenosis after coronary stent placement. *Hypertens Res*. 2004; **27**(8): 535-40.
376. Weber T, Auer J, O'Rourke M F, Kvas E, Lassnig E, Lamm G, et al. Increased arterial wave reflections predict severe cardiovascular events in patients undergoing percutaneous coronary interventions. *Eur Heart J*. 2005; **26**(24): 2657-63.

377. Chirinos JA, Zambrano JP, Chakko S, Veerani A, Schob A, Willens HJ, et al. Aortic pressure augmentation predicts adverse cardiovascular events in patients with established coronary artery disease. *Hypertension*. 2005; **45**(5): 980-5.
378. Williams B, Lacy PS, Thom SM, Cruickshank K, Stanton A, Collier D, et al. Differential impact of blood pressure-lowering drugs on central aortic pressure and clinical outcomes: principal results of the Conduit Artery Function Evaluation (CAFE) study. *Circulation*. 2006; **113**(9): 1213-25.
379. Covic A, Mardare N, Gusbeth-Tatomir P, Prisada O, Sascau R, Goldsmith DJ. Arterial wave reflections and mortality in haemodialysis patients--only relevant in elderly, cardiovascularly compromised? *Nephrol Dial Transplant*. 2006; **21**(10): 2859-66.
380. Dart AM, Gatzka CD, Kingwell BA, Willson K, Cameron JD, Liang YL, et al. Brachial blood pressure but not carotid arterial waveforms predict cardiovascular events in elderly female hypertensives. *Hypertension*. 2006; **47**(4): 785-90.
381. Vlachopoulos C, Aznaouridis K, O'Rourke MF, Safar ME, Baou K, Stefanadis C. Prediction of cardiovascular events and all-cause mortality with central haemodynamics: a systematic review and meta-analysis. *Eur Heart J*. 2010; **31**(15): 1865-71.
382. Alfakih K, Plein S, Thiele H, Jones T, Ridgway JP, Sivananthan MU. Normal human left and right ventricular dimensions for MRI as assessed by turbo gradient echo and steady-state free precession imaging sequences. *J Magn Reson Imaging*. 2003; **17**(3): 323-9.
383. Grothues F, Smith GC, Moon JC, Bellenger NG, Collins P, Klein HU, et al. Comparison of interstudy reproducibility of cardiovascular magnetic resonance with two-dimensional echocardiography in normal subjects and in patients with heart failure or left ventricular hypertrophy. *Am J Cardiol*. 2002; **90**(1): 29-34.
384. Moon JC, Lorenz CH, Francis JM, Smith GC, Pennell DJ. Breath-hold FLASH and FISP cardiovascular MR imaging: left ventricular volume differences and reproducibility. *Radiology*. 2002; **223**(3): 789-97.
385. Jenkins C, Moir S, Chan J, Rakhit D, Haluska B, Marwick TH. Left ventricular volume measurement with echocardiography: a comparison of left ventricular opacification, three-dimensional echocardiography, or both with magnetic resonance imaging. *Eur Heart J*. 2009; **30**(1): 98-106.
386. Rehr RB, Malloy CR, Filipchuk NG, Peshock RM. Left ventricular volumes measured by MR imaging. *Radiology*. 1985; **156**(3): 717-9.
387. Hudsmith LE, Petersen SE, Francis JM, Robson MD, Neubauer S. Normal human left and right ventricular and left atrial dimensions using steady state free precession magnetic resonance imaging. *J Cardiovasc Magn Reson*. 2005; **7**(5): 775-82.
388. Pattynama PM, Lamb HJ, van der Velde EA, van der Wall EE, de Roos A. Left ventricular measurements with cine and spin-echo MR imaging: a study of reproducibility with variance component analysis. *Radiology*. 1993; **187**(1): 261-8.
389. Semelka RC, Tomei E, Wagner S, Mayo J, Caputo G, O'Sullivan M, et al. Interstudy reproducibility of dimensional and functional measurements between cine magnetic resonance studies in the morphologically abnormal left ventricle. *American heart journal*. 1990; **119**(6): 1367-73.
390. Semelka RC, Tomei E, Wagner S, Mayo J, Kondo C, Suzuki J, et al. Normal left ventricular dimensions and function: interstudy reproducibility of measurements with cine MR imaging. *Radiology*. 1990; **174**(3 Pt 1): 763-8.
391. Bellenger NG, Davies LC, Francis JM, Coats AJ, Pennell DJ. Reduction in sample size for studies of remodeling in heart failure by the use of cardiovascular magnetic resonance. *J Cardiovasc Magn Reson*. 2000; **2**(4): 271-8.
392. White HD, Norris RM, Brown MA, Brandt PW, Whitlock RM, Wild CJ. Left ventricular end-systolic volume as the major determinant of survival after recovery from myocardial infarction. *Circulation*. 1987; **76**(1): 44-51.

393. Bikkina M, Levy D, Evans JC, Larson MG, Benjamin EJ, Wolf PA, et al. Left ventricular mass and risk of stroke in an elderly cohort. *The Framingham Heart Study*. *Jama*. 1994; **272**(1): 33-6.
394. Casale PN, Devereux RB, Milner M, Zullo G, Harshfield GA, Pickering TG, et al. Value of echocardiographic measurement of left ventricular mass in predicting cardiovascular morbid events in hypertensive men. *Annals of internal medicine*. 1986; **105**(2): 173-8.
395. Koren MJ, Devereux RB, Casale PN, Savage DD, Laragh JH. Relation of left ventricular mass and geometry to morbidity and mortality in uncomplicated essential hypertension. *Annals of internal medicine*. 1991; **114**(5): 345-52.
396. Levy D, Garrison RJ, Savage DD, Kannel WB, Castelli WP. Prognostic implications of echocardiographically determined left ventricular mass in the Framingham Heart Study. *The New England journal of medicine*. 1990; **322**(22): 1561-6.
397. Carabello BA. Evolution of the study of left ventricular function: everything old is new again. *Circulation*. 2002; **105**(23): 2701-3.
398. McMurray JJ, Adamopoulos S, Anker SD, Auricchio A, Bohm M, Dickstein K, et al. ESC Guidelines for the diagnosis and treatment of acute and chronic heart failure 2012: The Task Force for the Diagnosis and Treatment of Acute and Chronic Heart Failure 2012 of the European Society of Cardiology. Developed in collaboration with the Heart Failure Association (HFA) of the ESC. *Eur Heart J*. 2012; **33**(14): 1787-847.
399. Mertens LL, Friedberg MK. Imaging the right ventricle--current state of the art. *Nature reviews Cardiology*. 2010; **7**(10): 551-63.
400. Sechtem U, Pflugfelder PW, Gould RG, Cassidy MM, Higgins CB. Measurement of right and left ventricular volumes in healthy individuals with cine MR imaging. *Radiology*. 1987; **163**(3): 697-702.
401. Caudron J, Fares J, Lefebvre V, Vivier PH, Petitjean C, Dacher JN. Cardiac MRI assessment of right ventricular function in acquired heart disease: factors of variability. *Academic radiology*. 2012; **19**(8): 991-1002.
402. Pellerin D, Sharma R, Elliott P, Veyrat C. Tissue Doppler, strain, and strain rate echocardiography for the assessment of left and right systolic ventricular function. *Heart (British Cardiac Society)*. 2003; **89 Suppl 3**: iii9-17.
403. Hor KN, Gottliebson WM, Carson C, Wash E, Cnota J, Fleck R, et al. Comparison of magnetic resonance feature tracking for strain calculation with harmonic phase imaging analysis. *JACC Cardiovasc Imaging*. 2010; **3**(2): 144-51.
404. Rosen BD, Edvardsen T, Lai S, Castillo E, Pan L, Jerosch-Herold M, et al. Left ventricular concentric remodeling is associated with decreased global and regional systolic function: the Multi-Ethnic Study of Atherosclerosis. *Circulation*. 2005; **112**(7): 984-91.
405. Rosen BD, Saad MF, Shea S, Nasir K, Edvardsen T, Burke G, et al. Hypertension and smoking are associated with reduced regional left ventricular function in asymptomatic individuals the Multi-Ethnic Study of Atherosclerosis. *J Am Coll Cardiol*. 2006; **47**(6): 1150-8.
406. Castillo E, Osman N, Rosen B, El-Shehaby I, Pan L, Jerosch-Herold M, et al. Quantitative Assessment of Regional Myocardial Function with MR-Tagging in a Multi-Center Study: Interobserver and Intraobserver Agreement of Fast Strain Analysis with Harmonic Phase (HARP) MRI. *Journal of Cardiovascular Magnetic Resonance*. 2005; **7**(5): 783-91.
407. Augustine D, Lewandowski AJ, Lazdam M, Rai A, Francis J, Myerson S, et al. Global and regional left ventricular myocardial deformation measures by magnetic resonance feature tracking in healthy volunteers: comparison with tagging and relevance of gender. *J Cardiovasc Magn Reson*. 2013; **15**: 8.
408. Maret E, Todt T, Brudin L, Nylander E, Swahn E, Ohlsson JL, et al. Functional measurements based on feature tracking of cine magnetic resonance

images identify left ventricular segments with myocardial scar. *Cardiovasc Ultrasound*. 2009; **7**: 53.

409. Schuster A, Kutty S, Padiyath A, Parish V, Gribben P, Danford DA, et al. Cardiovascular magnetic resonance myocardial feature tracking detects quantitative wall motion during dobutamine stress. *J Cardiovasc Magn Reson*. 2011; **13**: 58.

410. Bistoquet A, Oshinski J, Skrinjar O. Myocardial deformation recovery from cine MRI using a nearly incompressible biventricular model. *Medical image analysis*. 2008; **12**(1): 69-85.

411. McLaughlin VV, Archer SL, Badesch DB, Barst RJ, Farber HW, Lindner JR, et al. ACCF/AHA 2009 expert consensus document on pulmonary hypertension a report of the American College of Cardiology Foundation Task Force on Expert Consensus Documents and the American Heart Association developed in collaboration with the American College of Chest Physicians; American Thoracic Society, Inc.; and the Pulmonary Hypertension Association. *J Am Coll Cardiol*. 2009; **53**(17): 1573-619.

412. Peng HH, Chung HW, Yu HY, Tseng WY. Estimation of pulse wave velocity in main pulmonary artery with phase contrast MRI: preliminary investigation. *J Magn Reson Imaging*. 2006; **24**(6): 1303-10.

413. Hooper MM, Oudiz RJ, Peacock A, Tapson VF, Haworth SG, Frost AE, et al. End points and clinical trial designs in pulmonary arterial hypertension: clinical and regulatory perspectives. *J Am Coll Cardiol*. 2004; **43**(12 Suppl S): 48S-55S.

414. Sanz J, Kariisa M, Dellegrottaglie S, Prat-Gonzalez S, Garcia MJ, Fuster V, et al. Evaluation of pulmonary artery stiffness in pulmonary hypertension with cardiac magnetic resonance. *JACC Cardiovasc Imaging*. 2009; **2**(3): 286-95.

415. Bogren HG, Klipstein RH, Mohiaddin RH, Firmin DN, Underwood SR, Rees RS, et al. Pulmonary artery distensibility and blood flow patterns: a magnetic resonance study of normal subjects and of patients with pulmonary arterial hypertension. *Am Heart J*. 1989; **118**(5 Pt 1): 990-9.

416. Hayashi K, Handa H, Nagasawa S, Okumura A, Moritake K. Stiffness and elastic behavior of human intracranial and extracranial arteries. *J Biomech*. 1980; **13**(2): 175-84.

417. Kawasaki T, Sasayama S, Yagi S, Asakawa T, Hirai T. Non-invasive assessment of the age related changes in stiffness of major branches of the human arteries. *Cardiovasc Res*. 1987; **21**(9): 678-87.

418. Gan CT, Lankhaar JW, Westerhof N, Marcus JT, Becker A, Twisk JW, et al. Noninvasively assessed pulmonary artery stiffness predicts mortality in pulmonary arterial hypertension. *Chest*. 2007; **132**(6): 1906-12.

419. Toshner MR, Gopalan D, Suntharalingam J, Treacy C, Soon E, Sheares KK, et al. Pulmonary arterial size and response to sildenafil in chronic thromboembolic pulmonary hypertension. *J Heart Lung Transplant*. 2010; **29**(6): 610-5.

420. Paz R, Mohiaddin RH, Longmore DB. Magnetic resonance assessment of the pulmonary arterial trunk anatomy, flow, pulsatility and distensibility. *Eur Heart J*. 1993; **14**(11): 1524-30.

421. Bouchard A, Higgins CB, Byrd BF, 3rd, Amparo EG, Osaki L, Axelrod R. Magnetic resonance imaging in pulmonary arterial hypertension. *Am J Cardiol*. 1985; **56**(15): 938-42.

422. Stone IS, Barnes NC, Petersen SE. Chronic obstructive pulmonary disease: a modifiable risk factor for cardiovascular disease? *Heart*. 2012; **98**(14): 1055-62.

423. Ertan C, Tarakci N, Ozeke O, Demir AD. Pulmonary artery distensibility in chronic obstructive pulmonary disease. *Echocardiography*. 2013; **30**(8): 940-4.

424. Miller MR, Hankinson J, Brusasco V, Burgos F, Casaburi R, Coates A, et al. Standardisation of spirometry. *Eur Respir J*. 2005; **26**(2): 319-38.

425. Dubois AB, Botelho SY, Bedell GN, Marshall R, Comroe JH, Jr. A rapid plethysmographic method for measuring thoracic gas volume: a comparison with a

- nitrogen washout method for measuring functional residual capacity in normal subjects. *J Clin Invest.* 1956; **35**(3): 322-6.
426. Miller MR, Crapo R, Hankinson J, Brusasco V, Burgos F, Casaburi R, et al. General considerations for lung function testing. *Eur Respir J.* 2005; **26**(1): 153-61.
427. Hankinson JL, Odencrantz JR, Fedan KB. Spirometric reference values from a sample of the general U.S. population. *Am J Respir Crit Care Med.* 1999; **159**(1): 179-87.
428. Macintyre N, Crapo RO, Viegi G, Johnson DC, van der Grinten CP, Brusasco V, et al. Standardisation of the single-breath determination of carbon monoxide uptake in the lung. *Eur Respir J.* 2005; **26**(4): 720-35.
429. Wilkinson I.B MCM, Schillaci G, Boutouyrie P, Segers P, Donald A, Chowienczyk PJ, On behalf of the ARTERY Society. ARTERY Society guidelines for validation of non-invasive haemodynamic measurement devices: Part 1, arterial pulse wave velocity. *Artery Res.* 2010; **4**(2): 34-40.
430. Childs H, Ma L, Ma M, Clarke J, Cocker M, Green J, et al. Comparison of long and short axis quantification of left ventricular volume parameters by cardiovascular magnetic resonance, with ex-vivo validation. *J Cardiovasc Magn Reson.* 2011; **13**: 40.
431. Hogan MC, Petersen SE, Hudsmith LE, Francis JM, Neubauer S, Robson MD. Effects of steady state free precession parameters on cardiac mass, function, and volumes. *The international journal of cardiovascular imaging.* 2007; **23**(5): 583-9.
432. Shapiro MD, Nieman K, Nasir K, Nomura CH, Sarwar A, Ferencik M, et al. Utility of cardiovascular magnetic resonance to predict left ventricular recovery after primary percutaneous coronary intervention for patients presenting with acute ST-segment elevation myocardial infarction. *Am J Cardiol.* 2007; **100**(2): 211-6.
433. Hudsmith LE, Petersen SE, Francis JM, Robson MD, Neubauer S. Normal human left and right ventricular and left atrial dimensions using steady state free precession magnetic resonance imaging. *J Cardiovasc Magn Reson.* 2005; **7**(5): 775-82.
434. Strugnell WE, Slaughter I R, Riley RA, Trotter AJ, Bartlett H. Modified RV short axis series--a new method for cardiac MRI measurement of right ventricular volumes. *J Cardiovasc Magn Reson.* 2005; **7**(5): 769-74.
435. Kawut SM, Lima JA, Barr RG, Chahal H, Jain A, Tandri H, et al. Sex and race differences in right ventricular structure and function: the multi-ethnic study of atherosclerosis-right ventricle study. *Circulation.* 2011; **123**(22): 2542-51.
436. Fratz S, Schuhbaeck A, Buchner C, Busch R, Meierhofer C, Martinoff S, et al. Comparison of accuracy of axial slices versus short-axis slices for measuring ventricular volumes by cardiac magnetic resonance in patients with corrected tetralogy of fallot. *Am J Cardiol.* 2009; **103**(12): 1764-9.
437. Morton G, Jogiya R, Plein S, Schuster A, Chiribiri A, Nagel E. Quantitative cardiovascular magnetic resonance perfusion imaging: inter-study reproducibility. *Eur Heart J Cardiovasc Imaging.* 2012; **13**(11): 954-60.
438. Papavassiliu T, Kuhl HP, Schroder M, Suselbeck T, Bondarenko O, Bohm CK, et al. Effect of endocardial trabeculae on left ventricular measurements and measurement reproducibility at cardiovascular MR imaging. *Radiology.* 2005; **236**(1): 57-64.
439. Mosteller RD. Simplified calculation of body-surface area. *N Engl J Med.* 1987; **317**(17): 1098.
440. Hof IE, Velthuis BK, Van Driel VJ, Wittkampfh FH, Hauer RN, Loh P. Left atrial volume and function assessment by magnetic resonance imaging. *J Cardiovasc Electrophysiol.* 2010; **21**(11): 1247-50.
441. Ceelen F, Hunter RJ, Boubertakh R, Sommer WH, Armbruster M, Schilling RJ, et al. Effect of atrial fibrillation ablation on myocardial function: insights from cardiac magnetic resonance feature tracking analysis. *Int J Cardiovasc Imaging.* 2013.



442. Harrild DM, Han Y, Geva T, Zhou J, Marcus E, Powell AJ. Comparison of cardiac MRI tissue tracking and myocardial tagging for assessment of regional ventricular strain. *The international journal of cardiovascular imaging*. 2012; **28**(8): 2009-18.
443. Zwanenburg JJ, Kuijter JP, Marcus JT, Heethaar RM. Steady-state free precession with myocardial tagging: CSPAMM in a single breathhold. *Magn Reson Med*. 2003; **49**(4): 722-30.
444. Ibrahim el SH, Stuber M, Schar M, Osman NF. Improved myocardial tagging contrast in cine balanced SSFP images. *J Magn Reson Imaging*. 2006; **24**(5): 1159-67.
445. Maclay JD, McAllister DA, Mills NL, Paterson FP, Ludlam CA, Drost EM, et al. Vascular dysfunction in chronic obstructive pulmonary disease. *American journal of respiratory and critical care medicine*. 2009; **180**(6): 513-20.
446. Bland JM, Altman DG. Statistical methods for assessing agreement between two methods of clinical measurement. *Lancet*. 1986; **1**(8476): 307-10.
447. Davies JM, Bailey MA, Griffin KJ, Scott DJ. Pulse wave velocity and the non-invasive methods used to assess it: Complior, SphygmoCor, Arteriograph and Vicorder. *Vascular*. 2012.
448. Vedam H, Phillips CL, Wang D, Barnes DJ, Hedner JA, Unger G, et al. Short-term hypoxia reduces arterial stiffness in healthy men. *Eur J Appl Physiol*. 2009; **105**(1): 19-25.
449. Shahin Y, Barakat H, Barnes R, Chetter I. The Vicorder device compared with SphygmoCor in the assessment of carotid-femoral pulse wave velocity in patients with peripheral arterial disease. *Hypertens Res*. 2012.
450. Nemeth ZK, Studinger P, Kiss I, Othmane Tel H, Nemcsik J, Fekete BC, et al. The method of distance measurement and torso length influences the relationship of pulse wave velocity to cardiovascular mortality. *Am J Hypertens*. 2011; **24**(2): 155-61.
451. Janner JH, McAllister DA, Godtfredsen NS, Prescott E, Vestbo J. Is chronic obstructive pulmonary disease associated with increased arterial stiffness? *Respir Med*. 2012; **106**(3): 397-405.
452. Edvardsen T, Gerber BL, Garot J, Bluemke DA, Lima JA, Smiseth OA. Quantitative assessment of intrinsic regional myocardial deformation by Doppler strain rate echocardiography in humans: validation against three-dimensional tagged magnetic resonance imaging. *Circulation*. 2002; **106**(1): 50-6.
453. Miyatake K, Yamagishi M, Tanaka N, Uematsu M, Yamazaki N, Mine Y, et al. New method for evaluating left ventricular wall motion by color-coded tissue Doppler imaging: in vitro and in vivo studies. *J Am Coll Cardiol*. 1995; **25**(3): 717-24.
454. Castro PL, Greenberg NL, Drinko J, Garcia MJ, Thomas JD. Potential pitfalls of strain rate imaging: angle dependency. *Biomedical sciences instrumentation*. 2000; **36**: 197-202.
455. Amundsen BH, Helle-Valle T, Edvardsen T, Torp H, Crosby J, Lyseggen E, et al. Noninvasive myocardial strain measurement by speckle tracking echocardiography: validation against sonomicrometry and tagged magnetic resonance imaging. *J Am Coll Cardiol*. 2006; **47**(4): 789-93.
456. Blessberger H, Binder T. NON-invasive imaging: Two dimensional speckle tracking echocardiography: basic principles. *Heart*. 2010; **96**(9): 716-22.
457. R-Core-Team. R: A language and environment for statistical computing. Vienna, Austria: R Foundation for Statistical Computing; 2015.
458. Armitage P, Berry G. *Statistical Methods in Medical Research*. 3rd ed. Oxford: Blackwell Scientific Publications; 1993.
459. Morton G, Schuster A, Jogiya R, Kutty S, Beerbaum P, Nagel E. Inter-study reproducibility of cardiovascular magnetic resonance myocardial feature tracking. *J Cardiovasc Magn Reson*. 2012; **14**: 43.

460. Donekal S, Ambale-Venkatesh B, Berkowitz S, Wu CO, Choi EY, Fernandes V, et al. Inter-study reproducibility of cardiovascular magnetic resonance tagging. *J Cardiovasc Magn Reson*. 2013; **15**: 37.
461. Castillo E, Osman NF, Rosen BD, El-Shehaby I, Pan L, Jerosch-Herold M, et al. Quantitative assessment of regional myocardial function with MR-tagging in a multi-center study: interobserver and intraobserver agreement of fast strain analysis with Harmonic Phase (HARP) MRI. *J Cardiovasc Magn Reson*. 2005; **7**(5): 783-91.
462. Moore CC, Lugo-Olivieri CH, McVeigh ER, Zerhouni EA. Three-dimensional systolic strain patterns in the normal human left ventricle: characterization with tagged MR imaging. *Radiology*. 2000; **214**(2): 453-66.
463. Kuetting D, Sprinkart AM, Doerner J, Schild H, Thomas D. Comparison of magnetic resonance feature tracking with harmonic phase imaging analysis (CSPAMM) for assessment of global and regional diastolic function. *European journal of radiology*. 2015; **84**(1): 100-7.
464. Ambale-Venkatesh B, Armstrong AC, Liu CY, Donekal S, Yoneyama K, Wu CO, et al. Diastolic function assessed from tagged MRI predicts heart failure and atrial fibrillation over an 8-year follow-up period: the multi-ethnic study of atherosclerosis. *European heart journal cardiovascular Imaging*. 2014; **15**(4): 442-9.
465. Moody WE, Taylor RJ, Edwards NC, Chue CD, Umar F, Taylor TJ, et al. Comparison of magnetic resonance feature tracking for systolic and diastolic strain and strain rate calculation with spatial modulation of magnetization imaging analysis. *J Magn Reson Imaging*. 2015; **41**(4): 1000-12.
466. Murray CJ, Lopez AD. Global mortality, disability, and the contribution of risk factors: Global Burden of Disease Study. *Lancet*. 1997; **349**(9063): 1436-42.
467. Christakis NA, Escarce JJ. Survival of Medicare patients after enrollment in hospice programs. *N Engl J Med*. 1996; **335**(3): 172-8.
468. Puhan MA, Hansel NN, Sobradillo P, Enright P, Lange P, Hickson D, et al. Large-scale international validation of the ADO index in subjects with COPD: an individual subject data analysis of 10 cohorts. *BMJ open*. 2012; **2**(6).
469. Collins GS, Altman DG. Predicting the 10 year risk of cardiovascular disease in the United Kingdom: independent and external validation of an updated version of QRISK2. *BMJ*. 2012; **344**: e4181.
470. D'Agostino RB, Sr., Vasan RS, Pencina MJ, Wolf PA, Cobain M, Massaro JM, et al. General cardiovascular risk profile for use in primary care: the Framingham Heart Study. *Circulation*. 2008; **117**(6): 743-53.
471. Conroy RM, Pyorala K, Fitzgerald AP, Sans S, Menotti A, De Backer G, et al. Estimation of ten-year risk of fatal cardiovascular disease in Europe: the SCORE project. *Eur Heart J*. 2003; **24**(11): 987-1003.
472. Stone NJ, Robinson JG, Lichtenstein AH, Bairey Merz CN, Blum CB, Eckel RH, et al. 2013 ACC/AHA guideline on the treatment of blood cholesterol to reduce atherosclerotic cardiovascular risk in adults: a report of the American College of Cardiology/American Heart Association Task Force on Practice Guidelines. *Circulation*. 2014; **129**(25 Suppl 2): S1-45.
473. Redheuil A, Wu CO, Kachenoura N, Ohyama Y, Yan RT, Bertoni AG, et al. Proximal aortic distensibility is an independent predictor of all-cause mortality and incident CV events: the MESA study. *J Am Coll Cardiol*. 2014; **64**(24): 2619-29.
474. Maroules CD, Khera A, Ayers C, Goel A, Peshock RM, Abbara S, et al. Cardiovascular outcome associations among cardiovascular magnetic resonance measures of arterial stiffness: the Dallas heart study. *J Cardiovasc Magn Reson*. 2014; **16**: 33.
475. Armstrong AC, Gidding S, Gjesdal O, Wu C, Bluemke DA, Lima JA. LV mass assessed by echocardiography and CMR, cardiovascular outcomes, and medical practice. *JACC Cardiovasc Imaging*. 2012; **5**(8): 837-48.

476. DeFilippis AP, Young R, Carrubba CJ, McEvoy JW, Budoff MJ, Blumenthal RS, et al. An analysis of calibration and discrimination among multiple cardiovascular risk scores in a modern multiethnic cohort. *Ann Intern Med.* 2015; **162**(4): 266-75.
477. Shahab L, Jarvis MJ, Britton J, West R. Prevalence, diagnosis and relation to tobacco dependence of chronic obstructive pulmonary disease in a nationally representative population sample. *Thorax.* 2006; **61**(12): 1043-7.
478. Pepin JL, Cockcroft JR, Midwinter D, Sharma S, Rubin DB, Andreas S. Long-acting bronchodilators and arterial stiffness in patients with COPD: a comparison of fluticasone furoate/vilanterol with tiotropium. *Chest.* 2014; **146**(6): 1521-30.
479. Dransfield MT, Cockcroft JR, Townsend RR, Coxson HO, Sharma SS, Rubin DB, et al. Effect of fluticasone propionate/salmeterol on arterial stiffness in patients with COPD. *Respir Med.* 2011; **105**(9): 1322-30.
480. Duvoix A, Dickens J, Haq I, Mannino D, Miller B, Tal-Singer R, et al. Blood fibrinogen as a biomarker of chronic obstructive pulmonary disease. *Thorax.* 2013; **68**(7): 670-6.
481. Vanfleteren LE, Spruit MA, Groenen MT, Bruijnzeel PL, Taib Z, Rutten EP, et al. Arterial stiffness in patients with COPD: the role of systemic inflammation and the effects of pulmonary rehabilitation. *Eur Respir J.* 2014; **43**(5): 1306-15.
482. Agusti A, Sobradillo P, Celli B. Addressing the complexity of chronic obstructive pulmonary disease: from phenotypes and biomarkers to scale-free networks, systems biology, and P4 medicine. *Am J Respir Crit Care Med.* 2011; **183**(9): 1129-37.
483. Chemla D, Hebert JL, Coirault C, Zamani K, Suard I, Colin P, et al. Total arterial compliance estimated by stroke volume-to-aortic pulse pressure ratio in humans. *Am J Physiol.* 1998; **274**(2 Pt 2): H500-5.
484. Lind L, Andren B, Sundstrom J. The stroke volume/pulse pressure ratio predicts coronary heart disease mortality in a population of elderly men. *J Hypertens.* 2004; **22**(5): 899-905.
485. Lilly SM, Jacobs D, Bluemke DA, Duprez D, Zamani P, Chirinos J. Resistive and pulsatile arterial hemodynamics and cardiovascular events: the Multiethnic Study of Atherosclerosis. *Journal of the American Heart Association.* 2014; **3**(6): e001223.
486. Fagard RH, Pardaens K, Staessen JA, Thijs L. The pulse pressure-to-stroke index ratio predicts cardiovascular events and death in uncomplicated hypertension. *J Am Coll Cardiol.* 2001; **38**(1): 227-31.
487. Duprez DA, Jacobs DR, Jr., Lutsey PL, Bluemke DA, Brumback LC, Polak JF, et al. Association of small artery elasticity with incident cardiovascular disease in older adults: the multi-ethnic study of atherosclerosis. *Am J Epidemiol.* 2011; **174**(5): 528-36.
488. Andreas S, Haarmann H, Klarner S, Hasenfuss G, Raupach T. Increased sympathetic nerve activity in COPD is associated with morbidity and mortality. *Lung.* 2014; **192**(2): 235-41.
489. Clarenbach CF, Senn O, Sievi NA, Camen G, van Gestel AJ, Rossi VA, et al. Determinants of endothelial function in patients with COPD. *Eur Respir J.* 2013; **42**(5): 1194-204.
490. Schoos MM, Dalsgaard M, Kjaergaard J, Moesby D, Jensen SG, Steffensen I, et al. Echocardiographic predictors of exercise capacity and mortality in chronic obstructive pulmonary disease. *BMC cardiovascular disorders.* 2013; **13**: 84.
491. Pocock SJ, Ariti CA, McMurray JJ, Maggioni A, Kober L, Squire IB, et al. Predicting survival in heart failure: a risk score based on 39 372 patients from 30 studies. *Eur Heart J.* 2013; **34**(19): 1404-13.
492. Mineo TC, Pompeo E, Rogliani P, Dauri M, Turani F, Bollero P, et al. Effect of lung volume reduction surgery for severe emphysema on right ventricular function. *American journal of respiratory and critical care medicine.* 2002; **165**(4): 489-94.

493. Kaufmann MR, Barr RG, Lima JA, Praestgaard A, Jain A, Tandri H, et al. Right ventricular morphology and the onset of dyspnea: the MESA-right ventricle study. *PLoS One*. 2013; **8**(2): e56826.
494. Hsiao SH, Chiou KR. Left atrial expansion index predicts atrial fibrillation in dyspnea. *Circulation journal : official journal of the Japanese Circulation Society*. 2013; **77**(11): 2712-21.
495. Kojima T, Kawasaki M, Tanaka R, Ono K, Hirose T, Iwama M, et al. Left atrial global and regional function in patients with paroxysmal atrial fibrillation has already been impaired before enlargement of left atrium: velocity vector imaging echocardiography study. *European heart journal cardiovascular Imaging*. 2012; **13**(3): 227-34.
496. Louvaris Z, Kortianou EA, Spetsioti S, Vasilopoulou M, Nasis I, Asimakos A, et al. Intensity of daily physical activity is associated with central hemodynamic and leg muscle oxygen availability in COPD. *J Appl Physiol (1985)*. 2013; **115**(6): 794-802.
497. Vanfleteren LE, Kocks JW, Stone IS, Breyer-Kohansal R, Greulich T, Lacedonia D, et al. Moving from the Oslerian paradigm to the post-genomic era: are asthma and COPD outdated terms? *Thorax*. 2014; **69**(1): 72-9.
498. Scirba FC, Rogers RM, Keenan RJ, Slivka WA, Gorcsan J, 3rd, Ferson PF, et al. Improvement in pulmonary function and elastic recoil after lung-reduction surgery for diffuse emphysema. *N Engl J Med*. 1996; **334**(17): 1095-9.
499. Come CE, Divo MJ, San Jose Estepar R, Scirba FC, Criner GJ, Marchetti N, et al. Lung deflation and oxygen pulse in COPD: results from the NETT randomized trial. *Respir Med*. 2012; **106**(1): 109-19.
500. Dambrosio M, Cinnella G, Brienza N, Ranieri VM, Giuliani R, Bruno F, et al. Effects of positive end-expiratory pressure on right ventricular function in COPD patients during acute ventilatory failure. *Intensive Care Med*. 1996; **22**(9): 923-32.
501. Dambrosio M, Fiore G, Brienza N, Cinnella G, Marucci M, Ranieri VM, et al. Right ventricular myocardial function in ARF patients. PEEP as a challenge for the right heart. *Intensive Care Med*. 1996; **22**(8): 772-80.
502. Liu C-Y, Parikh M, Gomes A, Vogel-Claussen J. Chronic Obstructive Pulmonary Disease (COPD) is associated with pulmonary artery stiffness - the MESA COPD study. *Journal of Cardiovascular Magnetic Resonance*. 2013; **15**(Suppl 1): 062.
503. Hilde JM, Skjorten I, Grotta OJ, Hansteen V, Melsom MN, Hisdal J, et al. Right ventricular dysfunction and remodeling in chronic obstructive pulmonary disease without pulmonary hypertension. *J Am Coll Cardiol*. 2013; **62**(12): 1103-11.
504. Peinado VI, Barbera JA, Ramirez J, Gomez FP, Roca J, Jover L, et al. Endothelial dysfunction in pulmonary arteries of patients with mild COPD. *Am J Physiol*. 1998; **274**(6 Pt 1): L908-13.
505. Peinado VI, Barbera JA, Abate P, Ramirez J, Roca J, Santos S, et al. Inflammatory reaction in pulmonary muscular arteries of patients with mild chronic obstructive pulmonary disease. *Am J Respir Crit Care Med*. 1999; **159**(5 Pt 1): 1605-11.
506. Milnor WR, Bergel DH, Bargainer JD. Hydraulic power associated with pulmonary blood flow and its relation to heart rate. *Circ Res*. 1966; **19**(3): 467-80.
507. Stevens GR, Garcia-Alvarez A, Sahni S, Garcia MJ, Fuster V, Sanz J. RV dysfunction in pulmonary hypertension is independently related to pulmonary artery stiffness. *JACC Cardiovasc Imaging*. 2012; **5**(4): 378-87.
508. Vestbo J, Anderson J, Brook RD, Calverley PM, Celli BR, Crim C, et al. The Study to Understand Mortality and Morbidity in COPD (SUMMIT) study protocol. *Eur Respir J*. 2013; **41**(5): 1017-22.
509. Maclean EN, Stone IS, Ceelen F, Garcia-Albeniz X, Sommer WH, Petersen SE. Reporting standards in cardiac MRI, CT, and SPECT diagnostic accuracy

studies: analysis of the impact of STARD criteria. European heart journal cardiovascular Imaging. 2014; **15**(6): 691-700.